

REMEDIATION OF ACID MINE DRAINAGE USING NATURAL ZEOLITE

By

TAFADZWA MOTSI

A thesis submitted to
The University of Birmingham
for the degree of
DOCTOR OF PHILOSOPHY

School of Chemical Engineering
The University of Birmingham
United Kingdom

March 2010

UNIVERSITY OF
BIRMINGHAM

University of Birmingham Research Archive

e-theses repository

This unpublished thesis/dissertation is copyright of the author and/or third parties. The intellectual property rights of the author or third parties in respect of this work are as defined by The Copyright Designs and Patents Act 1988 or as modified by any successor legislation.

Any use made of information contained in this thesis/dissertation must be in accordance with that legislation and must be properly acknowledged. Further distribution or reproduction in any format is prohibited without the permission of the copyright holder.

Abstract

This research focuses on the removal of Fe, Cu, Zn and Mn from synthetic metal solutions and real AMD from Wheal Jane mine using natural zeolite. Laboratory experiments were performed to investigate the effectiveness of natural zeolite as a potential low cost material for the removal of these heavy metals from AMD. These include, equilibrium tests, batch kinetic studies, column studies and desorption studies.

Equilibrium studies showed that the capacity of natural zeolite for heavy metals increased with an increase in initial solution pH. Fitting of the Langmuir and Freundlich isotherms to experimental data gave good fits, R^2 values ranging from 0.9 – 0.99. The selectivity series of natural zeolite was: $\text{Fe}^{3+} > \text{Zn}^{2+} > \text{Cu}^{2+} > \text{Mn}^{2+}$. The amount of exchangeable cations increased at equilibrium, indicating that ion exchange had taken place. Higher metal uptakes were achieved by increasing agitation speed, initial solution pH, particle size reduction, and thermal pre-treatment. The rate limiting step for this process was intraparticle diffusion.

Column studies showed that natural zeolite was capable of removing heavy metals from a continuously flowing solution. The breakthrough time increased with a longer bed height and slower flow rate. The bed depth service time model (BDST) was used to simulate experimental data and deviated from these by 12 – 14%.

The treatment of actual Wheal Jane mine AMD showed that about 71-99% Fe and 97-99% Cu were removed from solution. Results from the treatment of actual AMD revealed that natural zeolite was best suited for treating dilute metal solutions, and hence should be used downstream of other AMD treatment technologies.

Dedication

To my dearly beloved parents, Mr A. Motsi and Mrs L. Motsi, for their constant love,
support and wisdom.

Acknowledgements

I would like to gratefully acknowledge the valuable assistance and encouragement I received throughout this project from my supervisors, Dr Neil Rowson and Dr Mark Simmons.

I would also like to express my appreciation to IMERYS Minerals Ltd, UK for supplying the natural zeolite samples used in this project and their technical assistance in analysing some of these samples.

I would also like to acknowledge the financial support I received from the Overseas Research Scholarship Award (ORSAS), which gave me the opportunity to carry out this project.

I am grateful to my family for their support, love and encouragement. To my father for continually challenging me and reminding me to give it my best all the time. Special thanks to my mum for her refreshing words and love. To my young sister, Tatenda, thank you for being a continual inspiration. I am immensely grateful to my friends for their love, support and company without which this project would have been very difficult.

Finally, I would like to give my heartfelt thanks to God for blessing me with the wonderful people that surrounded me during my study and also for blessing me with favour, strength and good health to complete it.

Table of Contents

Abstract.....	ii
Dedication.....	iii
Acknowledgement.....	iv
List of Figures.....	ix
List of Tables.....	xiii
Nomenclature.....	xvi

Chapter 1: Introduction

1.1 Evaluation of the Acid Mine Drainage Problem.....	1
1.2 Treatment of Acid Mine Drainage.....	3
1.3 Motivation and Aims of Thesis.....	5
1.4 Thesis Structure.....	6

Chapter 2: Literature Review

2.1 Introduction.....	9
2.2 Acid Mine Drainage.....	10
2.2.1 Sources of Acid Mine Drainage.....	10
2.2.2 Formation and Constituents of Acid Mine Drainage.....	11
2.2.3 Environmental and Ecological Impact of Acid Mine Drainage.....	13
2.2.4 Preventing Acid Mine Drainage Formation.....	18
2.2.5 Technologies used for treating Acid Mine Drainage.....	20
2.2.6 Recovery of valuable products from AMD treatment.....	30
2.3 Adsorption of Acid Mine Drainage.....	31
2.3.1 Adsorption Process.....	31
2.3.2 Examples of Adsorbents.....	33
2.3.3 Natural Zeolite.....	34
2.3.3.1 Occurrence of Natural Zeolites.....	35
2.3.3.2 Framework and Structure of zeolites.....	37
2.3.3.3 Application of Natural Zeolites.....	39
2.3.3.4 Using Natural Zeolite to treat Acid Mine Drainage.....	41

Chapter 3: Case Study, Wheal Jane Mine

3.1	Brief History.....	43
3.2	Composition of Wheal Jane Mine AMD.....	45
3.3	Treatment technologies used at Wheal Jane Mine.....	46
3.3.1	Active Treatment.....	46
3.3.2	Passive Treatment.....	47
3.4	Conclusion.....	48

Chapter 4: Materials and Methods

4.1	Introduction.....	49
4.2	Materials and Sample Preparation.....	49
4.2.1	Synthetic solutions and other chemicals.....	49
4.2.2	Characterisation of Natural Zeolite.....	50
4.3	Experimental Procedure.....	53
4.3.1	Batch Adsorption Studies.....	53
4.3.2	Column Studies.....	57
4.3.3	Treatment of AMD from Wheal Jane Mine.....	59
4.4	Sample Analysis.....	60

Chapter 5: Characterisation of Natural Zeolite

5.1	Introduction.....	62
5.2	Scanning Electron Microscopy (SEM).....	63
5.3	Energy Dispersive Spectroscopy (EDS).....	69
5.4	X – Ray Diffraction	71
5.5	X – Ray Fluorescence.....	72
5.6	Other particle characteristics.....	74

Chapter 6: Equilibrium Studies

6.1	Introduction.....	76
6.2	Equilibrium isotherms.....	77
6.2.1	Langmuir adsorption isotherm.....	77
6.2.2	Freundlich adsorption isotherm.....	79

6.3	Results and discussion.....	80
6.3.1	Removal of copper.....	80
6.3.2	Removal of zinc.....	87
6.3.3	Removal of iron.....	92
6.3.4	Removal of manganese.....	96
6.4	Selectivity of natural zeolite.....	101
6.5	Conclusion.....	104

Chapter 7: Kinetic Studies

7.1	Introduction.....	106
7.2	General Kinetic study results.....	107
7.3	Factors that affect rate of Adsorption.....	109
7.3.1	Effect of adsorbent mass.....	109
7.3.2	Effect of particle size.....	111
7.3.3	Effect of initial solution pH.....	113
7.3.4	Effect of initial solution concentration.....	117
7.3.5	Effect of agitation.....	120
7.3.6	Effect of competing cations.....	122
7.3.7	Effect of thermal pre – treatment.....	124
7.4	Desorption/Regeneration studies.....	128
7.5	Treatment of Synthetic Acid Mine Drainage (sAMD).....	132
7.6	Kinetic Modelling.....	135
7.6.1	Chemical Reaction control.....	135
7.6.2	Film transfer diffusion control (external mass transfer).....	141
7.6.3	Intra – Particle diffusion control.....	146
7.6.4	Interruption Tests.....	153
7.7	Conclusion.....	156

Chapter 8: Column Studies

8.1	Introduction.....	158
8.2	Breakthrough Curves.....	160
8.3	Modelling of fixed bed columns.....	163

8.3.1	Bed depth service time model.....	163
8.3.2	Results and discussion.....	165
8.4	Column operation.....	168
8.4.1	Effect of flow rate.....	168
8.4.2	Effect of bed height.....	171
8.5	Treatment of synthetic acid mine drainage (sAMD).....	175
8.5.1	Adsorption studies.....	175
8.5.2	Desorption studies.....	179
8.6	Conclusion.....	183

Chapter 9: Treatment of Wheal Jane AMD

9.1	Introduction.....	185
9.2	Batch Experiments.....	186
9.2.1	Use of thermally pre – treated natural zeolite in treating real AMD.....	186
9.2.2	Standing tests for the treatment of Wheal Jane AMD.....	189
9.2.3	Comparison between natural zeolite and synthetic zeolite in treating Wheal Jane mine AMD.....	194
9.2.4	Proposed design of a passive AMD treatment reactor vessel.....	196
9.3	Column Experiments.....	199
9.3.1	Adsorption and desorption studies.....	199
9.4	Conclusions.....	206

Chapter 10: Conclusions and Recommendations

10.1	Conclusions.....	208
10.1.1	Characterisation of natural zeolite.....	208
10.1.2	Equilibrium studies.....	209
10.1.3	Kinetic studies.....	210
10.1.4	Column studies.....	212
10.1.5	Treatment of Wheal Jane AMD.....	214
10.2	Recommendations.....	215

References

APPENDICES

List of Figures

Figure 1.1: Fish kills like the one pictured above are typical of mine spills. Spills from Los Pelambres Mine (above) resulted in 5,307,000 litres of AMD showing higher than normal levels of sulphates and molybdenum, being released into the Cuncumén River, Chile.....	2
Figure 2.1: An example of a common Passive treatment system (Reprinted from: http://www.scrip.pa-conservation.org/aboutamd.htm).....	24
Figure 2.2: Representation of $[\text{SiO}_4]^{4-}$ or $[\text{AlO}_4]^{5-}$ tetrahedral (Dyer, 1988).....	34
Figure 2.3: Secondary building units in zeolite frameworks; (a) single four ring (S4R), (b) single six ring (S6R), (c) single eight ring (S8R), (d) double six ring (D6R), (e) complex 4-4-1 (f) double four ring (D4R), (g) complex 4-1 and (h) complex 5-1 (Dyer, 1988).....	38
Figure 2.4: Shape selectivity in zeolite channels (Csicsery, 1985).....	39
Figure 3.1: Aerial photograph of the mouth of Restronguet Creek and Carrick Roads taken during the Wheal Jane incident [<i>Photograph courtesy of the Environment Agency</i>].....	44
Figure 3.2: Simplified process flow diagram for the Passive treatment plant at Wheal Jane Mine (Whitehead et al., 2005).....	47
Figure 4.1: Schematic diagram of the column set – up.....	57
Figure 5.1: SEM Micrograph of natural zeolite (Clinoptilolite) at a magnification of x3000; the natural zeolite was washed in distilled water.....	64
Figure 5.2: SEM Micrographs of acid washed natural zeolite (Clinoptilolite) at different magnifications: (a) x 1000 and (b) x 2000.....	64
Figure 5.3: SEM microstructure of unwashed natural zeolite thermally pre – treated in a muffle furnace for 30 minutes at (a, b) 400 °C (c) 200 °C.....	65
Figure 5.4: SEM microstructure of natural zeolite thermally pre – treated in a microwave for 15 minutes.....	66
Figure 5.5: Micrographs of thermally pre – treated natural zeolite at <i>i.</i> 800 °C (a, b) and <i>ii.</i> 30 minute exposure to microwave energy at 950 W, (c).....	67
Figure 5.6: SEM microstructure of natural zeolite whose pores have completely collapsed due to thermal runaway, (a) x39, (b) x5000.....	68

Figure 5.7: EDS analysis showing the elemental composition and scanning method for natural zeolite.....	70
Figure 6.1: Equilibrium isotherms for the removal of copper from solution.....	82
Figure 6.2: Equilibrium pH change with respect to various initial copper concentrations. The initial solutions were at different pH values, (a) 2.5, (b) 3.5 and, (c) 5.7. Error in pH reading is ± 0.05	84
Figure 6.3: Amount of exchangeable Ca^{2+} ions in solution after equilibrium, at different initial copper concentrations.....	86
Figure 6.4: Equilibrium isotherms for the removal of zinc from solution by natural zeolite at different initial solution pH levels.....	88
Figure 6.5: Change in equilibrium pH with respect to various initial zinc concentrations. The initial solutions were at different pH values, which are: (a) 2.5, (b) 3.5 and, (c) 5.7 ± 0.05	90
Figure 6.6: Amount of exchangeable Ca^{2+} ions in solution at equilibrium, for different initial zinc concentrations.....	91
Figure 6.7: Equilibrium isotherms for the removal of iron from solution by natural zeolite at different initial solution pH levels.....	93
Figure 6.8: Equilibrium pH change with respect to different initial iron concentrations. The initial solutions were at different pH values, which are: (a) 2.0 and, (b) 2.5 ± 0.05	94
Figure 6.9: Equilibrium isotherms for the removal of manganese from solution by natural zeolite at different initial solution pH levels.....	97
Figure 6.10: Equilibrium pH change with respect to various initial manganese concentrations. The initial solutions were at pH: (a) 2.5, (b) 3.5 and, (c) 5.7 ± 0.05	99
Figure 6.11: Amount of exchangeable Ca^{2+} ions in solution at equilibrium, for different initial manganese concentrations.....	100
Figure 7.1: The effect of the mass of natural zeolite on the adsorption of iron, copper, zinc and manganese from solution (particle size: 1 – 3 mm; pH: 3.5).....	110
Figure 7.2: Effect of particle size on the adsorption of iron, copper, zinc and manganese from solution (15 g of zeolite in 100 ml solution; solution pH 3.5).....	112
Figure 7.3: Effect of initial solution pH on the adsorption capacity of natural zeolite (3.7 g zeolite; 100 ml single component solution; particle size 1 – 3 mm).....	114

Figure 7.4: Change in solution pH as adsorption of heavy metals proceeds (3.7 g zeolite; 100 ml single component solution; particle size 1 – 3 mm).....	116
Figure 7.5: Effect of agitation on the adsorption of heavy metals by natural zeolite (3.7 g in 100 ml solution).....	121
Figure 7.6: Comparison of the adsorption capacity of natural zeolite for iron, manganese, zinc and copper from single and multi – component solutions.....	123
Figure 7.7: Comparison of natural and thermally pre – treated natural zeolite, 3.7 g mixed with 100ml single component solutions at pH 3.5.....	125
Figure 7.8: Change in the adsorption capacity of natural zeolite due to regeneration...	130
Figure 7.9: Comparison of adsorption capacities from single component solutions and from synthetic acid mine drainage (sAMD).....	133
Figure 7.10: Effect of adsorbent particle size on the reaction rate constant.....	138
Figure 7.11: Effect of agitation speed on the reaction rate constant.....	139
Figure 7.12: Fitting film transfer diffusion control model to the experimental results...	144
Figure 7.13: Intraparticle diffusion control: Vermeulen’s versus Nernst-Plank’s approximations.....	151
Figure 7.14: The effect of interruption upon the rate of exchange according to controlling diffusion mechanism (schematic) (Harland, 1994).....	154
Figure 7.15: Interruption tests on the removal of heavy metals from solution by natural zeolite (3.7g natural zeolite, 100 ml single component solution, pH 3.5).....	155
Figure 8.1: Schematic diagram of the column set – up.....	159
Figure 8.2: Schematic representation of the displacement of the adsorption zone or mass transfer zone and the resulting breakthrough curve (Harland, 1994).....	161
Figure 8.3: Comparison of the BDST model with experimental results, bed height 15 cm, flow rate 20 ml/min and the BDST model was calculated at 30 % breakthrough...	167
Figure 8.4: Breakthrough curves for the effect of flow rate on the adsorption of heavy metals by natural zeolite.....	169
Figure 8.5: Effect of bed height on the adsorption of iron by natural zeolite; $C_o = 400$ mg/l.....	172

Figure 8.6: Effect of bed height on the adsorption of zinc by natural zeolite; $C_0 = 120$ mg/l.....	174
Figure 8.7: Breakthrough curves for the removal/adsorption of heavy metals from synthetic solutions by natural zeolite, bed height 50 cm and flow rate 20 ml/min...	176
Figure 8.8: Breakthrough curves for the effect of competing cations in the removal of zinc and iron from single component and sAMD solutions; bed height 50 cm, flow rate 20 ml/min.....	178
Figure 8.9: Desorption of heavy metals from natural zeolite; column bed height 50 cm, cycle 1.....	181
Figure 9.1: Effect of thermally pre-treating natural zeolite on its capacity to remove heavy metals from Wheal Jane mine AMD.....	187
Figure 9.2: Treatment of Wheal Jane mine AMD using natural zeolite (no agitation for about 9 days).....	191
Figure 9.3: Sketch of the proposed reactor for the passive treatment of Wheal Jane AMD.	196
Figure 9.4: Proposed flow diagram for the passive treatment of AMD from Wheal Jane mine.....	198
Figure 9.5: Breakthrough curves for the treatment of Wheal Jane AMD; bed height 50 cm and flow rate 20 ml/min.....	200
Figure 9.6: Desorption of heavy metals from natural zeolite using 2 % (w/w) sulphuric acid at 40 °C; flow rate 20 ml/min; column bed height 50 cm.....	205

List of Tables

Table 2.1: Typical composition of Acid Mine Drainage.....	13
Table 2.2: Chemicals for <i>AMD</i> oxidation, neutralisation and coagulation /floculation.....	22
Table 3.1: Chemical quality of Wheal Jane Mine water (<i>AMD</i>).....	45
Table 5.1: Chemical analysis of natural zeolite performed by XRF (% wt/wt).....	73
Table 5.2: Physical properties of natural zeolite (clinoptilolite) used in this study, compared with samples used by other researchers.....	74
Table 6.1: Calculated equilibrium adsorption isotherm constants for the uptake of copper from solution by natural zeolite.....	80
Table 6.2: Minimum pH values for complete precipitation of heavy metal ions as hydroxides (Brown et al., 2002).....	85
Table 6.3: Calculated equilibrium adsorption isotherm constants for the uptake of zinc from solution by natural zeolite.....	87
Table 6.4: Calculated equilibrium adsorption isotherm constants for the uptake of iron from solution by natural zeolite.....	92
Table 6.5: The amount of Ca^{2+} ions released from natural zeolite at equilibrium, for different initial iron concentrations; initial solution pH = 2.0.....	95
Table 6.6: Calculated equilibrium adsorption isotherm constants for the uptake of manganese from solution by natural zeolite.....	96
Table 6.7: Some examples of maximum capacities obtained using different natural zeolite (clinoptilolite) samples in batch mode applications for the removal of Fe^{3+} , Cu^{2+} , Zn^{2+} and Mn^{2+} in literature.....	101
Table 6.8: Examples of experimentally derived selectivity series of natural zeolite for different heavy metals from literature.....	103
Table 7.1: Effect of natural zeolite mass on the removal of heavy metals from solution at pH 3.5 and 22 °C.....	109
Table 7.2: Effect of initial solution concentration on the adsorption capacity of natural zeolite. Total contact time: 360 minutes.....	118

Table 7.3: Surface area of thermally pre – treated samples of natural zeolite.....	127
Table 7.4: The percentage recovery of heavy metals from natural zeolite by regeneration.....	128
Table 7.5: Calculated percentage change in adsorption capacity over 3 cycles.....	131
Table 7.6: Variation of rate constant with agitation speed and adsorbent particle size...	140
Table 7.7: Calculated film mass transfer coefficients.....	145
Table 7.8: Summary of the diffusion coefficients calculated from Vermeulen’s approximation for natural zeolite.....	150
Table 7.9: Diffusion coefficients determined using the Nernst-Plank’s Approximation.....	152
Table 8.1: Values of BDST model parameters for the adsorption of heavy metals from single component solutions by natural zeolite at 30 % breakthrough, 15 cm column height and a flow rate of 20 ml/min.....	165
Table 8.2: Effect of flow rate on the volume of solution treated, at $C_t/C_o = 0.4$ and 15 cm bed height.....	171
Table 8.3: Effect of bed height on the adsorption of iron from solution by natural zeolite in fixed bed columns.....	173
Table 8.4: Effect of bed height on the adsorption of zinc from solution by natural zeolite in fixed bed columns.....	175
Table 8.5: Bed service time at 40 % breakthrough for the treatment of synthetic acid mine drainage.....	177
Table 8.6: Calculated desorption efficiencies for the desorption of heavy metals from natural zeolite in fixed bed columns using 2 % (w/w) H_2SO_4 at 40 °C; bed height 50 cm, flow rate 20 ml/min; contact time 540 minutes.....	182
Table 9.1: Comparison between thermally pre-treated natural zeolite and untreated natural zeolite in treating Wheal Jane AMD after 360 minutes.....	188
Table 9.2: Treatment of Wheal Jane mine AMD using natural zeolite (no mixing, total contact time 9 days, 22 °C, particle size: 1 – 3mm).....	193
Table 9.3: Comparison of natural zeolite and synthetic zeolite in treating AMD from Wheal Jane mine.....	195

Table 9.4: Removal efficiencies of heavy metals from Wheal Jane mine passive treatment plant (Whitehead et al., 2005).....	197
Table 9.5: Calculated column efficiencies for the 3 cycles (Contact time for each cycle was about 500 minutes).....	202
Table 9.6: Comparison between results from Wheal Jane (W.J.) active treatment plant and those found in this study (fixed bed column studies).....	203
Table 9.7: Research carried out at the University of Birmingham for the treatment of Wheal Jane mine AMD and the results obtained.....	204

Nomenclature

A_c	area under the packed bed column breakthrough curve
b	Langmuir adsorption coefficient
C_e	residual liquid phase concentration at equilibrium
C_o	initial concentration of heavy metal ions
C_t	metal ion concentration at time, t
d_p	average particle diameter
D'_i	solid phase self-diffusion coefficient of ion i
k_2	pseudo second order rate constant
k_s	film mass transfer coefficient
m	mass of adsorbent
m_d	mass of solute desorbed
m_s	mass of adsorbent particle per unit volume of particle free slurry
m_{ads}	mass of solute that has been adsorbed
m_f	total amount of metal ions fed into the column
n_r	number of data
N_o	dynamic adsorption capacity
q_b	amount of solute adsorbed at breakthrough point per unit mass adsorbent in column
q_e	amount of solute adsorbed per unit mass of adsorbent at equilibrium
$q_{e \max}$	maximum experimental adsorption capacity at equilibrium
q_o	amount of solute adsorbed per unit mass of adsorbent corresponding to complete coverage of available adsorption sites
Q_v	volumetric flow rate
R^2	correlation coefficient
r	natural zeolite particle radius
S_s	outer surface area of zeolite particles per unit volume of particle free slurry
T_b	represents the column breakthrough point

T_s	time required for full bed exhaustion under ideal conditions
$U(t)$	fractional attainment of equilibrium in the ion exchanger
V	volume of solution from which adsorption occurs
X_j^p	predicted fractional concentration
X_j	measured (experimental) fractional concentration
Z	column bed depth

Symbols:

ε_p	porosity of the zeolite particles.
ρ_t	density of particle

CHAPTER 1

INTRODUCTION

1.1 Evaluation of the Acid Mine Drainage Problem

Acid Mine Drainage (*AMD*) is predominantly caused by the weathering of pyrite (FeS_2). Pyrite oxidises to produce very acidic waters ($\text{pH} < 3$), which can solubilise heavy metals and other toxic elements and cause them to be transported downstream into river bodies, eventually ending up in the sea (Pentreath, 1994; Jenkins et al., 2000).

Pyrite is a mineral composed of iron and sulphur (FeS_2). Mineral deposits containing pyrite are usually present as sulphides, deposited beneath the earth's surface, where there is little or no oxygen. When mining occurs, these minerals are exposed and brought to the surface where a combination of weathering and mining activities results in the production of acid waters. These acid waters solubilise some of the elements contained in the mineral deposits, elements such as iron, copper, zinc, cadmium, manganese and many such toxic metals, forming Acid Mine Drainage. These elements are not biodegradable and thus tend to accumulate in living organisms, causing various diseases, disorders and even death (Alvarez-Ayuso et al., 2003; Spyrnskyy et al., 2006; Bailey et al., 1999), see Figure 1.1. Although current mining activities do result in the formation of *AMD*, the largest and “worst” pollution comes from old, abandoned deep mines, mainly in places where vast amounts of mining took place in the past, for example in Cornwall, U.K.



Figure 1.1: Fish kills like the one pictured above are typical of mine spills. Spills from Los Pelambres Mine (above) resulted in 5,307,000 litres of AMD showing higher than normal levels of sulphates and molybdenum, being released into the Cuncumén River, Chile

(Reprinted from: http://patagonia-under-siege.blogspot.com/2007_12_01_archive.html).

In the United Kingdom, *AMD* is also common, it is mainly formed in abandoned metalliferous mines for example Wheal Jane in Cornwall and also in abandoned coal mines (which contain significant amounts of FeS_2) located mainly in the Midlands and Northern England. The sulphur content of most coal used in the UK is in the range of 1-3 %, the average sulphur content being about 1.6 % (ACE Information Programme).

1.2 Treatment of Acid Mine Drainage

There are a number of Acid Mine Drainage (*AMD*) Treatment technologies, and these fall mainly into two broad categories, Passive and Active treatment. Comparing the two remediation processes; Active treatment is generally more complex, requires more unit processes and thus higher running costs compared to the simpler passive treatment techniques which do not require specialised machinery or chemicals.

1.2.1 Active Treatment

Active treatment involves physically adding a neutralising agent to the source of the *AMD* or directly to the stream that has been polluted. Active treatment can be very successful; however, it necessitates a long-term and continuous commitment to treatment. Equipment failure, weather conditions, and budget reductions can result in lapses in treatment which may have devastating consequences.

The addition of neutralising agents/chemicals does not only neutralise the *AMD*, but it serves to precipitate the metals out of the solution. There are a number of chemicals that are used in active remediation of *AMD*, these include:

- Calcium Carbonate (CaCO_3),
- Calcium Oxide (CaO),
- Calcium Hydroxide ($\text{Ca}(\text{OH})_2$),
- Ammonia (NH_3),
- Sodium Hydroxide (NaOH),
- Sodium Carbonate (Na_2CO_3).

1.2.2 Passive Treatment

The major methods of passive treatment with regards to the remediation of *AMD* are:

- Anoxic Limestone Drains (ALD),
- Limestone sand dosing,
- Open Limestone Channels and Channel bars,
- Limestone diversion wells,
- Aerobic wetlands,
- Anaerobic wetlands,
- Settling ponds.

1.2.3 Other Treatments

The other treatment methods in use for *AMD* treatment are:

- Electro-dialysis,
- Ultra-filtration,
- Electrolysis,
- Reverse osmosis,
- Use of adsorbent material for example natural zeolites, activated carbon, blast furnace slag, dead biomass etc.

Some of these, such as electrolysis and electro-dialysis are not in large scale use because of both their high capital and running costs.

1.3 Motivation and Aims of Thesis

The importance of solving the *AMD* problem has been briefly highlighted above. Since conventional methods have a number of shortcomings; which are, greater land utilisation, production of large secondary solid waste, high capital and running costs especially when treating relatively dilute solutions (Alvarez-Ayuso et al., 2003), alternative technologies need to be developed.

The aim of this investigation is to develop a low cost alternative method for the treatment of *AMD*. The efficiency of natural zeolite (clinoptilolite) for the removal of heavy metal ions from solution was investigated. Only 4 heavy metal ions were considered in this investigation; these are Fe^{3+} , Cu^{2+} , Mn^{2+} and Zn^{2+} . These were chosen because they are the main heavy metal ions contained in Wheal Jane mine *AMD* (Swash and Monhemius, 2005; Coulton et al., 2003). The effectiveness of natural zeolite as an adsorbent in *AMD* treatment was further investigated by using the zeolite to treat real *AMD* from Wheal Jane Mine, which was used as a case study in this research.

The ideal method for treating *AMD* should include the following:

- Low cost (that is, capital and running costs),
- Simple to run/operate,
- Produce considerably small amounts or no solid waste,
- Should have small land utilisation,
- Reduce the liquid waste volume,
- It should also be relatively more effective and efficient compared to conventional methods.

1.4 Thesis Structure

This thesis is divided into a number of chapters, each explaining different aspects of the investigation. A summary of each chapter is given below.

Chapter 1: Introduction

A brief background of the *AMD* problem is given together with the different solutions to the problem. An outline of the motivation, aims and objectives of this research is also briefly discussed.

Chapter 2: Literature Review

An in – depth explanation into the *AMD* problem is given; its sources, environmental impact, prevention and the different treatment technologies available. The treatment of *AMD* using natural zeolite is also explained, that is, the treatment mechanism. Natural zeolites are also described in greater detail with their general characteristics. A review of previous research involving the use of different adsorbents including natural zeolite is also presented.

Chapter 3: Case Study: Wheal Jane Mine, UK

A brief history of the mine is given together with a description of the incident that occurred in 1992, which resulted in the release of *AMD* into the environment. The *AMD* treatment technologies presently being employed at the mine are also described and discussed.

Chapter 4: Materials and Methods

The materials used in this research, that is, chemicals and adsorbent materials are described in this chapter. The experimental techniques used in order to determine the potential of natural zeolite as a low cost material in treating acid mine drainage (*AMD*) are also described in detail.

Chapter 5: Characterisation of Natural Zeolite

Different methods of characterising the properties of natural zeolite are described in this chapter. The main methods used are Scanning Electron Microscopy (SEM) and Energy Dispersive Spectroscopy (EDS), X – Ray Diffraction (XRD) and X – Ray Fluorescent (XRF). The other properties of natural zeolite such as density, porosity, moisture content and surface area were also determined.

Chapter 6: Equilibrium Studies

In this chapter equilibrium experiments are described for the removal of iron, copper, zinc and manganese from their single component solutions under different conditions. The experimental data were also analysed using adsorption isotherms, mainly the Freundlich and Langmuir adsorption isotherms. From these studies the selectivity of natural zeolite for the heavy metals under investigation was determined.

Chapter 7: Kinetic Studies

This chapter describes the kinetic studies performed in order to determine the efficiency of natural zeolite in removing heavy metals from solution. Natural zeolite was contacted with solutions containing heavy metals under different conditions, for example, different

initial pH or initial concentration and agitation speeds. The rate limiting step for the removal of heavy metals from solution by natural zeolite was also determined.

Chapter 8: Column Studies

Column studies are described in detail in this chapter; this includes a description of the effect of flow rate, bed height and regeneration of natural zeolite.

Chapter 9: Treatment of Wheal Jane AMD

In this chapter the actual treatment of acid mine drainage from Wheal Jane Mine is described. The results are compared with removal rates from technologies currently being used at Wheal Jane mine.

Chapter 10: Conclusions and Recommendations

This chapter presents a summary of the findings and conclusions of the work performed in this project and recommendations are given for further study.

CHAPTER 2

LITERATURE REVIEW

2.1 Introduction

Acidic mine drainage is an environmental pollutant of major concern in mining regions throughout the world. The oxidative dissolution of sulphide minerals (principally pyrite, FeS_2) in the presence of water and oxygen gives rise to these acidic, metal laden waters. The high acidity of *AMD* and the large amounts of dissolved heavy metals, such as copper, zinc, manganese, iron, arsenic, lead etc, generally make *AMD* extremely toxic to most living organisms (Pentreath, 1994).

In the United Kingdom *AMD* is now becoming a problem due to the increasing number of abandoned mines and the closure of whole coalfields. The pumps which currently keep these mines dry are being switched off and groundwater is returning to its pre – mining industry levels leading to *AMD* discharges into the surrounding areas (Hughes, 1994).

The objective of this chapter is to discuss the acid mine drainage problem; main focus will be on its formation, environmental impact, treatment and prevention and the use of low cost materials to treat it. A detailed description of natural zeolite will be given since it was used in this research as a low cost adsorbent for *AMD* treatment.

2.2 Acid Mine Drainage

2.2.1 Sources of Acid Mine Drainage

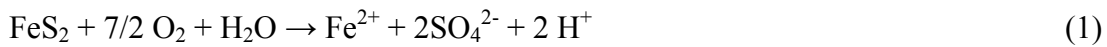
Mining activities expose a significant amount of mineral deposits containing pyrite deposited in the layers of rock beneath the earth's surface, where there is little or no oxygen. Mining activities bring these deposits to the surface where they are crushed to release valuable minerals like copper, zinc, gold, nickel etc, the tailings are left on the mine site. Thus large amounts of pyrite becomes exposed to surface conditions, that is, air and water which will assist in the oxidation of the pyrite to produce *AMD* (Jenkins et al., 2000). Pyrite is recognised as the major source of *AMD*, due to its abundance in the environment (Evangelou, 1998)

In the case of abandoned mines, water may enter the mines through a number of ways including via mine faults, galleries and adits from the surface as rainwater or from ground water (National Rivers Authority, 1999). If this water is not pumped out in a timely manner *AMD* will be formed due to the reaction of water and the exposed sulphide minerals (mainly FeS_2) deep in the mine. An example of this scenario is Wheal Jane Mine, Cornwall, the mine flooded because the water drainage pumps were switched off, resulting in an adit failure and hence the formation and discharge of *AMD* into the surrounding environment (Hallberg and Johnson, 2003).

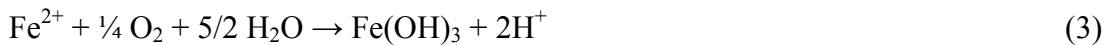
2.2.2 Formation and Constituents of Acid Mine Drainage

As discussed above, *AMD* is produced when sulphide minerals are oxidised in the presence of oxygen (from air or dissolved in water) and water (as vapour or liquid) to produce sulphuric acid. The primary reactions for the formation of *AMD* from pyrite are presented below (Singer and Strumm, 1970):

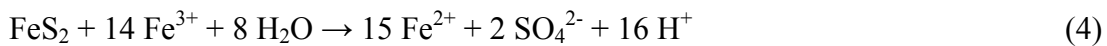
Pyrite is initially oxidised by atmospheric oxygen producing sulphuric acid and ferrous iron (Fe^{2+}) according to the following reaction:



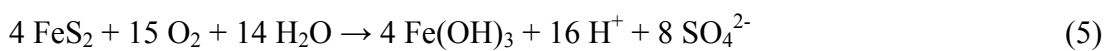
The ferrous iron may be further oxidized by oxygen releasing more acid into the environment and precipitating ferric hydroxide:



The pH of the solution decreases as acid production increases, resulting in further oxidation of pyrite by Fe^{3+} , resulting in more acid production:

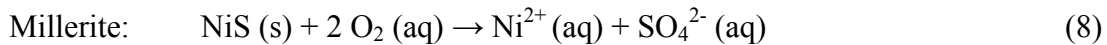
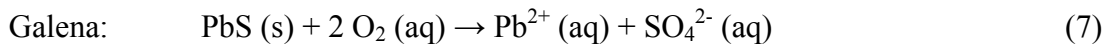
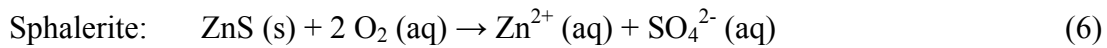


Reaction [4] is catalysed by bacteria, most notably *Thiobacillus ferrooxidans*. The overall reaction for the formation of *AMD* is thus:



The rate of *AMD* formation depends on several factors, such as the presence and type of activating micro – organisms, type of sulphide and non – sulphide minerals present, particle size of the rock, solution pH, temperature and the availability of oxygen, nutrients and water (Evangelou, 1998; Valenzuela et al., 2005).

Other metals commonly found in *AMD*, such as aluminium, copper, lead, nickel, zinc etc, exist because they are present in the rocks with pyrite. For example, there are a variety of other metal sulphides that may release these metal ions into solution (Younger et al., 2002; Costello, 2003):



It is apparent that the formation of *AMD* is complicated due to the number of factors that influence its production and hence it would be highly probable that the constituents of *AMD* vary from region to region. Since factors like number and type of micro – organisms, temperature (weather and seasonal conditions) and type of minerals vary from place to place, thus influencing the quality (pH and metals content) and amount of *AMD* produced (Steffen et al., 1989; Sanchez et al., 2005).

The chemical composition of several representative *AMD* solutions from different countries is given in Table 2.1.

Table 2.1: Typical composition of Acid Mine Drainage.

Constituent	U.K., Wheal Jane Mine ^a	Spain, Rio Tinto River ^b	Spain, Odiel River ^b	Norway, Storwartz Mine
pH	2.6 – 3.1	2.9	3.8	6.5
Fe	1720 – 1900	123	4.9	1.60
Cu	14 – 18	15.7	5.4	0.06
Al	170 – 197	66.5	32.8	0.03
Zn	1260 – 1700	24.1	11.5	2.13
Mn	11 – 25	6.8	8.1	1.35
Ni	---	0.135	0.145	---
As	---	0.147	0.004	---
Co	---	0.476	0.269	---
Pb	---	0.121	0.045	---

^a Hamilton et al., 1994; ^b Nieto et al., 2007. Units for all metal concentrations are in mg/l.

2.2.3 Environmental and Ecological Impact of Acid Mine Drainage

As discussed above, *AMD* introduces sulphuric acid and heavy metals into the environment. Usually the environment is capable of absorbing the effects of *AMD* through a combination of dilution, biological action and neutralisation, but at high metal concentrations this ability is drastically reduced (Evangelou, 1998). These heavy metals pose a serious threat to human health, animals and ecological systems. This is because *AMD* contains heavy metal contaminants, such as Cu^{2+} , Fe^{3+} , Mn^{2+} , Zn^{2+} , Cd^{2+} and Pb^{2+} which are not biodegradable and tend to accumulate in living organisms, causing various diseases and disorders (Moreno et al., 2001; Sprynskyy et al., 2006; Bailey et al., 1999).

Moreover, *AMD* is initially clear but turns a vivid orange colour as it undergoes neutralisation in rivers downstream because of the precipitation of iron oxide and hydroxide. This precipitate is usually called *ochre*; it is a low density solid material which is not very stable. In conditions where water is flowing ochre can easily be transported and deposited, coating large surface areas posing a significant environmental concern.

2.2.3.1 Impact of dissolved metals

Acid mine drainage contains a number of dissolved metals as highlighted earlier, which are toxic by nature. The environmental impact of a number of these metals will be discussed in this section.

2.2.3.1.1 Effect of dissolved metals on aquatic life

Dissolved heavy metals not only increase the toxicity of *AMD* but act as metabolic poisons. These heavy metals can act together to suppress algal growth and affect fish and benthos (these are organisms that live on, in or near the seabed, such as crabs, lobsters and clams) (Hoehn and Sizemore, 1977). When the conditions allow, the dissolved metals can precipitate out of solution as hydroxides. The formation of precipitates consumes dissolved oxygen, thereby reducing the oxygen content available for aquatic organisms. When formed, these hydroxides may coat fish body surfaces, smother eggs and cover the bottom of the stream hence making it unfit for habitation by benthic organisms (Hoehn and Sizemore, 1977).

Aluminium rarely occurs naturally in water at high concentrations, however higher concentrations can occur due to *AMD* discharges (Hem, 1970). Significant amounts of aluminium in water combined with a low pH increases the rate of sodium loss from blood and tissue resulting in death. Brown and Sadler (1989) state that the main cause of fish death in water contaminated by *AMD* is the loss of sodium ions from blood and the loss of oxygen in the tissue. If dissolved aluminium precipitates, it may accumulate in fish gills and affect their breathing (Brown and Sadler, 1989).

Iron is a common constituent of *AMD* which can also have detrimental effects on aquatic life. Water contaminated with *AMD* which contains significant levels of iron has little signs of life in it (Earle and Callaghan, 1998). If iron precipitates out of solution, the precipitate will cause almost similar effects as those caused by the aluminium precipitate; the iron precipitate will blanket the stream bottom consequently affecting both macro-invertebrates and fish. This ferric hydroxide solid greatly diminishes the total biomass of benthic organisms and thus affects the food chain. It has been found that streams that have normal pH levels but high iron concentrations have a small fish population (Koryak et al., 1972).

Manganese is also a common constituent of *AMD*. There are uncertainties concerning its toxicity on aquatic life. Regardless, of these uncertainties it is desirable to remove it from solution because like iron and aluminium, manganese hydrolysis also contributes to the total mineral acidity of *AMD* (Hallberg and Johnson, 2005):



Another metal which is commonly found in *AMD* is zinc. Zinc is toxic at relatively low concentrations; at 0.14 mg/l it affects the reproduction of *Daphnia magna* (Biesinger et al., 1986). At higher concentrations it has been observed that zinc significantly affects the blood circulation and respiration of fish (Wong et al., 1977).

2.2.3.1.2 Effect of dissolved metals on plant and animal life

Studies concerning heavy metal effects on microbial and fungal activity in soils found that copper, manganese, zinc and other metals inhibited mineralisation of nitrogen and

phosphorus in contaminated forest soils. Regression analysis indicated that copper was more important than other metals in controlling these processes. Studies reported lower fungal species diversity in soils contaminated with heavy metals. Copper was found to be more toxic to these species than other metals. This evidence suggests that while other metals in contaminated soils contributed to the observed effects, copper may be the most important in terms of toxicity (Lide, 1997).

Moreover, copper negatively influences the activity of micro – organisms and earthworms resulting in the slowing down of the decomposition of organic matter, this significantly alters soil fertility and hence the growth of plants. That is why there is very little *plant diversity* near copper-disposing factories or areas contaminated by copper rich *AMD*. Due to these effects on soil based activities, copper is a serious threat to the productivity of farmlands.

AMD also contains dissolved lead which poses a threat to plants, animals and human. In humans and other animals lead acts as a central nervous system toxin. High levels of exposure may cause brain damage. Lead exposure is also linked to blood disorders, kidney damage, miscarriages, and reproductive disorders. The World Health Organisation (WHO) has determined that certain lead compounds are carcinogenic to humans.

2.2.3.1.3 Impact of AMD Acidity

The pH of *AMD* is critical in determining its environmental impact, since the lower the pH, the more severe the potential effects of mine drainage on plants, aquatic and animal life. If the pH falls below the tolerance range, death will occur due to respiratory or osmo – regulatory failure (Kimmel, 1983). At low pH levels, hydrogen ions may be absorbed

by the body cells displacing vital sodium ions (Morris et al., 1989), which are important for normal body operation. Sodium is important in nerve and muscle function and in regulating body fluids.

AMD also affects man made structures, mainly because of its corrosive nature. The following is a quote from a 1937 report on the detrimental aspects of mine drainage; *AMD* from a coal mine had been discharged into a river: "...the acid water caused excessive corrosion of the federal navigation locks and dams, ships and barges, bridges and culverts, pipelines and plumbing. The acid, iron sulphate, and iron oxide (red water) ... caused unsightly reddish brown spots on fabrics in laundries and textile factories and scum in washbowls, sinks and tubs. The water was destructive, scale forming, and unsuitable for use in locomotive and power plant boilers, in manufacturing industries, and in municipal waterworks..." (Hodge, 1937).

2.2.3.2 Impact of solid waste precipitate produced from *AMD*

When *AMD* is neutralised, a precipitate called ochre (iron oxide and iron hydroxide) is produced. This is a fine, low density material which is orange in colour. This fine solid usually covers the river bed and thus prevents small animals that live on the bottom of the rivers (benthic organisms) from feeding, which leads to their death. This has a domino effect which drastically affects the food chain and hence results in the depletion of aquatic life. Ochre also reduces the surface area available for fish to lay their eggs hence affecting breeding (Pentreath, 1994). Ochre can also accumulate in fish gills; this may affect their respiratory system resulting in death.

Ochre is not stable, thus if it comes in contact with acidic water downstream, it will re-dissolve releasing toxic heavy metals into the water stream, thereby resulting in the pollution of a larger area (McGinness, 1999).

2.2.4 Preventing Acid Mine Drainage Formation

The best method of controlling *AMD* is stopping its formation altogether, as the axiom says “*prevention is better than cure*”, but this is not always practical. There are a number of methods that can be used for this purpose involving the separation of reactants (mine tailing, water and air) that combine in the production of *AMD* and the use of biocides which inhibit or destroy colonies of iron and sulphur oxidising bacteria. All these methods are collectively known as “source controls”. The two main drawbacks of preventative methods are the cost of implementing the methods and retrofitting them to existing plant equipment.

2.2.4.1 Flooding/sealing

The flooding and sealing of abandoned deep mines, serves to deprive the pyrite oxygen which is necessary for *AMD* formation. The dissolved oxygen present in the flooding waters (ca. 8 – 9 mg/l) will be consumed by mineral – oxidising and other micro – organisms present in the water. Atmospheric oxygen is prevented from entering the mine by sealing of the mine (Johnson and Hallberg, 2005). This method is effective where the location of all mine shafts and adits are known and where oxygen containing water does not seep into the mine.

2.2.4.2 Underwater storage of mine tailings

Underwater storage can also be used for disposing and storing mine tailings that are potentially acid producing (Li et al., 1997). Shallow water covers may be used as a way to prevent the contact of the minerals and dissolved oxygen. The effectiveness of these covers may be improved by covering the tailings with a layer of sediment or organic material. This prevents the tailings from re-suspending under the influence of wind and wave action (Johnson and Hallberg, 2005).

2.2.4.3 Land based storage in sealed waste heaps

Surface storage of reactive mineral spoils are potential sources of *AMD*. There are a number of covers used to minimise the movement of water and oxygen into these waste heaps, for example dry covers made from clay can be used (Swanson et al., 1997). Plastic covers can also be used, but these can be expensive when covering large surface areas.

2.2.4.4 Blending of mineral wastes

AMD production can be minimised or prevented by blending acid-generating and acid consuming materials, producing environmentally friendly composites (Mehling et al., 1997). For example the addition of solid-phase phosphates (such as apatite) to pyritic mine waste in order to precipitate iron (III) as ferric phosphate, thereby reducing its potential to act as an oxidant of sulphide minerals (Evangelou, 1998).

2.2.4.5 Application of anionic surfactants (Biocides)

Certain micro – organisms catalyse the production of *AMD* as stated earlier, hence in preventing the formation of *AMD* the control of these micro – organisms is important. Biocides are used to inhibit the activities of bacteria in mineral spoils and tailings.

Biocides are anionic surfactants such as sodium dodecyl sulphate (SDS), which is highly toxic to this group of micro – organisms. However, the effectiveness of biocide application has been found to only give short-term control of the problem and requires repeated applications of the chemicals (Loos et al., 1989). This is mainly because most biocides are water soluble and in running streams, they can be washed away after application.

2.2.4.6 Mine Capping

A cap refers to an overlying "impermeable" zone created through placement of compacted, fine grained soil material, combustion by-products (fly ash, fluidized bed wastes), kiln dust, or synthetic (plastic) fabric. The cap is significantly less permeable than the surrounding material. Caps restrict or prevent the infiltration of rainfall from reaching pyrite minerals in a backfilled mine, mainly from above. Capping is generally used for surface mines (Fripp et al., 2000).

2.2.5 Technologies used for treating Acid Mine Drainage

As highlighted in the previous section, inhibiting the formation of *AMD* at the source has a number of practical and economic challenges thus the alternative is to minimise the impact of already formed *AMD* on the environment. Such measures require that the *AMD* be treated to the legal discharge concentration before release into the environment.

The treatment of *AMD* can be divided into “active” and “passive” treatment processes. Active treatment involves the continuous application of alkaline material to neutralise *AMD* and precipitate the metal ions out of solution. This system requires constant maintenance and transportation of waste away from the site (Hallberg and Johnson, 2003;

McGinness, 1999). Passive treatment on the other hand usually makes use of natural and constructed wetlands which require little maintenance. While initial costs of passive treatment can be higher than active treatment, passive treatment uses processes that are not operationally intensive hence operational costs are less (Fripp et al., 2000).

2.2.5.1 Active Treatment

The most widespread method for treating *AMD* is active treatment, which involves the addition of a chemical – neutralising agent (Coulton et al., 2003). The addition of an alkaline material to *AMD* will raise its pH, accelerating the rate of chemical oxidation of ferrous iron and causing most of the dissolved metals to precipitate out as hydroxides or carbonates. Examples of alkaline materials added to *AMD* are lime, soda ash and ammonia, Table 2.2.

Typical active treatment involves *AMD* oxidation, neutralisation (adding an alkali) and sedimentation (addition of flocculants and coagulants). Oxidation is important because it introduces oxygen to *AMD* which is necessary for metal precipitation at low pH values. Neutralisation raises the *AMD* pH so that metals can precipitate out of solution as hydroxides or carbonates and the addition of flocculants leads to the production of a dense sludge which settles faster in settling ponds. High density sludge is advantageous because of reduced costs associated with disposal and storage due to reduced volume (Coulton et al., 2003).

Table 2.2 shows the chemicals that are typically used in active treatment of *AMD*.

Table 2.2: Chemicals for AMD oxidation, neutralisation and coagulation/flocculation.

Name	Chemical Formula	Comments
Oxidants		
Calcium Hypochlorite	Ca(ClO) ₂	Strong oxidant
Sodium Hypochlorite	NaClO	Also a strong oxidant
Calcium Peroxide	CaO ₂	Trapzene, an acid neutraliser
Hydrogen Peroxide	H ₂ O ₂	Strong oxidant
Potassium Permanganate	KMnO ₄	Very effective, commonly used
Acid Neutralisation		
Limestone	CaCO ₃	Used in anoxic limestone drains and open limestone channels.
Hydrated Lime	Ca(OH) ₂	Cost effective reagent, requires mixing.
Pebble Quick Lime	CaO	Very reactive, needs metering equipment.
Soda Ash Briquette	Na ₂ CO ₃	System for remote locations, but expensive.
Caustic Soda	NaOH	Very soluble, can be in solid or liquid form, but cheaper in liquid form.
Ammonia	NH ₃ or NH ₄ OH	Very reactive and soluble.
Fly Ash	CaCO ₃ , Ca(OH) ₂	Neutralisation value varies with each product.
Coagulants/Flocculants		
Alum (aluminium sulphate)	Al ₂ (SO ₄) ₃	Acidic material, forms Al(OH) ₃ .
Copperas (ferrous sulphate)	FeSO ₄	Acidic material, usually slower reacting than alum.
Ferric sulphate	Fe ₂ (SO ₄) ₃	Ferric products react faster than ferrous.
Sodium Aluminate	NaAlO ₂	Alkaline coagulant.

(Source: Skousen et al., 1998)

2.2.5.1.1 Advantages of Active treatment

Since active treatment is the most widespread method used to treat *AMD*, it must have a number of advantages, some of these are listed below:

- Effective and fast removal of acid and metals,
- Frequent process monitoring,
- Precise process control,
- Can be accommodated at small sites.

2.2.5.1.2 Disadvantages of Active treatment

There are a number of drawbacks for active treatment, these include:

- High initial capital costs,
- Chemicals used in this process are very expensive,
- Ongoing operational costs are quite high,
- The production of a bulky metal laden sludge poses a disposal challenge.

2.2.5.2 Passive Treatment

Since the early 1990s, passive treatment systems have been developed to treat *AMD*; these require only periodic maintenance, which greatly reduces long term costs. Passive treatment technologies take advantage of naturally occurring chemical and biological reactions in a controlled environment to treat *AMD* with minimal operational or maintenance cost (Gazea et al., 1996; Johnson and Hallberg, 2005). A typical passive treatment plant is shown in Figure 2.1.

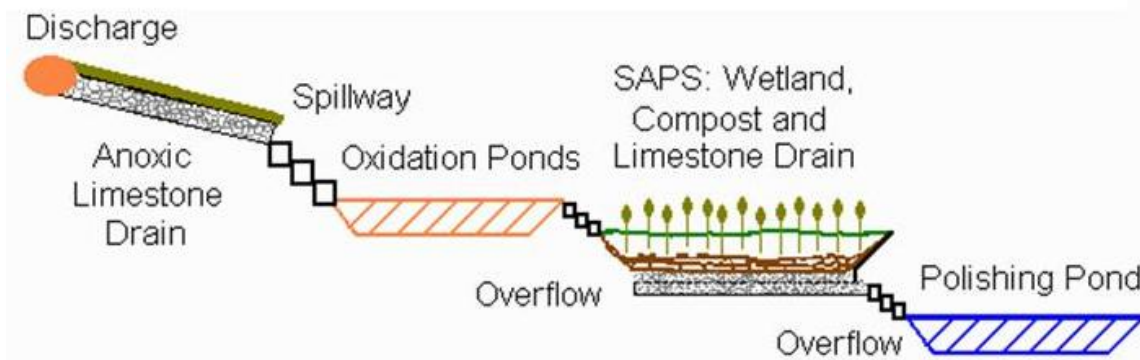


Figure 2.1: An example of a common Passive treatment system (Reprinted from: <http://www.scrip.pa-conservation.org/aboutamd.htm>).

The primary passive technologies include aerobic and anaerobic wetlands; anoxic limestone drains (ALD), limestone ponds, open limestone channels (OLC), vertical flow reactors and settling ponds. A brief description of these systems will be given in this section.

2.2.5.2.1 Anoxic limestone drains (ALD)

One method used to reduce wetland size is pre – treatment of *AMD* using anoxic limestone drains (ALD). ALDs are limestone-filled trenches that can rapidly produce bicarbonate alkalinity via limestone dissolution. They are installed at the point of discharge to capture the *AMD* subterraneously. ALDs are capped with clay or compacted soil to prevent *AMD* contact with oxygen (Hedin and Watzlaf, 1994). The acidic water flowing through the trench dissolves the limestone and releases bicarbonate alkalinity, equation [11]. ALD pre – treatment of *AMD* allows for the construction of smaller, more effective treatment systems due to the decreased metal loadings and increased alkalinity of the ALD effluent discharged into them. The effluent pH of ALDs is typically between 6 and 7.5 (Skousen et al., 1998).



The objective of these systems is to add alkali to *AMD* while maintaining the iron in its reduced form to avoid the oxidation of ferrous iron and precipitation of ferric hydroxide on the limestone (“armouring”), which otherwise would severely reduce the effectiveness of the neutralising agent (Hedin et al., 1994; Johnson and Hallberg, 2005).

2.2.5.2.2 Aerobic wetlands

Aerobic wetlands are typically designed to promote precipitation of metal oxides or hydroxides by providing the necessary residence time and aeration. Typical wetlands contain about 15 to 46 cm of water, cattails and other wetland vegetation which are capable of removing metals through oxidation reactions that form oxides or hydroxides. The cattails and microbes in the water also adsorb some metals, and the slow rate at which water moves through the wetlands allows time for precipitate and sediments to drop out. *AMD* entering these wetlands is typically mildly acidic or alkaline, containing elevated iron concentrations (Zipper and Jage, 2001).

The extent of metal removal depends on dissolved metal concentrations, exposure to air and the resulting dissolved oxygen content, pH and net alkalinity of *AMD*, the presence of active microbial biomass, and retention time of *AMD* in the wetland (Skousen et al., 1998). Metal hydrolysis does produce H^+ ions, but since the water is alkaline it buffers the pH and allows metal precipitation to continue.

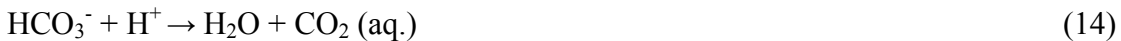
2.2.5.2.3 Anaerobic wetlands

Anaerobic wetlands are similar to regular wetlands with cattails and other typical vegetation above the water, but they have a layer of organic material along with some limestone underneath (Hedin et al., 1994). The *AMD* slowly flows down through the organic material, which can be mushroom compost, peat moss, wood chips, sawdust or even hay. Micro – organisms in the organic layer reduce sulphates, and the substrate promotes chemical and micro – organism actions that generate alkalinity and increase pH.

Anaerobic wetlands neutralise *AMD* by encouraging the generation of bicarbonate alkalinity (HCO_3^-) by both anaerobic microbial sulphate reduction [12], with CH_2O representing biodegradable organic compounds and limestone dissolution [13].



Bicarbonate then neutralises the acidity of the *AMD*, thereby raising pH [14] and increasing the precipitation of acid-soluble metals such as iron.



The main factor that limits the effectiveness of anaerobic wetlands is the slow mixing of the alkaline substrate water with *AMD* near the surface. This slow mixing can be overcome by constructing very large wetlands to provide longer retention times (Skousen et al., 1998). This demand on land area is a major drawback in the use of anaerobic wetlands.

2.2.5.2.4 Open limestone channels (OLC)

Where *AMD* must be conveyed over some distance prior to or during treatment, use of open channels lined with limestone has been shown to be an effective mechanism for removing iron and generating small amounts of alkalinity (Ziemkiewicz et al., 1997). Even though the limestone in such channels typically becomes armoured with iron, research indicates that the armoured limestone retains some treatment effectiveness. Optimum performance is attained on slopes exceeding 20%, where flow velocities keep precipitates in suspension, clean precipitates from limestone surfaces and the abrasive action of fast-moving water tends to dislodge the armouring iron. Open limestone channels can be effective as one element of a passive treatment system, but typically are not relied upon for stand-alone *AMD* treatment (Zipper and Jage, 2001).

2.2.5.2.5 Vertical flow systems

Vertical flow systems combine the treatment mechanisms of anaerobic wetlands and ALDs in an attempt to compensate for the limitations of both, also known as Successive Alkalinity Producing Systems (SAPS) (Kepler and McCleary, 1994). These systems are similar to the anaerobic wetland, but a drainage system is added within the limestone layer to force the *AMD* into direct contact with both the organic matter and the limestone.

The drainage system, a limestone layer, and an organic layer constitute the major elements of vertical flow systems. The system is constructed within a water-tight basin, and the drainage system is constructed with a standpipe to regulate water depths and ensure that the organic and limestone layers remain submerged. As *AMD* flows downward through the organic layer, two essential functions are performed: dissolved

oxygen in the *AMD* is removed by aerobic bacteria utilizing biodegradable organic compounds as energy sources, and sulphate-reducing bacteria in the anaerobic zone of the organic layer generate alkalinity. In the limestone layer, CaCO_3 is dissolved by the acidic, anoxic waters moving down to the drainage system, producing additional alkalinity. The final effluent is discharged from the drainage system standpipe into a settling pond to allow acid neutralization and metal precipitation prior to ultimate discharge.

In order to avoid clogging of the limestone layer with iron and other metal precipitates, a flushing pipe is typically included as part of the drainage system (Kepler and McCleary, 1997).

For severe *AMD* discharges, several vertical-flow systems can be linked in series to generate alkalinity successively until acceptable concentrations are reached.

2.2.5.2.6 Limestone Ponds

Limestone ponds are a new passive treatment idea in which a pond is constructed on the upwelling of an *AMD* seep or underground water discharge point. Limestone is placed at the bottom of the pond and the water flows upward through the limestone (Faulkner and Skousen 1995). The pond is sized and designed to retain the water for 1 or 2 days to allow for limestone dissolution, and to keep the seep and limestone under water. Limestone ponds are more effective when treating *AMD* with low concentrations of dissolved oxygen, iron and aluminium. Since the limestone is not buried, in the event that it is being coated by precipitate, the limestone can be periodically disturbed with a backhoe to uncover or to scrape off the precipitates. If the limestone is exhausted by

dissolution and acid neutralization, then more limestone can be added to the pond over the seep.

2.2.5.3 Other Treatment methods

2.2.5.3.1 Reverse Osmosis

This process involves the use of a semi – permeable membrane to treat *AMD*. Pressure is applied on *AMD* (which is the more concentrated solution) and it is forced through the membrane into a more dilute solution. The semi – permeable membrane only allows the passage of solvent and not solute. This leaves a more concentrated solution on the *AMD* side of the membrane. This process has a number of drawbacks which are the high cost of purchasing and operating the membrane, high pressures are needed to effect separation, high level of pre-treatment is required in some cases, and membranes are prone to fouling.

2.2.5.3.2 Adsorption

Adsorption is becoming a popular method for the removal of heavy metals from the *AMD* (Omer et al., 2003). Natural materials that are available in large quantities or certain waste products from industrial or agricultural activities may have potential as inexpensive sorbents (Bailey et al., 1999). Examples include dead biomass, blast furnace slag, fly ash, clay, bark, tea leaves and natural zeolite (Bhattacharyya and Gupta, 2006; Bailey et al., 1999).

2.2.5.3.3 Ion exchange

Ion exchange is the exchange of ions between a liquid phase and a porous solid, which may be synthetic or natural (resins or zeolites). Ion exchange is firmly established as a

unit operation in the mining industry and is an extremely valuable supplement to other procedures such as filtration, distillation, and adsorption. It is used in a wide range of applications from the recovery of metals from industrial wastes to the separation of gas mixtures and from catalysis of organic reactions to decontamination of cooling water of nuclear reactors. However, so far the most important application is the purification and demineralization of water. Ion exchange material is capable of removing base metals from *AMD* like zinc and copper (McGinness, 1999) and also raise the pH of *AMD* by adsorbing H^+ ions (Erdem et al., 2004).

2.2.5.3.4 Electrochemical technology

As the behaviour of metals in solution is often controlled by their electrochemistry, the use of electrical technologies in the treatment of *AMD* has received some attention. This process involves the use of electrical energy to drive unfavourable chemical reactions. One of the problems that may be associated with the use of such technology is its heavy dependence on a constant electrical supply (McGinness, 1999).

2.2.6 Recovery of valuable products from AMD treatment.

It is possible using some of the technologies available to extract and retain valuable metals from *AMD* and use these to offset the costs of treatment (McGinness, 1999). The basic idea behind this is to:

- Selectively concentrate certain metals from *AMD* until they reach a commercial concentration/grade which may be sold,
- Produce “grey” water from *AMD* which may have industrial use, like being used as a source water for a pump storage electricity generating facility,

- Produce a by product from *AMD* treatment that has a commercial value, and hence can be sold, for example iron oxide from *AMD* can be sold to a paint company as a pigment,
- There are also proposals to make building materials from *AMD* sludge.

All these proposals are there to offset the treatment costs by bringing revenue from by-products of *AMD* treatment. Moreover, waste from *AMD* could be a valuable secondary source of metals.

2.3 Adsorption of Acid Mine Drainage

It is clear from the previous section that there has been a growing interest in treating *AMD* and hence the need for an economic process capable of achieving the desired results. Adsorption has been found to be an effective and economic method with great potential for the removal, recovery and recycle of metals from *AMD* (Kadirvelu and Namasivayam, 2003; Chironet et al., 2003). Natural materials that are available in large quantities or certain waste products from industrial or agricultural operations may have potential as inexpensive adsorbents (Bailey et al., 1999).

2.3.1 Adsorption Process

Adsorption involves the movement or diffusion of solute molecules (adsorbate) from a bulk fluid to the surface of a solid (adsorbent), forming a distinct adsorbed phase (Richardson et al., 2002). The separation efficiency of an adsorption process depends on the selectivity and affinity of the adsorbent for a particular solute over another in the mixture (Tien, 1994).

There are two main types of adsorption processes; these are physical adsorption and chemisorption. Physical adsorption occurs when a solute is loosely bound to the solid surface usually via weak van de Waals forces or dipole interactions. Physical adsorption is generally considered fast and reversible. Chemisorption on the other hand is often associated with heterogeneous catalysis and involves the formation of strong bonds between the adsorbate and adsorbent. This bonding often results in a change in both the surface and adsorbate chemical character. Unlike physical adsorption, chemisorption is usually slow, irreversible and is associated with the liberation of significant heat of adsorption.

2.3.1.1 Characteristics of Adsorbents

The primary requirements for an economic and commercially attractive adsorbent are listed below (Ruthven, 1984; Richardson et al., 2002):

- The adsorbent must have a large internal surface area, this is mainly manifested by porous material,
- This surface area should be accessible through pores big enough to allow certain molecules passage during adsorption, that is it should be highly selective,
- The adsorbent should be mechanically strong, enough to withstand bulk handling and vessel vibrations,
- The adsorbent should be easy to regenerate,
- There should not be any rapid exhausting (that is, loss of adsorptive capacity) of the adsorbent due to continual recycling.

2.3.2 Examples of Adsorbents

There are a number of micro – porous adsorbents in use for adsorption purposes in industry; these include silica gels, activated alumina, activated carbon and molecular sieves (Ruthven, 1984; Richardson et al., 2002).

2.3.2.1 Silica Gels

Silica gel is a partially dehydrated form of polymeric colloidal silicic acid. It is formed when a silicate like sodium silicate is acidified, producing an agglomerate of micro – particles, subsequent heating expels water leaving a hard, glassy porous structure. The surface of silica gel is hydrophilic and hence its use in drying gases.

2.3.2.2 Activated Alumina

Activated alumina is a porous high surface area form of aluminium oxide, prepared either directly from bauxite ($\text{Al}_2\text{O}_3 \cdot 3\text{H}_2\text{O}$) or from the monohydrate by dehydration and re – crystallisation at elevated temperatures. The surface of activated alumina exhibits both acidic and basic characteristics, thus reflecting the amphoteric nature of aluminium metal. These also show a high affinity for water. Activated alumina is usually used for adsorption at elevated temperatures in preference to silica gel, which loses its adsorptive capacity at high temperatures.

2.3.2.3 Activated Carbon

Most coal is not porous and hence the need to activate it in order to generate a system of fine pores. This is achieved by thermal decomposition of carbonaceous material followed by activation with steam or carbon dioxide at elevated temperatures (700 – 1100 °C). Activation is simply the removal of tarry carbonisation products formed during pyrolysis,

thereby creating pores. Activated carbon is made of randomly stacked micro – crystallites of graphite, it is the spaces between these crystals that form the micropores. Activated carbon is usually used for adsorbing organic material since it tends to be organophilic.

2.3.2.4 Molecular sieves

These usually effect separation by their shape and size selectivity. Examples of molecular sieves are natural and synthetic zeolites.

2.3.3 Natural Zeolite

Zeolites are a well defined class of naturally occurring crystalline aluminosilicate minerals (Dyer, 1988). The zeolite framework consists of an assemblage of $[\text{SiO}_4]^{4-}$ and $[\text{AlO}_4]^{5-}$ tetrahedral (Figure 2.2) joined together in various regular arrangements through shared oxygen atoms, to form an open crystal lattice containing pores of molecular dimensions into which guest molecules (water and cations) can penetrate (Mortier et al., 1982).

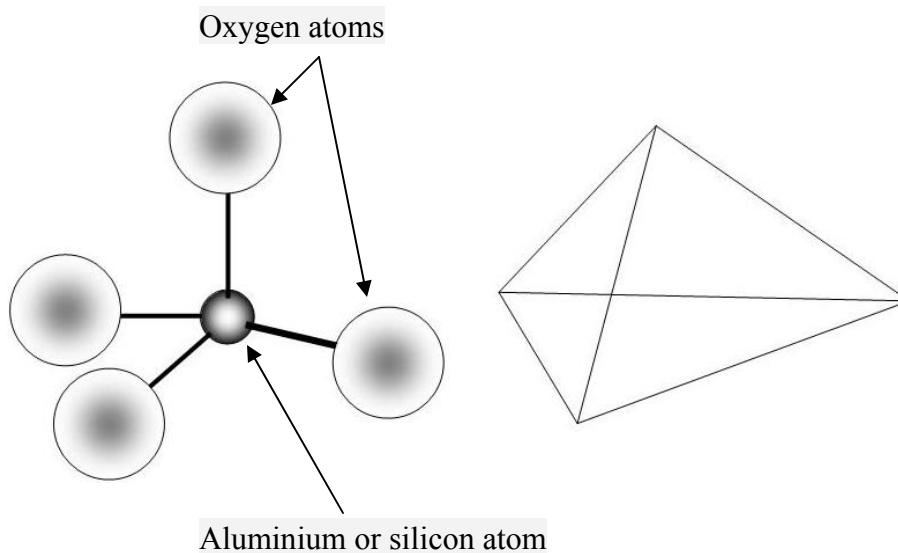


Figure 2.2: Representation of $[\text{SiO}_4]^{4-}$ or $[\text{AlO}_4]^{5-}$ tetrahedral (Dyer, 1988).

The amount of cations in zeolite is determined by the number of $[\text{AlO}_4]^{5-}$ tetrahedral in the framework, this arises from the isomorphous substitution of Al^{3+} for Si^{4+} in the structure, resulting in a net negative charge which must be counterbalanced by cations (Alvarez et al., 2003). These exchangeable cations are located at preferred sites within the framework and play an important role in determining the adsorptive capacity of zeolite.

2.3.3.1 Occurrence of Natural Zeolites

Zeolites occur in rocks of many types, ages and geological settings. Zeolites are formed by reaction of pore water with solid material. Some common solid material reactants in zeolite formation are volcanic glass (debris), montmorillonite, plagioclase, nepheline, poorly crystalline clay and quartz. Zeolites and clay can be formed from the same material, but whether it is zeolite or clay that is formed depends on the physical environment and the activities of dissolved species such as H^+ ions, alkali- and alkaline earth ions, H_4SiO_4 and $\text{Al}(\text{OH})^4$ (Sand and Mumpton, 1978). The more common zeolites are clinoptilolite, analcime, heulandite and phillipsite.

As discussed above, natural zeolites are found in a variety of geological environments mainly from volcanic debris. Some examples include the formation of zeolites by burial diagenesis, in open flowing systems, in marine deposits and in saline alkaline lakes (Dyers, 1988).

2.3.3.1.1 Zeolites from burial diagenesis

Zeolites formed from this process are also referred to as the burial metamorphic type. These have been formed as a result of their depth of burial, by subsequent layers of geologic species and the consequential geothermal gradient (Sand and Mumpton, 1978).

These conditions are associated with deep – sea and hydrothermal conditions. Zeolites formed by this process are found in certain parts of Japan and the United States.

2.3.3.1.2 Zeolites from saline alkaline lakes

Saline alkaline lakes are usually closed basins in arid and semi – arid regions which contain water with high pH levels, about 9.5. The lake water is rich in dissolved sodium carbonate-bicarbonate. Zeolites are thus formed from the reactive material deposited in the lake such as volcanic glass, biogenic silica, poorly crystalline clay and quartz (Sand and Mumpton, 1978). The most common zeolites formed in this environment are phillipsite, clinoptilolite and erionite. Such deposits are found in the western parts of the United States.

2.3.3.1.3 Zeolites from open flowing systems

When flowing water of high pH and salt content interact with vitric volcanic ash rapid crystallisation may occur resulting in the formation of zeolites. Common zeolites associated with open flowing systems are clinoptilolite, chabazite and analcime.

2.3.3.1.4 Zeolites found in marine deposits

Zeolites also occur in a number of marine sediments and sedimentary rocks and are relatively common in many strata. Zeolites may be formed at shallow depths and low temperatures. Zeolites formed in this way seem to have been formed mainly from the action of trapped salt solutions (pore fluids) on glasses of underwater volcanic origin (Dyer, 1988). The zeolites found under the Indian and Atlantic Ocean have been formed in this manner. The most dominant zeolites in marine deposits are phillipsite and clinoptilolite (Sand and Mumpton, 1978).

2.3.3.2 Framework and Structure of zeolites

As briefly described earlier, zeolites have a three dimensional framework structure arising from the joining of $[\text{SiO}_4]^{4-}$ and $[\text{AlO}_4]^{5-}$ tetrahedral. Each oxygen atom is shared between two tetrahedral Al and Si atoms; this creates infinite lattices comprised of identical building blocks (cell units) in a way typical for crystalline materials (Dyer, 1988).

It is difficult to classify zeolites based on these unit cells, hence another method to classify zeolites is based on using recurring secondary building units, Figure 2.3 (Dyer, 1988).

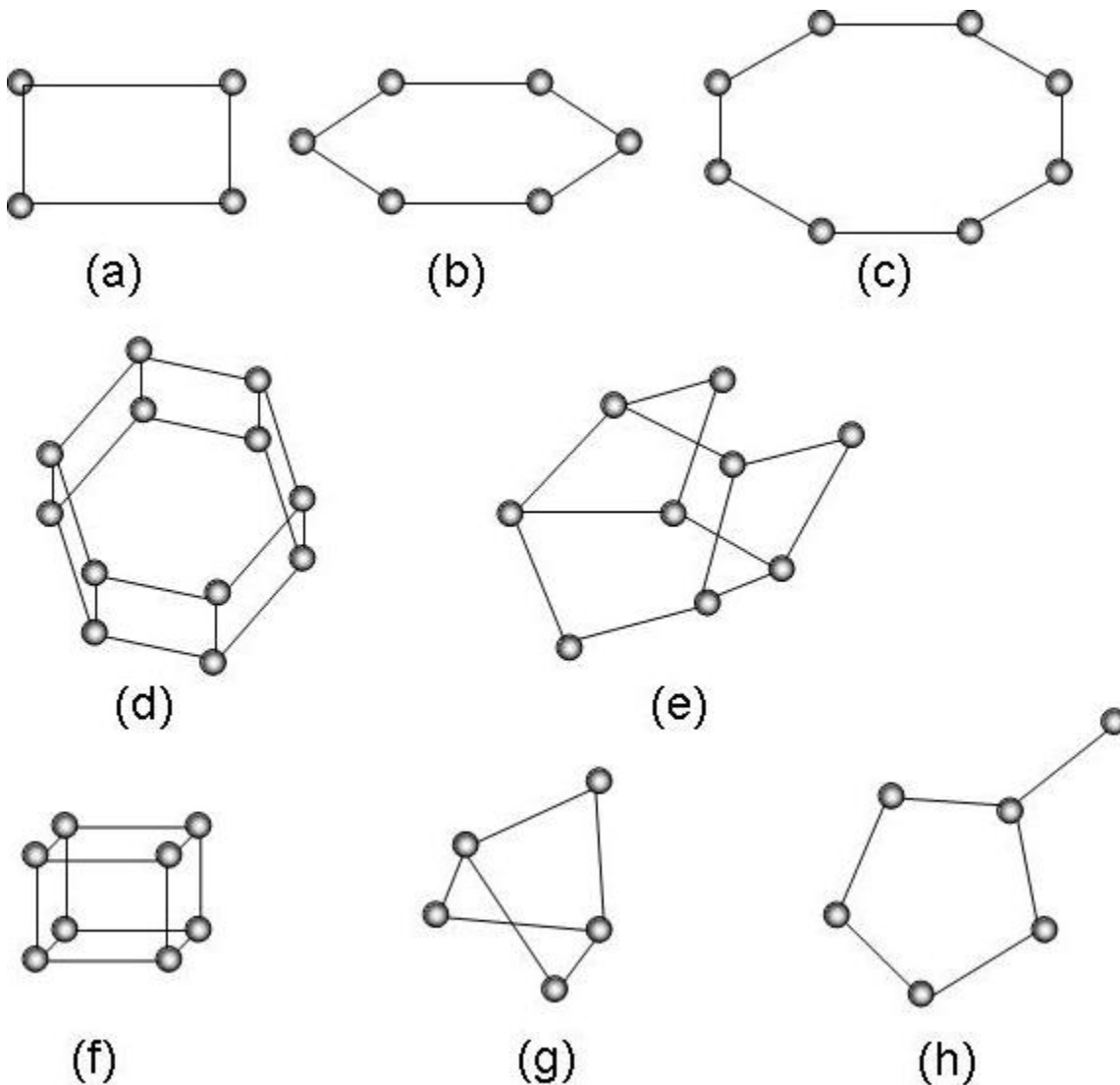


Figure 2.3: Secondary building units in zeolite frameworks; (a) single four ring (S4R), (b) single six ring (S6R), (c) single eight ring (S8R), (d) double six ring (D6R), (e) complex 4-4-1 (f) double four ring (D4R), (g) complex 4-1 and (h) complex 5-1 (Dyer, 1988).

Clinoptilolite is the natural zeolite used in this research as the low cost material for the removal of heavy metals from *AMD*. The typical price range of clinoptilolite is USD 50-70 per ton (www.gsaresources.com/smz.html; Mumpton and Fishman, 1977). Clinoptilolite is assigned to the framework (HEU) (Baerlocher et al., 2007), in which the

secondary building unit is the complex 4-4-1, as shown in Figure 2.3 (e). Clinoptilolite is regarded as the most abundant zeolite (Sprynskyy et al., 2006).

2.3.3.3 Application of Natural Zeolites

Zeolite has been used in various industries recently; this is due to its many attractive characteristics. Some of the applications will be discussed in this section.

2.3.3.3.1 In adsorption and separation processes

Zeolite contains water molecules and cations, when water is removed from zeolite, empty voids are created within its framework which can be occupied by other molecules. The occupation of these voids by other molecules (*guests*) is called adsorption.

As highlighted previously, the structural architecture of zeolite is made up of interconnected cages and channels of certain sizes (molecular dimensions), which allow certain sizes of molecules to pass through whilst excluding others, as shown in Figure 2.4. This property of zeolites, of separating mixtures of molecules (liquid or gases) on the basis of their effective size and shape, has led to their use as molecular sieves.

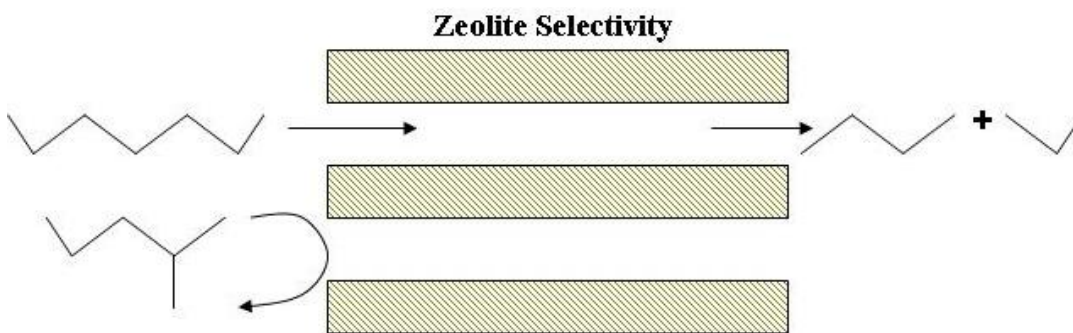


Figure 2.4: Shape selectivity in zeolite channels (Csicsery, 1985).

These properties have been utilised in areas such as the dewaxing of diesel fuels, purification of para – xylene, the removal of noxious gases from air streams (SO₂, NO₂, H₂S and HCl gases) and the separation of fructose from sucrose and other sugars.

2.3.3.3.2 In catalysis

Zeolites have been used extensively as catalysts; this is because of a number of reasons such as its micro – porous nature which gives zeolite a high surface area where reactions can take place, the shape and size of particular pore systems which exerts a steric influence on the reaction thus controlling the access of only the required reactants, Figure 2.4 above. Because of the shape selective nature of zeolite, they are sometimes referred to as *shape selective catalysts*.

Hydrogen-exchanged zeolites, whose framework-bound protons give rise to very high acidity, are used extensively in many organic reactions, including crude oil cracking, isomerisation and fuel synthesis. Zeolites account for more than 99% of the world's petrol production from crude oils (Dyer, 1988). Zeolites can also serve as oxidation or reduction catalysts, often after metals have been introduced into their framework. Examples are the use of titanium ZSM-5 in the production of caprolactam, and copper zeolites in NO_x decomposition (Bell, 2001).

2.3.3.3.3 In ion exchange reactions

The zeolite structure contains some exchangeable cations, which are readily exchanged for other types of cations from solution. This property of zeolite has been exploited in a major way in water softening, where alkali metals such as sodium or potassium prefer to exchange out of the zeolite, being replaced by the "hard" calcium and magnesium ions

from the water. Many commercial washing/laundry powders thus contain substantial amounts of zeolite. Commercial waste water containing heavy metals (for example *AMD*) and nuclear effluents containing radioactive isotopes can also be cleaned up using zeolites. The ion exchange property of zeolites is also used in controlling soil pH and nutrient levels (soil conditioning), and also as an animal feed supplement (Alvarez et al., 2003; Sand and Mumpton, 1978).

2.3.3.4 Using Natural Zeolite to treat Acid Mine Drainage

The treatment of *AMD* by natural zeolite is mainly an ion exchange reaction, where the exchangeable cations in the zeolite structure (Na^+ , Ca^{2+} , K^+ and Mg^{2+}) are displaced by heavy metal cations such as lead, copper, zinc, iron, nickel and aluminium (Barrer, 1978). The fact that cations being displaced from zeolite are relatively harmless makes zeolite attractive for the removal of undesirable and toxic heavy metal ions from *AMD* effluents.

The other factors that make natural zeolite an attractive alternative for the treatment of *AMD* are:

- Cheap since they are relatively abundant (Heping Cui et al, 2006),
- Have a favourable cation exchange capacity (CEC) (Yuan et al., 1999),
- They have good selectivity for cations (Malliou et al., 1994),
- Zeolites have a high surface area due to their porous and rigid structure (Alvarez et al., 2003),
- They also act as molecular sieves and this property can easily be modified to increase the performance of the zeolite (Sprynskyy et al., 2006),

- Zeolites have good structural stability even in acidic conditions, hence it is expected that they can easily be regenerated with little effect on their structure and adsorption capacity,
- Zeolites can neutralise acidic solutions; this is achieved through the exchange of H^+ ions from solution with the exchangeable cations in the zeolite structure (Leinonen and Lehto, 2001).

Therefore, because of these attractive characteristics there has been a growing interest in adsorbing heavy metals from solution using natural zeolite. A number of researchers have shown the feasibility of using natural zeolite to adsorb heavy metals under different experimental conditions like temperature, pH, concentration and agitation speed (Inglezakis et al., 2003; Zamzow et al., 1990; Erdem et al., 2004; Mier et al., 2001; Cincotti et al., 2006). However, the treatment of actual *AMD* has not received a lot of attention (Heping Cui et al., 2006; Wingenfelder et al., 2005; Moreno et al., 2001).

CHAPTER 3

CASE STUDY: WHEAL JANE MINE

3.1 Brief History

Wheal Jane Mine is located in the Carnon Valley area in Cornwall, United Kingdom. This region has been mined extensively for centuries. Initially mining was carried out on the surface, but as surface mineral deposits were depleted, underground mining became inevitable. A major problem with working underground is that the mine workings might eventually penetrate below the local water table resulting in mine flooding, this problem was solved initially by building a series of tunnels (adits) running out of the mine.

Wheal Jane Mine has a long history of mining activities. Tin was the major product from the mine from the mid 1700s, although other metals were mined such as zinc, copper, arsenic and silver. Around 1885 most mines around Wheal Jane were closing down because of economic hardships, Wheal Jane survived a little longer because of revenues coming from the sale of arsenic. Wheal Jane finally closed in 1895 but was re-opened in 1906 under the auspices of Falmouth Consolidated. The period from 1906 to 1969 was characterised by a number of closures and re-openings. In 1969 Wheal Jane was opened and eventually bought by Rio Tinto Zinc and mining commenced profitably for some time due to improved mining techniques and technology. In 1985 with the end of the International Tin Agreement and the subsequent collapse of world tin prices, Wheal Jane began a downward spiral and underground operations were eventually stopped in 1991.

In 1992 the failure of an adit plug (Nangiles adit) due to flooding of Wheal Jane Mine, led to the catastrophic release of acidic, heavy metal laden water (*AMD*) into the Carnon River and the Fal River/Estuary (Younger et al., 2004; Neal et al., 2004; Hallberg and Johnson, 2003), as shown in Figure 3.1. About 50 000 m³ of untreated *AMD* were released in 24 hours and subsequently the discharge rate reduced to 6 000 m³ per day for several weeks. The drop in flow-rate was due to the emergency controls enforced by the Environmental Agency.



Figure 3.1: Aerial photograph of the mouth of Restronguet Creek and Carrick Roads taken during the Wheal Jane incident [*Photograph courtesy of the Environment Agency*].

3.2 Composition of Wheal Jane Mine AMD

The legally and environmentally acceptable concentrations for heavy metals discharges were exceeded by many orders of magnitude due to this release of *AMD* into the Carnon River and the surrounding waterways.

Table 3.1 shows the water quality in the Carnon River, initially when *AMD* was discharged in 1992, the water quality in 1995 and the legal discharge concentrations from mines according to the Environmental Quality Standard (EQS). Mine discharges rather than watercourses may not have to meet EQS standards (Bone, 2003) as such metal and mine waste is dealt with on a case by case basis (Griffiths, 2005) by insurance of consent limits by regulatory bodies such as the Environmental Agency.

Table 3.1: Chemical quality of Wheal Jane mine water (AMD).

	Jan 1992 ^a	1995 ^b	EQS Values ^c	Wheal Jane consent limits ^c
pH	2.6 – 3.1	3.5	6 – 9	≤ 10.0
Aluminium	170 – 197	30	0.01-0.025	10.0
Arsenic	26 – 29	9	0.05	0.1
Cadmium	1.4 – 1.9	1	0.005	0.04
Copper	14 – 18	1.5	0.028	0.08
Iron	1720 – 1900	300	1.0	5.0
Manganese	11 – 25	12	0.03	1.0
Zinc	1260 – 1700	120	0.5	2.5

(^a Hamilton et al., 1994; ^b Dobbs – Smith et al., 1995; ^c Bone, 2003).

[All Units are in mg/l dissolved metals, except pH].

The concentrations in 1995 are drastically lower than those in 1992; nevertheless the concentrations are still higher than the legal requirement for waste water discharges into the environment, hence treatment is still required.

3.3 Treatment technologies used at Wheal Jane Mine

The treatment methods for Wheal Jane Mine *AMD* can be divided into two categories, which are; active treatment and passive treatment.

3.3.1 Active Treatment

The Environmental Agency commissioned the design and construction of an active treatment plant at Wheal Jane, which oxidised and chemically neutralised the *AMD*. The active treatment plant was based on the “Unipure” process, which consists of three stages (Brown et al., 2002):

- Mixing of the *AMD* and sludge,
- Aeration of the mixture,
- Clarification/Sedimentation of sludge.

The active treatment plant is also capable of treating water from the mine drain, supernatant from the tailings pond and effluent from the pilot passive treatment plant.

The treatment process begins with the addition of 5 % lime slurry to the *AMD*, in order to raise its pH to about 9.5. The mixture is then aerated in aeration tanks installed with a diffuser at their base. The product of the aeration tanks is pumped to the clarifiers where it is mixed with flocculants to facilitate settling. The settled sludge is about 30 – 40 % solids, this sludge is disposed of at a tailing pond (Whitehead et al., 2005). The metal removal efficiency of this process is about 99.2%.

3.3.2 Passive treatment

The Wheal Jane Mine incident in 1992 provided an opportunity to test passive treatment technologies. A pilot passive treatment plant was constructed to determine the effectiveness of this method in giving a cost effective alternative to the expensive active treatment option.

The constructed passive treatment plant consisted of three individual wetland circuits which differ only in the pre – treatment, that is, pH control of the inflowing *AMD*. The three systems incorporate a limestone treatment tank, a series of five aerobic cells, one anaerobic cell and nine rock filters (Swash and Monhemius, 2005; Whitehead et al., 2005; Hallberg and Johnson, 2003). See Figure 3.2.

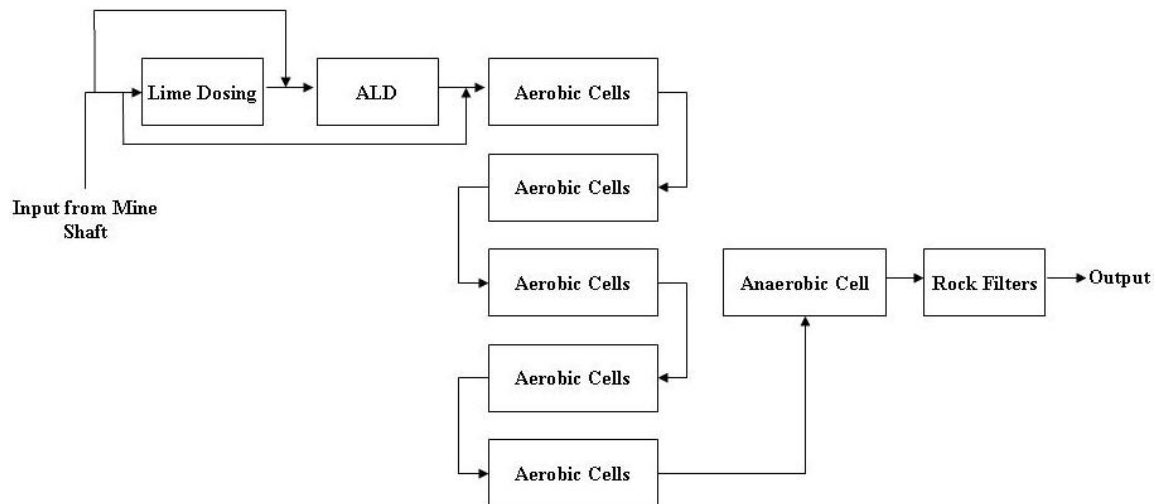


Figure 3.2: Simplified process flow diagram for the Passive treatment plant at Wheal Jane Mine (Whitehead et al., 2005).

Lime dosing is performed to raise the pH of *AMD* without the removal of excess iron. The anoxic limestone drains (ALD) were designed to remove dissolved oxygen from *AMD* so as to reduce the formation of iron hydroxide and to raise the pH of *AMD* through limestone dissolution (Whitehead et al., 2005).

The *aerobic cells* were designed to facilitate the removal of iron, through the oxidation of ferrous iron and the hydrolysis of the ferric iron produced. Iron is removed as ferric hydroxide/oxyhydroxide, with arsenic also being removed by co – precipitation and adsorption onto the iron precipitate (Hallberg and Johnson, 2003).

Anaerobic cells were constructed to remove metals such as cadmium, zinc, copper and residual iron. Removal occurs through the reaction of hydrogen sulphide and the dissolved metals to form metal sulphides.

Rock filters were also designed to promote the growth of algae, as well as the removal of manganese as an oxide, along with the reduction in biochemical oxygen demand (BOD) of the anaerobic cell effluent.

The passive treatment plant was only capable of treating 6 litres of AMD per second, which is far less than the volume needed to be treated (about 330 L/s). This meant that if passive treatment was to be employed more land had to be used, but the land area available in the Carnon Valley was not adequate to accommodate a full scale passive treatment plant (Environmental Agency, 2007). Moreover, passive systems are generally less controllable and consistent than active treatment plants. Therefore, the active treatment plant is the main method for treating Wheal Jane AMD.

3.4 Conclusion

In this study, as mentioned earlier, Wheal Jane Mine will be used as a case study. The acidic solutions produced at this mine will be collected/sampled and contacted with natural zeolite under different conditions in order to determine the potential of natural zeolite as a low cost adsorbent for treating AMD.

CHAPTER 4

MATERIALS AND METHODS

4.1 Introduction

This chapter describes in detail the methods and materials used in the determination of natural zeolite as a potential adsorbent in AMD treatment. Some of the methods used include kinetic studies, equilibrium studies, the effect of thermal pre-treatment of adsorbent, effect of initial solution pH and column studies. The preparation and analysis of different solutions used in this research is also discussed; these solutions simulate, in terms of concentration and pH, those in Wheal Jane AMD.

4.2 Materials and Sample Preparation

4.2.1 Synthetic solutions and other chemicals

Synthetic single component solutions of Fe^{3+} , Cu^{2+} , Mn^{2+} and Zn^{2+} were prepared from analytical grade $\text{Fe}_2(\text{SO}_4)_3 \cdot 5\text{H}_2\text{O}$, $\text{CuSO}_4 \cdot 5\text{H}_2\text{O}$, $\text{MnSO}_4 \cdot 4\text{H}_2\text{O}$ and $\text{ZnSO}_4 \cdot 7\text{H}_2\text{O}$ respectively (Fisher Scientific, UK). The required metal concentrations were 400, 120, 20 and 20 mg/l of Fe^{3+} , Zn^{2+} , Cu^{2+} and Mn^{2+} respectively; these simulate the respective metal concentrations in actual AMD from Wheal Jane Mine (McGinness, 1999). The pH was adjusted to 3.5 ± 0.1 using sulphuric acid.

Sulphuric acid was used for all the desorption tests in this research; the acid concentration used was 2 % (wt) H_2SO_4 . Sulphuric acid was also used to clean all the vessels used in order to remove residual metals on their surfaces. Sodium chloride (NaCl) solution, 20 g/l was also prepared and used in desorption tests.

Synthetic acid mine drainage, *sAMD*, was prepared by mixing 400 ± 5 , 120 ± 5 , 20 ± 1.5 and 20 ± 1.5 mg of Fe^{3+} , Zn^{2+} , Cu^{2+} and Mn^{2+} in a litre of distilled water. The solution pH was adjusted to 3.5 ± 0.1 using sulphuric acid. The synthetic solution was used to observe the behaviour of each cation in the presence of competing cations, that is, the other 3 cations.

Real AMD from Wheal Jane mine was collected in 25 litre bottles and sealed. The real AMD was used to determine the effectiveness of natural zeolite in treating actual AMD.

Standard solutions for metal analysis using the atomic absorption spectrometer (AAS) were prepared from standard metal solutions from Fischer Scientific. The range of standards used was 0.1, 0.25, 0.5, 1, 2 and 5 mg/l.

4.2.2 Characterisation of Natural Zeolite

In this study natural zeolite (clinoptilolite) samples from Turkey were used, and these were supplied by IMERYS Minerals Ltd, UK. The samples were used in their natural state (“as received”) with no chemical modifications, unless stated. The natural zeolite samples were washed with distilled water to remove dust from their surfaces before use.

4.2.2.1 Adsorbent Particle size

The particle size distribution of the samples was determined using sieve screens. The sieves were mechanically vibrated using a vibratory shaker for about 15 minutes which was sufficient for separation to take place. The particle size range of the natural zeolite used in this study was 1 to 3 mm, unless stated otherwise.

4.2.2.2 Scanning Electron Microscopy (SEM)

The surface morphology of natural zeolite was studied using a scanning electron microscope, Philips XL-30 Environmental SEM-FEG. This particular microscope is also fitted with an Oxford Inca 300 EDS system. EDS, stands for Energy Dispersive Spectroscopy; it is an analytical technique used for the elemental analysis of a sample.

The samples were carbon coated in a vacuum chamber in order to make them conductive, to enable better scanning and analysis. The carbon coating is very thin; otherwise the definition of the sample will be compromised. Samples were placed on a brass disc/stage using sticky carbon tape. The carbon coating of the samples and the sticky carbon tape were used to prevent the accumulation of surface charge on the sample during analysis. Samples were placed into a vacuum chamber of the microscope and analysed using different magnifications.

Samples that were analysed using SEM are natural zeolite and thermally pre-treated zeolite. The Inca scanning software was used to study the samples' surface morphology and for data analysis.

4.2.2.3 X-Ray Diffraction and X-Ray Fluorescent

Mineralogical analysis of the natural zeolite samples was carried out using X-Ray Diffraction (*XRD*). Chemical analysis to determine the chemical composition of the samples was obtained by X-Ray Fluorescence (*XRF*) these two analytical procedures were carried out by the supplier of the natural zeolite samples, IMERYS Minerals Ltd, UK.

4.2.2.4 Surface area (BET)

Surface area measurements for the natural zeolite and thermally pre – treated zeolite were determined by Nitrogen adsorption fitted to the BET equation (Brunauer, 1943), using the TRISTAR 3000 apparatus from Micromeritics. These tests were also carried out by IMERYYS Minerals, Ltd.

4.2.2.5 Other physical characteristics

Other physical properties namely porosity, moisture content and density of the natural zeolite samples were measured. The density of natural zeolite was determined using a helium gas pycnometer from Micromeritics, model AccuPyc II 1340. The porosity of natural zeolite was measured using a mercury porosimeter, Micromeritics, AutoPore (IV).

4.3 Experimental Procedure

4.3.1 Batch Adsorption Studies

Batch adsorption tests were carried out using different amounts of zeolite mixed with solutions containing the desired concentration of heavy metal ions. The mixtures were agitated in 300 ml plastic bottles over a tumbling mill at 110 rpm unless stated otherwise.

4.3.1.1 Kinetic Studies

The mass of zeolite used was 3.7, 7.5, 15 and 30 g in a constant volume (100 ml) of synthetic solution containing different metal ions, at different concentrations (20 to 400 mg/l). The agitation time was varied from 15 – 360 min, in the following intervals: 15, 30, 45, 60, 120, 180, 240, 300 and 360 min. The sorption experiments were carried out in duplicates in order to observe the reproducibility of the results, and the mean value was used. The deviation between duplicate samples in analysing the cations was $\pm 6.6\%$, 6.5% , 5.7% and 6.6% for Fe^{3+} , Cu^{2+} , Mn^{2+} and Zn^{2+} respectively.

4.3.1.1.1 Effect of adsorbent particle size

The effect of adsorbent particle size on the kinetics of the process was also investigated. Three different sizes were used; $20 \mu\text{m} < d_p < 180 \mu\text{m}$, 1 – 3 mm and 5.6 – 6.7 mm. 15 g of adsorbent at the required particle size was mixed with 100 ml solution of the appropriate single component solution for 360 minutes and samples were collected at regular intervals and analysed.

4.3.1.1.2 Effect of adsorbent mass

Three different masses were used in this study, 3.7, 7.5 and 15 g of natural zeolite in 100 ml solution. The mixture was agitated for 360 minutes and samples taken at regular intervals for AAS analysis. The particle size of the dry zeolite samples used was 1 – 3 mm.

4.3.1.1.3 Effect of initial solution pH

The solution pH was varied as follows: 2.5, 3.5 and 4.5 ± 0.1 for the single component solutions. Solution pH was adjusted using 2 % (wt) H_2SO_4 . 100ml of the single component solution was contacted with 3.7 g of natural zeolite for 360 minutes. The change in solution pH as the reaction proceeded was measured using the Hanna PH211 pH meter.

4.3.1.1.4 Effect of initial solution concentration

The effect of initial metal concentration on the removal of the cations from solution by zeolite was investigated using single component solution concentrations ranging from 10 – 800 mg/l. 100 ml solutions at pH 3.5 were contacted with 3.7 g of zeolite samples of size 1 – 3 mm. The experiments were run for 360 minutes.

4.3.1.1.5 Effect of agitation

Agitation or mixing of the solution and zeolite was carried out using two methods. The first method was agitation in a beaker using a stirrer at different speeds (190 – 390 – 645 rpm) and the second was carried out in 300 ml bottles over a tumbling mill rotating at a speed of 110 rotations per minute. 3.7 g of natural zeolite was mixed with 100 ml solution for 360 minutes and samples were collected at regular intervals and analysed.

4.3.1.1.6 Effect of competing cations

Acid mine drainage normally contains more than one cation, it is a mixture of different cations for example Fe^{3+} , Cu^{2+} , Mn^{2+} , Zn^{2+} , Pb^{2+} , Cr^{3+} etc. Tests were performed to investigate the influence of the presence of other cations on the adsorption capacity of natural zeolite for each of the cations under investigation in this study. Multi-component solutions containing equal concentrations of Fe^{3+} , Cu^{2+} , Mn^{2+} and Zn^{2+} were made and contacted with natural zeolite for 360 minutes. Two initial concentrations of the multi – component solutions were made, that is, 40 and 120 mg/l for each metal, at a pH of 3.1 ± 0.1 . The initial concentration of one of the solutions was 40 mg/l for each metal ion and hence the total metal concentration was 160 mg/l; and for the initial concentration of 120 mg/l for each ion, the total metals concentration in that solution was 480 mg/l.

4.3.1.1.7 Thermal pre – treatment of adsorbent

Thermal pre – treatment of natural zeolite was carried out using two processes:

- Heating in an air atmosphere muffle furnace for 30 minutes at 200, 400 and 800°C and,
- Exposing the natural zeolite to microwave energy of 2.45 GHz at 950 W for 15 and 30 minutes in an air atmosphere.

The thermally modified natural zeolite samples, 3.7 g, were then contacted with single component solutions, 100 ml, for 360 minutes. Agitation was carried out using a tumbling mill.

4.3.1.2 Equilibrium Adsorption Isotherms

Equilibrium isotherm experiments were conducted by mixing 3.7 g of natural zeolite with 100 ml single component solutions. The range of initial metal concentration was from 10 – 800 mg/l. The solutions prepared were at three different initial solution pH levels, which are, 2.5, 3.5 and 5.7 ± 0.1 . The particle size of adsorbent used was 1 – 3 mm. The mixtures were agitated for 360 minutes, until equilibrium was reached and then the solution was filtered and analysed using the AAS.

4.3.1.3 Desorption

15 g of natural zeolite was mixed with single component solutions, 200 ml, of Fe^{3+} , Cu^{2+} , Mn^{2+} and Zn^{2+} and agitated for 360 minutes. The mixture was filtered and solution analysed using the AAS. The solids loaded with the different metals were washed using distilled water and dried in an oven.

The dried metal loaded solids from the adsorption tests above were then mixed with 200 ml solution of desorption reagent for 180 min. Samples were collected at regular intervals, 5 – 180 minutes. Two different desorption reagents were used in this study: H_2SO_4 at a concentration of 2 % (wt) and $\text{pH} \approx 0.75 \pm 0.1$ and NaCl at a concentration of 20 g/l and $\text{pH} \approx 5.5$. Desorption experiments were carried out at 22 and 40 ± 2 °C.

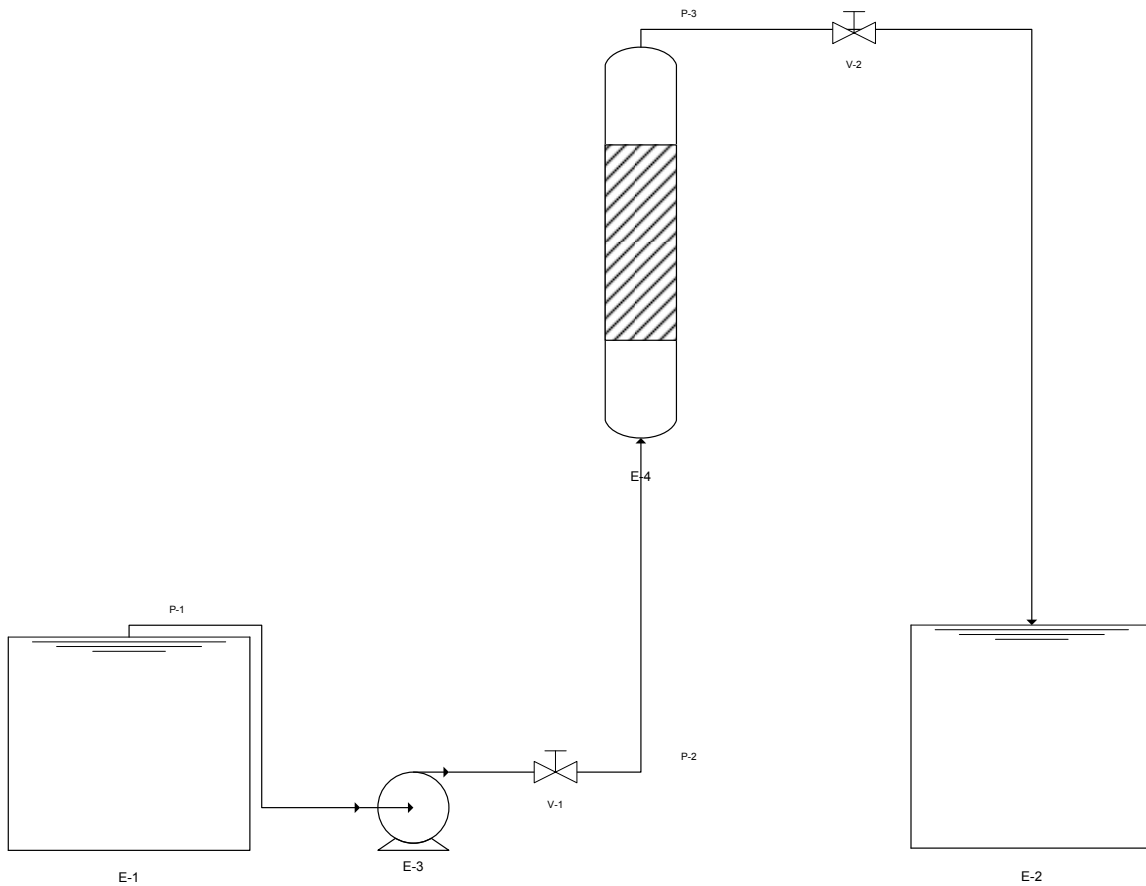
4.3.1.4 Treatment of synthetic acid mine drainage, *sAMD*

The objective of this study is to treat acid mine drainage. Thus synthetic solutions containing a mixture of Fe^{3+} , Cu^{2+} , Mn^{2+} and Zn^{2+} at 400, 20, 20 and 120 mg/l respectively were prepared (these concentrations are similar to the ones in AMD produced at Wheal Jane Mine (McGinness, 1999)). 100 ml of the solution was contacted

with 3.7 g of natural zeolite for 360 minutes. After the desired contact period the mixture was filtered and the filtrate was analysed using the AAS.

4.3.2 Column Studies

Fixed bed column experiments were carried out in laboratory scale Plexiglas columns of inside diameter 4.4 cm and 52.2 cm height, as shown in Figure 4.1 below. The column had wire mesh at both ends (inlet and outlet) to prevent adsorbent particles from flowing out of the column.



Vessel Catalogue:

E-1 and E-2:	Solution storage tanks (25 L),
E-3:	Watson Marlow peristaltic pump,
E-4:	Fixed bed column, packed with natural zeolite,
V-1 and V-2:	Control valves,
P-1, P-2, and P-3:	Connecting pipelines.

Figure 4.1: Schematic diagram of the column set – up.

The solutions were fed into the column in an upward flow motion using a peristaltic pump (Watson Marlow 502S). Upward flow was preferred because it insures that there is total coverage of the adsorbent by the solution and it also prevents the formation of channels during the column's operation (Harland, 1994).

These experiments were conducted in order to examine the uptake of Fe^{3+} , Cu^{2+} , Mn^{2+} and Zn^{2+} from their single component solutions under a number of operating conditions such as different volumetric flow rates and bed heights. The effect of competing cations was also investigated. The solution leaving the top of the column was collected at regular intervals and analysed using the AAS.

4.3.2.1 Effect of flow rate

The effect of flow rate on the uptake of heavy metals from solution by natural zeolite was investigated using 3 flow rates, 20, 50 and 80 ± 2 ml/min. Single component solutions of Fe^{3+} , Cu^{2+} , Mn^{2+} and Zn^{2+} were pumped through the fixed bed of natural zeolite each with an initial concentration of 400, 20, 20 and 120 mg/l respectively. The column bed height for each experiment was 15 cm. The experiments were run for about 600 minutes.

4.3.2.2 Effect of bed height

Iron and zinc were used to investigate the effect of bed height on the adsorption of these metals from their solutions. The breakthrough curves for these cations were obtained at two different bed heights, 15 and 50 cm. The initial concentration of iron was 400 ± 5 mg/l and that of zinc was 120 ± 5 mg/l. The solution flow rate was kept constant at 20 ± 2 ml/min for both metals. The experiments were run for about 600 minutes.

4.3.2.3 Treatment of synthetic AMD

Synthetic acid mine drainage, *sAMD*, was made using metal ion concentrations that simulate real acid mine drainage, that is, a mixture of Fe^{3+} , Cu^{2+} , Mn^{2+} and Zn^{2+} at 400, 20, 20 and 120 mg/l respectively. This solution was pumped in an up flow mode into the column at a flow rate of 20 ml/min. The bed height used was 50 cm. The experiments were run for approximately 600 minutes.

4.3.2.4 Desorption Studies

Column desorption tests were only carried out using solids that were used in treating synthetic acid mine drainage, *sAMD* (see *section 4.3.2.3* above). The flow of regenerating reagent was in the same direction as the loading solution, that is, up flow mode. This is called co – flow regeneration. Sulphuric acid, that is, 2 % (wt) H_2SO_4 at 40 ± 2 °C (which was the regenerating reagent), was pumped at 20 ml/min for 180 minutes through the 50 cm column bed. Samples were collected at regular intervals and analysed using the AAS.

4.3.3 Treatment of AMD from Wheal Jane Mine

The treatment of actual AMD from Wheal Jane Mine was carried out using two main methods, these are batch and continuous.

4.3.3.1 Batch Experiments

Experiments using real AMD from Wheal Jane Mine were carried out. Natural zeolite, thermally pre – treated zeolite and synthetic zeolite were used to treat real acid mine drainage under different conditions:

- Natural zeolite (20, 30 and 50 g) was contacted with 100 ml of real AMD for 360 minutes; this mixture was not agitated, it was left standing,

- 20 g of thermally pre – treated zeolite samples and natural zeolite, were separately mixed with 100 ml of real AMD and the respective mixtures were agitated for 360 minutes,
- A comparison between the efficiencies of natural and synthetic zeolite in treating real AMD was carried out; this was done by contacting 30 g of natural zeolite with 100 ml of AMD and 3.7 g of synthetic zeolite with 100 ml of real AMD for 360 minutes.

All samples were collected at regular intervals and analysed using the AAS. The pH of real AMD was about 2.48 ± 0.1 .

4.3.3.2 Continuous Experiments

A fixed column, as described earlier, Figure 4.1, was used to treat real AMD from Wheal Jane Mine. The bed height was 50 cm, flow rate 20 ml/min and flow during adsorption was upward. Adsorption was carried out at 22 ± 2 °C. Solutions exiting the column were collected at regular intervals and analysed using the AAS.

The adsorbent was washed with distilled water and regenerated after every adsorption stage using 2 % (wt) H₂SO₄ at 40 ± 2 °C. Co – flow regeneration was used in this study. *Co – flow Regeneration* is when the solution flow in both the adsorption and desorption stage are in the same direction, in this case up flow mode.

4.4 Sample Analysis

Samples collected from the different experiments were analysed using an atomic absorption spectrometer (AAS), [Model 751, Instrumentation Laboratory, USA]. The AAS uses an air – acetylene flame and single element hollow cathode lamps. The

samples were prepared for analysis by adding 2 % (wt) sulphuric acid to insure that any precipitate is dissolved. The AAS is generally used to analyse relatively low metal concentrations and hence dilution of some of the samples was necessary. The AAS was calibrated using standard solutions of the respective metals in the range 0.1 – 5 mg/l. Distilled water was used for all dilution purposes. The deviation between two duplicate samples when analysing for iron, copper, manganese and zinc was \pm 6.6%, 6.5%, 5.7% and 6.6% respectively. A detailed explanation of how the AAS works is given in Appendix A.

CHAPTER 5

CHARACTERISATION OF NATURAL ZEOLITE

5.1 Introduction

The stability, chemical reactivity and physical strength of many materials are affected by the size distribution and shape/structure of their particles, hence the importance of characterising the particles. The characterisation of natural zeolite is undertaken in this chapter. Particle characterisation reveals information on the physical and chemical nature of natural zeolite particles, which is related to its ability to remove heavy metal ions from solution.

Different analytical techniques were used in this study; these include scanning electron microscopy (SEM), X – Ray diffraction (XRD), X – Ray fluorescence (XRF), energy dispersive spectroscopy (EDS) and surface area determination using BET (*BET* stands for Brunauer, Emmett, and Teller, the three scientists who optimized the theory for measuring surface area (Brunauer et al., 1938)).

5.2 Scanning Electron Microscopy (SEM)

A scanning electron microscope (SEM) was used to observe the sample surface. The SEM is an instrument that produces a largely magnified image by using electrons instead of light to form an image. A beam of electrons is produced at the top of the microscope by an electron gun. The electron beam follows a vertical path through the microscope, which is held within a vacuum. The beam travels through electromagnetic fields and lenses, which focus the beam down onto the sample. Once the beam hits the sample, electrons and X-rays are ejected from the sample. The electrons interact with the atoms that make up the sample producing signals that contain information about the sample's surface morphology and topography and composition. Detectors collect these X – Rays, backscattered electrons, and secondary electrons and convert them into a signal that can be displayed as a greyscale SEM image on a computer.

5.2.1 Results and discussion of characterisation using SEM

Micrographs of “as received” natural zeolite samples obtained from SEM analysis are given in Figure 5.1. The micrographs clearly show a number of macro-pores in the zeolite structure ($1\ \mu\text{m} \leq d_{\text{pore}} \leq 2\ \mu\text{m}$). The micrographs also show well defined crystals of clinoptilolite; these “plate” like structures are well defined in samples that have been acid washed, as shown in Figure 5.2.

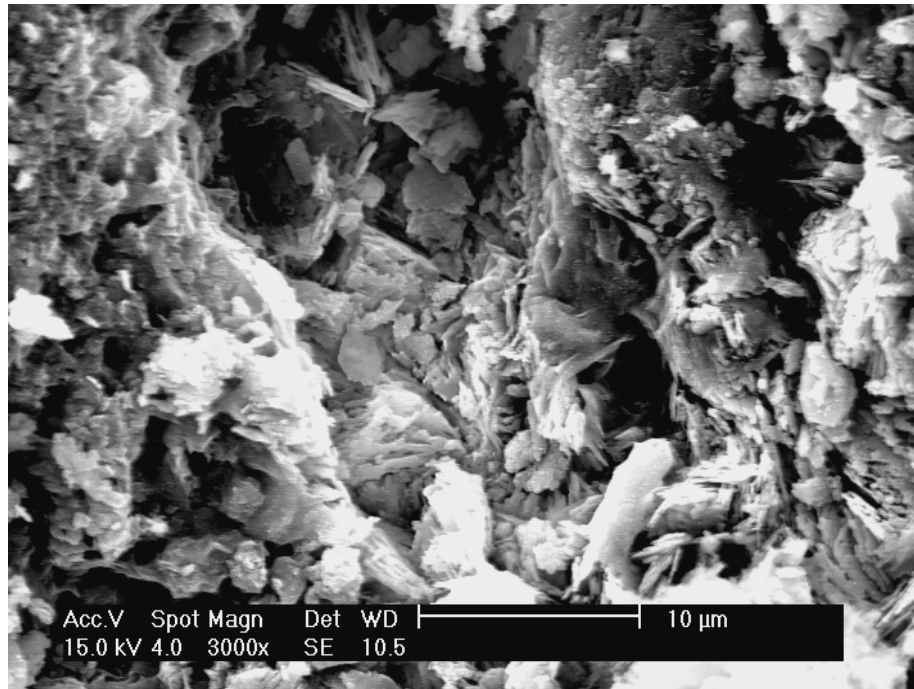


Figure 5.1: SEM micrograph of natural zeolite (Clinoptilolite) at a magnification of x3000; the natural zeolite was washed in distilled water.

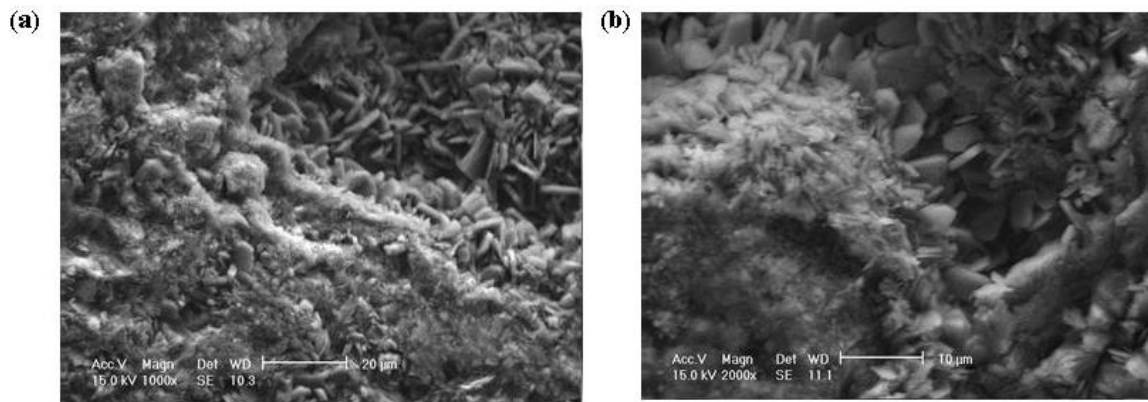


Figure 5.2: SEM micrographs of acid washed natural zeolite (Clinoptilolite) at different magnifications: (a) x 1000 and (b) x 2000.

Acid washing the zeolite removes all dust particles, unwanted waste material from the zeolite surface, leaving a clean surface and well defined crystal structures.

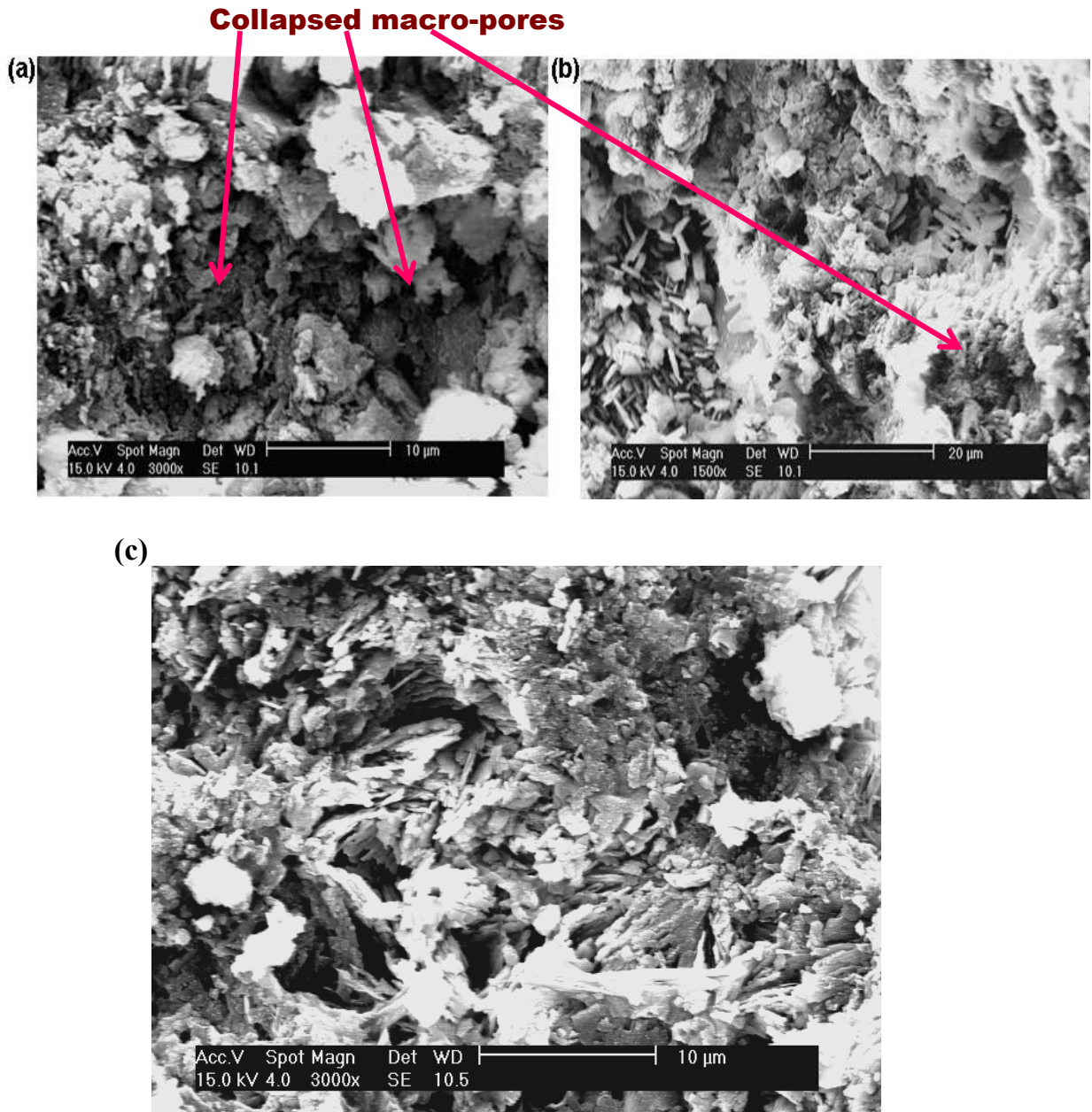


Figure 5.3: SEM microstructure of unwashed natural zeolite thermally pre – treated in a muffle furnace for 30 minutes at (a, b) 400 °C (c) 200 °C.

Figure 5.3 (c) shows that there is not much difference between the microstructure of natural zeolite and natural zeolite that has been pre – treated at 200 °C. Figure 5.3 (b) shows some well defined clinoptilolite crystals but these are within macro – pores or at the entrance of macro – pores in the zeolite particle. The surface crystals are shown to

have lost their crystalline structure due to direct heating at 400 °C; this can be clearly seen in Figure 5.3 (a), which is a micrograph (x 3000 magnification) of natural zeolite that has been pre – treated at this temperature. The macro – pores on the natural zeolite structure seem to have slightly collapsed.

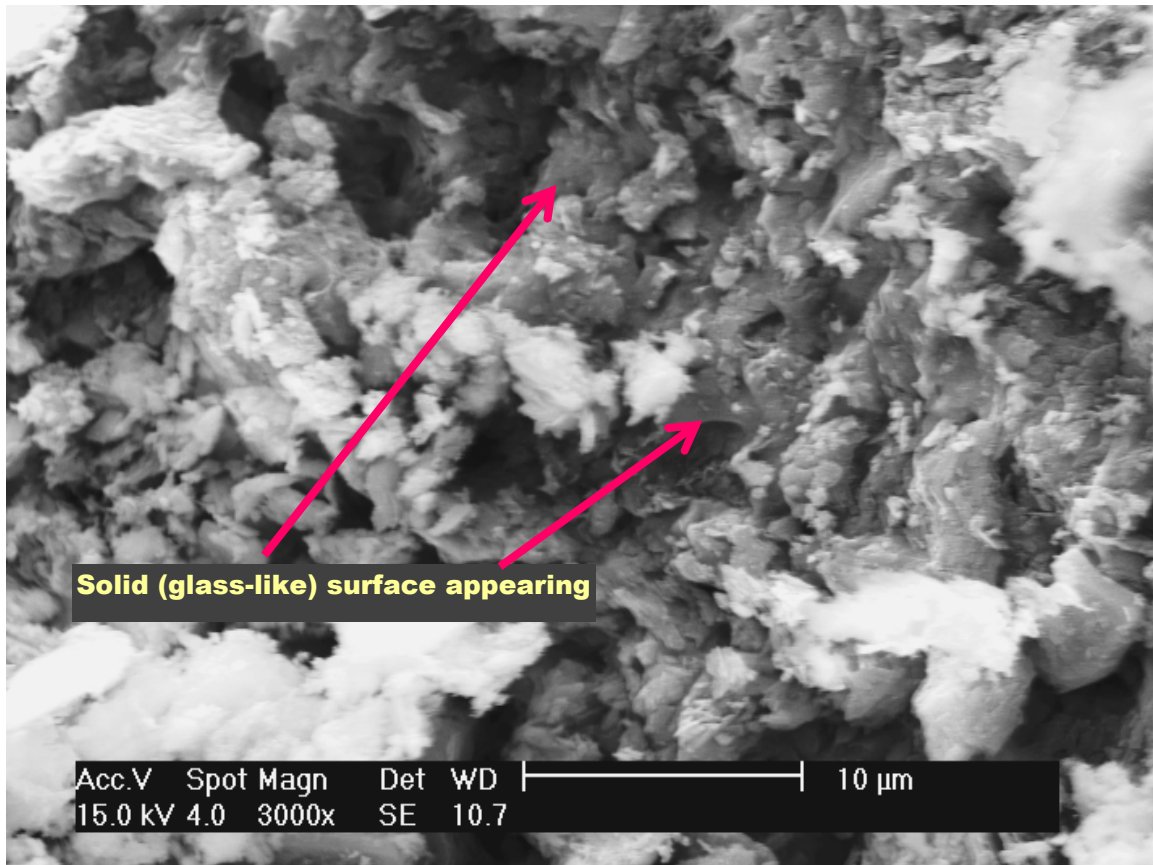


Figure 5.4: SEM microstructure of natural zeolite thermally pre – treated in a microwave for 15 minutes.

Figure 5.4 shows that the zeolite structure is still porous, but the distinct crystal structures of clinoptilolite have disappeared, that is, the “plate” like structures. A more solid non porous surface is appearing on the zeolite, this may be a result of the collapse of some macro – pores and crystals due to microwave heating.

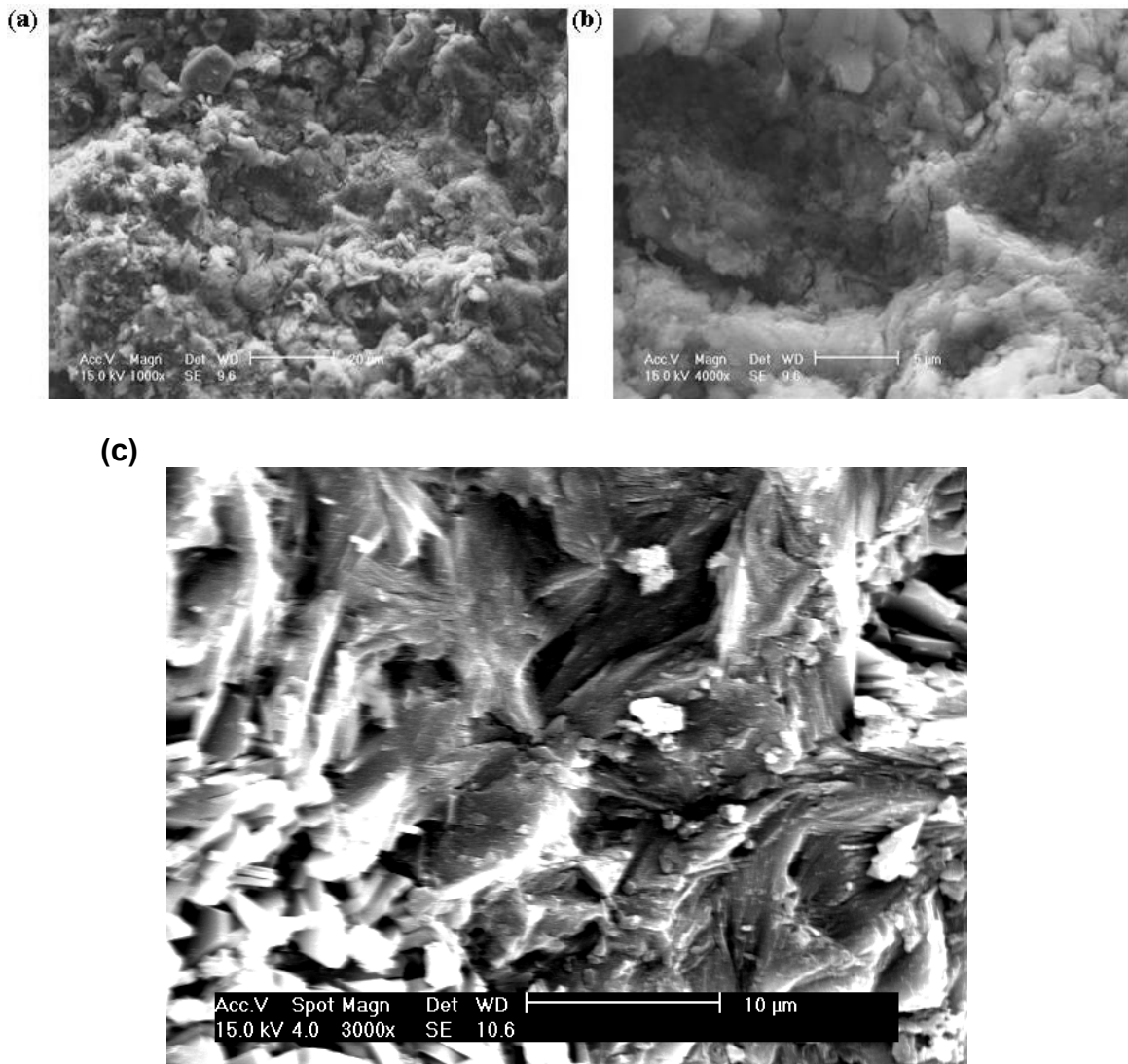


Figure 5.5: Micrographs of thermally pre – treated natural zeolite at *i.* 800 °C (a, b) and *ii.* 30 minute exposure to microwave energy at 950 W, (c).

The SEM micrographs in Figure 5.5 show natural zeolite which has partially lost its porosity due to thermal runaway. Thermal runaway occurs when an exothermic reaction goes out of control, leading to a destructive result. The samples heated at 800 °C, show an almost solid surface, with virtually no macro – pores, only cracks appear where macro – pores and crystals used to be. Figure 5.5 (c), shows how microwave radiation had a negative impact on the structure of natural zeolite. The “plate like” crystals of

clinoptilolite have almost disappeared due to partial melting and adherence to each other (sintering) producing a more glass like solid surface.

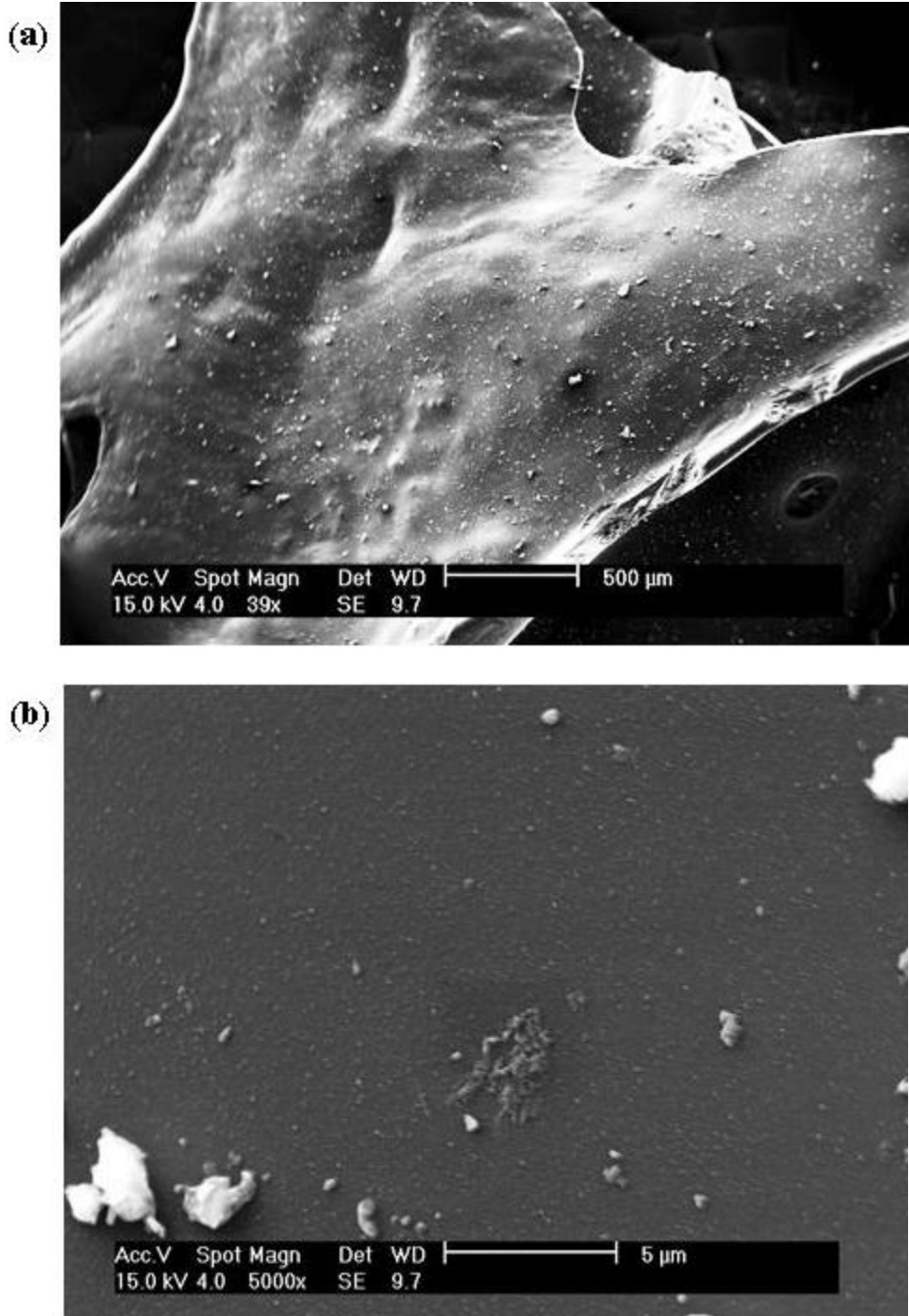


Figure 5.6: SEM microstructure of natural zeolite whose macro – pores have completely collapsed due to thermal runaway, (a) x39, (b) x5000.

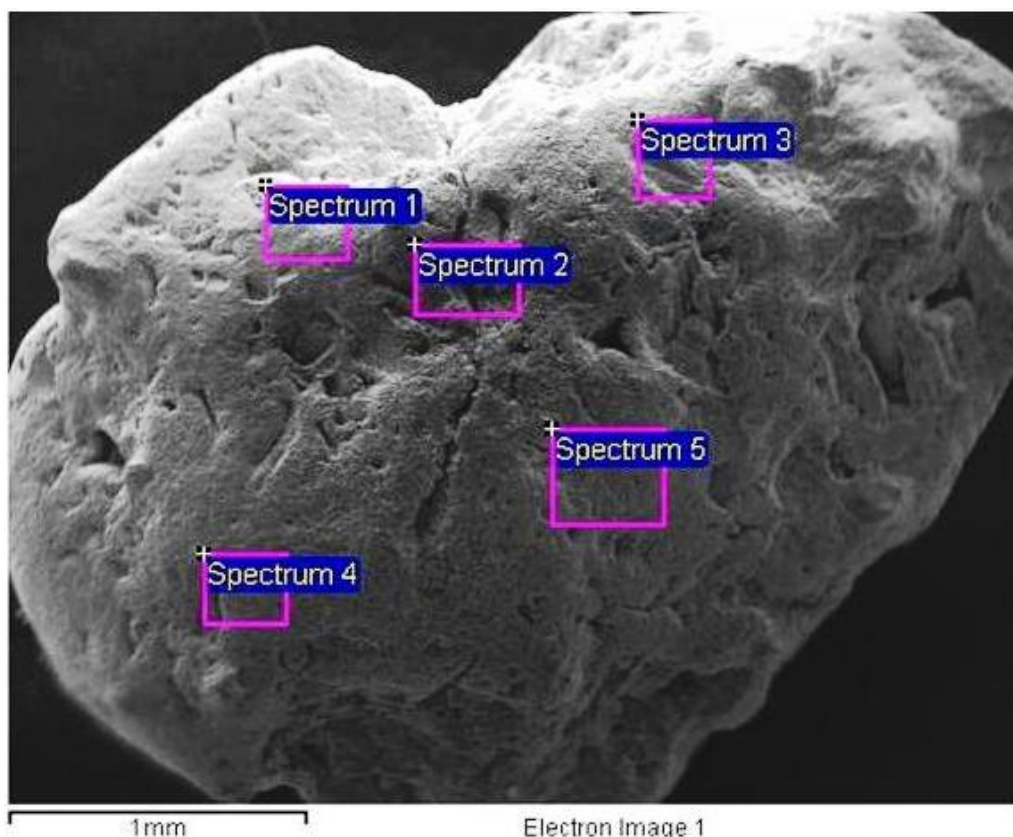
The sample shown in Figure 5.6 was exposed to extreme thermal conditions, that is, more than 30 minutes exposure to microwave radiation/energy. The zeolite structure completely collapsed and a solid glass like material was formed.

5.3 Energy Dispersive Spectroscopy (EDS)

The scanning electron microscope used in this study was also fitted with an EDS system, which means it could also perform energy dispersive spectroscopy. EDS is an analytical technique used to identify the elemental composition of a sample based on the emission of characteristic X – Rays by the sample when subjected to a high energy beam of charged particles such as electrons or protons (Goldstein et al., 2003).

5.3.1 Energy dispersive spectroscopy (EDS) results

An electron beam was directed onto different parts of the samples in order to get a more accurate analysis. Figure 5.7 shows how the different parts of the sample were analysed and the elemental composition of natural zeolite (clinoptilolite).



Spectrum	O	Na	Mg	Al	Si	K	Ca	Fe	Total
Spectrum 1	52.30	0.62	0.77	7.20	32.98	3.35	1.80	0.98	100.00
Spectrum 2	50.40	0.55	0.72	6.53	36.23	2.96	1.71	0.89	100.00
Spectrum 3	50.41	0.58	0.79	6.42	36.59	2.77	1.60	0.84	100.00
Spectrum 4	51.05	0.57	0.76	6.41	35.60	2.79	1.61	1.22	100.00
Spectrum 5	51.86	0.58	0.88	6.94	34.85	2.50	1.45	0.95	100.00
Mean	51.20	0.58	0.78	6.70	35.25	2.87	1.63	0.97	100.00
Std. deviation	0.85	0.03	0.06	0.35	1.43	0.31	0.13	0.15	

Figure 5.7: EDS analysis showing the elemental composition and the scanning method for natural zeolite.

Results of EDS analysis showed that the predominant exchangeable cations in natural zeolite (clinoptilolite) structure were Na^+ , Mg^{2+} , K^+ and Ca^{2+} .

5.4 X – Ray Diffraction

About 95% of all solid materials can be described as crystalline. When X – Rays interact with a crystalline substance, a characteristic diffraction pattern is produced. In 1919 A. W. Hull gave a paper titled, “A New Method of Chemical Analysis.” In it he pointed out that “...every crystalline substance gives a pattern; the same substance always gives the same pattern; and in a mixture of substances each produces its pattern independently of the others.”

Therefore, the X – Ray diffraction pattern of a pure substance is like a fingerprint of the substance. X – Ray diffraction (XRD) is thus ideally suited for characterisation of heterogeneous solid mixtures to determine relative abundance of crystalline compounds. XRD was used to investigate the mineralogical structure of natural zeolite samples. This technique is based on observing the scattering intensity of an X – Ray beam hitting a sample as a function of incident and scattered angle, polarization, and wavelength or energy. The diffraction data obtained are compared to the database maintained by the *International Centre for Diffraction Data*, in order to identify the material in the solid samples.

The results of XRD showed that the natural zeolite contained clinoptilolite in the majority, and small quantities of quartz, feldspar and mica acting as impurities, as shown in Appendix B (*Courtesy of IMERYS Minerals Ltd, UK*).

5.5 X – Ray Fluorescence

X – Ray fluorescence (XRF) is the emission of characteristic "secondary" (or fluorescent) X – Rays from a material that has been excited by bombarding with high-energy X – Rays or gamma rays. The phenomenon is widely used for elemental analysis and chemical analysis. When primary X – Rays from an X – Ray tube or a radioactive source strikes a sample, the X – Ray can either be absorbed by the atom or scattered through the material. The process in which an X – Ray is absorbed by the atom by transferring all of its energy to an innermost electron is called the "photoelectric effect." During this process, if the primary X – Ray had sufficient energy, electrons are ejected from the inner shells, creating vacancies. These vacancies present an unstable condition for the atom. As the atom returns to its stable condition, electrons from the outer shells are transferred to the inner shells and in the process give off a characteristic X – Ray whose energy is the difference between the two binding energies of the corresponding shells. Because each element has a unique set of energy levels, each element produces X – Rays at a unique set of energies, allowing one to non-destructively measure the elemental composition of a sample.

The results of chemical analysis performed using XRF are presented in Table 5.1. The predominant exchangeable cations for the natural zeolite were found to be Na^+ , K^+ , Mg^{2+} and Ca^{2+} , and this is in agreement with the results obtained using EDS analysis.

Table 5.1: Chemical analysis of natural zeolite performed using XRF (% wt/wt).

Natural Zeolite	
Chemical Composition (%) from XRF*	
SiO ₂	72.43
Al ₂ O ₃	11.92
Fe ₂ O ₃	1.18
TiO ₂	0.08
K ₂ O	3.38
CaO	2.12
MgO	1.38
Na ₂ O	1.10
Si/Al (mol/mol)	5.16
TCEC (meq/g)	2.52

* Courtesy of IMERYS Minerals Ltd, UK; TCEC – Theoretical cation exchange capacity.

The Si/Al ratio was also calculated from the XRF results and is presented in Table 5.1, this value is typical of clinoptilolite, whose Si/Al ratio typically ranges from 4 to 5.5, (Tsitsishvili et al., 1992; Culfaz and Yagiz, 2004). Erdem et al. (2004) claimed that low – silica members of clinoptilolite are enriched with calcium, whereas high-silica clinoptilolite is enriched with potassium, sodium and magnesium. However, XRF analyses reveal that, the samples used in this research are also enriched with calcium even though they are high silica clinoptilolites. A small value of the Si/Al ratio means the zeolite surface has a large net negative charge and hence has more capacity for cations; these cations will be strongly bound to the surface and hence the ion exchange capacity of the zeolite will be drastically reduced.

Table 5.1 also gives the value of the theoretical cation exchange capacity (TCEC) of natural zeolite; this was calculated from XRF results and determined to be 2.52 meq/g. Theoretical cation exchange capacity is a measure of the ion exchange between the zeolite sample and metal laden solution. The ion exchange process involves the

replacement of singly – charged exchangeable atoms in the zeolite by other singly – charged atoms from solution or replacing two singly – charged exchangeable atoms in the zeolite by one doubly – charged atom from the solution. The theoretical cation exchange capacity obtained in this study is typical of natural zeolite. Englert and Rubio (2005) obtained the cation exchange capacity of Chilean natural zeolite as 2.05 meq/g, Cincotti et al. (2006) determined the CEC of Sardinian natural zeolite as 2.78 meq/g and Inglezakis (2005) found that the TCEC of natural zeolite from Greece was 2.16 meq/g. However, not all cations that are identified as “exchangeable” cations within the zeolite are available for ion exchange; this is mainly because of two reasons. Firstly, some of these “exchangeable” cations are located at inaccessible sites of the zeolite structure; secondly the “exchangeable” cations might be components of impurities such as feldspar, quartz and mica and thus can not take part in ion exchange (Inglezakis et al., 2002).

5.6 Other particle characteristics

The other characteristics of natural zeolite that were investigated are listed in Table 5.2.

Table 5.2: Physical properties of natural zeolite (clinoptilolite) used in this study, compared with samples used by other researchers.

Physical Properties	This Study (Turkey)	Erdem et al., 2004 (Turkey)	Korkuna et al., 2006 (Ukraine)	Englert and Rubio, 2005 (Chile)	Alvarez-Ayuso et al., 2003 (Greece)
Surface area (m^2g^{-1})	15.9	---	14.0	---	20.3
Interstitial Porosity (%)	47.6	41.5	---	---	---
Density (g/cm^3)	2.28	2.27	---	2.20	---
Moisture Content (% wt.)	9.4	---	9.0	5.0	---
Particle size (mm)	1 – 3	0.6	0.36-0.5	0.15	0.1
Colour	Buff	Whiteness (68%)	---	---	---

The density of natural zeolite was determined using a helium gas pycnometer from Micromeritics, model AccuPyc II 1340. The density of dry natural zeolite was found to be 2.2751 g/cm^3 , and the standard deviation was 0.0004 g/cm^3 .

Surface area measurements were determined by Nitrogen adsorption fitted to the BET equation (Brunauer, 1943), using the TRISTAR 3000 apparatus from Micromeritics.

Moisture content of zeolite was determined by measuring a known mass of zeolite and drying it in an oven at $200 \text{ }^\circ\text{C}$. The mass of the sample was continuously monitored and when the mass was constant the samples were removed from the oven and final weight measured. It was found that the moisture content was $9.4 \% \pm 0.2 \text{ (w/w)}$.

The porosity of natural zeolite was measured using a mercury porosimeter. The porosity of natural zeolite was 47.63% .

Appendix B gives a description of the physical and chemical characteristics of natural zeolite provided by the supplier.

CHAPTER 6

EQUILIBRIUM STUDIES

6.1 Introduction

Equilibrium studies generally involve the determination of the adsorption capacity of a given material, this is important in accessing the potential of the material as an economic and commercially viable adsorber. The material is contacted with the solute until equilibrium is achieved. The adsorption equilibrium is a dynamic concept achieved when the rate at which molecules are adsorbed onto a surface is equal to the rate at which they are desorbed (Richardson et al., 2002).

The main objective of the equilibrium studies was to determine the maximum capacity of natural zeolite towards copper, iron, zinc and manganese removal under the studied conditions and accordingly to make a selectivity comparison for these cations. Furthermore, the determination of the mechanism involved in removing heavy metals from solution was carried out; mainly by measuring the amount of exchangeable cations released from the natural zeolite samples at equilibrium.

Experimental data were also fitted to conventional adsorption mathematical models, namely the Freundlich and Langmuir models. These were used to predict the adsorption performance of natural zeolite. The performance of natural zeolite was also assessed at different initial solution pH levels.

6.2 Equilibrium isotherms

Equilibrium behaviour is usually described in terms of equilibrium isotherms which depend on the system temperature, the total initial concentration of the solution in contact with the exchanger and on the characteristics of the ion exchange system, such as solution composition, mineral type and pH (Inglezakis et al., 2002). The Langmuir and Freundlich adsorption isotherms were used in this study because they are the most widely used mathematical models due to their simplicity and ability to describe equilibrium data in a wide range of concentrations (Altin et al., 1998, Peric et al., 2004).

6.2.1 Langmuir adsorption isotherm

The Langmuir model was originally developed for the adsorption of gases onto solids and is based on the assumption that adsorption occurs on localised sites with no interaction between adsorbate molecules (Langmuir, 1918). Maximum adsorption occurs when the surface is covered by a monolayer of adsorbate. For the adsorption of a solute (adsorbate) from solution the Langmuir isotherm can be written as follows:

$$q_e = \frac{q_o b C_e}{1 + b C_e} \quad (1)$$

$$q_e = \frac{m_s}{m} = (C_o - C_e) \frac{V}{m}, \quad (2)$$

Where, q_e is the amount of solute adsorbed per unit mass of adsorbent at equilibrium (mg/g),

q_o is the amount of solute adsorbed per unit mass of adsorbent corresponding to complete coverage of available sites (mg/g),

C_o is the initial concentration of heavy metal ions (mg/l);

C_e is the residual liquid phase concentration at equilibrium (mg/l),

V is the volume of solution from which adsorption occurs (litres),

m_s is the mass of solute adsorbed (mg),

m is the mass of the adsorbent (g),

b is the Langmuir adsorption coefficient, this constant is related to the affinity between the adsorbent and solute (L/mg).

A number of assumptions were made in the development of the Langmuir adsorption isotherm; these include (Richardson et al., 2002; Tien, 1994):

- Monolayer coverage of the adsorbent surface,
- There are no interactions between adjacent molecules on the adsorbent surface,
- The energy of adsorption is the same all over the adsorbent surface, and each adsorption site accommodates one adsorbate molecule only,
- Molecules are adsorbed at fixed sites and do not migrate over the surface (localised).

For solid – liquid systems the linear form of the isotherm can be expressed by equation [3], below:

$$\frac{1}{q_e} = \frac{1}{bq_o C_e} + \frac{1}{q_o} \quad (3)$$

There are a number of researchers who have successfully used the Langmuir adsorption isotherm to model their equilibrium data for the removal of heavy metals from solution using natural zeolite; these include Gunay et al. (2007), Sprynskyy et al. (2006) and Erdem et al. (2004).

6.2.2 Freundlich adsorption isotherm

A well used empirical isotherm is the Freundlich adsorption isotherm, which describes equilibrium on a heterogeneous surface that is more often seen in natural systems. The mathematical model assumes that the energy of adsorption is not equivalent for all adsorption sites (unlike the Langmuir isotherm); hence the isotherm gives room for multi-layer adsorption. The Freundlich isotherm is mathematically expressed as:

$$q_e = kC_e^{1/n} \quad (4)$$

Where, q_e is the amount of solute adsorbed per unit mass of adsorbent at equilibrium (mg/g),

C_e is the residual liquid phase concentration at equilibrium (mg/l),

k and n are empirical Freundlich constants that are dependent on experimental conditions. k is an indicator of adsorption capacity while n is related to the adsorption intensity or binding strength.

The linear form of the Freundlich adsorption isotherm is:

$$\ln q_e = \ln k + \frac{1}{n} \ln C_e \quad (5)$$

$1/n$ is the heterogeneity factor; values of $1/n \ll 1$ indicate heterogeneous adsorbents, while values closer to or even 1 indicate a material with relatively homogeneous binding sites (Papageorgiou et al., 2006). Natural zeolite should be a heterogeneous adsorbent due to its porous nature. Cincotti et al. (2006), Alvarez-Ayuso et al. (2003) and Gunay et al. (2007) successfully used the Freundlich adsorption isotherm to model their results from equilibrium experiments.

6.3 Results and discussion

In order to carry out the equilibrium studies, 3.7 g of natural zeolite was mixed with 100 ml solution of the respective cation at different initial pH levels and concentrations, and agitated for 360 minutes. The results of equilibrium studies for each cation are presented and discussed in this section.

6.3.1 Removal of copper

It is clear from Figure 6.1 that as the initial concentration of heavy metal cations increases, the amount of metal adsorbed per gram of natural zeolite (q_e) increases. This is mainly due to the fact that at high metal concentrations, there is a higher solute concentration gradient; and this provides the necessary driving force for metal ions to displace exchangeable cations on the surface and from the internal micro-pores of natural zeolite (Du et al., 2005; Abadzic and Ryan, 2001). However, this increasing trend is valid up to a point at which the maximum capacity of the natural zeolite samples for the respective heavy metal cation is achieved, that is, its saturation point.

Experimental data obtained from equilibrium experiments were fitted to the Langmuir and Freundlich adsorption isotherms. The values of the parameters for the two isotherms are presented in Table 6.1. The error in analysing copper using AAS was $\pm 6.5\%$.

Table 6.1: Calculated equilibrium adsorption isotherm constants for the uptake of copper from solution by natural zeolite.

Initial pH	Experimental		Langmuir			Freundlich		
	$q_{e \max}$ (mg/g)	C_e (mg/l)	q_0 (mg/g)	b (L/mg)	R^2	k (L/mg)	$1/n$	R^2
2.5	2.82	590.24	3.31	0.011	0.97	0.164	2.138	0.90
3.5	3.32	477.14	3.37	0.110	0.90	1.088	0.180	0.86
5.7	5.77	523.85	6.09	0.010	0.96	0.678	0.330	0.97

Table 6.1 shows that both the Langmuir and Freundlich isotherms for the adsorption of copper from solution gave good fits of the experimental results, as revealed by the values of the correlation coefficients, R^2 , which range from 0.86 to 0.98. The adsorption capacity generally increases from pH 2.5 to 5.7, the maximum adsorption capacity, q_0 , according to the Langmuir model at pH 5.7 is about 6.1 mg/g and that at 2.5 is just 3.3 mg/g. The fitting of Langmuir and Freundlich models to experimental results for the adsorption of copper are also shown graphically in Figure 6.1.

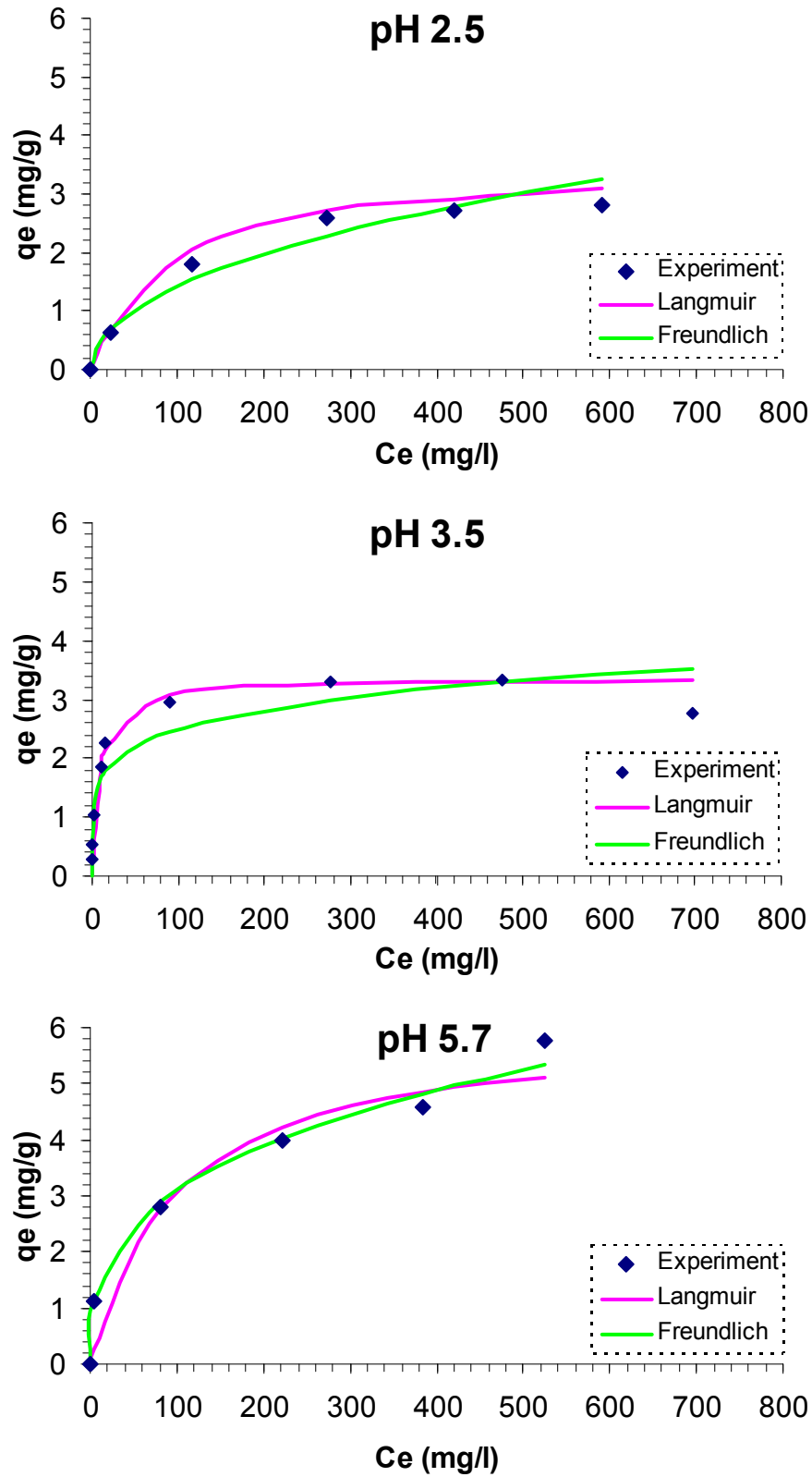


Figure 6.1: Equilibrium isotherms for the removal of copper from solution.

Figure 6.1 also shows the adsorption capacity of natural zeolite for copper at different initial solution pH levels. It can be observed that there is a general increase in adsorption capacity as the solution pH increases. This is mainly attributed to the decrease in H^+ ion concentration as the initial pH level increases from 2.5 to 5.7. H^+ ions act as competitors for available adsorption sites on the natural zeolite surface, and hence at low pH levels, H^+ ions are more concentrated and thus because of the concentration driving force will be adsorbed in preference to copper ions, resulting in lower adsorption capacities for copper ions (Inglezakis et al., 2001; Wingenfelder et al., 2005; Alvarez-Ayuso et al., 2003). The effect of initial solution pH on the adsorption of heavy metals by natural zeolite is discussed in detail in *section 7.3.3*.

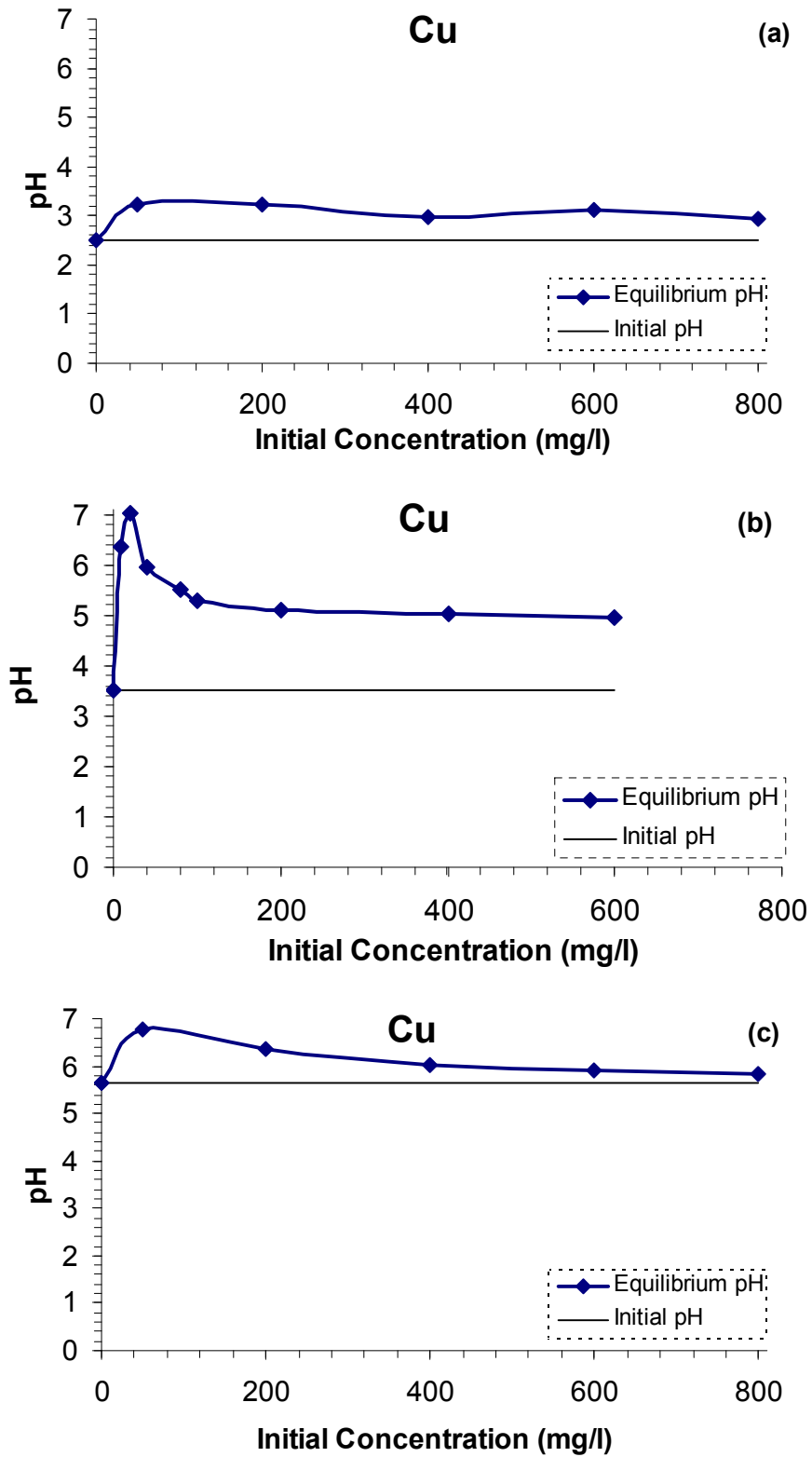


Figure 6.2: Equilibrium pH change with respect to various initial copper concentrations. The initial solutions were at different pH values, (a) 2.5, (b) 3.5 and, (c) 5.7. Error in pH reading is ± 0.1 .

Figure 6.2 presents the variation in the equilibrium pH values with respect to initial copper concentration in each equilibrium study. The equilibrium pH values are greater than the initially adjusted pH values and the difference between equilibrium pH and initial pH exhibits a descending trend with increasing initial copper concentration. The increase in pH is a result of the adsorption of H^+ ions from solution, but as the initial concentration of copper increases, the concentration driving force begins to favour the adsorption of Cu^{2+} ions in preference to H^+ ions, thus the descending trend of the equilibrium pH at higher initial copper concentrations. The highest equilibrium pH was about 7; see Figure 6.2 (c). The equilibrium pH values for the copper solutions were less than the minimum pH value (7.2) needed for complete precipitation of copper as a hydroxide (Table 6.2), thus no precipitate was observed during the experiment.

Table 6.2: Minimum pH values required for complete precipitation of heavy metal ions as hydroxides (Brown et al., 2002).

Heavy Metals	Minimum pH
Fe^{3+}	4.3
Cu^{2+}	7.2
Zn^{2+}	8.4
Mn^{2+}	10.6

As discussed earlier, in the characterisation studies, it was shown that natural zeolite contains exchangeable cations in its structure which include Ca^{2+} , Mg^{2+} , K^+ and Na^+ ions (Figure 5.7). Therefore, these ions should be present in solution at equilibrium if ion exchange took place in the removal of heavy metal cations from solution. The amount of Ca^{2+} ions was monitored in this study to investigate whether ion exchange took place between the solution and natural zeolite.

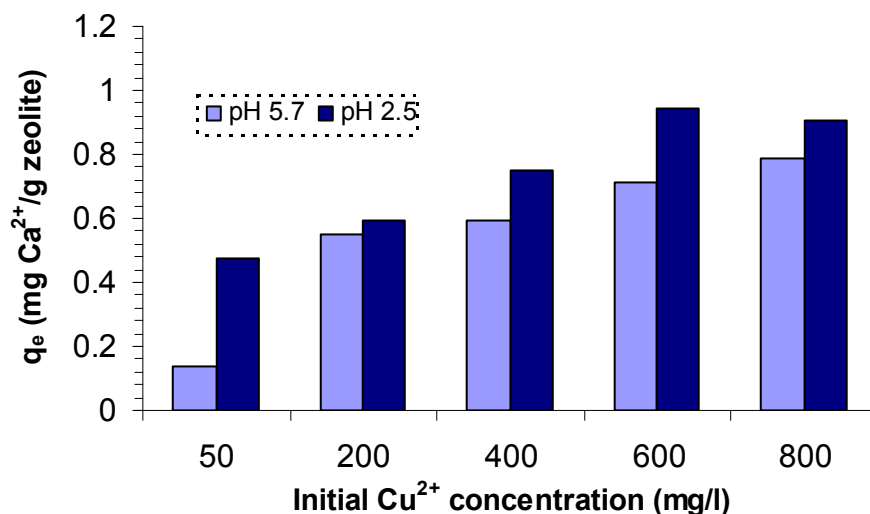


Figure 6.3: Amount of exchangeable Ca^{2+} ions in solution after equilibrium, at different initial copper concentrations.

The concentration of Ca^{2+} ions in solution was measured using AAS. It is clear from Figure 6.3 that significant amounts of Ca^{2+} ions were displaced from the natural zeolite. It can be seen that as the initial concentration of copper increases so does the amount of Ca^{2+} ions present at equilibrium, this is because there is an increase in the amount of copper ions adsorbed resulting in more Ca^{2+} ions being displaced from the adsorption sites by the adsorbed Cu^{2+} ions. Therefore, one of the processes involved in the removal of copper from solution by natural zeolite is ion exchange.

6.3.2 Removal of Zinc

The equilibrium adsorption capacities of natural zeolite for zinc at different initial solution pH levels are shown in Table 6.3. The highest experimental amount of zinc removed, $q_{e \max}$, was 6.51 mg/g, from a solution whose initial pH was 5.7. The amount of zinc removed from solution increased with an increase in initial solution pH. The error in analysing zinc samples using the AAS was $\pm 6.6\%$. Table 6.3 also presents the Langmuir and Freundlich adsorption isotherm parameters.

Table 6.3: Calculated equilibrium adsorption isotherm constants for the uptake of zinc from solution by natural zeolite.

Initial pH	Experimental		Langmuir			Freundlich		
	$q_{e \max}$ (mg/g)	C_e (mg/l)	q_0 (mg/g)	b (L/mg)	R^2	k (L/mg)	$1/n$	R^2
2.5	5.76	586.90	4.82	0.017	0.80	0.252	0.492	0.99
3.5	5.97	578.95	6.05	0.011	0.93	0.873	0.288	0.95
5.7	6.51	559.05	8.85	0.005	0.98	0.579	0.383	0.99

Table 6.3 shows that there is a general increase in the equilibrium adsorption capacity, q_0 , from pH 2.5 to 5.7 according to the Langmuir isotherm. The maximum adsorption capacity being, 8.85 mg zinc per gram natural zeolite. The Freundlich isotherm gave good fits of the experimental results, as shown by the correlation coefficient, R^2 value, ranging from 0.95 – 0.99. The Langmuir and Freundlich models fitting to experimental results for the adsorption of zinc are shown graphically in Figure 6.4.

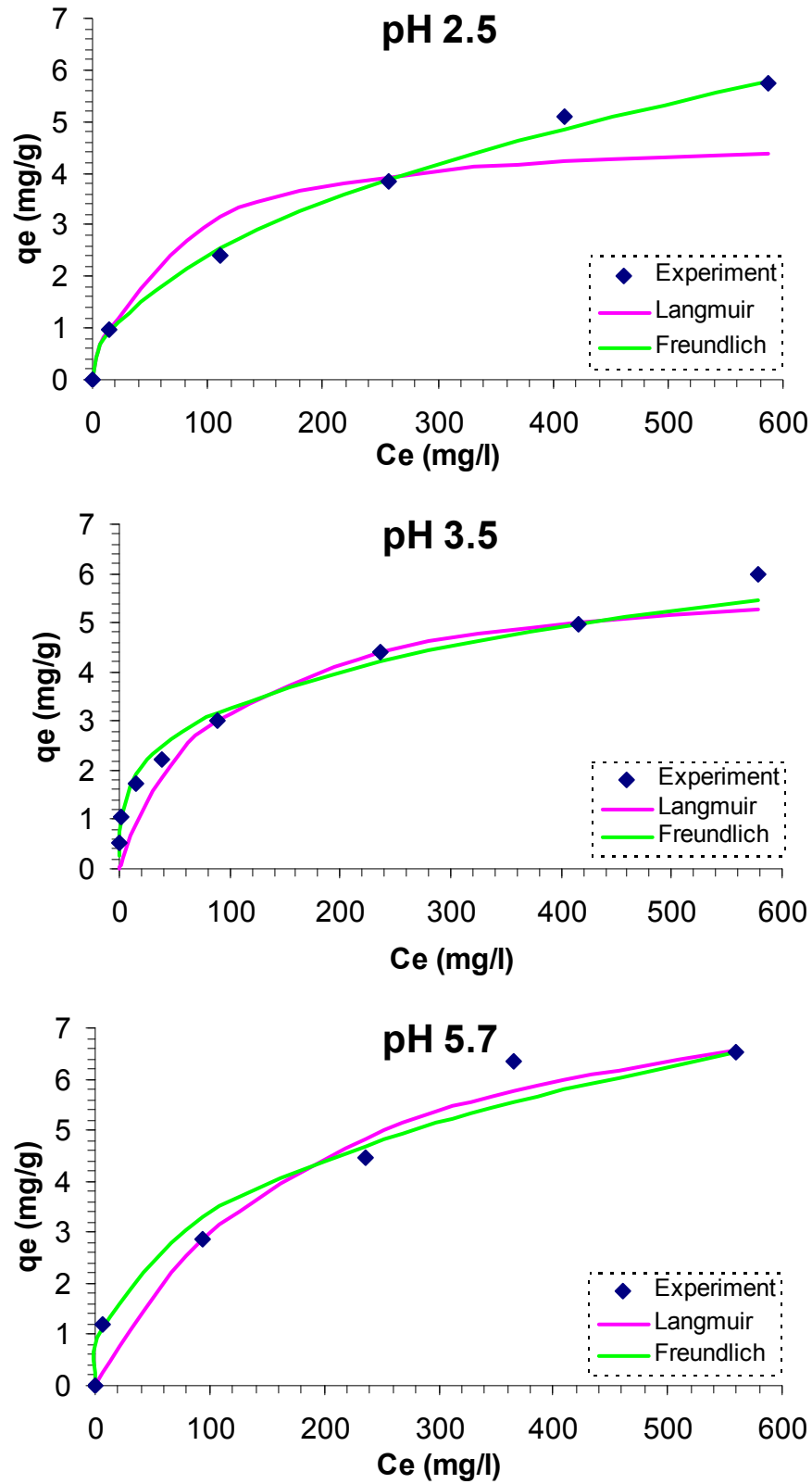


Figure 6.4: Equilibrium isotherms for the removal of zinc from solution by natural zeolite at different initial solution pH levels.

As observed in the adsorption of copper, there is a general increase in the final solution pH compared to the initial pH (Figure 6.5), which is a result of the adsorption of H^+ ions from solution by natural zeolite. The decrease in the equilibrium pH as the initial concentration of zinc increases is mainly due to the preferential adsorption of Zn^{2+} ions to H^+ ions due to the concentration driving force which favours Zn^{2+} adsorption at higher zinc concentrations. The probability of zinc precipitating out of solution is very small since the equilibrium pH ranges from 3.15 – 6.72 (Figure 6.5), and this is lower than the minimum pH (8.4) needed for the precipitation of zinc, see Table 6.2.

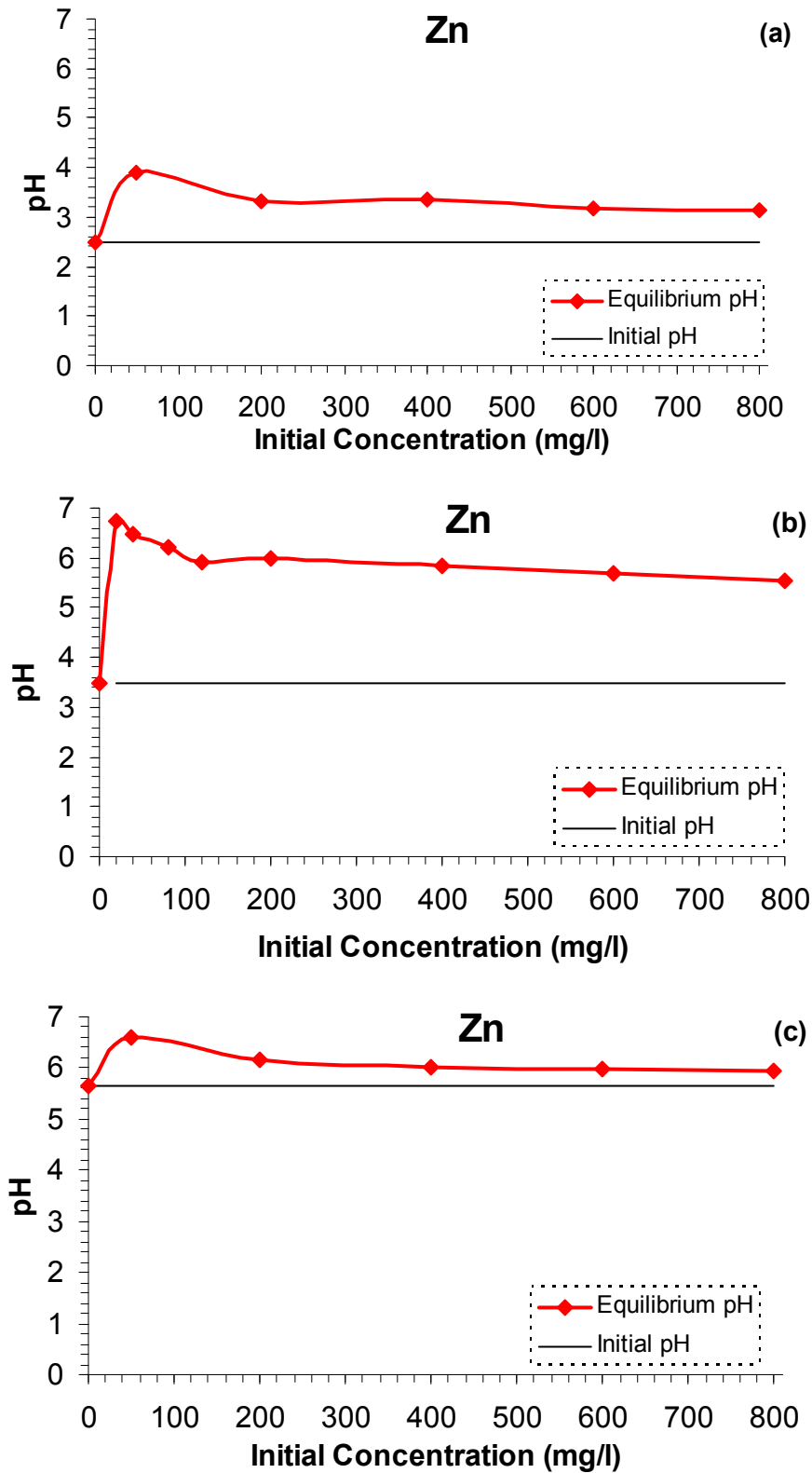


Figure 6.5: Change in equilibrium pH with respect to various initial zinc concentrations. The initial solutions were at different pH values, which are: (a) 2.5, (b) 3.5 and, (c) 5.7 ± 0.1 .

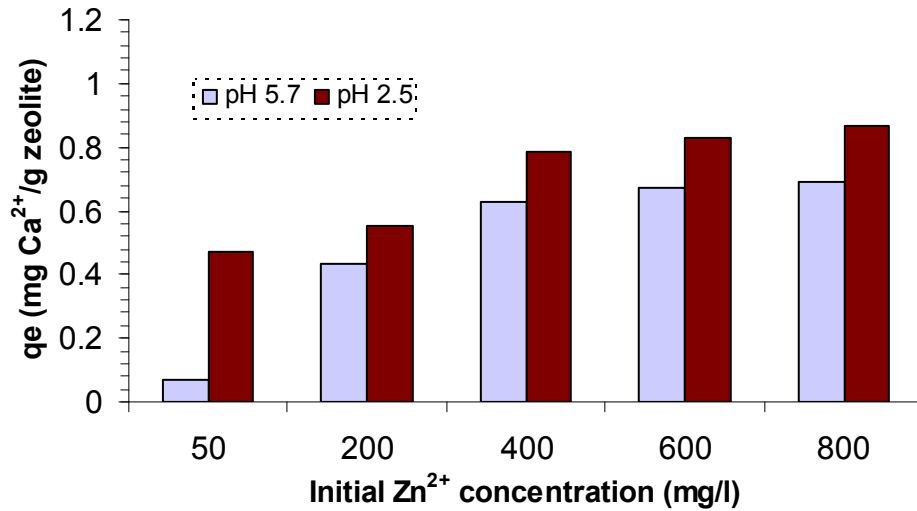


Figure 6.6: Amount of exchangeable Ca²⁺ ions in solution at equilibrium, for different initial zinc concentrations.

In the zinc – natural zeolite system, the decrease in the concentration of zinc in the liquid phase is partly due to exchange with ions from the structure of natural zeolite and partly because of other possible uptake mechanisms (adsorption). The exchange with ions from natural zeolite results in an increase in the concentration of exchangeable ions (Ca²⁺) in solution at equilibrium. The increase in Ca²⁺ ion concentration may also be due to the dissolution of natural zeolite in acidic conditions (Trgo and Peric, 2003). From Figure 6.6 it can be seen that there is higher Ca²⁺ ion concentration at lower initial solution pH levels, that is, at pH 2.5 compared to pH 5.7. At the lower solution pH level the solution is more acidic and thus may cause slight dissolution of natural zeolite, resulting in the release of exchangeable cations into solution. Therefore, the increase in Ca²⁺ ions may be a result of two possible processes; ion exchange with Zn²⁺ and the dissolution of natural zeolite. The fact that Ca²⁺ ions are also released at high solution pH levels, where the solution is not too acidic, is an indication that ion exchange between natural zeolite and heavy metal ions in solution does also contribute to the increase in Ca²⁺ ions at equilibrium.

6.3.3 Removal of iron

The uptake capacity of natural zeolite for iron from solution is shown in Table 6.4 and graphical presentations of the adsorption isotherms are shown in Figure 6.7. The error in analysing iron samples using the AAS was $\pm 6.6\%$.

Table 6.4: Calculated equilibrium adsorption isotherm constants for the uptake of iron from solution by natural zeolite.

Initial pH	Experimental		Langmuir			Freundlich		
	$q_{e \max}$ (mg/g)	C_e (mg/l)	q_0 (mg/g)	b (L/mg)	R^2	k (L/mg)	$1/n$	R^2
2.0	3.28	166.43	2.81	0.048	0.78	0.269	0.492	0.81
2.5	6.56	57.13	6.61	2.628	0.98	2.867	6.116	0.90

Table 6.4 shows that more iron is removed from solutions at higher initial pH, that is, almost double the amount of iron is removed at pH 2.5 compared to pH 2.0. The removal of iron from solution was also due to precipitation, this was determined by observation. There was a rust red precipitate produced in the reaction vessel, especially when treating solutions with low initial iron concentration (less than 100 mg/l), whose equilibrium pH values were higher or closer to 4.3, which is the minimum pH necessary for iron precipitation (Table 6.2). Therefore, the apparently high adsorption capacities that characterise iron removal from solution by natural zeolite may be due to the combination of ion exchange and iron precipitation (Moreno et al., 2001; Alvarez-Ayuso et al., 2003).

The fitting of the Langmuir and Freundlich isotherms to experimental data was relatively good, with the R^2 values ranging from 0.78 – 0.98. The maximum adsorption capacity, q_0 , according to the Langmuir isotherm was 6.61 at pH 2.5.

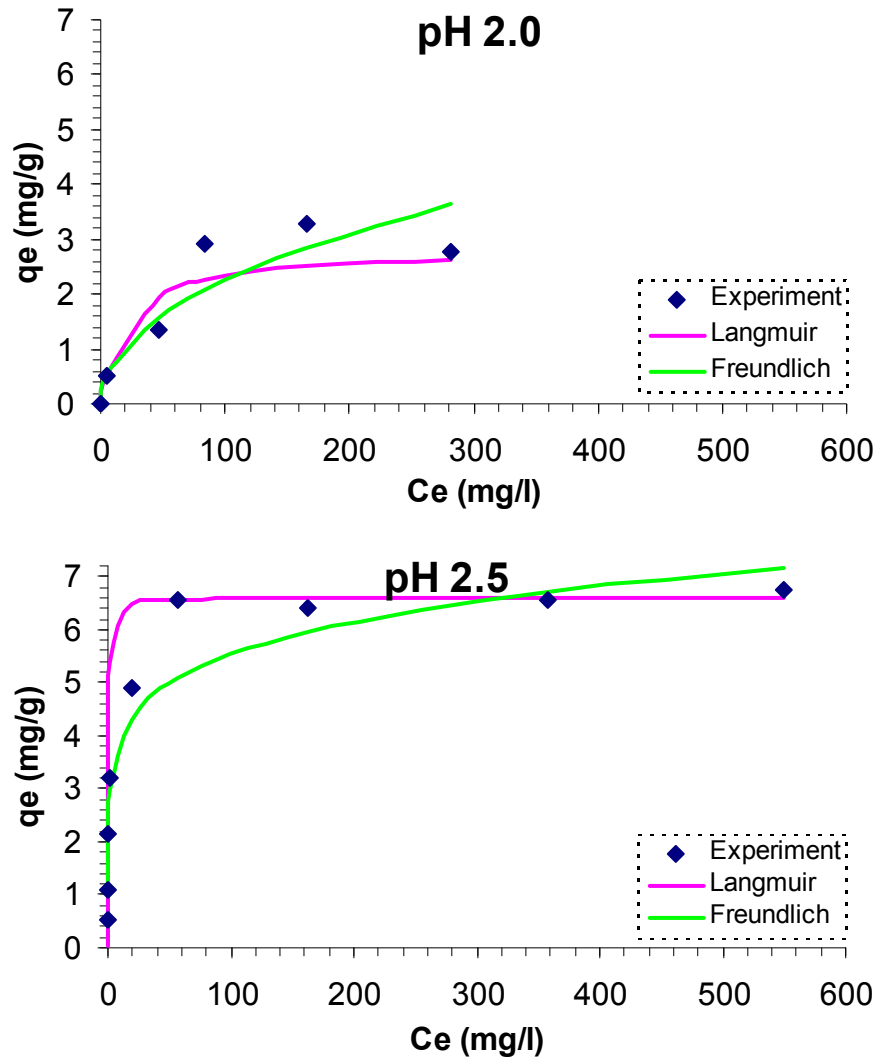


Figure 6.7: Equilibrium isotherms for the removal of iron from solution by natural zeolite at different initial solution pH levels.

There is an increase in iron removal, but this is up to a limit due to the formation of charged metal hydroxyl species and adsorption/ion exchange of these species on the active sites of natural zeolite surface (Figure 6.7). However, with the formation of neutral metal-hydroxyl species iron uptake decreases due not only to the clogging of the pores of natural zeolite because of surface precipitation, but also to the loss of electrostatic attraction (Doula et al., 2002; Ersoy and Celik, 2002). The loss in electrostatic attraction

is due to the formation of a layer of precipitate over the natural zeolite surface thus preventing direct contact between the heavy metal cations and the zeolite's surface.

Figure 6.8 shows the variation in the equilibrium pH values with respect to initial iron concentration in each equilibrium study.

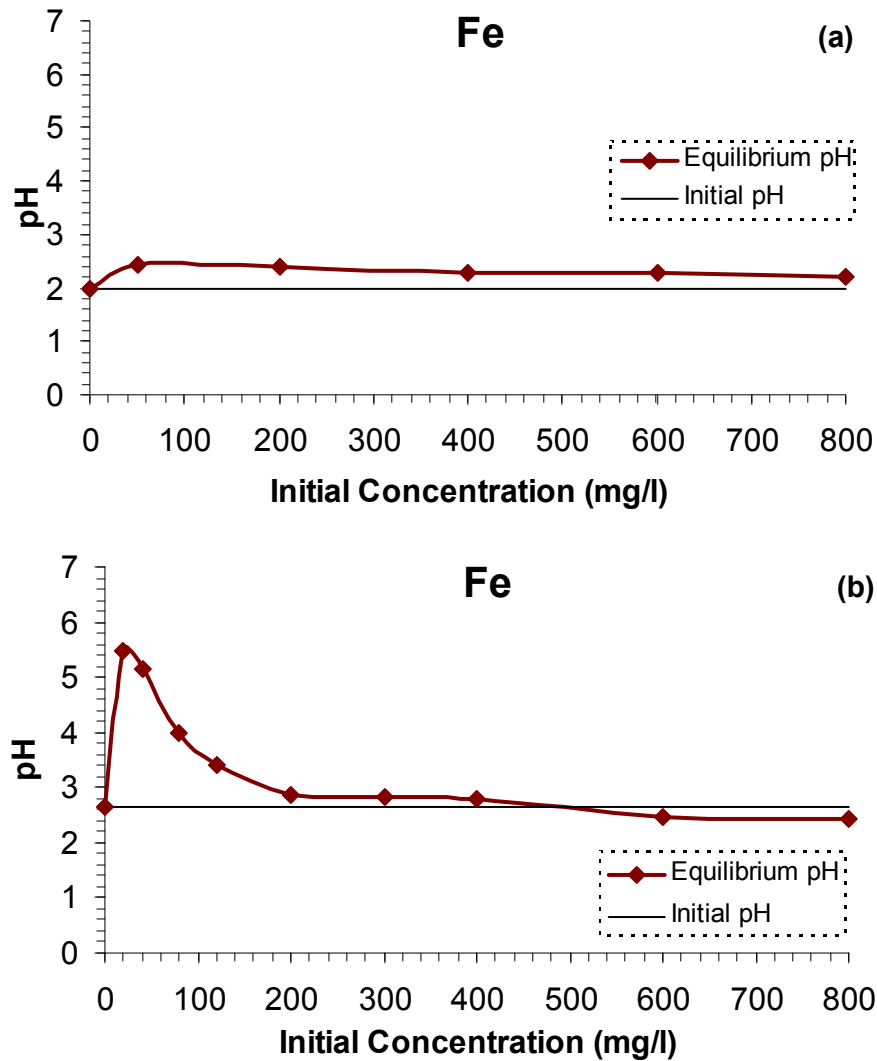


Figure 6.8: Equilibrium pH change with respect to different initial iron concentrations. The initial solutions were at different pH values, which are: (a) 2.0 and, (b) 2.5 ± 0.1 .

The equilibrium pH values, as shown in Figure 6.8, are generally greater than the initially adjusted pH values and this difference exhibits a descending trend with increasing initial iron concentration, as more iron is preferentially adsorbed compared to H⁺ ions. Figure 6.8 (b) shows that the equilibrium pH values of solutions with iron concentrations less than 100 mg/l are greater or close to the minimum pH (pH = 4.3, see Table 6.2) necessary for precipitation to occur, hence the evident precipitate in the reaction vessels. The equilibrium pH values observed for iron adsorption from the solution with initial pH of 2.5 (Figure 6.8 (b)) shows that for iron concentrations greater than 450 mg/l, the equilibrium pH values are less than the initial pH value. The reason for this may be due to the formation of charged iron hydroxyl species, due to the hydrolysis of iron at higher initial concentrations which results in the liberation of H⁺ ions (Doula et al., 2002). It is this liberation of H⁺ ions which results in a reduction in solution pH at equilibrium.

Table 6.5: The amount of Ca²⁺ ions released from natural zeolite at equilibrium, for different initial iron concentrations; initial solution pH = 2.0.

Initial iron concentration (mg/l)	Amount of Ca ²⁺ ions released (mg Ca ²⁺ /g zeolite)
50	0.80
200	1.01
400	0.99
600	1.08
800	1.16

From Table 6.5, it is evident that ion exchange is also one of the mechanisms responsible for the removal of iron from solution by natural zeolite since there is an increase in the amount of exchangeable Ca²⁺ ions in solution at equilibrium as the initial iron concentration increases.

6.3.4 Removal of manganese

The removal of manganese from solution by natural zeolite and the capacity of natural zeolite for manganese are shown in Table 6.6. The maximum experimental capacity, $q_{e \max}$, of natural zeolite was 2.84 mg/g, from the solution with initial pH of 5.7. The error in analysing manganese samples using the AAS was $\pm 5.7\%$.

Table 6.6: Calculated equilibrium adsorption isotherm constants for the uptake of manganese from solution by natural zeolite.

Initial pH	Experimental		Langmuir			Freundlich		
	$q_{e \max}$ (mg/g)	C_e (mg/l)	q_0 (mg/g)	b (L/mg)	R^2	k (L/mg)	$1/n$	R^2
2.5	2.50	727.32	1.61	0.025	0.75	0.148	0.449	0.83
3.5	2.60	710	2.42	0.155	0.98	0.643	0.216	0.86
5.7	2.84	694.82	2.60	0.049	0.90	0.534	0.259	0.99

The maximum adsorption capacity, q_0 , of natural zeolite for manganese according to the Langmuir isotherm was 2.60 mg/g for the solution with initial pH of 5.7. The heterogeneous factor, $1/n$, from the Freundlich isotherm is less than one for all the solutions, that is, 0.449, 0.216 and 0.259 for solutions with initial pH of 2.5, 3.5 and 5.7 respectively. The values of $1/n$ less than 1 imply that the surface is heterogeneous. The values of $1/n$ from Table 6.6 indicate that the surface of natural zeolite is slightly heterogeneous during the removal of manganese, and this is expected since natural zeolite is a porous material. The correlation coefficients, R^2 values, for the adsorption of manganese from solution are in the range, 0.75 – 0.98 for the Langmuir isotherm and 0.83 – 0.99 for the Freundlich isotherm. The lower R^2 values (< 0.85) were obtained for the adsorption of manganese from more acidic solutions; hence these isotherms can not be generally used to describe the adsorption of heavy metals from very acidic solutions by natural zeolite.

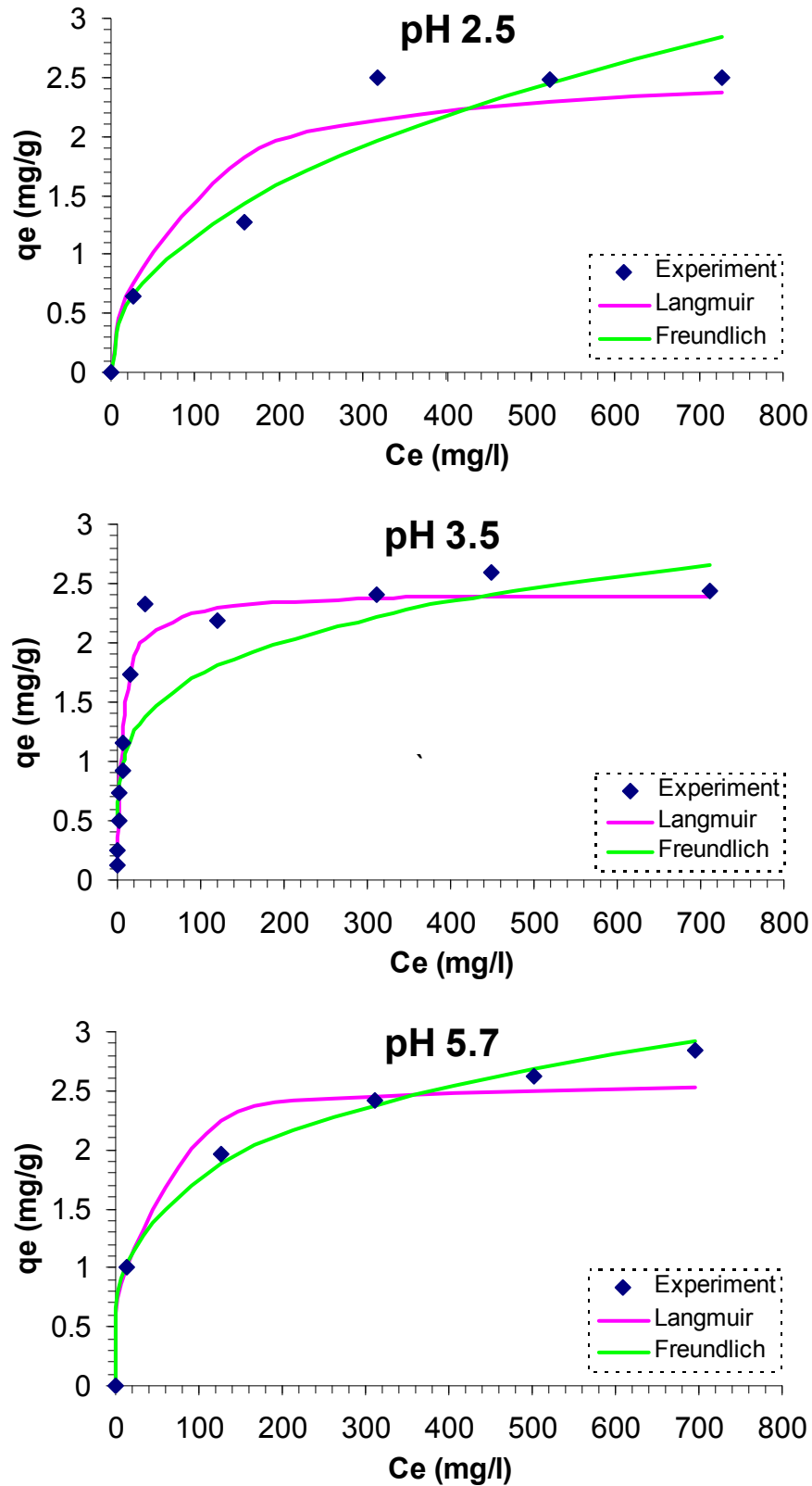


Figure 6.9: Equilibrium isotherms for the removal of manganese from solution by natural zeolite at different initial solution pH levels.

The adsorption isotherms for the removal of manganese from solution, Figure 6.9, show a favourable convex shape, thus manganese removal using natural zeolite at the initial solution pH levels under investigation is favourable.

Figure 6.10 presents the variation in the equilibrium pH values with respect to initial manganese concentration in each equilibrium study.

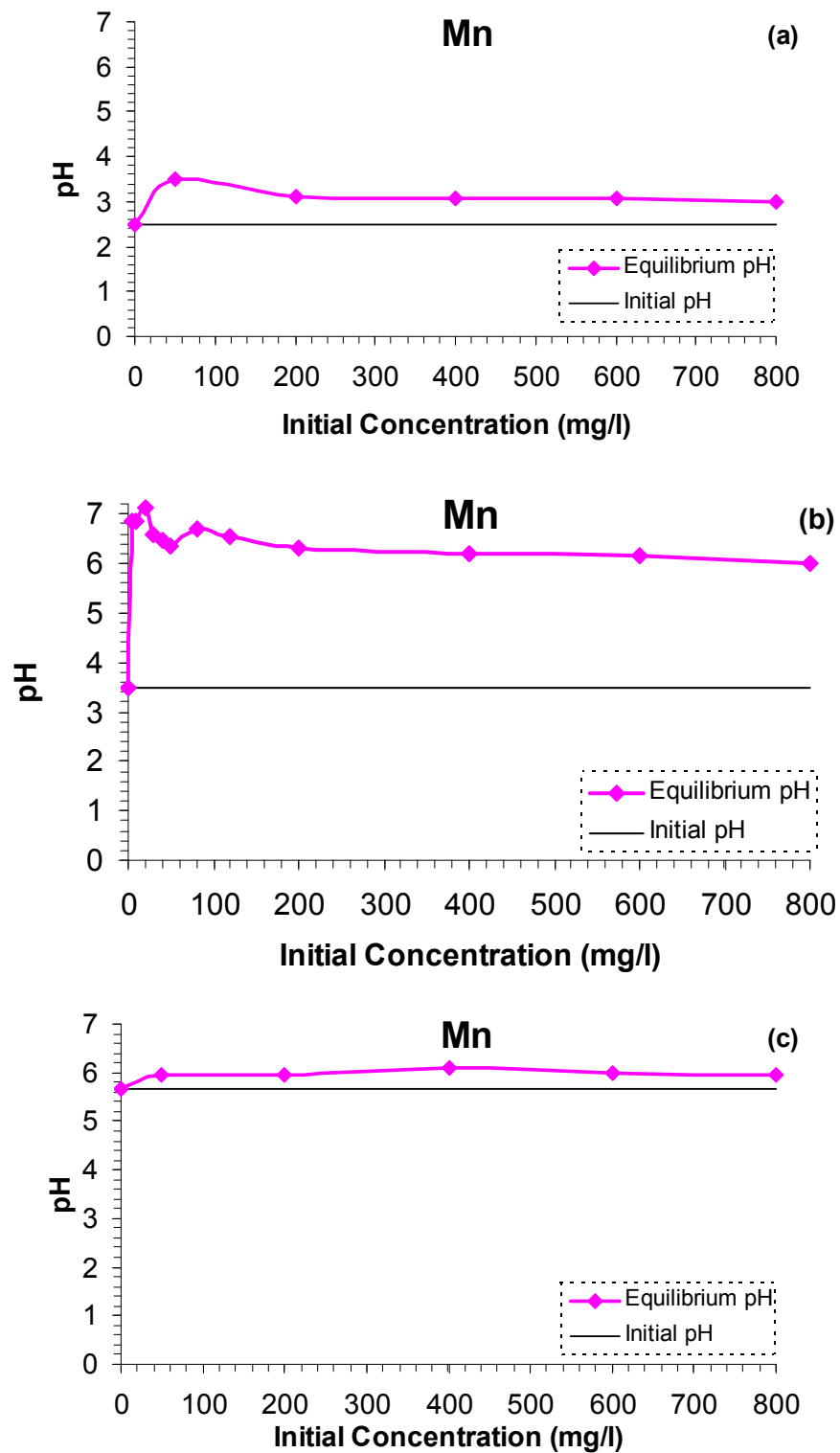


Figure 6.10: Equilibrium pH change with respect to various initial manganese concentrations. The initial solutions were at pH: (a) 2.5, (b) 3.5 and, (c) 5.7 ± 0.1 .

The equilibrium pH values are greater than the initially adjusted pH values. However, as the initial concentration of manganese increases the equilibrium solution pH begins to decrease. The increase in pH is a result of the adsorption of H^+ ions from solution, but as the concentration of manganese ions increases the concentration driving force begins to favour the adsorption of Mn^{2+} ions in preference to H^+ ions. This preferential adsorption of Mn^{2+} ions at higher manganese concentrations results in a decrease in the adsorption of H^+ ions from solution thereby causing a slight difference in solution pH at equilibrium compared to the initial pH at higher Mn^{2+} concentrations.

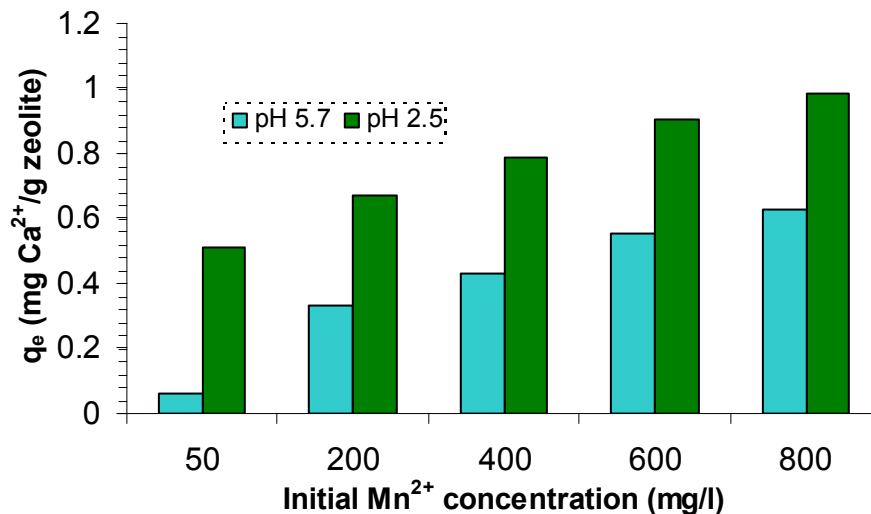


Figure 6.11: Amount of exchangeable Ca^{2+} ions in solution at equilibrium, for different initial manganese concentrations.

As shown in Figure 6.11, there is an increase in the amount of Ca^{2+} ions in solution at equilibrium as the initial manganese concentration increases. This is an indication that the removal of manganese from solution by natural zeolite incorporates an ion exchange process. Doula (2006) and Moreno et al. (2001) also reported the ion exchange nature of natural zeolite in the removal of manganese from solution.

6.4 Selectivity of natural zeolite

Many researchers have carried out equilibrium studies with various natural zeolite samples (clinoptilolite) under different experimental conditions to determine the effectiveness and capacity of their adsorbent materials in adsorbing heavy metal cations from solution (Wingenfelder et al., 2005; Alvarez-Ayuso et al., 2003; Bailey et al., 1998).

In Table 6.7 the maximum removal capacities obtained in various studies are presented.

Table 6.7: Some examples of maximum capacities obtained using different natural zeolite (clinoptilolite) samples in batch mode applications for the removal of Fe³⁺, Cu²⁺, Zn²⁺ and Mn²⁺ in literature.

Heavy metal	Particle Size, mm	Initial pH	T, °C	q _o (mg/g)	Reference
Copper	0.063-0.106	6 – 7	25	8.96	Erdem et al., 2004
	< 0.1	5	22	5.91	Alvarez-Ayuso et al., 2003
	---	---	---	6.74	Panayotova and Velikov, 2002
	1 – 3	5.7	22	6.09	This study.
Iron	0.6 – 0.85	2.0	25	5.86	Garcia-Mendieta e al., 2009
	< 1.0	---	20	5.58-5.89	Sheta et al., 2003
	1 – 3	2.5	22	6.61	This study
Zinc	0.063-0.106	6 – 7	25	8.75	Erdem et al., 2004
	< 0.1	6	22	3.45	Alvarez-Ayuso et al., 2003
	1 – 3	---	25	3.65	Markovska et al., 2006
	---	---	---	2.7-2.3	Panayotova and Velikov, 2002
	< 1.0	---	20	1.9-2.9	Sheta et al., 2003
	1 – 3	5.7	22	8.85	This study.
Manganese	0.063-0.106	6 – 7	25	4.22	Erdem et al., 2004
	< 0.02	---	25	7.69	Doula, 2006
	1 – 3	5.7	22	2.60	This study.

Although these adsorption capacity values correspond to different experimental conditions and there is no experimental relation between them, they are representative of natural zeolite's tendency to retain heavy metal ions from solution.

Equilibrium studies are usually useful in determining the selectivity of natural zeolite for heavy metals under certain experimental conditions (Inglezakis et al., 2002). In this study the Langmuir adsorption isotherm was used to determine the selectivity of natural zeolite, this was done by comparing the maximum adsorption capacity (q_0) of natural zeolite for the respective heavy metal ion. The selectivity series obtained was: $Fe^{3+} > Zn^{2+} > Cu^{2+} > Mn^{2+}$, this series was the same for equilibrium studies performed using solutions with initial pH of 2.5, 3.5 and 5.7.

The difference in adsorption capacity of the natural zeolite for the heavy metal ions may be due to a number of factors which include hydration diameters, hydration enthalpies and solubility of the cations. The hydration radii of the cations are: $r_{H}Zn^{2+} = 4.30\text{\AA}$, $r_{H}Fe^{3+} = 4.57\text{\AA}$, $r_{H}Cu^{2+} = 4.19\text{\AA}$ and $r_{H}Mn^{2+} = 4.38\text{\AA}$ (Nightingale, 1959). The smallest cations should ideally be adsorbed faster and in larger quantities compared to the larger cations, since the smaller cations can pass through the micropores and channels of the zeolite structure with ease (Erdem et al., 2004). Furthermore, adsorption should be described using hydration enthalpy, which is the energy that permits the detachment of water molecules from cations and thus reflects the ease with which the cation interacts with the adsorbent. Therefore, the more a cation is hydrated the stronger its hydration enthalpy and the less it can interact with the adsorbent (Amarasinghe and Williams, 2004). The hydration energies of the cations are: -2010, -1955, -1760 and -4265 kJmol^{-1} for Cu^{2+} , Zn^{2+} , Mn^{2+} and Fe^{3+} respectively (Marcus, 1991; Nightingale, 1959). According to the hydration diameters the order of adsorption should be $Cu^{2+} > Zn^{2+} > Mn^{2+} > Fe^{3+}$ and according to the hydration enthalpies the order should be $Mn^{2+} > Zn^{2+} > Cu^{2+} > Fe^{3+}$. Fe^{3+}

has a greater charge density compared to the other 3 cations which have an ionic charge of 2+, hence its greater hydration diameter and enthalpy.

The above series according to the hydration diameters and enthalpy are different from the experimentally obtained series which is $Fe^{3+} > Zn^{2+} > Cu^{2+} > Mn^{2+}$. The difference in the series may be an indicator that adsorption is not necessarily the only mechanism responsible for the removal of heavy metal ions from solution; precipitation of metal hydroxides may have a significant influence in the removal of heavy metals using natural zeolite (Moreno et al., 2001; Alvarez-Ayuso et al., 2003).

A number of researchers have investigated the selectivity of natural zeolite for different heavy metal ions; results of their work are presented in Table 6.8.

Table 6.8: Examples of experimentally derived selectivity series of natural zeolite for different heavy metals from literature.

Researcher	Experimental selectivity series
Zamzow et al., 1990	$Pb^{2+} > Cd^{2+} > Cs^{2+} > Cu^{2+} > Co^{2+} > Cr^{3+} > Zn^{2+} > Ni^{2+} > Hg^{2+}$
Erdem et al., 2004	$Co^{2+} > Cu^{2+} > Zn^{2+} > Mn^{2+}$
Inglezakis et al., 2002	$Pb^{2+} > Cr^{3+} > Fe^{3+} > Cu^{2+}$
Sprynskyy et al., 2006	$Pb^{2+} > Cu^{2+} > Cd^{2+} > Ni^{2+}$
Blanchard et al., 1984	$Pb^{2+} > NH_4^+ > Ba^{2+} > Cu^{2+} \approx Zn^{2+} > Cd^{2+} \approx Sr^{2+} > Co^{2+}$
Alvarez-Ayuso et al., 2003	$Cu^{2+} > Cr^{3+} > Zn^{2+} > Cd^{2+} > Ni^{2+}$
Moreno et al., 2001	$Fe^{3+} \approx Al^{3+} > Cu^{2+} > Pb^{2+} > Cd^{2+} > Zn^{2+} > Mn^{2+} > Ca^{2+} \approx Sr^{2+} > Mg^{2+}$
Cincotti et al., 2001	$NH_4^+ > Pb^{2+} > Cd^{2+} > Cu^{2+} \approx Zn^{2+}$

Table 6.8 shows that most of the clinoptilolite samples have their own unique selectivity series. The reason for this difference may be attributed not only to the different experimental conditions (such as, initial solution pH and concentration, agitation speed, pre-treatment of zeolite and zeolite particle size) used in each study, but also to the

chemical composition of the natural zeolite (clinoptilolite) samples used (Inglezakis et al., 2003).

6.5 Conclusion

Equilibrium studies showed that natural zeolite was capable of removing heavy metals from single component solutions. The maximum experimental removal capacities, $q_{e \text{ exp}}$, were 5.77, 6.51, 6.56 and 2.84 mg metal/ g natural zeolite for copper, zinc, iron and manganese respectively. The adsorption capacity increased with an increase in initial solution pH, from 2.5 to 5.7. The maximum adsorption capacities were all obtained at pH 5.7. The capacity of the natural zeolite used in this study was comparable with other natural zeolite samples used by other researchers in removing heavy metals from solution.

The Langmuir and Freundlich adsorption isotherms were used to evaluate the adsorption behaviour of natural zeolite for copper, zinc, manganese and iron. These models were able to give good fits to experimental data (pH 3.5 and 5.7), with correlation coefficients, R^2 , ranging from about 0.86 – 0.99. However, at low initial solution pH, that is, pH = 2.5, the models were not effective in describing the equilibrium data.

The selectivity series of natural zeolite for the adsorption of iron, copper, zinc and manganese from solution, according to the Langmuir isotherm was found to be: $\text{Fe}^{3+} > \text{Zn}^{2+} > \text{Cu}^{2+} > \text{Mn}^{2+}$.

Moreover, there was an increase in the concentration of exchangeable cations (Ca^{2+}) in solution at equilibrium. This was an indication that ion exchange between the solution

and natural zeolite was also responsible for the removal of heavy metal ions from solution. Precipitation was also found to affect the removal rate and amount of heavy metals from solution, especially iron, whose minimum pH necessary for precipitation is much lower than that of the other 3 cations.

CHAPTER 7

KINETIC STUDIES

7.1 Introduction

Kinetic studies are important because they supply information about the process dynamics, that is, the adsorption rate, residence time and mass transfer parameters such as external mass transfer coefficients and intraparticle diffusivity. These parameters are essential in the design and operation of any adsorption column in waste water treatment plants. Therefore, kinetic studies help to evaluate the suitability of any material as a potential adsorbent in removing pollutants from solution (Connors, 1990). A study of kinetics also reveals the nature of various fundamental ionic transport mechanisms that contribute to the overall exchange rate (Harland, 1994).

The rate at which adsorption proceeds is a complex function of several factors such that the overall reaction rate may be influenced by the separate or combined effect of these factors. Examples of such factors are adsorbent particle size, initial solution pH and concentration, temperature, agitation speed in the case of batch experiments and flow rate in columns. In this chapter, a number of these factors will be investigated with regards to their effect on the efficiency of natural zeolite in removing iron, copper, zinc and manganese from solution.

A number of kinetic models were identified and used to describe the uptake process/mechanism. The models used in this investigation are the pseudo second order

kinetic model, Nernst Plank's model, Vermeulen's approximation and the film diffusion model as proposed by Furusawa and Smith.

7.2 General Kinetic study results

The results of the kinetic experiments to measure the adsorption of cations from aqueous solutions onto the untreated natural zeolite as a function of zeolite mass and time are shown in Figure 7.1. Single component solutions were mixed with natural zeolite and agitated for 360 minutes. The concentration of the single component solutions were 400, 20, 20 and 120 mgL⁻¹ Fe³⁺, Cu²⁺, Mn²⁺ and Zn²⁺ respectively (these concentrations are similar to the ones in AMD produced at Wheal Jane Mine [McGinness, 1999]).

The results shown in Figure 7.1 show that adsorption is a heterogeneous process with an initial rapid adsorption rate followed by a slower rate. This is particularly noticeable for Fe³⁺ and Zn²⁺ cations which are adsorbed more slowly. In the first 40 minutes, the adsorption sites are available and the cations interact easily with the sites and hence a higher rate of adsorption is observed. This initial stage of fast adsorption corresponds to ion exchange in micro-pores on the surface of the zeolite grains (Inglezakis et al., 2002). Furthermore, the driving force for adsorption, which is the concentration difference between the bulk solution and the solid-liquid interface, is initially very high and this also results in a higher initial adsorption rate. However, after the initial period, slower adsorption may be due to slower diffusion of cations into the interior channels of natural zeolite, the cations subsequently occupy the exchangeable positions within the crystal structure (Amarasinghe and Williams, 2004; Myroslav et al., 2006). In this case it is suggested that ion exchange is between the exchangeable cations (Ca²⁺, Na⁺, Mg²⁺ and

K^+) within the zeolite crystal structure and heavy metal ions (Fe^{3+} , Cu^{2+} , Mn^{2+} and Zn^{2+}) in solution.

7.3 Factors that affect rate of Adsorption

There are a number of conditions that affect the rate of adsorption. These include adsorbent particle size, initial solution pH and concentration, temperature, agitation speed and the presence of competing cations.

7.3.1 Effect of adsorbent mass

A series of kinetic experiments at different adsorbent masses, that is, 3.7 – 7.5 – 15 g, were performed using fixed initial metal concentrations for the respective cation. Typical plots of the amount of metal adsorbed versus time are shown in Figure 7.1. In terms of the percentage of heavy metals adsorbed from solution, it is evident that an increase in adsorbent mass resulted in an increase in the adsorption of the heavy metals, also see Table 7.1. This is because as adsorbent mass increases more adsorption sites are available per unit mass of adsorbent added.

Table 7.1: Effect of natural zeolite mass on the removal of heavy metals from solution at pH 3.5 and 22 °C.

Heavy metal ions	Adsorbent Mass (g)	Percentage Adsorbed (%)
Iron	3.7	59.3
	7.5	85.7
	15	97.3
Copper	3.7	100
	7.5	100
	15	100
Manganese	3.7	95.2
	7.5	98.3
	15	98.9
Zinc	3.7	67.9
	7.5	83.5
	15	94.1

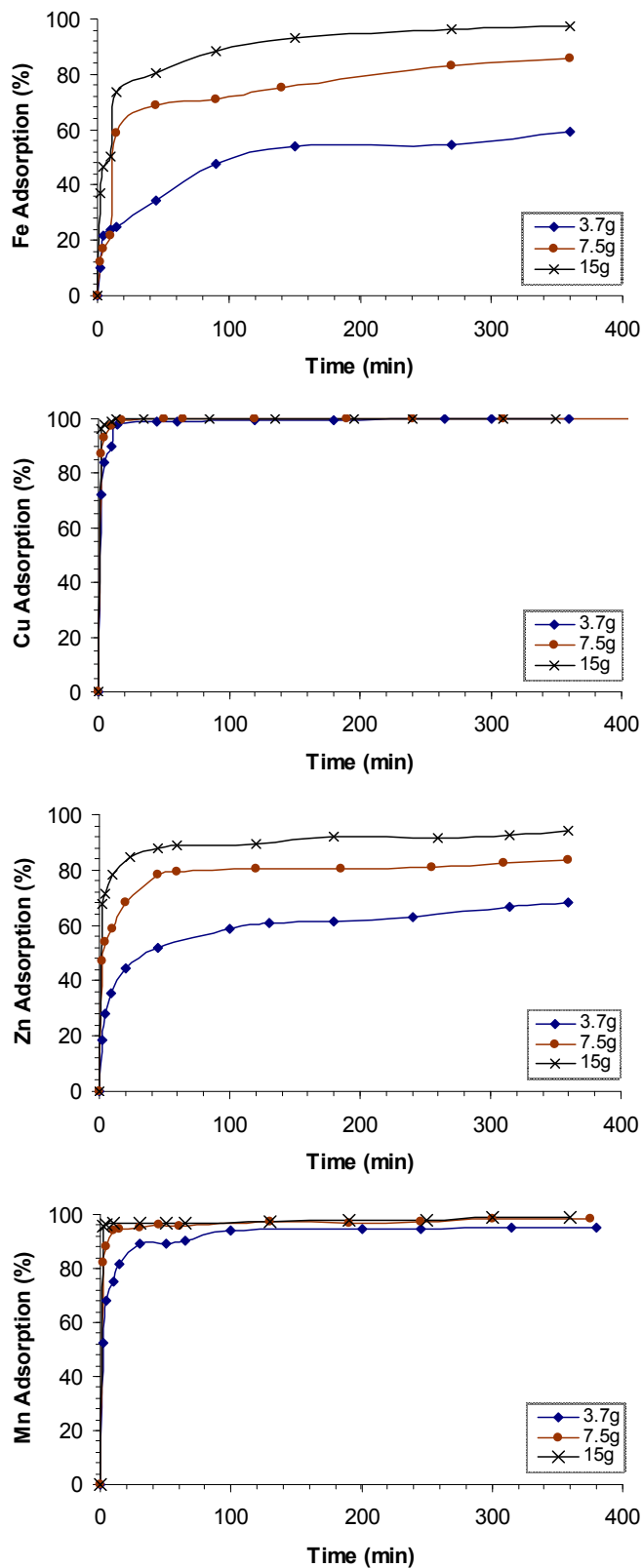


Figure 7.1: The effect of the mass of natural zeolite on the adsorption of iron, copper, zinc and manganese from solution (particle size: 1 – 3 mm; pH: 3.5).

7.3.2 Effect of particle size

Surface area of the adsorbent is an important parameter for adsorption. The uptake of heavy metals by natural zeolite takes place at sites on the exterior surface of the particle as well as sites within the particle. However, only a fraction of the internal adsorption sites are accessible to metal ions. The reason for this partial accessibility of internal sites may be attributed to intraparticle diffusion resistance. Therefore, increasing the external surface area by reducing the adsorbent particle size, results in an increase in the number of available sites for metal uptake (Inglezakis et al., 1999). Moreover, smaller particle sizes result in the shortening of the diffusion distance that heavy metals have to travel in order to get to an adsorption site, hence a faster rate of reaction. Three particle size ranges were used: $20 \mu\text{m} < d_p < 180 \mu\text{m}$, 1 – 3 mm and 5.6 – 6.7 mm. The results of this study are presented in Figure 7.2.

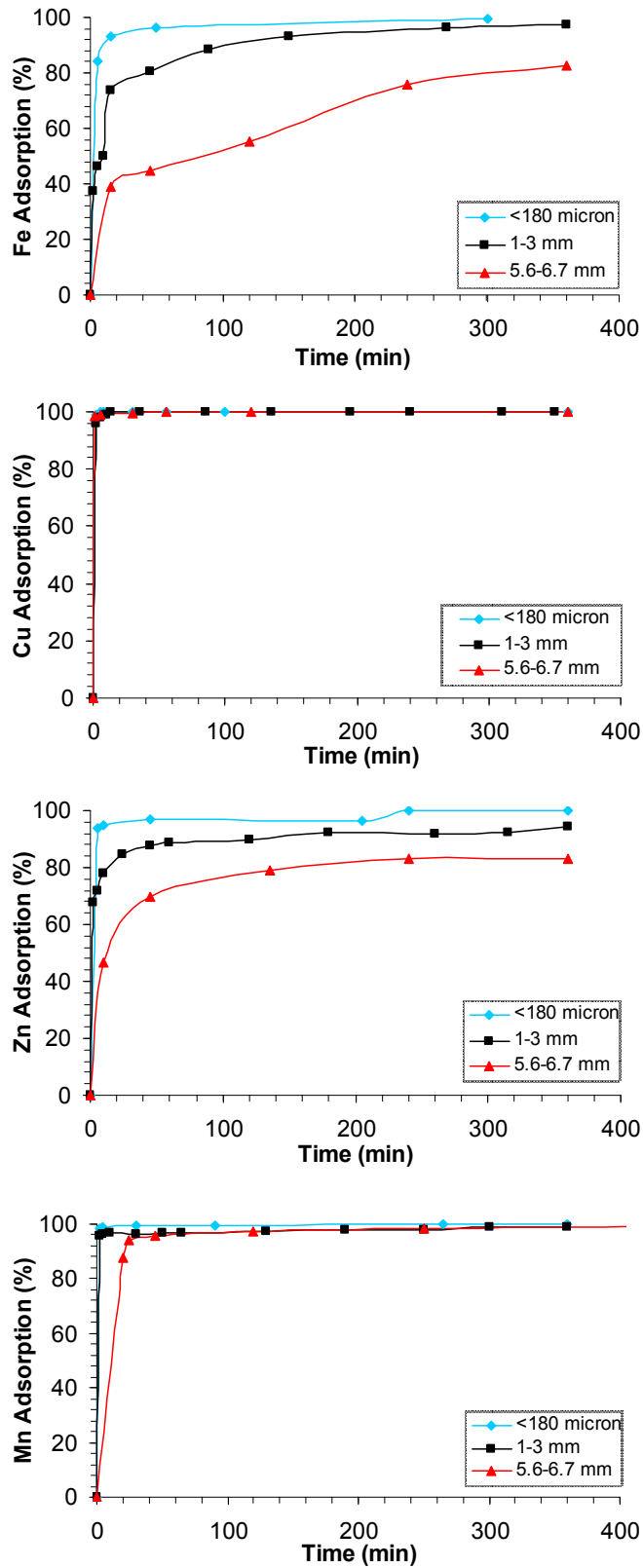


Figure 7.2: Effect of Particle size on the adsorption of iron, copper, zinc and manganese from solution (15 g of zeolite in 100 ml solution; solution pH 3.5).

The results, Figure 7.2 show that decreasing the particle size of natural zeolite results in higher heavy metal removal rates and efficiencies, but as contact time increases, (that is, tending toward equilibrium) there is a decrease in the degree of the effect of particle size on adsorption (Malliou et al., 1994; Erdem et al., 2004). Therefore, the impact of particle size is expected to be more significant in continuous column studies since such applications utilise relatively lower contact times compared to batch experiments. The use of very fine particles may also cause some operational problems such as difficulty in solid-liquid separation in batch mode, and considerably high pressure drops in fixed bed columns (Inglezakis et al., 2001). The typical adsorbent mean particle size used in industrial adsorption columns is 6 mm (Richardson et al., 2002).

7.3.3 Effect of initial solution pH

The pH of the solution in contact with natural zeolite has an obvious impact on its ability to remove metals since the acidic solution can influence both the character of the exchanging ions and the character (structure) of the zeolite itself. Figure 7.3 shows that as solution pH decreases, from 4.5 to 2.5, heavy metal removal efficiency also decreases, this is because H^+ ions compete with heavy metal cations for the same exchange sites (Inglezakis et al., 2001; Wingenfelder et al., 2005; Alvarez-Ayuso et al., 2003) and electrostatic repulsion between the heavy metal cations in solution and the protonated zeolite surface increases as more H^+ ions are adsorbed (Cabrera et al., 2005). Figure 7.3 shows how the adsorption capacity of natural zeolite is affected by solution pH. Therefore, low solution pH is found to inhibit the adsorption of heavy metals onto natural zeolite, hence the use of zeolite to treat *AMD* should be limited to slightly acidic solutions. An increase in initial pH from 2.5 to 4.5 resulted in an increase in the

adsorption capacity, q , of natural zeolite by about 43%, 34% and 23% for Mn^{2+} , Zn^{2+} and Cu^{2+} respectively. Therefore, the efficiency of metal adsorption depends on solution pH levels; this is in agreement with results obtained by Moreno et al., (2001) and Alvarez-Ayuso et al. (2003).

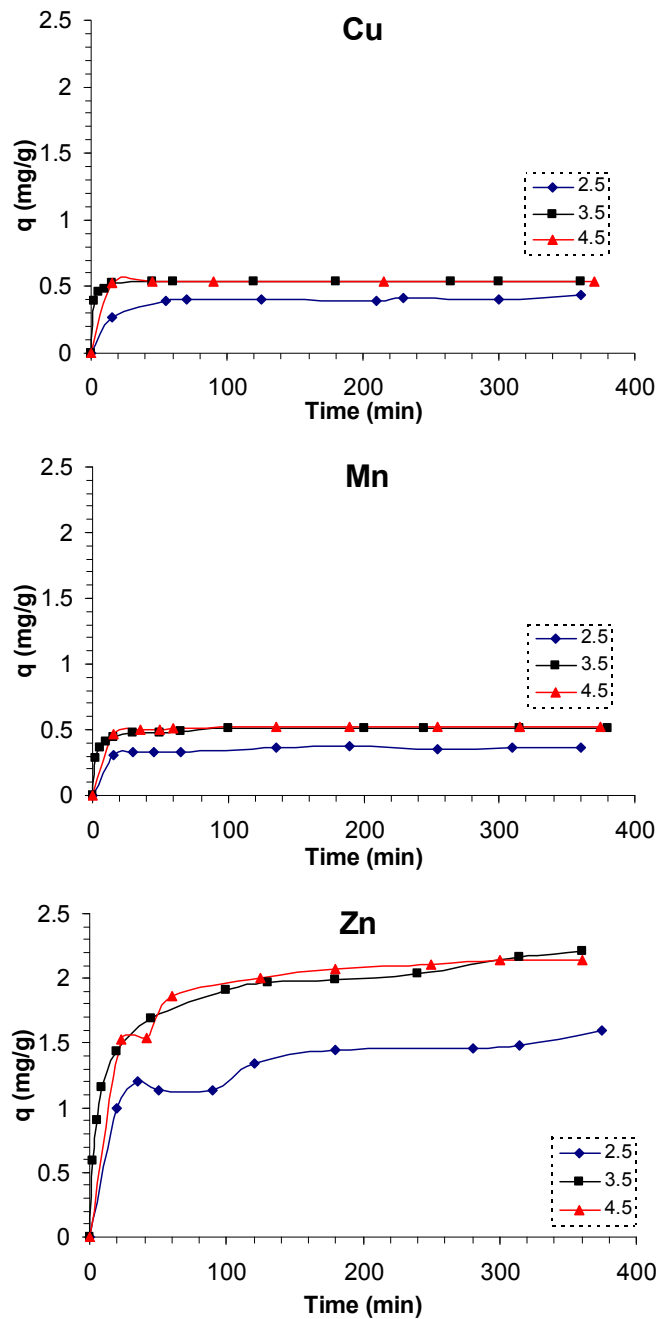
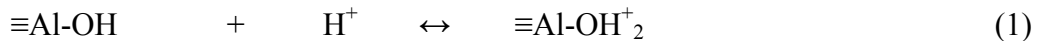


Figure 7.3: Effect of initial solution pH on the adsorption capacity of natural zeolite (3.7 g zeolite; 100 ml single component solution; particle size 1 – 3 mm).

There are several mechanisms that can describe the interaction of natural zeolite with acidic metal laden solutions. Three of these mechanisms are briefly described below:

- i. H^+ ions in the solution displaces Na^+ , K^+ , Ca^{2+} and Mg^{2+} ions on the outer surface or inner surface of zeolite samples in acid to neutral pH range (Doula et al., 2002; Rozic et al., 2002). This results in an increase in the solution pH, since H^+ ions are being removed from solution. The adsorption of H^+ ions by zeolite also results in a decrease in the adsorption of heavy metals from solution since H^+ ions will be competing for available adsorption sites on the zeolite, as already highlighted.
- ii. Acidic solutions result in the protonation of neutral and negative surface hydroxyl groups by H^+ ions (Ersoy and Celik, 2002; Doula et al, 2002) according to the following reactions:



These reactions result in the removal of H^+ ions from solution and hence an increase in solution pH as the reaction proceeds, this is shown in Figure 7.4 where the solution pH is seen to rise from 3.5 to approximately 6.

- iii. At relatively high pH values, OH^- ions may react with clinoptilolite surface;



The above reaction shows that the solution pH decreases since OH^- ions are being removed from solution. Moreover, there is an increase in the net negative charge on

the zeolite framework, which may result in an increase in the adsorption of heavy metal cations from solution (Doula et al., 2002; Ersoy and Celik, 2002).

The above mechanisms show how natural zeolite has a buffering effect (Erdem et al., 2004).

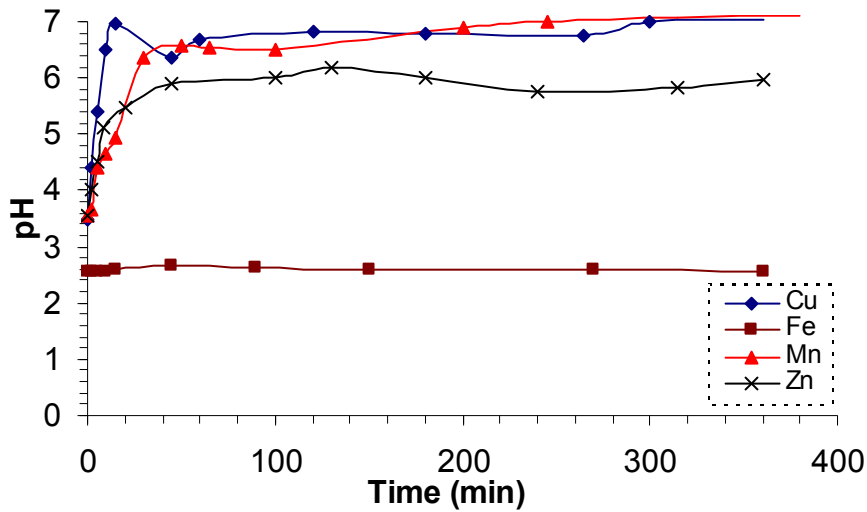


Figure 7.4: Change in solution pH as adsorption of heavy metals proceeds (3.7 g zeolite; 100 ml single component solution; particle size 1 – 3 mm).

The pH of the iron solution is not changing significantly with time; this is mainly due to the high initial concentration of iron (400 mg/l) and thus Fe^{3+} ions are preferentially adsorbed by natural zeolite to H^+ ions. Since little or no H^+ ions are being adsorbed, the solution pH remains almost constant throughout the reaction period.

7.3.4 Effect of initial solution concentration

The effect of initial concentration was investigated by contacting 3.7 g of natural zeolite with different concentrations of single component solutions ranging from 5 – 600 mg/l. An increase in concentration generally results in an increase in the amount of heavy metals adsorbed and the rate of adsorption. This may be a result of an increase in collisions between the reactants, leading to the observed increase in reaction rate and capacity according to the *Collision Theory* (Connors, 1990). The adsorption capacity will increase with an increase in initial concentration until the system reaches a saturation point, at which point further increase of the adsorbate (heavy metals) concentration will not result in any significant change in the amount adsorbed, q_e . Table 7.2 presents the results of this investigation.

Table 7.2: Effect of initial solution concentration on the adsorption capacity of natural zeolite. Total contact time: 360 minutes.

Heavy Metals	Initial Concentration (mg/l)	Amount Adsorbed, q_e (mg/g)	Percentage Adsorbed (%)
Iron	20	0.5	99.9
	40	1.1	99.8
	80	2.2	99.6
	120	3.2	98.6
	200	4.9	90.5
	300	6.6	80.9
	400	6.4	59.3
	600	6.5	40.3
Copper	10	0.3	100.0
	20	0.5	100.0
	40	1.0	95.9
	80	1.8	85.3
	100	2.3	84.1
	200	2.9	54.4
	400	3.3	30.6
	600	3.3	20.5
Manganese	5	0.1	93.0
	10	0.3	92.1
	20	0.5	92.1
	30	0.7	89.8
	40	0.9	85.2
	80	1.7	80.1
	120	2.3	71.7
	200	2.2	40.4
	400	2.4	22.2
	600	4.1	25.2
Zinc	20	0.5	99.9
	40	1.1	96.9
	80	1.8	80.8
	120	2.2	67.9
	200	3.0	55.9
	400	4.4	40.9
	600	4.9	30.7

The above results indicate that the amount of heavy metals adsorbed by natural zeolite at equilibrium is dependent on the initial metal concentration. The increase in the amount of metals adsorbed as initial concentration increases is a consequence of an increase in the

concentration driving force. The concentration driving force is important because it is responsible for overcoming the mass transfer resistance associated with the adsorption of metals from solution by the zeolite (Barrer, 1978). Therefore, as initial concentration increases, the driving force also increases resulting in an increase in metals uptake by the zeolite.

Table 7.2 also reveals that an increase in initial concentration not only results in an increase in the amount adsorbed (q_e) but a decrease in the efficiency of natural zeolite for the removal of heavy metals from solution. This can be seen by a general decrease in the percentage adsorption of the four heavy metals from about 100 % to 25 %, for an increase in initial concentration from 5 – 600 mg/l. Sprynskyy et al. (2006) also found a similar trend, that is, a decrease in efficiency, in their work on the adsorption of lead, copper, nickel and cadmium from solution by clinoptilolite.

7.3.5 Effect of agitation

Agitation is an important parameter in adsorption, the main reason for this being that agitation helps in overcoming the external mass transfer resistance. At higher agitation speeds, that is, rapid stirring of the solution, the mass transfer resistance related to ion diffusion through the liquid film surrounding the zeolite particles is reduced as the film thickness reduces due to agitation, resulting in greater metal uptake. Agitation of the mixture not only results in a decrease in film transfer resistance but also results in the abrasion of zeolite grains, producing freshly broken and highly reactive locations on the surface. So this mechanical effect increases the number of possible adsorption locations, resulting in an increase in the rate of adsorption (Trgo and Peric, 2003). However, the production of fine particles due to abrasion, has its disadvantages, mainly that it becomes increasingly difficult to separate the solids from the liquid (Inglezakis et al., 1999).

Agitation or mixing of the solution and zeolite was carried out using two methods. The first method was agitation in a reactor using a mechanical stirrer at different blade speeds (190 – 390 – 645 rpm) and the second was carried out in 300 ml bottles over a tumbling mill rotating at a speed of 110 rotations per minute. The results of the effect of agitation are shown in Figure 7.5.

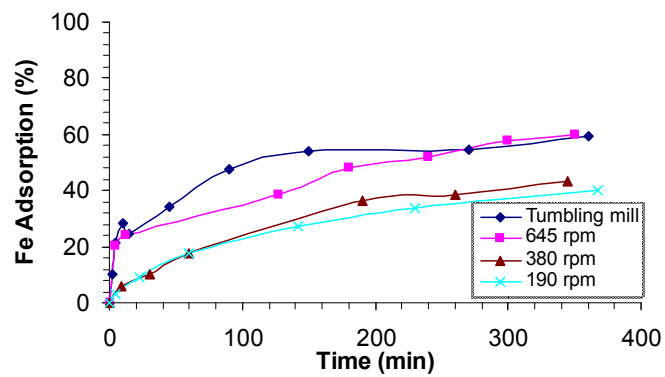
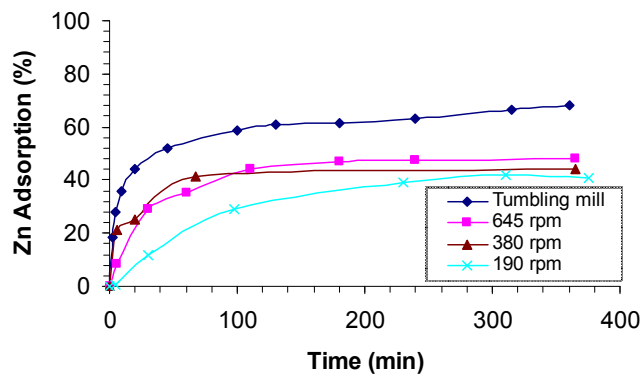
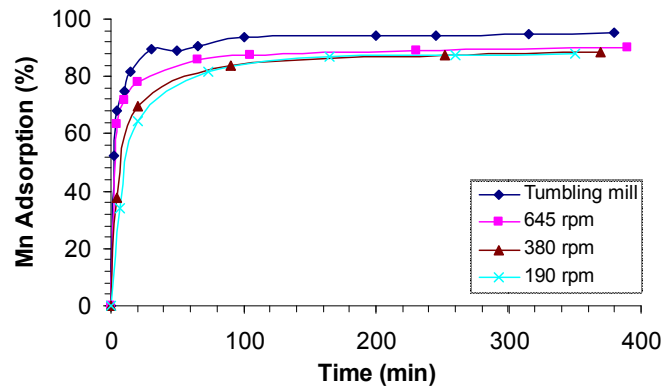
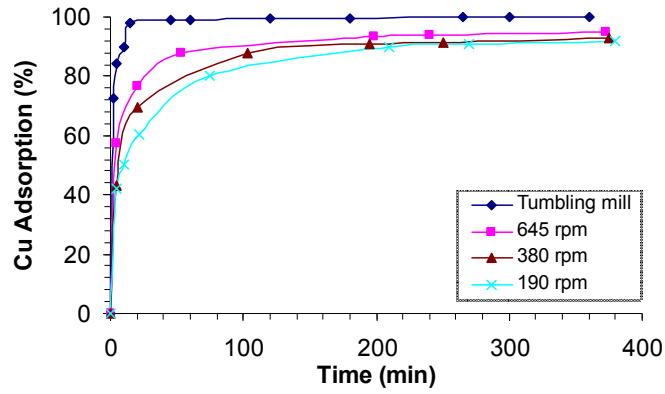


Figure 7.5: Effect of agitation on the adsorption of heavy metals by natural zeolite (3.7 g in 100 ml solution).

Figure 7.5 shows that the metal removal efficiency and rate increased as the speed of agitation increased. The difference in the amount removed from solution at the different speeds reduces with time; after about 400 minutes the total amount of copper and manganese removed at the different speeds is almost the same. Therefore, agitation apparently affects the rate of adsorption, and its effects are more observable at the beginning of the reaction.

7.3.6 Effect of competing cations

Industrial wastewater and acid mine drainage typically contain many different metal ions as a mixture. These ions have the potential to affect the effectiveness of an adsorbent in treating the wastewater; based on their competition for exchange sites on and in the adsorbent. Therefore, it is important to investigate the impact of competing cations on the removal of each pollutant from solution. Experiments were carried out to investigate the influence of the presence of competing cations on the individual adsorption of Cu^{2+} , Fe^{3+} , Zn^{2+} and Mn^{2+} from a solution containing a mixture of all 4 metal ions, by natural zeolite. Figure 7.6 compares the adsorption of each heavy metal ion from both single- and multi-component solutions.

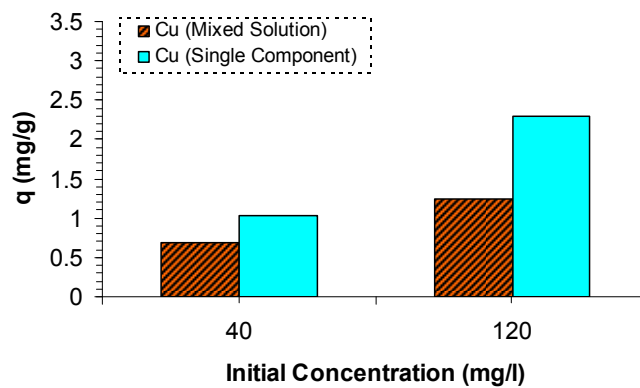
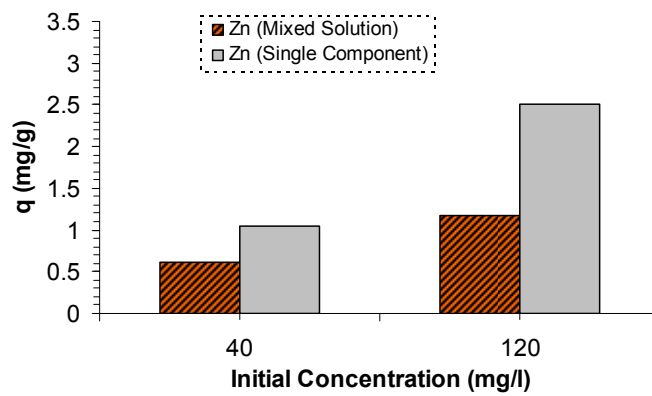
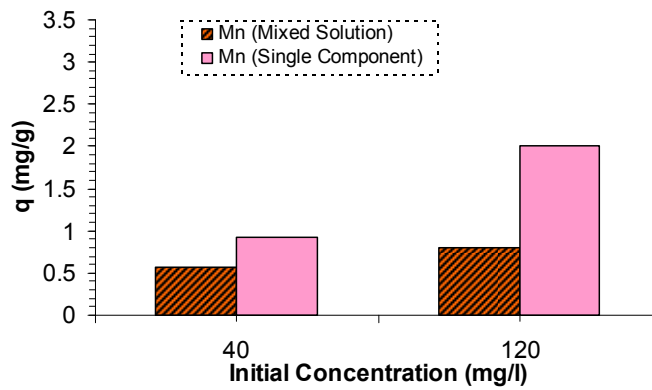
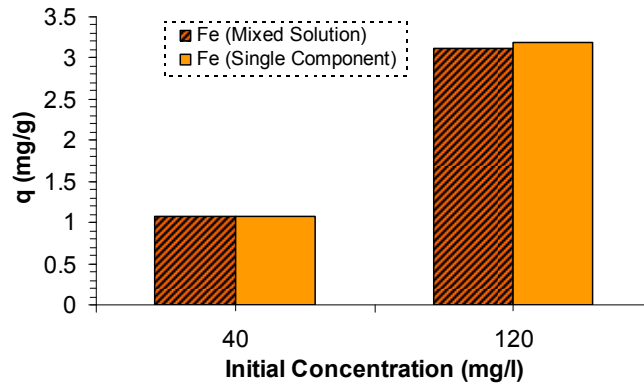


Figure 7.6: Comparison of the adsorption capacity of natural zeolite for iron, manganese, zinc and copper from single and multi – component solutions.

Figure 7.6 shows that the adsorption of Fe^{3+} was not significantly affected by the presence of competing ions. This may be because one of the mechanisms responsible for Fe^{3+} removal from solution is thought to be precipitation, from observation. Moreno et al. (2001) found that the precipitation of Fe^{3+} and Al^{3+} accounted for a sharp decrease in the concentration of these metals from solution in their treatment of AMD from the River Tinto (Spain) using zeolites. The adsorption of the other 3 cations was affected significantly: the amount adsorbed from multi-component solutions (initial concentration for each cation being 40 mg/l) decreased by 33%, 41% and 39% for Cu^{2+} , Zn^{2+} and Mn^{2+} respectively compared to their single component solutions at 40 mg/l. When the initial solution concentration for each cation was increased from 40 to 120 mg/l, the relative decrease in the amount adsorbed between the multi-component and single component solutions increased further. Moreover, the total amount of heavy metal ions adsorbed (all four cations) per unit mass of natural zeolite increased in all concentrations of multi-component solutions compared to the amount of solute adsorbed from single component solutions. This indicates that different adsorption mechanisms may be involved in the adsorption of each cation from solution (Amarasinghe and Williams, 2004).

7.3.7 Effect of thermal pre – treatment

Thermal pre – treatment of natural zeolite was performed in order to investigate whether pre – treatment could increase the adsorption capacity and rate of natural zeolite. Figure 7.7 shows how thermally pre-treating natural zeolite affected its efficiency in adsorbing heavy metals from solution. MTZ (15) and MTZ (30) are pre-treated natural zeolite samples that have been exposed to microwave radiation for 15 and 30 minutes respectively.

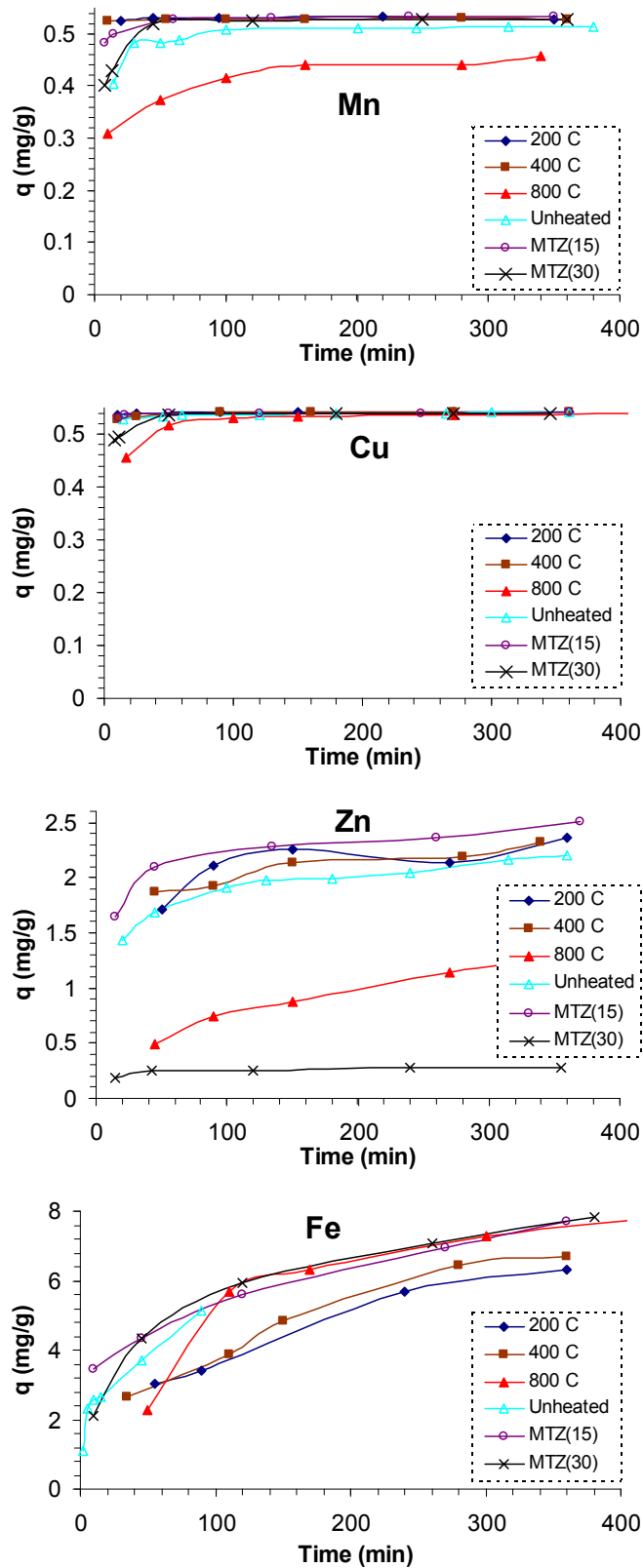


Figure 7.7: Comparison of natural and thermally pre – treated natural zeolite, 3.7 g mixed with 100ml single component solutions at pH 3.5.

For zeolite exposed to microwave radiation, the adsorption rate increased with exposure time, but to a limit. Rate of adsorption by zeolite exposed to microwave radiation begins to decrease as exposure time approaches 30 minutes, as shown for sample MTZ (30). Also, the rate of adsorption by calcined zeolite is faster compared to untreated zeolite, Figure 7.7, but the efficiency decreases for zeolite exposed to very high temperatures, 800 °C or more.

The increase in rate of adsorption and adsorption capacity as a result of thermal treatment may be a result of the removal of water from the internal channels of natural zeolite; this leaves the channels vacant and hence increases the adsorption capacity of the zeolite (Turner et al., 2000; Tatsuo and Nagae, 2003). The removal of water results in a change in the surface area of the samples after thermal pre – treatment, as shown in Table 7.3. Surface area measurements were determined by Nitrogen adsorption fitted to the BET equation (Brunauer, 1943) using TRISTAR 3000 apparatus from Micromeritics. The samples that were exposed to extreme thermal conditions had lower surface areas; this is due to the possible collapse of the porous zeolite structure (Akdeniz et al., 2007; Tatsuo and Nagae, 2005). When the structure collapses the porosity of natural zeolite decreases and thus the adsorption capacity is reduced since the heavy metal ions will no longer have access to exchangeable sites within the natural zeolite.

Table 7.3: Surface area of thermally pre – treated samples of natural zeolite.

Samples	Surface area (m²g⁻¹)
Natural Zeolite	15.879
<u>Microwave Heated Samples</u>	
MTZ (15)	16.601
MTZ (30)	15.400
<u>Furnace Heated Samples</u>	
200 °C	17.667
400 °C	14.331
800 °C	11.463

Surface area measurement, error $\pm 0.005 \text{ m}^2\text{g}^{-1}$.

The SEM micrographs in Figure 5.5 and 5.6 (*Characterisation section*) also show the difference in the surface of natural zeolite and zeolites exposed to extreme thermal conditions. The zeolites exposed to extreme thermal conditions have their surfaces almost smooth, with no pores or evident crystals. It is this loss of porosity which results in low surface area values being obtained for the samples exposed to extreme thermal conditions, as shown in Table 7.3.

7.4 Desorption/Regeneration studies

Desorption of heavy metal ions from an adsorbent or the regeneration of an adsorbent is of great practical importance. This is one of the characteristics that is considered in choosing an adsorbent for any practical application (Richardson et al., 2002). A favourable adsorbent is one that can be regenerated and re – used without a significant change in its adsorption efficiency after regeneration. Regeneration enables the reduction in volume of the waste material, which is of great practical and economic importance, as this reduces the storage costs and land utilisation.

In this study the regeneration of natural zeolite was carried out using sulphuric acid (2 %) and NaCl (20 g/l). The change in adsorption capacity of the natural zeolite was also investigated by contacting regenerated zeolite with single component solutions of the respective metal ions for 360 minutes.

7.4.1 Results and Discussion

Three adsorption – desorption cycles were performed for all 4 heavy metal ions. The desorption of the heavy metal ions was more effective using sulphuric acid at 40 °C compared to that at 22 °C or NaCl at 40 °C, as shown in Table 7.4.

Table 7.4: The percentage recovery of heavy metals from natural zeolite by regeneration.

Heavy Metals	% Recovered over 3 cycles		
	Acid (H ₂ SO ₄)		NaCl
	40 °C	22 °C	40 °C
Iron	56.37	42.07	12.72
Copper	84.51	62.19	50.47
Zinc	79.05	59.71	60.11
Manganese	88.65	73.91	70.35

Desorption takes place because of the displacement of the heavy metal ions from adsorption sites on the zeolite structure by either H^+ ions, in the case of acid or Na^+ ions from NaCl solution. This process is mainly driven by the concentration driving force, which favours H^+ and Na^+ ion adsorption because of the high solution concentrations used.

According to Table 7.4 it is evident that manganese is easily desorbed from the zeolite structure, this was expected since zeolite has a lower affinity for manganese as shown in the equilibrium studies earlier; hence it is easily displaced from the zeolite structure. Natural zeolite showed greater affinity for iron and zinc and hence their lower desorption efficiencies, as it is more difficult to displace them from the adsorption sites on zeolite. The desorption series is a reversal of the adsorption series; desorption series: $Mn^{2+} > Cu^{2+} > Zn^{2+} > Fe^{3+}$ and adsorption series: $Fe^{3+} > Zn^{2+} > Cu^{2+} > Mn^{2+}$.

The sulphuric acid used for desorption in all 3 cycles was recycled, this meant that the amount of metal ions in the acid increased and yet the volume of acid remained the same, thus a reduction in the volume of waste was achieved. The highly concentrated acidic solution could possibly be sold to a metal refinery, thus making revenue from the waste. Fresh sodium chloride was used for each new desorption cycle, since its regeneration efficiency was not very high.

The effect of regeneration on adsorption capacity was also investigated; the results are presented in Figure 7.8.

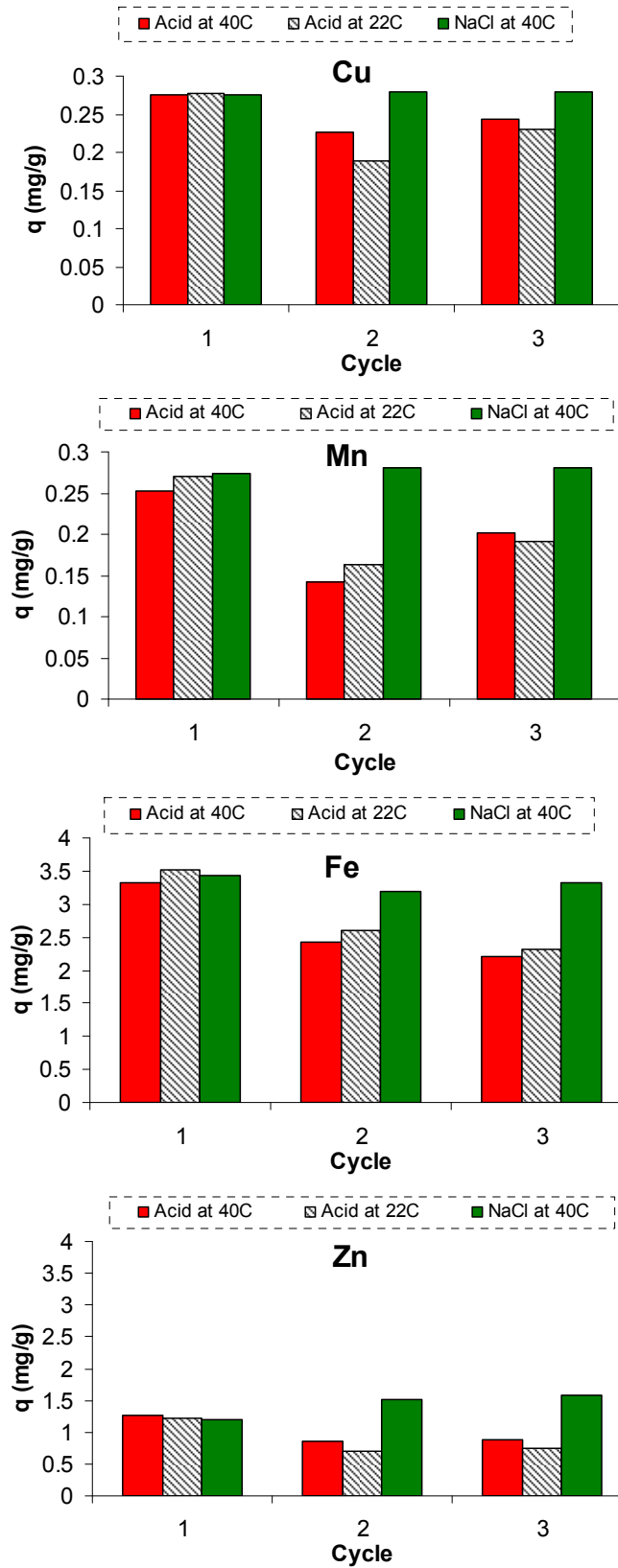


Figure 7.8: Change in the adsorption capacity of natural zeolite due to regeneration.

There is an observable drop in the adsorption capacity of natural zeolite that has been regenerated using sulphuric acid, as shown in Figure 7.8. The adsorption capacity of natural zeolite that has been regenerated using NaCl is either the same for the three adsorption stages or it increased slightly.

Table 7.5: Calculated percentage change in adsorption capacity over 3 cycles.

Heavy Metals	Average change in Adsorption capacity (%)		
	Acid (H ₂ SO ₄)		NaCl
	40 °C	22 °C	40 °C
Iron	- 20.2	- 19.8	- 3.2
Copper	- 9.8	- 16.4	+ 0.8
Zinc	- 20.4	- 27.1	+ 18.9
Manganese	- 21.4	- 22.8	+ 1.7

Table 7.5 shows the average percentage change in the adsorption capacity of natural zeolite for the 3 adsorption – desorption cycles. The adsorption capacities of acid-regenerated natural zeolite gave a negative change, since there was a drop in adsorption capacity from cycle 1 to 3, as seen in Figure 7.8. This drop in capacity may be due to the possible destruction of the zeolite structure by acid dissolution. The adsorption capacity of zeolite regenerated using NaCl was not negatively affected, actually the adsorption capacity for copper, zinc and manganese increased by 0.8%, 18.9% and 1.7% respectively. Inglezakis et al. (2001), Cincotti et al. (2006), Inglezakis and Grigoropoulou (2004) found that the adsorption capacity of natural zeolite increased when pre – treated with NaCl. Natural zeolite has a low preference for Na⁺ ions in comparison to most heavy metals; hence Na⁺ ions are easily displaced by heavy metals from the zeolite structure, thereby increasing the adsorption capacity of natural zeolite pre-treated with NaCl solution (Semmens and Martin, 1988; Kesraoui-Ouki et al., 1994; Curkovic et al., 1997).

7.5 Treatment of Synthetic Acid Mine Drainage (*sAMD*)

The potential of natural zeolite as an adsorbent for the treatment of acid mine drainage was determined using batch experiments. 3.7 g of natural zeolite was mixed with 100 ml solution of synthetic AMD (*sAMD*) for 360 minutes. The synthetic AMD was a mixture of all 4 heavy metals in a single solution, that is, Cu^{2+} , Fe^{3+} , Zn^{2+} and Mn^{2+} at a concentration of 20, 400, 120 and 20 mg/l respectively. A comparison was carried out for the removal of each metal ion from its single component solution and from *sAMD* as shown in Figure 7.9.

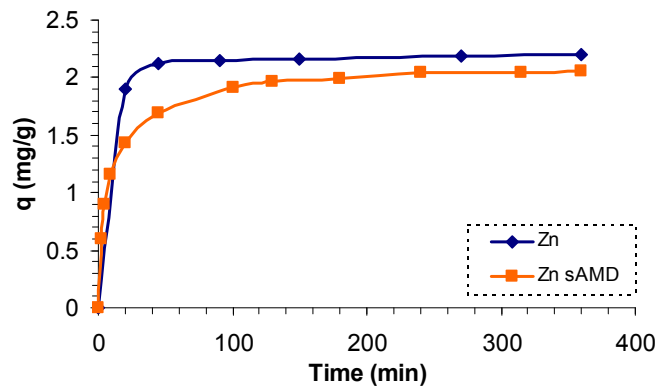
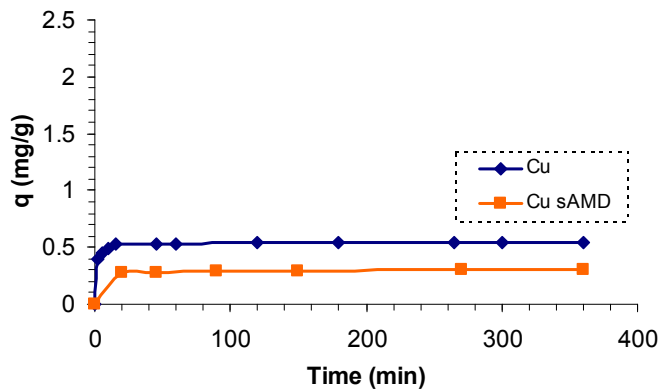
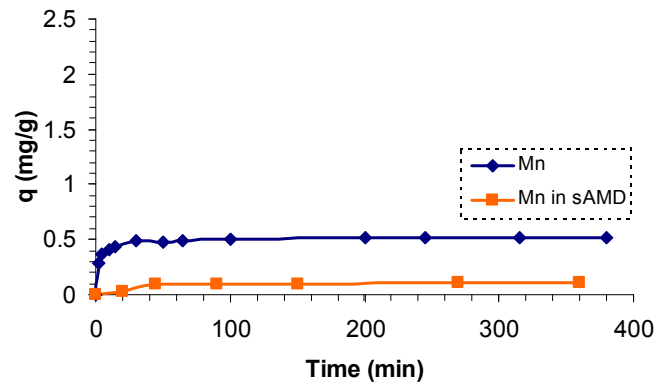
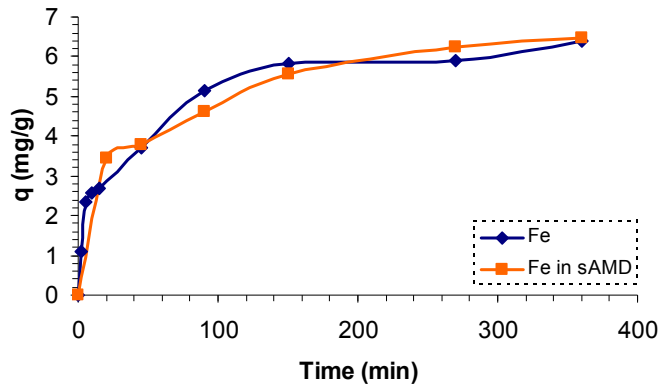


Figure 7.9: Comparison of adsorption capacities from single component solutions and from synthetic acid mine drainage (sAMD).

From the previous investigation on how adsorption is affected by the presence of competing cations, it was found that iron is the least affected of the 4 cations. The amount of Fe^{3+} ions adsorbed by natural zeolite from synthetic *AMD* was more or less equal to that adsorbed from its respective single component solutions. The order of adsorption from synthetic *AMD* was found to be: $\text{Fe}^{3+} > \text{Zn}^{2+} > \text{Cu}^{2+} > \text{Mn}^{2+}$, which is in agreement with the series obtained in equilibrium studies.

The above series shows that more Zn^{2+} ions were removed from synthetic *AMD* compared to Cu^{2+} and Mn^{2+} ions. The higher uptake of Zn^{2+} ions may be due to the higher concentration of Zn^{2+} (120 mg/l) compared to that of Cu^{2+} and Mn^{2+} , which is just 20 mg/l each. Thus the concentration driving force may be responsible for the greater adsorption capacity for zinc by natural zeolite.

Natural zeolite efficiently removed Zn^{2+} ions more than the other cations from synthetic *AMD*. Percent adsorptions of 63.1 %, 59.9 %, 56.8 % and 18.9 % for Zn^{2+} , Fe^{3+} , Cu^{2+} and Mn^{2+} respectively were achieved after 360 minutes contact with natural zeolite.

The final heavy metal concentration in synthetic *AMD* was 160.6, 38.6, 16.2 and 8.7 mg/l of Fe^{3+} , Zn^{2+} , Mn^{2+} and Cu^{2+} respectively, after mixing 3.7 g of natural zeolite with 100 ml *sAMD* solution for 360 minutes. These final concentrations fall short of the Environmental Quality Standard (EQS) values, which are 1.0, 0.5, 0.028 and 0.03 mg/l Fe^{3+} , Zn^{2+} , Cu^{2+} and Mn^{2+} respectively (Bone, 2003). A larger mass of zeolite, 15 g, was used and the final concentrations obtained were: 15, 29.1, 9.8 and 4.9 mg/l of Fe^{3+} , Zn^{2+} , Mn^{2+} and Cu^{2+} respectively. These concentrations still fall short of the EQS values, thus it is recommended that natural zeolite be used to treat relatively dilute solutions.

7.6 Kinetic Modelling

Kinetic modelling was carried out to investigate the rate controlling step in the removal of heavy metals from solution by natural zeolite. There are a number of possible rate controlling steps and these are (Helfferich, 1962):

- a. Diffusion of counter-ions in the external solution phase surrounding the particle (film diffusion control),
- b. Inter-diffusion of counter-ions within the exchanger itself (particle or intraparticle diffusion control),
- c. Chemical reaction at the sites of the functional group within the exchanger (chemical reaction kinetic control).

There are a number of kinetic models (Connors, 1990) that can be used to investigate the rate controlling step of a process, the following are the ones considered in this study:

- i. Pseudo second order kinetic model,
- ii. Nernst Plank model,
- iii. Vermeulen's approximation,
- iv. Furusawa and Smith's model.

7.6.1 Chemical Reaction control

The pseudo second order kinetic model was used to investigate whether chemical reaction at the adsorption sites of zeolite was rate controlling. The experimental data that fits to this model indicate that chemical reaction is involved in the removal of heavy metals from solution, that is, chemisorption (Amarasinghe and Williams, 2004). The

pseudo second order kinetic model is given by equation [4] and [5] (Amarasinghe and Williams, 2004),

$$\frac{dq}{dt} = k_2(q_e - q)^2 \quad (4)$$

$$\frac{t}{q} = \frac{t}{q_e} + \frac{1}{k_2 q_e^2} \quad (5)$$

Where q and q_e are the amount of metal adsorbed per unit weight of adsorbent (mg/g) at time t , and at equilibrium respectively. k_2 is adsorption rate constant. To test whether the rate of removal of heavy metals from solution by natural zeolite is controlled by chemical reactions (i.e. chemisorption) a number of conditions must be met. These conditions are (Harland, 1994):

- The rate constant should be constant for all values of initial concentration of counter-ions,
- The rate constant should not change with adsorbent particle size,
- The rate constant is *sometimes* independent of the degree of agitation (stirring rate).

If any of these conditions are not satisfied, chemical reaction kinetics is not rate controlling even if rate data is successfully fitted to the pseudo second order kinetic model.

7.6.1.1 Results and discussion

Batch adsorption tests were conducted by mixing 3.7 g of natural zeolite with 100 ml of single component solutions containing the desired concentration of heavy metal ions, at 22 ± 2 °C. Two of the above conditions were tested, that is, whether the rate constant

remains constant with a change in zeolite particle size and/or a change in agitation speed. The results obtained for the adsorption of Fe^{3+} , Cu^{2+} , Mn^{2+} and Zn^{2+} onto natural zeolite were fitted to equation [5]. This was achieved by plotting t/q versus t , as shown in Figure 7.10 and 7.11, and then tested for linearity.

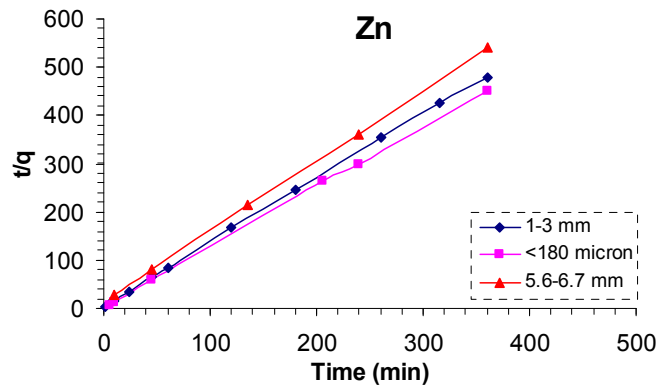
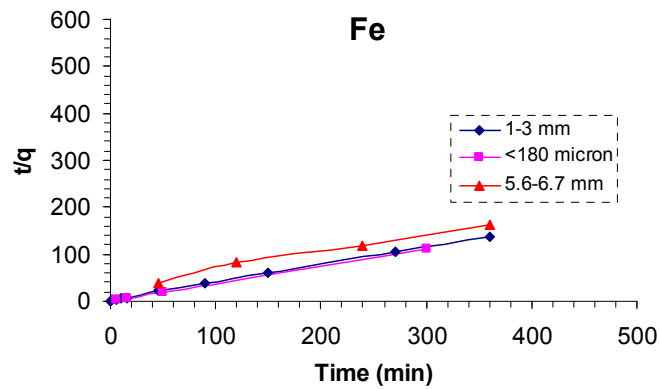
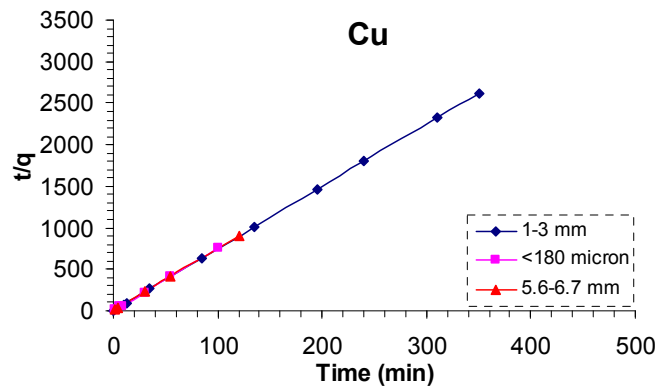
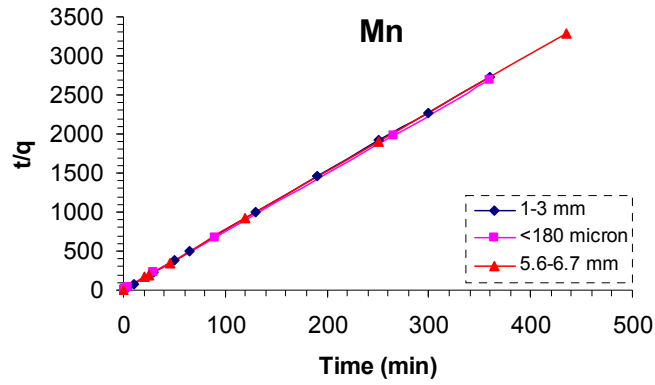


Figure 7.10: Effect of adsorbent particle size on the reaction rate constant.

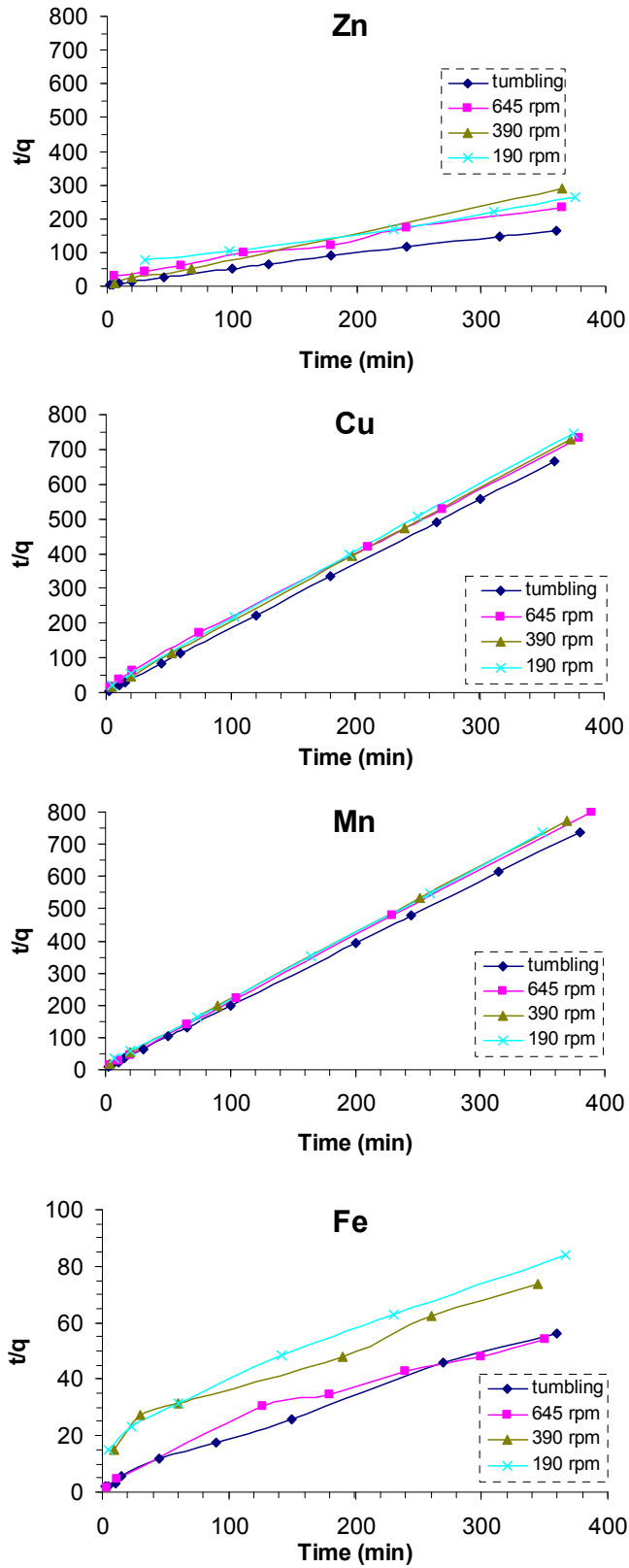


Figure 7.11: Effect of agitation speed on the reaction rate constant.

The experimental data (Figure 7.10 and 7.11) obtained for the effect of adsorbent particle size and effect of agitation speed gave a good fit to the pseudo second order kinetic model as expected, indicating that chemisorption does take place in the removal of heavy metals from solution by natural zeolite (Kocaoba et al., 2007; Bhattacharyya and Gupta, 2006). But from Table 7.6, it is seen that the rate constant, k_2 , for the removal of cations from solution, was not constant for different agitation speeds or adsorbent particle sizes. This lack of constancy is proof that even though the results gave a good fit to the kinetic model, the rate limiting step is not chemisorption. Bektas and Kara (2004) also found that the rate constant of the pseudo second order kinetic model varied for different agitation speeds (100 – 225 rpm) and adsorbent particle sizes (0.315-1.6 mm).

Table 7.6: Variation of rate constant with agitation speed and adsorbent particle size.

Heavy Metal	k_2 , rate constant ($\text{g mg}^{-1} \text{min}^{-1}$)						
	Adsorbent particle size			Agitation Speed			
	<180 μm	1-3 mm	5.6-6.7 mm	Tumbling Mill*	645 rpm	390 rpm	190 rpm
Fe³⁺	0.425	0.062	0.005	0.010	0.007	0.001	0.002
Cu²⁺	1361.804	142.060	123.253	2.660	0.222	0.585	0.389
Zn²⁺	1.120	0.591	0.152	0.046	0.017	0.211	0.012
Mn²⁺	45.477	11.562	4.388	0.853	0.872	0.481	0.333

*Tumbling Mill speed is 110 rotations per minute.

7.6.2 Film transfer diffusion control (external mass transfer)

Film transfer control was determined using a method proposed by Furusawa and Smith (1973). For film transfer resistance or control the main resistance is taken as that of the film diffusion of the metal ion across the boundary layer surrounding the adsorbent surface.

In a well agitated reactor, the concentration C of metal ions and concentration m_s of natural zeolite particles in the liquid are nearly uniform throughout the vessel. The change in C with respect to time is related to the fluid-particle mass transfer coefficient by the equations (Furusawa and Smith, 1973):

$$\frac{dC}{dt} = -k_s S_s (C - C_s), \quad [6]$$

$$C = C_0 \quad (t = 0), \quad [7]$$

Where k_s is the film mass transfer coefficient (cm s^{-1}), S_s is the outer surface of zeolite particles per unit volume of particle free slurry (cm^{-1}), C_s is the concentration in liquid at outer surface of particle and C_0 is the initial concentration of the bulk solution.

When intraparticle diffusion resistance is assumed to be negligible and the equilibrium isotherm is linear ($q = KC$),

$$m_s \frac{dq}{dt} = k_s S_s (C - C_s), \quad [8]$$

$$\frac{dq}{dt} = K \frac{dC_s}{dt}, \quad [9]$$

Where m_s is the mass of adsorbent particle per unit volume of particle free slurry (g cm^{-3}).

Furusawa and Smith solved equations [6 – 9], with initial conditions [7] and $q = 0$ at $t=0$ analytically, to give:

$$\frac{C}{C_o} = \frac{1}{1+m_s K} + \frac{m_s K}{1+m_s K} \exp\left[-\frac{1+m_s K}{m_s K} k_s S_s t\right], \quad [10]$$

Where K is the adsorption equilibrium constant (cm^3g^{-1}) and q is the amount of metal ions adsorbed onto natural zeolite (mgg^{-1}).

Equation [10] is applicable at $t = 0$ since the influence of intraparticle diffusion does not yet affect the results and since the isotherm becomes linear as $t \rightarrow 0$. Thus a plot of $\ln[(C/C_o) - (1/1+m_s K)]$ vs. t should give a straight line at $t = 0$. From the initial gradient/slope, $- [(1+m_s K)/(m_s K)] k_s S_s$, of the straight line, k_s can be evaluated. The outer surface area, S_s was obtained from:

$$S_s = \frac{6m_s}{d_p \rho_t (1 - \varepsilon_p)}, \quad [11]$$

Where d_p is the diameter of the zeolite particles (cm), ρ_t is the density of solid phase (gcm^{-3}) and ε_p is the porosity of the zeolite particles.

7.6.2.1 Results and discussion

Batch adsorption tests were conducted by mixing 3.7 g of natural zeolite with 100 ml of single component solutions containing the desired concentration of heavy metal ions, at 22 ± 2 °C. The results of the experiments were fitted to the model proposed by Furusawa and Smith.

Rearranging equation [10], and plotting $\ln[(C/C_0) - (1/(1+m_sK))]$ vs. time, should give a straight line. The gradient of the straight line is $- [(1+m_sK)/(m_sK)] k_s S_s$; the mass transfer coefficient between the bulk liquid and outer surface of the zeolite particle, k_s can then be evaluated. To determine how good the model fits the experimental data a plot of (C/C_0) versus time was made, Figure 7.12.

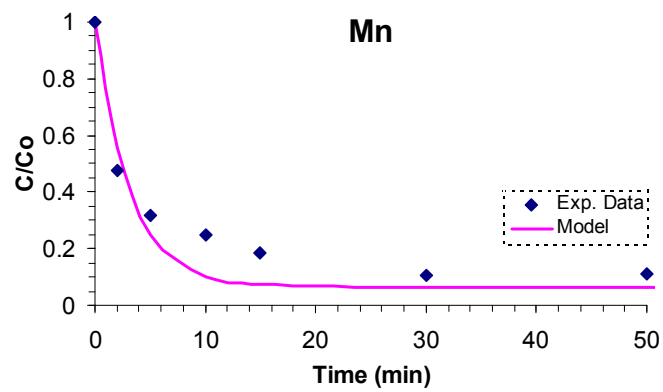
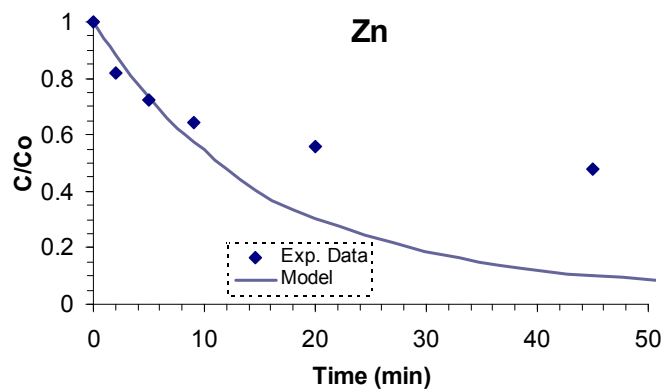
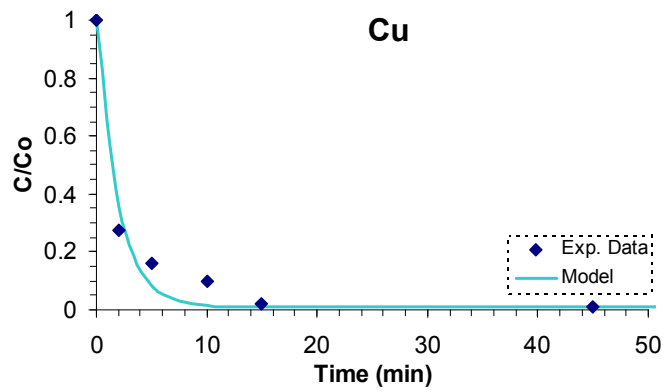
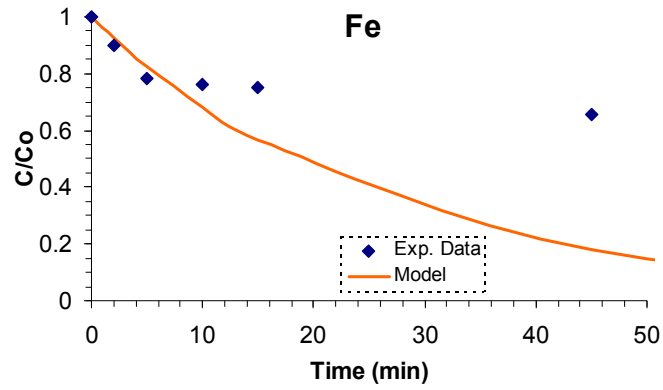


Figure 7.12: Fitting film transfer diffusion control model to the experimental results.

The fit was evidently not good for all the heavy metals, thus the rate controlling step during the adsorption of these heavy metals from solution by natural zeolite is not film resistance control. The trend in the removal of Cu^{2+} and Mn^{2+} shows a seemingly different trend to that of Zn^{2+} and Fe^{3+} , this is because most of Cu^{2+} and Mn^{2+} ions were removed within the first 20 to 30 minutes of reaction. Figure 7.12 clearly shows that for this *active* period (2 – 30 min), the removal of these two cations did not fit the film transfer control model.

Moreover, Figure 7.12 also shows that the film resistance model fits very well with all the cations as the process begins, this is expected since at these times ($t \rightarrow 0$) intraparticle diffusion will be negligible, and thus film resistance will be the more prominent of the two. The mass transfer coefficients for iron, copper, zinc and manganese removal from their single component solutions by natural zeolite are given in Table 7.7.

Table 7.7: Calculated film mass transfer coefficients.

Heavy Metals	k_s (cm s^{-1})
Iron	4.40×10^{-4}
Copper	5.95×10^{-3}
Zinc	5.75×10^{-4}
Manganese	3.50×10^{-3}

7.6.3 Intra – Particle diffusion control

The rate of adsorption, desorption, and ion exchange in porous materials are generally thought to be controlled by mass transport within the pore network/channels, rather than the kinetics of sorption or ion exchange itself (Erdem et al., 2004). Therefore, the most important parameter would be the pore/intraparticle diffusion coefficient.

There are a number of simplified models for the estimation of intraparticle diffusion coefficients, in this study only the Vermeulen's and Nernst-Plank's approximations were considered.

Assumptions (Inglezakis et al., 2001):

The zeolite particles are spherical containing counterion A^+ ; these are agitated in a solution of B^+ ions. It is assumed that the mixing is perfect and thus the composition in the bulk liquid phase is assumed constant throughout the reactor. B^+ ions diffuse from the bulk solution into the zeolite particles and are exchanged with the A^+ ions. Intraparticle diffusion is considered to be the rate limiting step.

Isotopic Exchange

The adsorption process is assumed to be isotopic exchange, that is, it is assumed that the diffusion coefficient is constant. The equation to be solved is (Inglezakis et al., 2001):

$$\frac{\partial C'_A}{\partial t} = D' \left(\frac{\partial^2 C'_A}{\partial r^2} + \frac{2}{r} \frac{\partial C'_A}{\partial r} \right), \quad [12]$$

With initial conditions:

$$C'_A(r) = 0 \quad \text{For } r > r_0 \text{ and } t = 0, \quad [13]$$

And

$$C'_A(r) = C' = \text{const} \quad \text{For } 0 < r < r_0 \text{ and } t=0, \quad [14]$$

Where C'_A is the solid phase concentration of ion A (equiv cm^{-3}), D' is the isotopic surface diffusion coefficient, constant throughout the process (cm^2s^{-1}), t is the time (s), r is the particle radius (cm), C' is the initial solid phase concentration of A ions (equiv cm^{-3}) and r_0 is the particle radius (cm).

Two boundary conditions can be considered, which are the infinite solution volume and the finite solution volume. For this study the appropriate boundary condition is the *infinite solution volume* which assumes that the concentration of A in the solution remains negligible throughout the process (Helfferich and Plesset, 1958). This assumption is true if a solution of constant composition is continuously passed through a thin layer of beads (shallow bed technique) or in *batch systems*, if solution volume is so large that the ratio of exchangeable ions in the solid phase to those in the liquid phase is much less than unity (single particle technique).

7.6.3.1 Vermeulen's Approximation

The solution of [12] is (Helfferich and Plesset, 1958):

$$U(t) = 1 - \frac{6}{\pi^2} \sum_{n=1}^{\infty} \frac{1}{n^2} \exp(-n^2 \pi^2 T), \quad [15]$$

Where $T = D't/r_0^2$ (dimensionless) and $U(t)$ is the fractional attainment of equilibrium in the ion exchanger (natural zeolite) at time t , defined as:

$$U(t) = \left(\frac{C_o - C(t)}{C_o - C_\infty} \right), \quad [16]$$

C_o is the initial metal concentration, $C(t)$ is the metal concentration a time (t) and C_∞ is the equilibrium metal concentration.

Instead of equation [15], Vermeulen's approximation can be used:

$$U(t) = [1 - \exp(-\pi^2 T)]^{0.5}, \quad [17]$$

Vermeulen's approximation is widely applied in related literature (Srivastava et al., 1989; Ames, 1965; Inglezakis et al., 2001), mainly in the case of the exchange of isotopes on resins.

7.6.3.2 Nernst – Plank's Model

The Nernst – Plank model incorporates the effect of the existence of an electric field generated by the motion of cations during the diffusion process, since there has to be a conservation of *electro – neutrality* during diffusion (Helfferich, 1962). Infinite solution volume is also assumed. The equation to be solved is:

$$\frac{\partial C'_A}{\partial t} = \frac{1}{r^2} (r^2 D'_{AB} \left(\frac{\partial C'_A}{\partial r} \right)), \quad [18]$$

Where

$$D'_{AB} = \frac{D'_A D'_B (z_A^2 C'_A + z_B^2 C'_B)}{z_A^2 C'_A D'_A + z_B^2 C'_B D'_B}, \quad [19]$$

D'_{AB} is the solid phase inter-diffusion coefficient (cm^2s^{-1}), D'_i is the solid phase self-diffusion coefficient of ion i (cm^2s^{-1}), C'_i is the solid phase concentration of ion i (equiv cm^{-3}), and z_i is the ionic charge of ion i (dimensionless).

The pertinent equations for solid diffusion control are solved with numerical methods and the results are expressed by Nernst – Plank's approximation, for complete conversion of solid to B^+ form,

$$U(t) = [1 - \exp(m)]^{0.5}, \quad [20]$$

Where

$$m = \pi^2 [c_1 T_A + c_2 T_A^2 + c_3 T_A^3], \quad [21]$$

Where $T_A = D'_A t / r_0^2$ (dimensionless), and the constants c_1 , c_2 , and c_3 are functions of a , where $a = D'_A / D'_B$, $1 \leq a \leq 20$. These constants depend on the type of ions involved in the ion exchange.

For univalent-bivalent exchange:

$$c_1 = -\frac{1}{0.64 + 0.36a^{0.668}}, \quad [22]$$

$$c_2 = -\frac{1}{0.96 - 2a^{0.4635}}, \quad [23]$$

$$c_3 = -\frac{1}{0.27 + 0.09a^{1.14}}, \quad [24]$$

If $a = 1$, isotopic exchange is presumed with the inter-diffusion coefficient D'_{AB} equal to the self-diffusion coefficients of each ion.

7.6.3.3 Results and discussion

Experimental results from the reaction of 3.7 g of natural zeolite and 100 ml single component solution were fitted to the Vermeulen's approximation and Nernst Plank model. The particle size of natural zeolite used was in the range 1 – 3 mm.

Vermeulen's Approximation:

The diffusion coefficient of the natural zeolite was calculated by rearranging equation [17], and plotting $-\ln[1-U(t)^2]$ vs. time, this should give a straight line with gradient equal to $\pi^2 D' / r_o^2$.

The time in seconds required to attain 50 % of equilibrium, $t_{1/2}$ is calculated as follows (Ames, 1965):

$$t_{1/2} = (0.030) \frac{r_o^2}{D'} \quad [25]$$

The diffusion coefficients of the heavy metals under investigation in this study are summarized in Table 7.8.

Table 7.8: Summary of the diffusion coefficients calculated from Vermeulen's approximation for natural zeolite.

Heavy Metals	$D' \text{ (cm}^2 \text{ s}^{-1}\text{)}$	R^2
Zinc	8.64×10^{-8}	0.92
Iron	1.05×10^{-7}	0.99
Manganese	1.74×10^{-7}	0.86
Copper	2.63×10^{-7}	0.67

The coefficients in Table 7.8 were substituted into the Vermeulen's approximation and the model was fitted to the experimental results, plot of $U(t)$ vs. time, Figure 7.13.

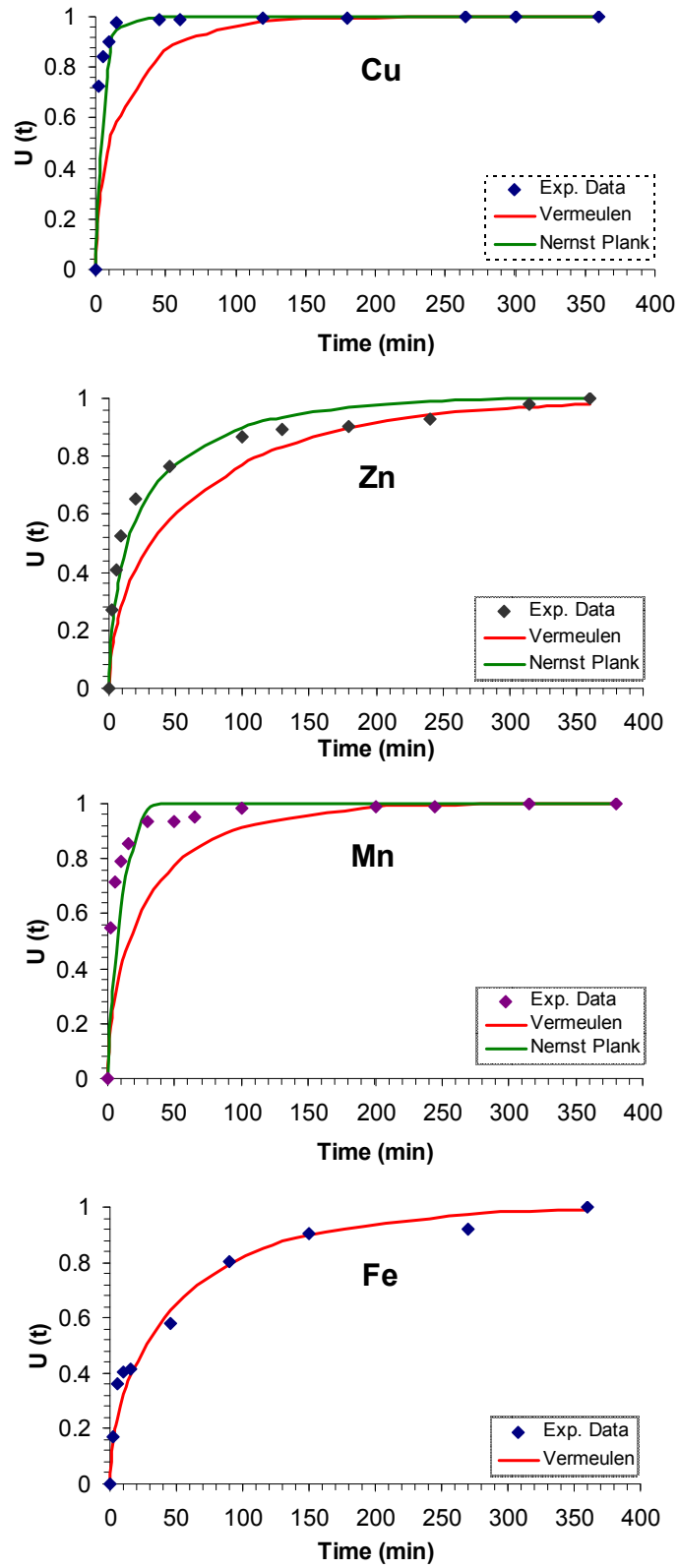


Figure 7.13: Intraparticle diffusion control: Vermeulen's versus Nernst-Plank's approximations.

Nernst-Plank's Model

The values of the diffusion coefficients obtained from the Nernst-Plank's approximation are presented in Table 7.9.

Table 7.9: Diffusion coefficients determined using the Nernst-Plank's Approximation.

Heavy Metals	D` (cm ² s ⁻¹)	t _{1/2} (min)	R ²
Copper	2.74 x 10 ⁻⁷	10.26	0.94
Manganese	1.64 x 10 ⁻⁷	17.13	0.98
Zinc	1.77 x 10 ⁻⁷	15.88	0.99
Iron	* -----	---	---

* No formula could be found for univalent-trivalent exchange.

The Nernst Plank's approximation gave a better fit compared to the Vermeulen's approximation for most of the cations, as shown by the R² values in Table 7.8 and 7.9. This is because the Nernst-Plank model does not neglect the effect of the *electric potential gradient* on the ionic fluxes (Helfferich, 1962). The above results show that the adsorption process is significantly affected by intraparticle diffusion. Similar results were also obtained by other researchers using natural zeolite (Cooney et al., 1999; Kocaoba et al., 2007; Barrer et al., 1967; Ames, 1965; Inglezakis and Grigoropoulou, 2001).

The hydration radii of the cations are: r_HZn²⁺ = 4.30Å, r_HFe³⁺ = 4.57Å, r_HCu²⁺ = 4.19Å and r_HMn²⁺ = 4.38Å (Nightingale, 1959). The smallest particles should ideally be adsorbed faster and in larger quantities compared to the larger particles, since the smaller particles can pass through the micropores and channels of the zeolite structure with ease (Erdem et al., 2004). According to the results shown in Table 7.9, the rates of diffusion are in the sequence: Cu²⁺ > Zn²⁺ > Mn²⁺; this is in agreement with the hydration radii of the cations.

7.6.4 Interruption Tests

These tests were performed to determine experimentally the rate controlling mechanism; that is, to distinguish between film transfer control and intraparticle diffusion control (Kocaoba and Akcin, 2008; Harland, 1994; Helfferich, 1962). These were carried out in the same way as the batch kinetic experiments (3.7 g zeolite and 100 ml solution agitated), with the exception that, after about 7 minutes of contact, the natural zeolite was separated from solution for about 5 minutes. After the period of interruption the natural zeolites were re-immersed into the solution and agitation continued. By removing zeolite from the solution, sufficient time is given for the concentration gradients in both phases to relax. Since intraparticle diffusion is much slower than film diffusion, when the exchange process is resumed (by re-immersing the zeolite into the solution) a relatively long period of time is required for a pre-interruption gradient to be re-established. As a result, the rate just after exchange begins is much higher than before the interruption if intraparticle diffusion is rate controlling as shown in the schematic, Figure 7.14. Samples of solution were taken before and after interruption and analysed using the AAS.

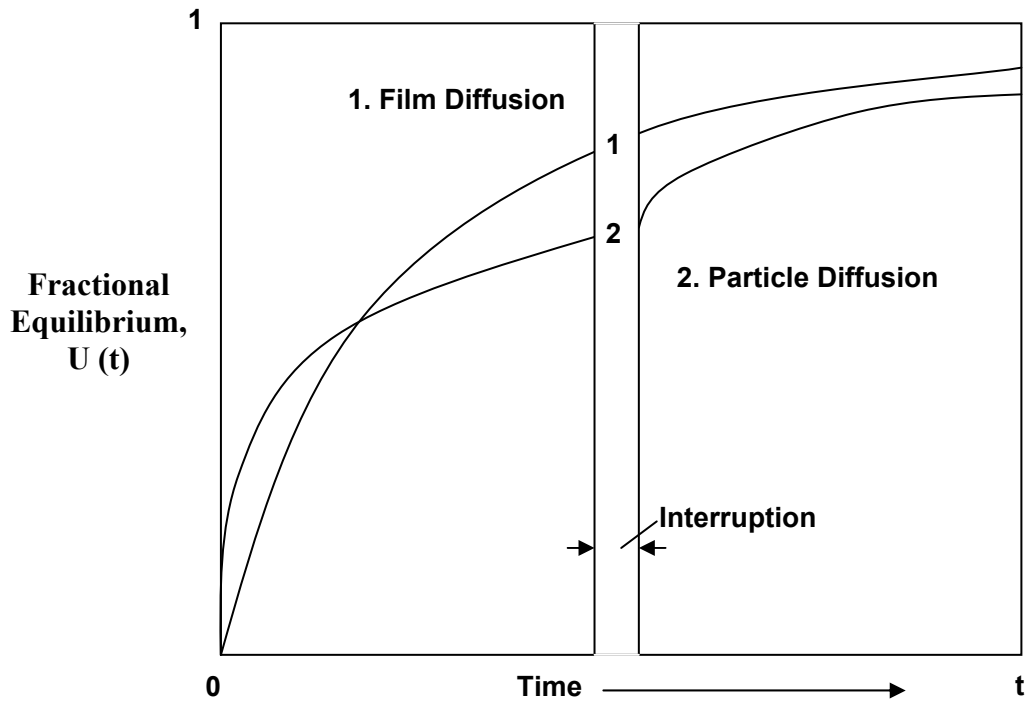


Figure 7.14: The effect of interruption upon the rate of exchange according to controlling diffusion mechanism (schematic) (Harland, 1994).

For each experiment, fractional attainment, U was plotted against time, t . U was calculated from equation [16].

7.6.4.1 Results and discussion

The results of the interruption tests performed indicate that intraparticle diffusion is rate controlling for the removal of heavy metals from solution by natural zeolite, Figure 7.15.

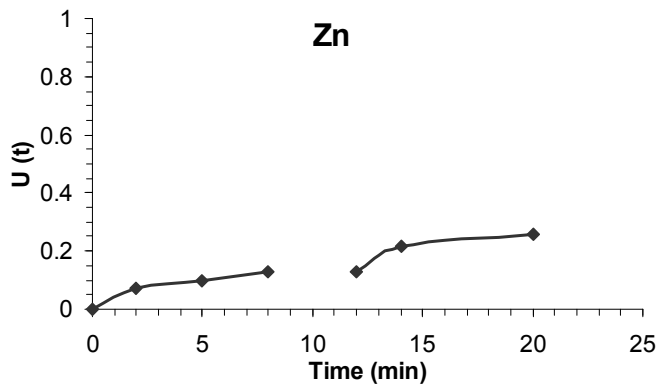
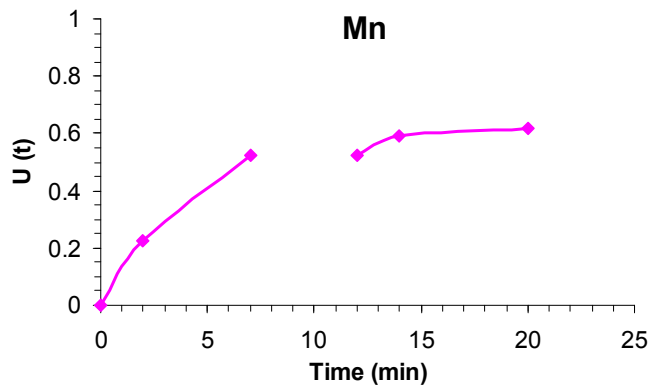
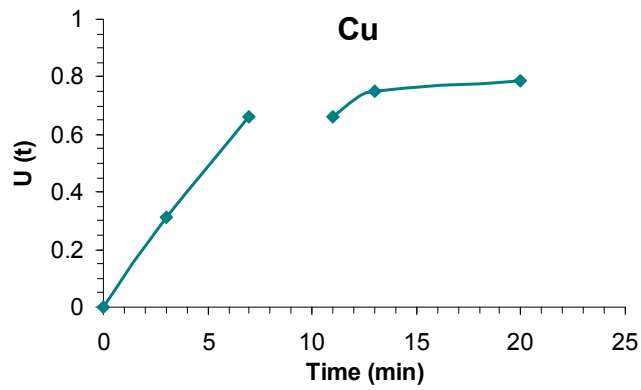
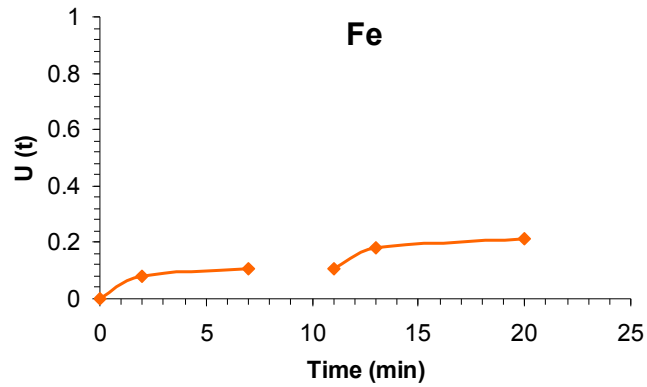


Figure 7.15: Interruption tests on the removal of heavy metals from solution by natural zeolite (3.7g natural zeolite, 100 ml single component solution, pH 3.5).

Figure 7.15 shows that the rate of adsorption of the heavy metals generally increased rapidly just after the natural zeolite was placed back into the solution, that is, after the interruption period, indicating that intraparticle diffusion is the rate controlling step. Cooney et al. (1999) also found similar results using natural zeolite from Australia.

7.7 Conclusion

The results of kinetic studies revealed that operational conditions such as rate of agitation, initial solution pH and concentration, adsorbent particle size, the presence of competing cations etc, are able to affect the adsorption capacity and efficiency of natural zeolite.

Adsorption was favoured by higher agitation speed, high pH values and smaller particle sizes. An increase in the initial solution pH from 2.5 to 4.5 resulted in an increase in the equilibrium adsorption capacity, q_e , of natural zeolite for Mn^{2+} , Zn^{2+} and Cu^{2+} by 43%, 34% and 23% respectively. Therefore, the efficiency of natural zeolite for metal adsorption is dependent on the initial solution pH.

An increase in the initial solution concentration resulted in more metals being adsorbed from solution until saturation point; but the adsorption efficiency of natural zeolite was drastically reduced from about 100% to 25% with an increase in concentration from 10-600 mg/l. Thermal pre – treatment resulted in an increase in adsorption capacity and efficiency of zeolite, but exposure to extreme thermal conditions led to the collapse of the porous structure of natural zeolite, which consequently reduced the effectiveness of natural zeolite.

The effect of competing cations was also investigated and it was observed that the adsorption of Fe^{3+} was not significantly affected by the presence of competing ions. This may be because one of the mechanisms responsible for Fe^{3+} removal from solution is thought to be precipitation. The other 3 heavy metals were significantly affected by the presence of competing cations: the amount adsorbed from multi-component solutions, decreased by 33%, 41% and 39% for Cu^{2+} , Zn^{2+} and Mn^{2+} respectively compared to that from single component solutions.

Both sulphuric acid, 2 % (wt.) and NaCl (20 g/l) were successfully used to regenerate natural zeolite. Sulphuric acid at 40 °C gave better desorption efficiencies compared to those from sulphuric acid at 22 °C and NaCl at 40 °C. Regeneration resulted in a decrease in the adsorption capacity of natural zeolite. For example, over 3 cycles of adsorption-desorption, the adsorption capacity of natural zeolite for iron, copper, zinc and manganese decreased by approximately 20.2, 9.8, 20.4 and 21.4 % respectively. This may be due to the destructive nature of sulphuric acid.

The rate limiting step for the removal of heavy metals from solution by natural zeolite was found to be intraparticle diffusion. The Nernst-Planck model gave a good fit of the experimental results; the correlation coefficient, R^2 , for the heavy metals ranged from 0.94 – 0.99. Moreover, interruption tests also proved that intraparticle diffusion was the rate limiting/controlling step.

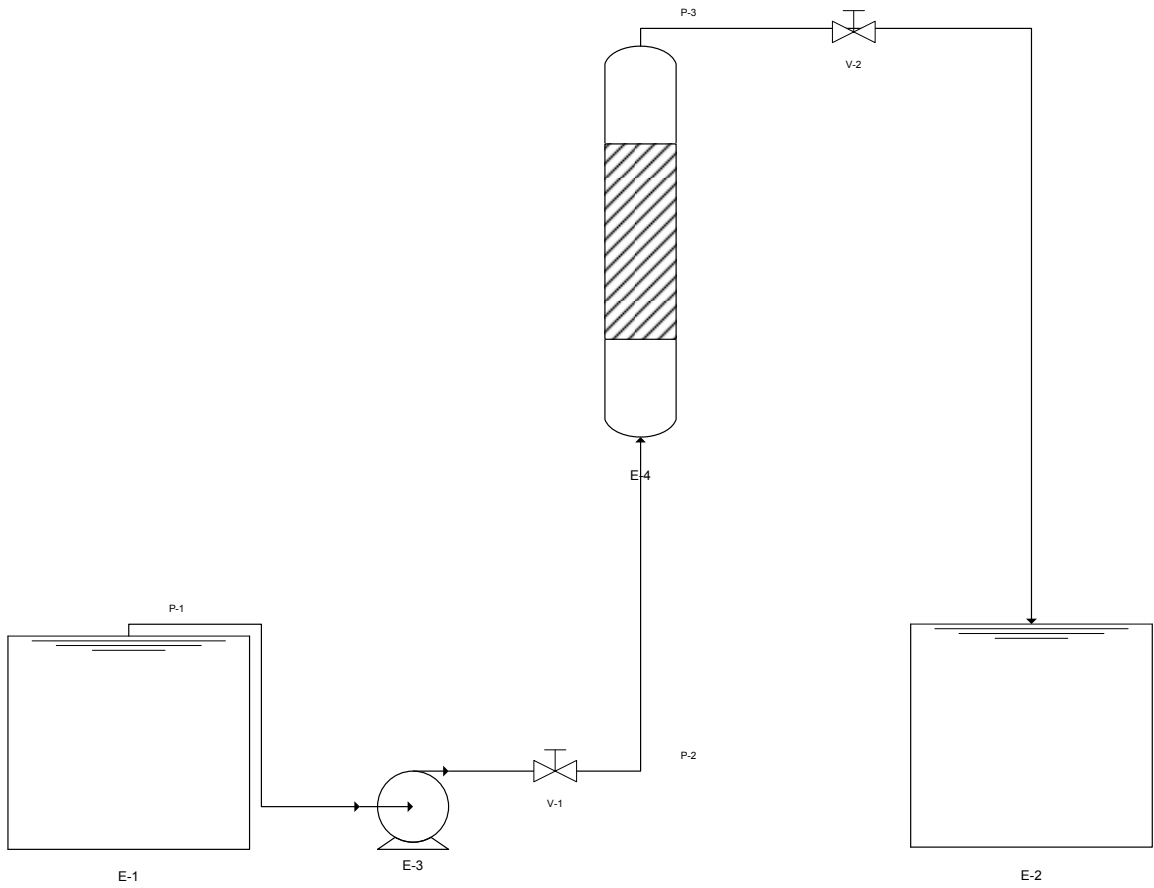
CHAPTER 8

COLUMN STUDIES

8.1 Introduction

Batch adsorption tests/studies provide information on adsorption equilibrium characteristics and adsorption kinetics, which is important in determining the effectiveness of the adsorbent in removing solute from solution. However, batch operations are not often economical in practice and the data obtained from these is not sufficient to give accurate scale – up data required in the design of industrial adsorption columns. Therefore, column studies have to be performed, whereby the most important parameter to be determined is the column breakthrough curve, which determines the operating life span of the fixed adsorbent bed.

In this chapter, fixed bed columns (Figure 8.1) packed with natural zeolite were used for the continuous removal of heavy metals from their respective single component solutions. The system variables or parameters studied include solution flow rate and bed height. Synthetic acid mine drainage, sAMD, which is a mixture of iron, copper, zinc and manganese with concentrations similar to those found in real AMD, was also treated using fixed bed columns. The metal loaded natural zeolite was regenerated using 2% (w/w) sulphuric acid at 40 °C.



Vessel Catalogue:

E-1 and E-2:	Solution storage tanks (25 L),
E-3:	Watson Marlow peristaltic pump,
E-4:	Fixed bed column, packed with natural zeolite,
V-1 and V-2:	Control valves,
P-1, P-2, and P-3:	Connecting pipelines.

Figure 8.1: Schematic diagram of the column set – up.

8.2 Breakthrough Curves

All the design models of fixed bed columns are based on determining the breakthrough curves for the specific system. The breakthrough curve depicts the time or volume of effluent treated versus the effluent concentration or dimensionless concentration, C_t/C_o , at different bed heights; hence it describes the performance of any fixed bed column. The characteristic shape of this curve will depend on the equilibrium between the solid and liquid phase, based on the kinetic adsorption process, which is divided into four stages; that is, diffusion in bulk fluid, external mass transfer, intraparticle diffusion and micro-pore diffusion (Moreno-Pirajan et al., 2006). From this curve it is possible to determine the time the adsorbent material will be able to sustain removing a specified amount of solute from solution before it needs regeneration or replacement, this period of time is called the service time of the bed.

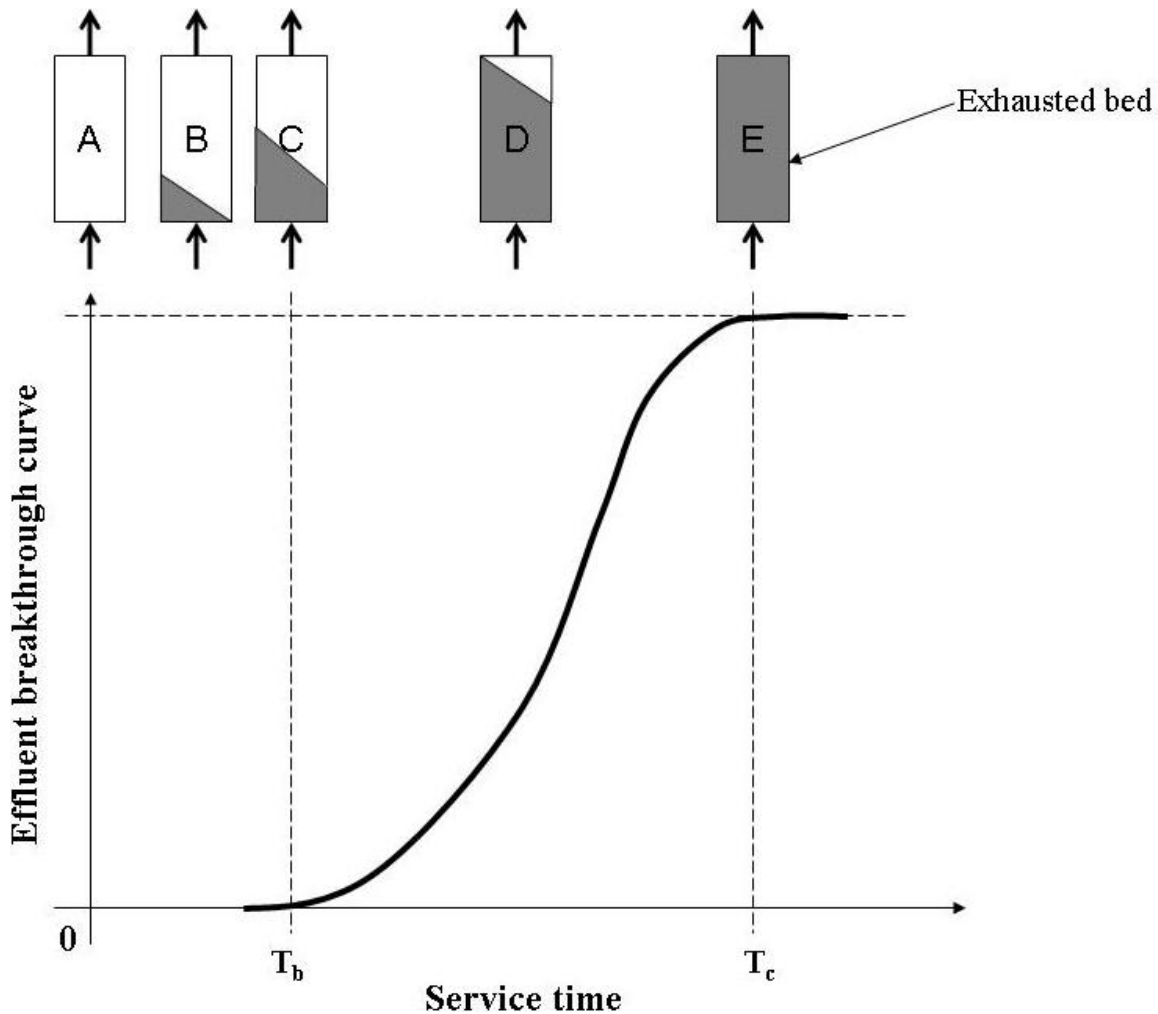


Figure 8.2: Schematic representation of the displacement of the adsorption zone or mass transfer zone and the resulting breakthrough curve (Harland, 1994).

Figure 8.2 can be used to describe how the breakthrough curve is established in a fixed bed column. Solution at solute concentration, C_0 enters the column and a concentration gradient is established within a finite zone, that is, the adsorption or mass transfer zone. In this zone the concentration of solution changes from C_0 to C_e , where C_e is close to zero. The loading of solute on the solid (adsorbent) also increases within the mass transfer zone until the solid is completely saturated. Since the system is a dynamic one, the mass transfer zone moves steadily from the influent end of the column to the outlet end. Figure 8.2 shows how the mass transfer zone moves along the column, from column

A, where the adsorbent is not yet in contact with the solution, to column E where the adsorbent is completely exhausted after time T_c . Time T_b represents the breakthrough point, where traces of solute start to be detected in the effluent from the column outlet.

The area above the breakthrough curve is a measure of the bed capacity, BC. The bed capacity can be calculated as follows (Treybal, 1980):

$$BC = Q_v \int_0^T (C_o - C) dt \quad (1)$$

Where Q_v is the flow rate, l/min; C_o and C are the inlet and outlet concentrations in mg/l at time, t respectively. T is the actual time required for full bed exhaustion. If the adsorption is infinitely rapid an ideal breakthrough curve will be a step change, and from these curves, T_s can be calculated, which is the time required for full bed exhaustion under ideal conditions (Amarasinghe and Williams, 2007; Cooney, 1998).

Usually in industry the column is stopped when the outlet concentration reaches a certain maximum allowable level, and at this breakthrough point the bed will not be fully utilized. The equivalent length of unused bed, LUB, is given by (Treybal, 1980):

$$LUB = \frac{Z}{T_s} (T_s - T_b) \quad (2)$$

The bed capacity, BC, is then given by:

$$BC = Q_v (C_o - C^*) T_s \quad (3)$$

Where Z is the bed height, cm, C^* is the concentration of the solution in equilibrium with the fresh adsorbent or concentration of the solution that initially comes out of the column, mg/l, T_b is the breakthrough time, min.

8.3 Modelling of fixed bed columns

The data collected from fixed bed column laboratory experiments serve as the basis for the design of full scale adsorption columns. A number of mathematical models have been developed for design purposes, among these, is the bed depth service time (BDST) model. This model has been successfully used in describing and predicting heavy metal column adsorption using different adsorbents (Jusoh et al., 2007; Ko et al., 1999; Cortes-Martinez et al., 2008; Mohan and Sreelakshmi, 2008).

8.3.1 Bed depth service time model

For an ideal fixed bed column with a single solute in dilute solution, the service time of the column can be expressed as a function of operational parameters. A simple approach has been proposed to correlate the service time, t , with the process variables. This approach or model is called the bed depth service time (BDST) model. The original work on the BDST model was carried out by Bohart and Adams (1920) who proposed a relationship between bed depth, Z , and the time taken for breakthrough to occur. The service time, t , is related to process conditions and operating parameters by the following equation (Bohart and Adams, 1920):

$$\ln\left(\frac{C_o}{C_b} - 1\right) = \ln\left(e^{K_a N_o Z / u} - 1\right) - K_a C_o t \quad (4)$$

Hutchins (1974), proposed a linear relationship between the bed depth and service time, which can be written as follows:

$$t = \frac{N_o Z}{C_o u} - \frac{1}{K C_o} \ln\left(\frac{C_o}{C_b} - 1\right) \quad (5)$$

Where, t is the service time at breakthrough point, min; C_o and C_b are the initial solute concentration and effluent solute concentration respectively, mg/l; u is the linear velocity, cm/min; K adsorption rate constant, l/(mg.min); N_o is the dynamic adsorption capacity, mg/l and Z column bed depth, cm.

Equation [5] shows how the service time and bed depth are correlated with the process parameters and initial solute concentration, solution flow rate and adsorption capacity.

This equation can also be written in the form of a straight line:

$$t = mZ - b \quad (6)$$

Therefore, the dynamic adsorption capacity (N_o) and the adsorption rate constant (K) can be evaluated from the slope (m) and intercept (b) by plotting t versus Z . At least three bed heights are required, for plotting the straight line; flow rate and solute concentration should be the same for the different bed heights.

The critical bed depth, Z_o , which represents the theoretical depth of adsorbent required to prevent the solute concentration from exceeding C_b , can be calculated from equation [5] by substituting $t = 0$ and solving for Z :

$$Z_o = \frac{u}{KN_o} \ln \left(\frac{C_o}{C_b} - 1 \right) \quad (7)$$

The gradient from equation [6] can be used to predict the performance of the column if there is a change in the initial solute concentration, C_o , to a new C'_o . Hutchins (1974) proposed that the new gradient, m' can be written as:

$$m' = m \left(\frac{C_o}{C_o'} \right) \quad (8)$$

And the new intercept would be:

$$b' = b \left(\frac{C_o}{C_o'} \right) + \left(\frac{\ln \left(\frac{C_o'}{C_t} - 1 \right)}{\ln \left(\frac{C_o}{C_t} - 1 \right)} \right) \quad (9)$$

8.3.2 Results and discussion

Data collected during laboratory column tests were used to determine the BDST model parameters, namely BDST adsorption capacity, N_o and rate constant, K and these are presented in Table 8.1.

Table 8.1: Values of BDST model parameters for the adsorption of heavy metals from single component solutions by natural zeolite at 30 % breakthrough, 15 cm column height and a flow rate of 20 ml/min.

Heavy Metals	q_b (mg/g)	K (L/mg.min)	N_o (mg/g)	Z_o (cm)	RMSE
Iron	0.79	0.00104	0.81	1.45	0.14
Zinc	1.43	0.00016	1.84	4.01	0.14
Manganese	0.87	0.00039	1.03	2.95	0.11
Copper	1.60	0.00022	1.90	2.95	0.12

N_o was calculated with the unit mg/l, but was converted to mg/g by multiplying it with the column bulk density = 0.921 g/cm³

The calculated values of the adsorption capacity, N_o , are consistent with the observed values from column operation, that is, q_b values. The critical bed depth, Z_o , which is the theoretical depth of adsorbent sufficient to prevent the solute concentration exceeding C_b ,

that is, the concentration at breakthrough, is lower for iron compared to the other three cations. This may be because of the higher affinity of natural zeolite for iron, as shown during equilibrium studies. Moreover, the rate constant for iron removal is larger than the other 3 metal cations, indicating that iron removal in fixed bed columns is faster than that of copper, manganese or zinc.

In order to determine how good a fit the BDST model is to the experimental results, a statistical measure of the root mean square error or RMSE was used. This measures the deviation of the model from the experimental data. Jusoh et al. (2007) successfully used the RMSE to determine the applicability of the BDST model in predicting the breakthrough curve for the removal of lead and cadmium from solution by granular activated carbon. The RMSE was calculated using the following equation:

$$RMSE = \left[\frac{\sum_{j=1}^m (X_j^p - X_j)^2}{n_r} \right]^{1/2} \quad (10)$$

Where, X_j^p is the predicted fractional concentration; X_j is the measured (experimental) fractional concentration and n_r is the number of data.

From Table 8.1 it can be observed that the breakthrough curve obtained from the BDST model deviated from the experimental results by between 12 – 14 %. This shows that the model can be used successfully to estimate and predict the breakthrough curve for the removal of heavy metals from solution by natural zeolite. Figure 8.3 also shows a comparison of the experimental breakthrough curves and those obtained from the BDST model for the adsorption of iron, copper, manganese and zinc by natural zeolite.

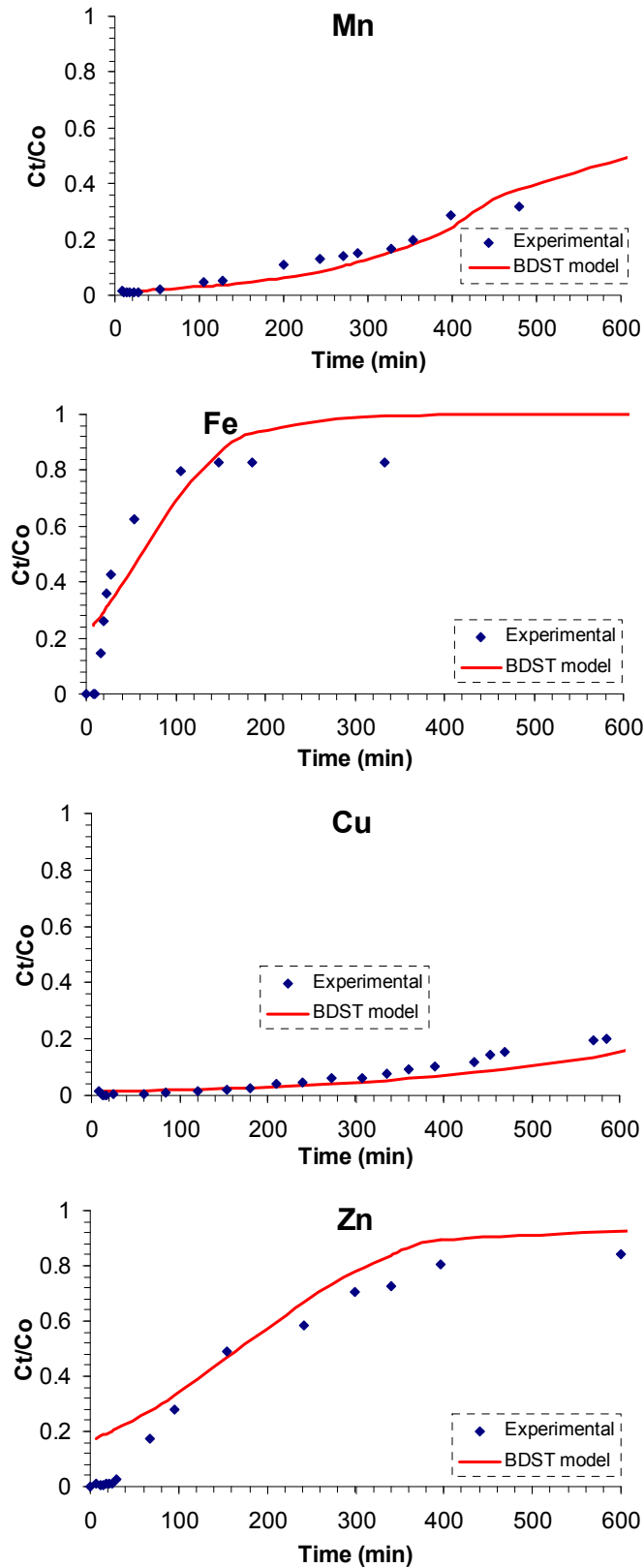


Figure 8.3: Comparison of the BDST model with experimental results, bed height 15 cm, flow rate 20 ml/min and the BDST model was calculated at 30 % breakthrough.

8.4 Column operation

There are a number of factors that affect the behaviour of breakthrough curves; these include effect of flow rate, adsorbent bed height and dimensions of the adsorption column.

8.4.1 Effect of flow rate

The effect of volumetric flow rate was investigated using natural zeolite particle size range 1 – 3 mm, column height of 15 cm and single component solutions. The solutions were pumped using a peristaltic pump in up flow mode at 20, 50 and 80 ml/min. The breakthrough curves for the different flow rates are shown in Figure 8.4.

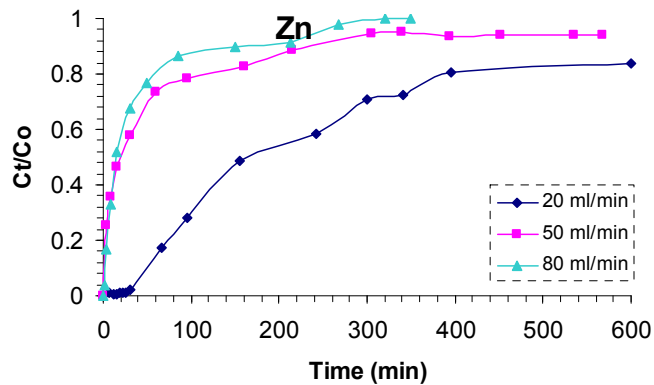
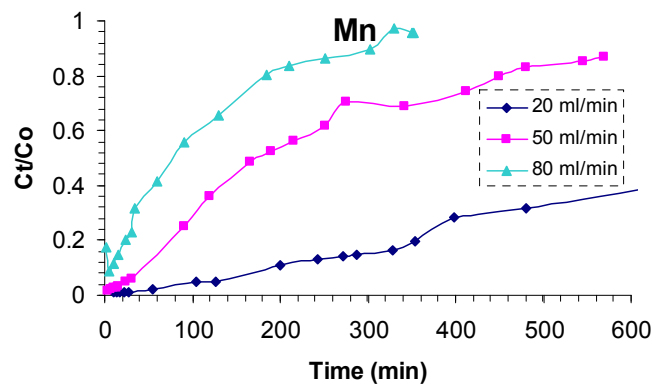
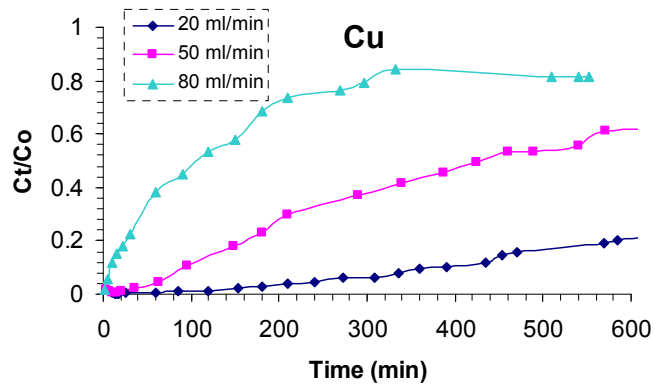
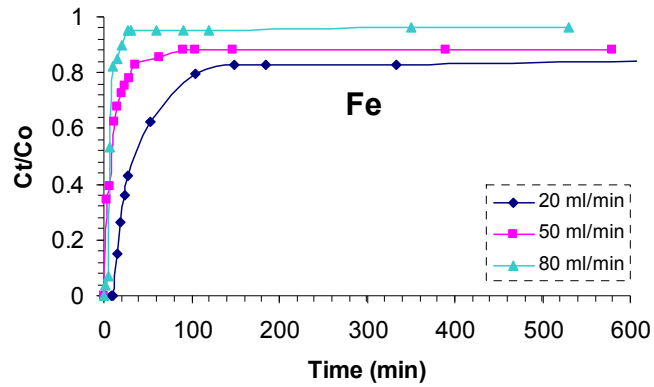


Figure 8.4: Breakthrough curves for the effect of flow rate on the adsorption of heavy metals by natural zeolite.

As can be seen in Figure 8.4, removal efficiency is favoured by lower volumetric flow rates; this is because breakthrough occurred earlier for faster flow rates, indicating a shorter column life. At higher flow rates there is less contact time between the natural zeolite and solution, and hence the system is not at equilibrium (Low et al., 1999). The failure to attain local equilibrium results in lower uptake of cations from the solution. Moreover, because of these shorter contact times, there is not enough time for the heavy metals to be distributed throughout all the available adsorption sites on zeolite, resulting in the evident premature breakthrough and lower adsorption capacities.

From the results of batch experiments it was seen that the rate limiting step for the adsorption of heavy metals from solution by natural zeolite was intraparticle diffusion, which is a slow process, hence the need for longer residence time if effective heavy metal removal is to take place. Thus, lowering the volumetric flow rate increases the residence time and the adsorption efficiency (Inglezakis and Grigoropoulou, 2004; Stylianou et al., 2007). The flow rate can only be lowered to a limit, after which the liquid hold-up of the bed is lowered and channelling begins to occur resulting in a reduction in the effectiveness of the process (Inglezakis and Grigoropoulou, 2004).

Table 8.2: Effect of flow rate on the volume of solution treated, at $C_t/C_0 = 0.4$ and 15 cm bed height.

Heavy Metals	Flow rate (ml/min)	Volume treated (L)	Time, T_b (min)	Time, T_s (min)	LUB (cm)
Copper	20	22.5	1070	---	---
	50	16.2	323	492	5.2
	80	5.4	68	184	9.5
Manganese	20	13.3	634	790	2.9
	50	6.7	134	240	6.6
	80	4.5	57	110	7.3
Zinc	20	2.7	129	235	6.8
	50	0.6	11.1	70	12.6
	80	0.5	10.9	45	12.9
Iron	20	0.6	26	58	8.3
	50	0.3	6.6	23	10.7
	80	0.3	6.4	8	10.9

From Table 8.2, it can be seen that generally more volume was treated at 20 ml/min compare to 50 or 80 ml/min. This was expected since, at 20 ml/min the heavy metals in solution have more time to interaction with the available adsorption sites in zeolite resulting in better removal efficiencies. Moreover, the length of unused bed (LUB), which represents the distance that is not saturated at breakthrough time, generally increased with an increase in flow rate. This may be a result of premature breakthrough that takes place at faster flow rates, and hence a reduction in the efficiency and effectiveness of the fixed bed column.

8.4.2 Effect of bed height

Breakthrough curves obtained for the adsorption of iron and zinc from their respective solutions by natural zeolite at different bed heights, that is, 15 and 50 cm and a constant flow rate of 20 ml/min are shown in Figure 8.5 and 8.6.

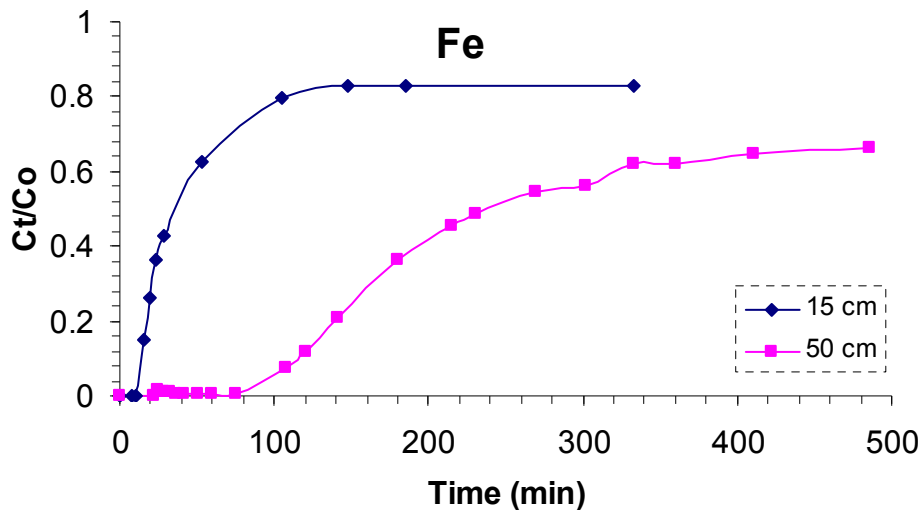


Figure 8.5: Effect of bed height on the adsorption of iron by natural zeolite; $C_0 = 400$ mg/l.

Figure 8.5 shows how the breakthrough curves for the removal of iron vary with column bed height. The volume of solution treated and the bed service time increased with an increase in bed height, as presented in Table 8.3. The increase in the volume of solution treated was because of an increase in the adsorbent mass (as the bed height was increased) which meant an increase in the adsorption binding sites available for heavy metal adsorption. Furthermore, an increase in bed height also results in an increase in residence time and hence there is more time for the heavy metals to interact with natural zeolite resulting in an increase in removal rates and amounts. The breakthrough curve for 15 cm bed height does not follow the characteristic “S” profile produced by ideal adsorption systems (Harland, 1994; Walker and Weatherley, 2001); therefore, adsorption is not favourable under these conditions as seen by the premature breakthrough.

The breakthrough volume from the 50 cm bed was about 7.5 times that from the 15 cm bed, at 40 % breakthrough. Similarly, the bed service time increased from about 26 minutes to 194 minutes, as the bed height increased, see Table 8.3. Moreover, the bed

adsorption capacity, q_b , (equation [11]) increases at the breakthrough point with increasing bed height, as also shown in Table 8.3. The bed adsorption capacity increases since an increase in bed height means an increase in adsorbent mass and thus more active adsorption sites, which result in an increase in the amount of iron removed from solution.

$$q_b = \frac{Q_v t_{40\%} C_o}{m_c} \quad (11)$$

Where, q_b is the amount of solute adsorbed at breakthrough point (mg/g); $t_{40\%}$ is the service time (min) when the effluent concentration reaches 40 % of the influent; Q_v is the volumetric flow rate (l/min) and m_c is the mass of adsorbent in the column (g).

The bed adsorption capacity for the 50 cm column used in iron removal, $q_b = 1.8$ mg/g, is lower than the maximum adsorption capacity for iron obtained from batch adsorption isotherms, $q_o = 6.61$ mg/g (from equilibrium studies). The efficiency of the 50 cm column was approximately 26 % (at 40 % breakthrough) compared to the maximum adsorption capacity of the adsorbent in the removal of iron under batch conditions. This is mainly because under batch conditions the adsorbent and solution are thoroughly mixed and in contact until equilibrium is reached, hence the higher adsorption capacity.

Table 8.3: Effect of bed height on the adsorption of iron from solution by natural zeolite in fixed bed columns.

Heavy Metal	Bed Height (cm)	Mass of adsorbent (g)	Treated volume, V_b (L)	Time at 40% breakthrough (min)	Bed adsorption capacity, q_b (mg/g)
Iron	15	207.8	0.547	26	1.0
	50	692.7	4.062	193	1.8

The effect of bed height on the adsorption of zinc from solution by natural zeolite is shown in Figure 8.6.

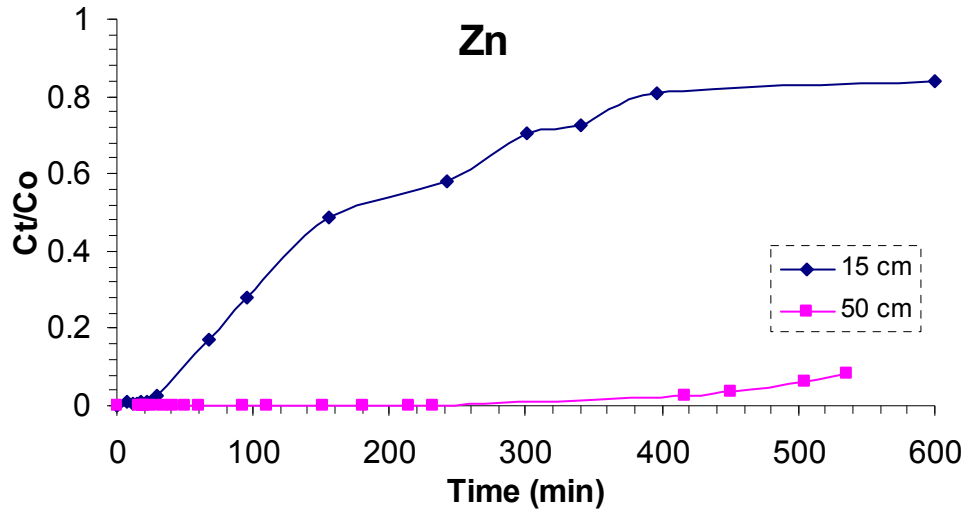


Figure 8.6: Effect of bed height on the adsorption of zinc by natural zeolite; $C_0 = 120$ mg/l.

Figure 8.6 shows that an increase in the bed height increases the breakthrough time, thus resulting in longer bed service times. The breakthrough curve for the 15 cm bed height reached breakthrough faster than the 50 cm bed height for zinc removal. The curve for the 50 cm bed shows a gradual increase of zinc in the effluent, indicating that it would take a relatively long time for the column to be completely exhausted and thus longer column service times.

The breakthrough volume, time and bed adsorption capacity for the adsorption of zinc by natural zeolite at the different bed heights, at 10 % breakthrough, are presented in Table 8.4. The efficiency of the 50 cm column in removing zinc from solution compared to batch equilibrium studies is approximately 41 %.

Table 8.4: Effect of bed height on the adsorption of zinc from solution by natural zeolite in fixed bed columns.

Heavy Metal	Bed Height (cm)	Mass of adsorbent (g)	Treated volume, V_b (L)	Time at 10% breakthrough (min)	Bed adsorption capacity, q_b (mg/g)
Zinc	15	210.3	1.014	49	0.7
	50	658.9	11.760	560	2.0

8.5 Treatment of synthetic acid mine drainage (sAMD)

Synthetic acid mine drainage was contacted with natural zeolite in order to establish the effectiveness of natural zeolite in treating *AMD* under continuous conditions. The synthetic solution contained a mixture of iron, zinc, copper and manganese at concentrations of 400, 120, 20 and 20 mg/l respectively. This solution was pumped at 20 ml/min through a 50 cm bed of natural zeolite, using a peristaltic pump. The natural zeolite was subjected to 3 cycles of adsorption and desorption. Sulphuric acid at 40 °C and a flow rate of 20 ml/min was used for desorption. The same acid was re-used/recycled for the three desorption stages. Both the adsorption and desorption were in up flow mode.

8.5.1 Adsorption studies

Breakthrough curves were obtained for the removal of iron, zinc, copper and manganese from sAMD for three adsorption cycles, as shown in Figure 8.7.

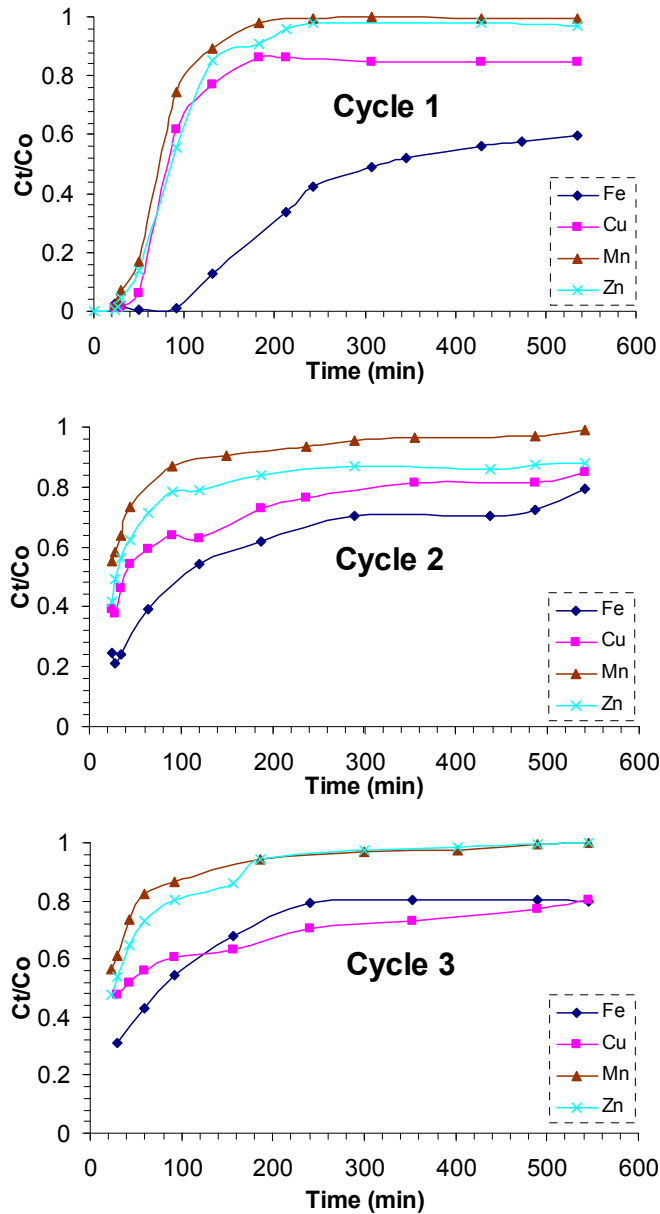


Figure 8.7: Breakthrough curves for the removal/adsorption of heavy metals from synthetic solutions by natural zeolite, bed height 50 cm and flow rate 20 ml/min.

Figure 8.7 shows that there is a general decrease in breakthrough time; for $C_t/C_o = 40\%$, the efficiency of natural zeolite is reduced by about 28 %, 60 %, 68 % and 72 % in the removal of manganese, copper, zinc and iron from synthetic acid mine drainage between cycle 1 to 2. This may be attributed to the occupation of adsorption sites by H^+ ions (from sulphuric acid which was used to regenerate the zeolite), which are tightly bound by

zeolite and hence more difficult to displace during the adsorption of heavy metals. Moreover, the electrostatic repulsion of heavy metals by the protonated zeolite surface may be another contributing factor toward the reduction in adsorption capacity (Cabrera et al., 2005). The breakthrough time for cycles 2 and 3 is almost the same within the bounds of experimental error, see Table 8.5.

Table 8.5: Bed service time at 40 % breakthrough for the treatment of synthetic acid mine drainage.

Heavy Metals	Bed service time (min)		
	Cycle 1	Cycle 2	Cycle 3
Manganese	25	18	17
Copper	75	30	25
Zinc	76	24	20
Iron	234	66	53

Table 8.5 clearly shows the loss in adsorption efficiency of natural zeolite due to regeneration using sulphuric acid at 40 °C. It is suggested that a lower concentration of acid be used or other less corrosive reagents such as EDTA and NaCl or NaNO₃.

The effects of competing cations in fixed bed column adsorption experiments, for iron and zinc removal are presented in Figure 8.8. These graphs show the breakthrough curves for the removal of iron and zinc from their respective single component solutions and from synthetic solutions containing a mixture of heavy metals, acting as competitors for the available adsorption sites on natural zeolite.

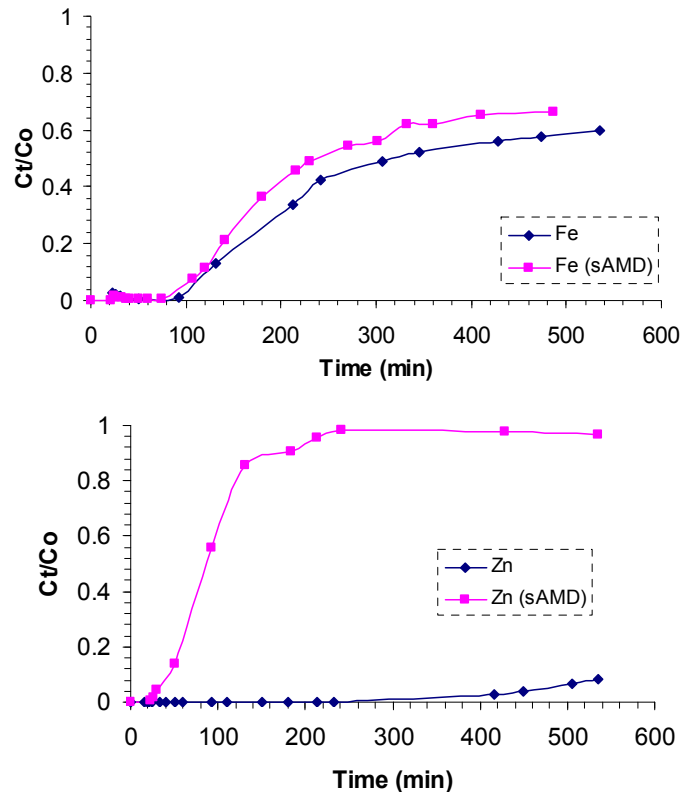


Figure 8.8: Breakthrough curves for the effect of competing cations in the removal of zinc and iron from single component and sAMD solutions; bed height 50 cm, flow rate 20 ml/min.

Figure 8.8 shows that the breakthrough curves for the removal of iron from both solutions were not drastically different. This is similar to the results obtained in batch experiments, where it was found that iron removal is generally not significantly affected by the presence of competing cations. Zinc removal on the other hand, was negatively affected by the presence of competing cations. Figure 8.8 clearly shows that the breakthrough

curve for zinc removal from sAMD reached breakthrough faster than that obtained from the removal of zinc from single component solutions. These results are similar to those obtained from batch experiments carried out to investigate the effect of competing cations.

8.5.2 Desorption studies

A good adsorbent, as noted earlier should not only have a high adsorption capacity, but must also exhibit good regeneration for multiple usages (Richardson et al., 2002). One of the aims of regeneration of metal loaded adsorbent is to reduce the liquid waste volume; that is, desorption liberates small volumes of concentrated metals solutions, which are more appropriate for conventional metal recovery processes such as electrolysis.

The mass of metal desorbed, m_d , can be calculated from the area below the desorption curve multiplied by the flow rate:

$$m_d = Q_v \int C_t dt \quad (12)$$

The desorption efficiency is simply a ratio of the amount of solute desorbed over the amount adsorbed by the adsorbent:

$$desorption(\%) = \frac{m_d}{m_{ads}} \times 100 \quad (13)$$

$$m_{ads} = Q_v \int_{t=0}^{t=t_{total}} C_s dt = Q_v A_c \quad (14)$$

Where, m_{ads} is the amount of solute that has been adsorbed, mg; t is service time, min; C_s is the adsorbed metal concentration, mg/l and Q_v is the flow rate, l/min. A_c is obtained by integrating the adsorbed metal concentration between $t = 0$ until the end of the adsorption period, this corresponds to the area under the curve for the plot of C_s versus t .

Regeneration of natural zeolite that was used to treat sAMD was carried out using 2 % (w/w) sulphuric acid at 40 °C, at a flow rate of 20 ml/min. Desorption curves of heavy metal removal from natural zeolite are presented in Figure 8.9.

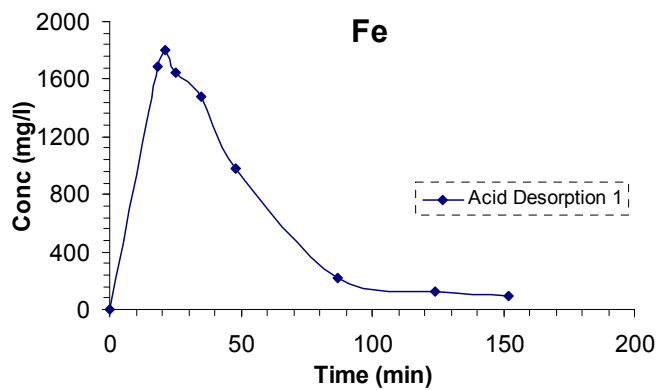
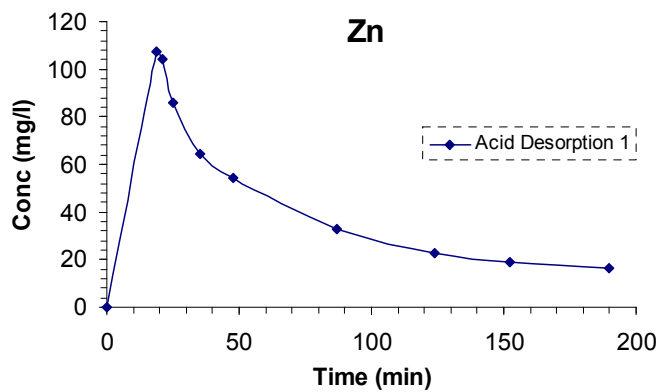
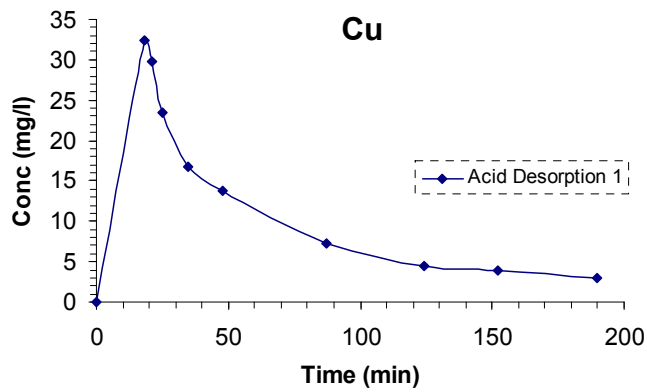
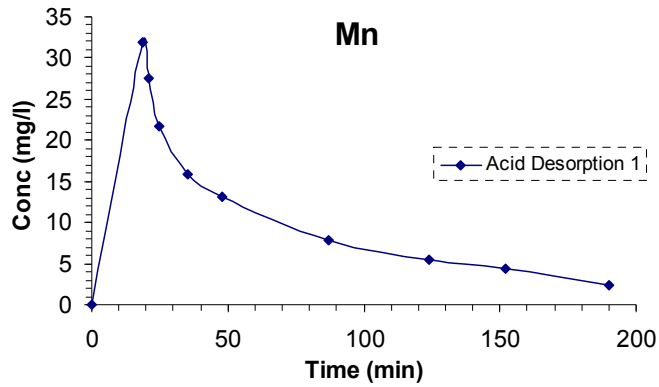


Figure 8.9: Desorption of heavy metals from natural zeolite; column bed height 50 cm, cycle 1.

There is more iron in the effluent from the column; this is due to the higher concentration of iron in sAMD compared to the other three heavy metals, thus more iron was adsorbed. The desorption curves for all four heavy metal ions, show that there is a general increase in the concentration of metal ions initially in the effluent, that is, within the first 20 minutes followed by a decrease at approximately the same rate and then the concentration gradually levels off after 50 minutes. Brigatti et al. (2000) and Celik et al. (2001) obtained a similar trend for the regeneration of sepiolite and clinoptilolite respectively. The amount of heavy metals desorbed from natural zeolite for the 3 cycles and desorption efficiencies are presented in Table 8.6.

Table 8.6: Calculated desorption efficiencies for the desorption of heavy metals from natural zeolite in fixed bed columns using 2 % (w/w) H₂SO₄ at 40 °C; bed height 50 cm, flow rate 20 ml/min; contact time 540 minutes.

Heavy Metals	Amount adsorbed from solution, m_{ads} (mg)	Amount desorbed from zeolite, m_d (mg)	Desorption efficiency (%)
Manganese			
Cycle 1	36.0	34	93
Cycle 2	25.2	21	83
Cycle 3	24.8	24	81
Iron			
Cycle 1	2152	1215	57
Cycle 2	1440	1500	63
Cycle 3	1032	495	48
Copper			
Cycle 1	60.4	28	46
Cycle 2	56.8	40	45
Cycle 3	69.2	58	49
Zinc			
Cycle 1	236	117	50
Cycle 2	236	127	36
Cycle 3	138	142	39

Table 8.6 shows that the total adsorption capacity, m_{ads} , of the natural zeolite (after 540 minutes) was not drastically altered by regeneration. This is a positive toward the determination of natural zeolite as a potential low cost adsorbent for AMD treatment. Moreover, desorption efficiencies for heavy metal removal were generally high; these could be further improved if optimised for practical applications. Manganese gave the highest desorption efficiencies, this is similar to results obtained in batch desorption studies. Manganese is less strongly bound by zeolite and hence is easily displaced from the zeolite structure. Natural zeolite showed greater affinity for iron, zinc and copper and hence their lower desorption efficiencies, as it is more difficult to displace them from the adsorption sites in the zeolite structure.

The above results indicate that natural zeolite can be regenerated and re-used in removing heavy metals from solution.

8.6 Conclusion

The results from column studies showed that the adsorption of heavy metals from solution was affected by operational conditions such as flow rate and bed height. Slower flow rates gave better removal efficiencies and capacities compared to faster ones, since slower flow rates lead to larger residence times, resulting in the column approaching equilibrium. Longer bed heights also resulted in greater adsorption efficiencies, because of an increase in residence time and available adsorption sites (due to an increase in adsorbent mass).

The bed depth service time (BDST) model was successfully used to simulate experimental results at 30 % breakthrough. This model provides the necessary parameters

needed for fixed bed column design. The breakthrough curves for iron copper, zinc, manganese and iron obtained from the BDST model deviated from experimental results by between 12 – 14 %.

The fixed bed column was also used to treat synthetic AMD, which simulated Wheal Jane mine AMD. Natural zeolite was exposed to 3 cycles of adsorption and desorption. The efficiency of the column in removing heavy metals from synthetic AMD drastically reduced after regeneration, that is, at 40 % breakthrough. This reduction in efficiency proves that acid regeneration negatively affected natural zeolite. It is recommended that other regenerating reagents be used, for example NaCl, NaNO₃ or EDTA. The reduction in efficiency may have been caused by the protonation of the zeolite surface by sulphuric acid. The protonated surface repels any heavy metals that may be approaching the zeolite surface, resulting in the evident reduction in efficiency of the acid regenerated zeolite.

The total amount of heavy metals adsorbed from solution after about 540 minutes, for the 3 cycles, was almost the same. This indicates that the capacity of natural zeolite was not drastically affected by regeneration; rather its efficiency is the one that was affected. It is the rate of adsorption that was mainly affected by acid regeneration.

CHAPTER 9

TREATMENT OF WHEAL JANE AMD

9.1 Introduction

Wheal Jane mine was used as a case study in this research, as highlighted earlier. Natural zeolite was used to treat AMD from the mine, and its potential as a low cost adsorbent was investigated. Different methods were used to assess this potential, this varied from batch experiments to continuous column experiments. This chapter gives the results and discussion on the use of natural zeolite in treating actual AMD from Wheal Jane Mine.

9.2 Batch Experiments

Batch experiments using real AMD from Wheal Jane Mine were carried out. Natural zeolite, thermally pre – treated zeolite and synthetic zeolite were used to treat real acid mine drainage, using different contacting methods.

9.2.1 Use of thermally pre – treated natural zeolite in treating real AMD

From the kinetic studies carried out earlier it was established that thermally pre – treating natural zeolite improved its adsorption capacity, especially pretreating:

- i. In a muffle furnace for 30 minutes at a temperature of 200 °C (sample NT 200 C)
and,
- ii. In a microwave for 15 minutes exposure to microwave radiation (sample MTZ 15).

Natural zeolite pre-treated using the above two methods and untreated natural zeolite were used to treat AMD from Wheal Jane mine. The mixture, that is, 20 g zeolite in 100 ml solution was agitated using the tumbling mill; the results are shown in Figure 9.1.

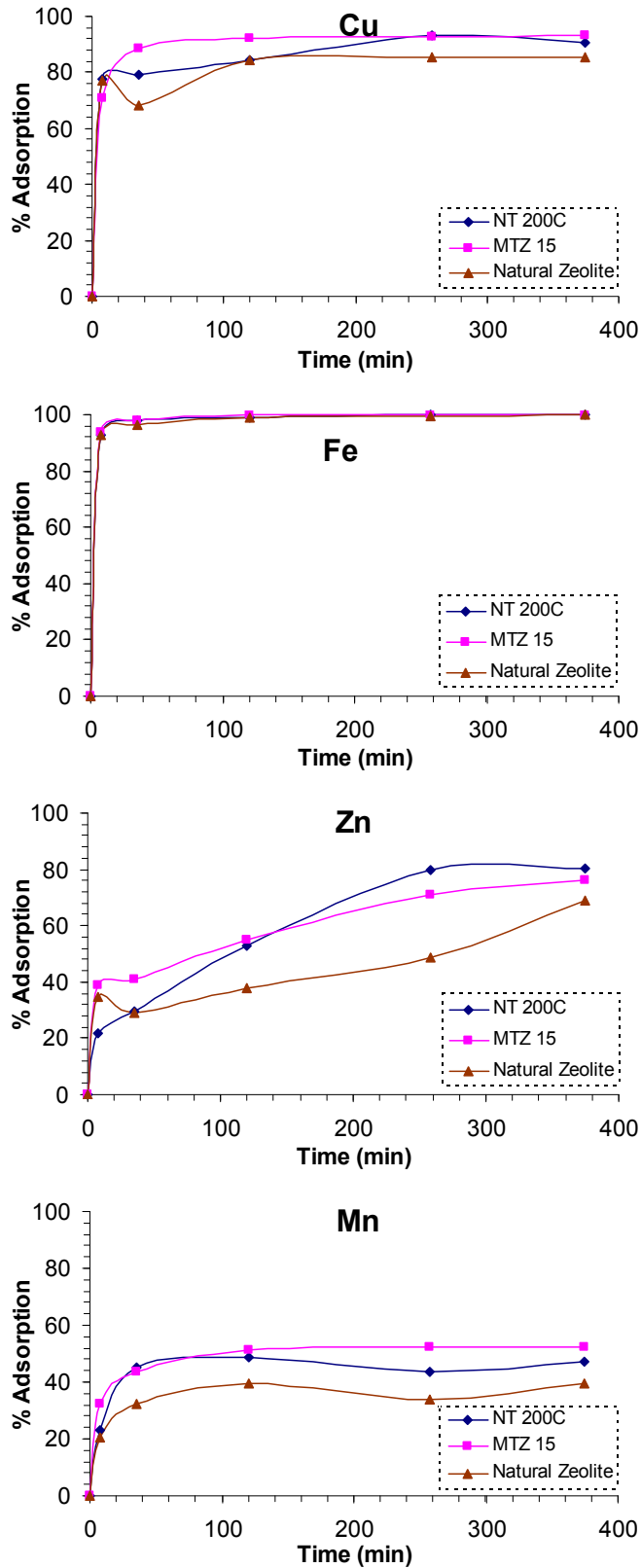


Figure 9.1: Effect of thermally pre-treating natural zeolite on its capacity to remove heavy metals from Wheal Jane mine AMD.

Generally the natural zeolite that was exposed to microwave energy for 15 minutes gave better removal efficiencies compared to the one heated in the muffle furnace. The natural zeolite exposed to microwave energy lost more mass during thermal pre-treatment, due to the evaporation of water from its micropores and channels. The moisture lost was about 7.8 % of the original weight compared to 6.4 % for natural zeolite heated in the muffle furnace at 200 °C. The difference in moisture lost may be the reason why the adsorption capacity of natural zeolite exposed to microwave energy is greater than that of zeolite heated at 200 °C, since the zeolite internal micropores and channels will be more vacant, thus making room for more cations to be adsorbed from solution (Sidheswaran and Bhat, 1998). Table 9.1 compares the adsorption capacities of the 3 zeolite samples.

Table 9.1: Comparison between thermally pre-treated natural zeolite and untreated natural zeolite in treating Wheal Jane AMD after 360 minutes.

Heavy metals	% Adsorption	Adsorption capacity (mg/g)	Final concentration (mg/l)	Wheal Jane maximum consent limit (mg/l)
Copper				
<i>Natural Zeolite</i>	85.6	0.0081	0.27	0.08
<i>MTZ 15</i>	93.4	0.0089	0.13	
<i>NZ 200 °C</i>	90.8	0.0086	0.17	
Iron				
<i>Natural Zeolite</i>	99.8	0.267	0.11	5.0
<i>MTZ 15</i>	100	0.268	0	
<i>NZ 200 °C</i>	100	0.268	0	
Zinc				
<i>Natural Zeolite</i>	68.7	0.13	11.89	2.5
<i>MTZ 15</i>	76.3	0.14	9.02	
<i>NZ 200 °C</i>	75.1	0.14	9.50	
Manganese				
<i>Natural Zeolite</i>	39.6	0.009	2.74	1.0
<i>MTZ 15</i>	52.4	0.012	2.16	
<i>NZ 200 °C</i>	46.9	0.011	2.41	

The initial concentrations of iron, copper, manganese and zinc in AMD from Wheal Jane mine are 63.95, 1.90, 4.54 and 37.98 mg/l respectively, and these were measured using the AAS.

The Wheal Jane mine-water maximum consent limits for iron, copper, manganese and zinc in discharge water are 5.0, 0.08, 1.0 and 2.5 mg/l respectively (Bone, 2003; United Utilities, 2007). Table 9.1 shows that iron was reduced to concentration levels less than the maximum consent limit. The concentration of copper, zinc and manganese were higher than their respective consent limits, but the final concentration can be reduced if more zeolite is used or the solution is further contacted with fresh natural zeolite. Samples MTZ (15), that is, natural zeolite exposed to microwave radiation for 15 minutes, gave the best removal efficiencies, which are 93.4%, 100%, 76.3% and 52.4% copper, iron, zinc and manganese respectively, from Wheal Jane mine AMD. The difference in the amount removed from solution by the 3 zeolite samples (that is, the 2 pre-treated and one untreated) was not that significant to justify the use of thermally pre-treated zeolite, since pre-treatment increases the cost of AMD treatment. Therefore, untreated natural zeolite was used to treat AMD for the rest of this study.

9.2.2 Standing tests for the treatment of Wheal Jane AMD

Natural zeolite (20, 30 and 50 g) was contacted with 100 ml of real AMD; this mixture was not agitated, it was left standing in a beaker for about 9 days. The particle size range of natural zeolite used was 1 – 3 mm. The purpose of this experiment was to establish whether natural zeolite can be used in settling ponds, in which natural zeolite will be placed at the bottom of the pond and AMD pumped upward through the natural zeolite,

this is the same concept employed in Limestone ponds which are used for passive treatment of AMD. The results of this experiment are shown in Figure 9.2.

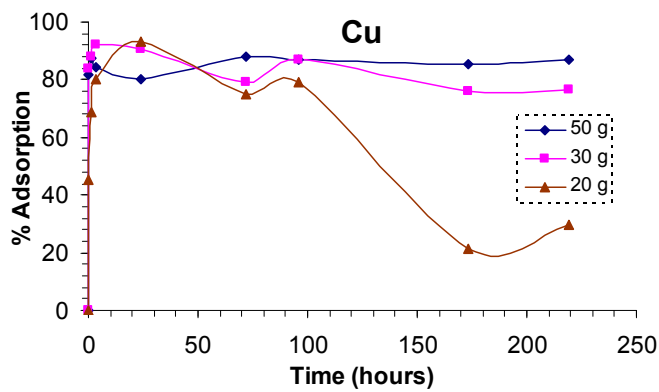
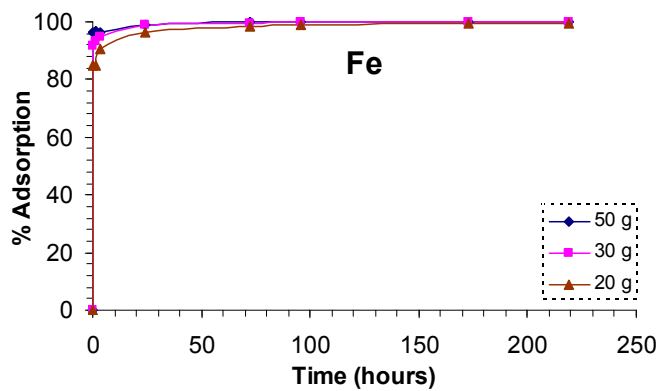
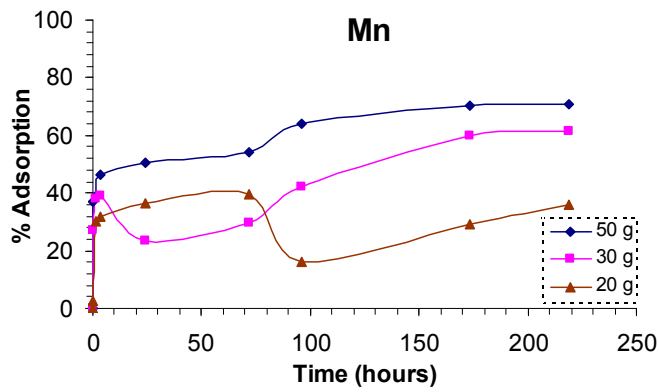
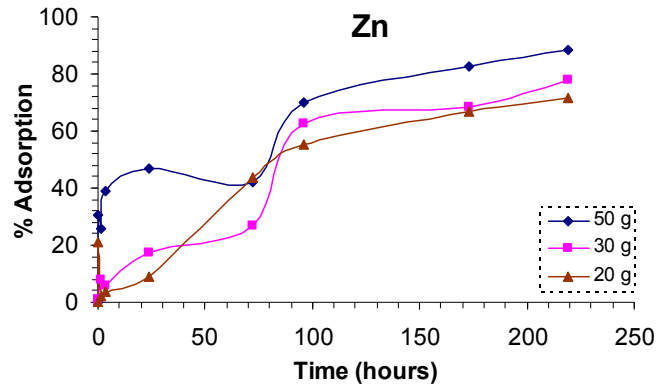


Figure 9.2: Treatment of Wheal Jane mine AMD using natural zeolite (no agitation for about 9 days).

Figure 9.2 shows that the rate of metal removal is initially fast, that is, within the first 10 hours most of the heavy metals are removed, especially iron and copper. This may be a result of the interaction of heavy metals with the adsorption sites on the surface of natural zeolite, which can easily be accessed by the diffusing heavy metals. The rate then slows down and begins to level off after about 50 hours of contact. Since the system is not being agitated the solid – liquid contact is not very good, resulting in poor adsorption rates and hence the slowing down of the uptake rate. The zeolite particles on the top layer are the ones in direct contact with AMD and hence become saturated initially before the zeolite at bottom layers. The saturation of surface zeolite results in the apparent slowing down of the uptake rate from 10 – 70 hours. A thin layer of iron precipitate began to deposit onto the top layer of natural zeolite as the experiment progressed. Moreover, since there is no agitation, the film mass transfer resistance increases, resulting in a reduction in the rate of adsorption.

After this slow period, desorption seems to take place, this is mainly evident in the uptake of copper and manganese. This phenomena may be a result of desorption of heavy metals (copper and manganese) from the saturated top layer of natural zeolite. Desorption is also more evident for lower solid to liquid ratios, that is, for the 20 g in 100 ml solution mixture. As the contact time increases from 100 hours, the uptake rate begins to increase since the heavy metals would have had enough time to diffuse from bulk solution to the zeolite surface and also to the particles at the bottom layers of the zeolite bed. This system could be made more efficient if AMD is flowing and not stagnant, resulting in better and faster contact between the solution and natural zeolite particles.

Table 9.2: Treatment of Wheal Jane mine AMD using natural zeolite (no mixing, total contact time 9 days, 22 °C, particle size: 1 – 3mm).

Heavy Metals	50 hours contact		4 days contact		9 days contact	
	Final Concentration (mg/l)	% Adsorption	Final Concentration (mg/l)	% Adsorption	Final Concentration (mg/l)	% Adsorption
Iron						
50 g	0.31	99.5	0	100	0	100
30 g	0.49	99.2	0	100	0	100
20 g	1.71	97.3	0.71	98.9	0.21	99.7
Copper						
50 g	0.29	84.4	0.25	86.9	0.25	86.9
30 g	0.29	84.4	0.25	86.9	0.45	76.5
20 g	0.31	83.5	0.40	79.1	1.33	29.8
Manganese						
50 g	2.16	52.4	1.62	64.3	1.32	70.9
30 g	3.32	27.0	2.63	42.0	1.74	61.7
20 g	2.81	38.1	3.81	16.1	2.90	36.1
Zinc						
50 g	21.20	44.2	11.38	70.0	4.31	88.6
30 g	29.44	22.5	14.28	62.4	8.33	78.1
20 g	27.51	27.6	16.99	55.3	10.80	71.6

Table 9.2 shows the percentage metals adsorbed from solution and the final concentrations after different contact times. It is generally not economical to have longer contact times hence; 9 days would be too long a residence time for any economical system. It can be seen that the removal rates after about 50 hours are slightly less than those after 4 or 9 days. If the system is optimised the removal rates after 50 hours could become comparable with those after 4 or 9 days. One way of doing this would be to pump the solution through the natural zeolite at very low flow rates. Pumping can be achieved using a pump or allowing the solution to cascade down the natural zeolite bed by gravitational forces.

Natural zeolite was able to remove significant amounts of heavy metals, especially iron, from solution, as shown in Table 9.2. The effectiveness of natural zeolite decreased with a reduction in mass, since smaller masses become saturated faster and are also prone to desorption. The final concentration of iron was within the consent limit for mine-water discharges from Wheal Jane after 4 days, that is, for natural zeolite at a mass of 30 and 50 g. The greater removal of iron may be attributed to precipitation, as highlighted earlier.

9.2.3 Comparison between natural zeolite and synthetic zeolite in treating Wheal Jane mine AMD.

Synthetic zeolite (zeolite - 4A) was used to treat AMD from Wheal Jane mine. The synthetic zeolite was in the form of a powder, with particle size less than 20 micron. Natural zeolite was milled using a ball mill to get a similar size range (that is, less than 20 micron) for comparison purposes. 30 g of natural zeolite powder was mixed with 100 ml solution of AMD and 3.7 g of synthetic zeolite was also mixed with 100 ml AMD

solution, these were agitated over a tumbling mill for about 360 minutes. The results of the adsorption experiments are presented in Table 9.3.

Table 9.3: Comparison of natural zeolite and synthetic zeolite in treating AMD from Wheal Jane mine.

Heavy metals	Zeolite Type	% Adsorption	Adsorption capacity (mg/g)
Copper	Natural zeolite	92.1	0.006
	Synthetic zeolite	95.9	0.049
Manganese	Natural zeolite	59.1	0.009
	Synthetic zeolite	100	0.123
Zinc	Natural zeolite	85.6	0.108
	Synthetic zeolite	100	1.027
Iron	Natural zeolite	100	0.255
	Synthetic zeolite	99.4	2.054

The results presented in Table 9.3 show that synthetic zeolite is more effective and efficient in removing heavy metals from AMD, since only 3.7 g of synthetic zeolite was used compared to 30 g of natural zeolite. For example, in the removal of manganese it can be seen that 3.7 g of synthetic zeolite removed all the Mn^{2+} ions from AMD and yet 30 g of natural zeolite was only able to remove 59.1 % of Mn^{2+} from AMD; this is a clear indication of the superiority of synthetic zeolite over natural. Furthermore, the adsorption capacity of synthetic zeolite for all the heavy metals is about 10 times that of natural zeolite.

Synthetic zeolite was not used in this study because it is expensive since the aim of this study was to come up with a low cost material for treating AMD. The cost of zeolite 4A is about USD 58 per kilogram (Wako Pure Chemical Industries) and that of natural

zeolite (clinoptilolite) is about USD 50 – 70 per ton (www.gsaresources.com/smz.html; Mumpton and Fishman, 1977), which is a massive price difference.

9.2.4 Proposed design of a passive AMD treatment reactor vessel

From the results obtained from batch experiments, removal rates and capacities from agitated experiments were much higher than those obtained from standing tests. Nevertheless, agitation is often expensive in practice; hence the proposed design is based on experiments carried out without agitation (standing tests).

The proposed reactor incorporates certain elements from the vertical flow reactors used in the passive treatment of AMD. The sizing calculations for this proposed reactor are shown in Appendix 3. The sketch of the reactor is presented in Figure 9.3.

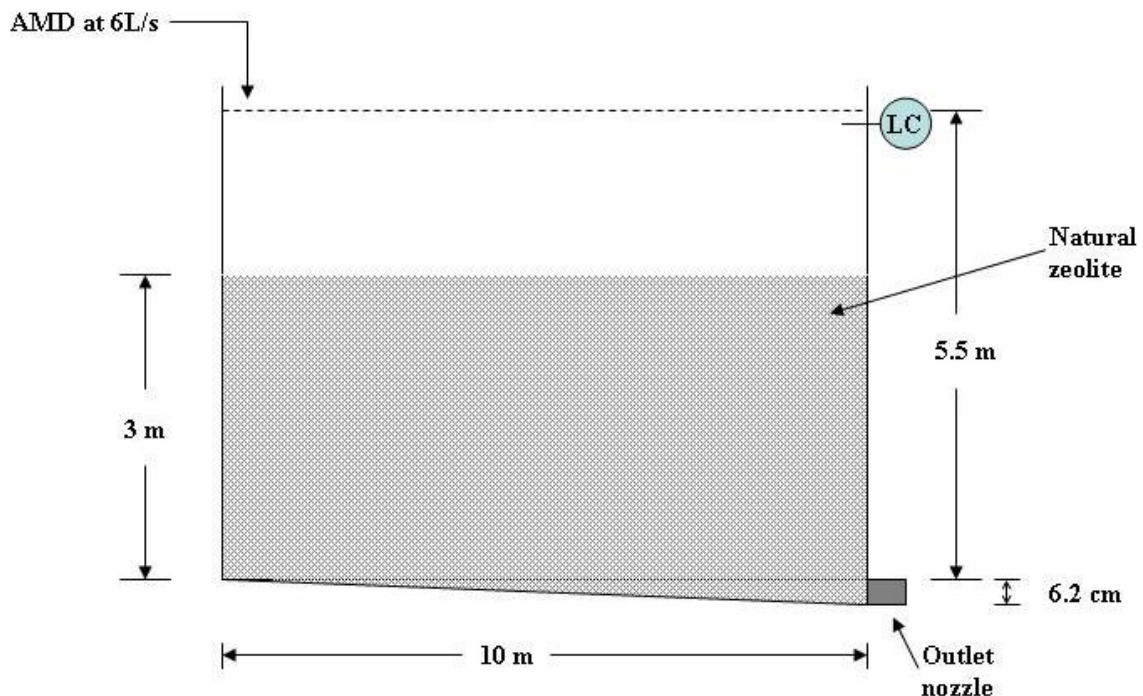


Figure 9.3: Sketch of the proposed reactor for the passive treatment of Wheal Jane AMD.

The reactor vessel will be a 10 m square tank with a working depth of 5.5 m, and working capacity of 550 m³. The reactors will be constructed from concrete, for longevity. The residence time for each tank will be 24 hours. The AMD solution is pumped at a flow rate of 6 litres per second; this is comparable with flow rates that were used at the Wheal Jane pilot passive treatment plant (Whitehead et al., 2005). The solution then cascades down through the bed of natural zeolite (3 m) and eventually drains out of the vessel through a drain pipe. The solution from the vessel can be drained into a settling pond. The purpose of the settling pond will be to increase the solution pH by adding lime, this results in the precipitation of trace heavy metals in the solution. The pond is designed to allow enough residence time for the precipitate to settle at the bottom of the pond. The clear solution is decanted from the surface of the pond to a chosen watercourse.

This system should give better removal efficiencies compared to those obtained from standing tests, but for comparison purposes the removal efficiencies from standing test (containing 50 g natural zeolite) are shown in Table 9.4 alongside those obtained from passive treatment technologies used at Wheal Jane mine.

Table 9.4: Removal efficiencies of heavy metals from Wheal Jane mine passive treatment plant (Whitehead et al., 2005).

System	Copper (%)	Manganese (%)	Zinc (%)	Iron (%)
LD	73	54	66	97
ALD	95	60	73	99
LF	42	45	47	95
Proposed*	84	52	44	99

*These results are from standing tests using 50 g natural zeolite.

From Table 9.4 it can be observed that the removal efficiencies expected from the proposed design should be comparable to those obtained from other passive treatment

technologies like Anoxic limestone drain system (ALD), Lime dosed system (LD) or the Lime free system (LF). Therefore, this proposed technology could be integrated into the AMD treatment flow diagram, preferably where the inlet concentrations are relatively dilute. In the case of Wheal Jane pilot passive treatment process flow diagram (Figure 3.2), the proposed reactor can be placed after the Lime dosing and ALD stages, thus eliminating the aerobic cells, anaerobic cells and rock filters; the proposed flow diagram is shown in Figure 9.4.

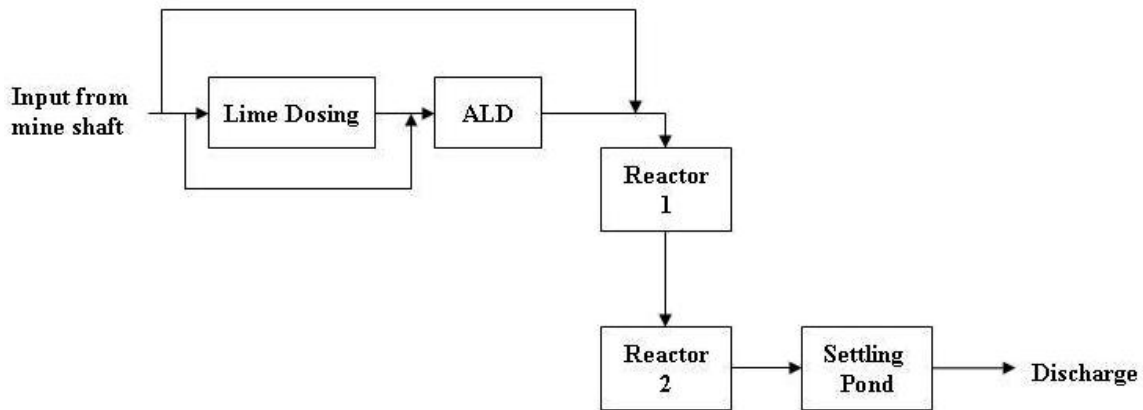


Figure 9.4: Proposed flow diagram for the passive treatment of AMD from Wheal Jane mine.

9.3 Column Experiments

Column tests were performed so as to investigate the effectiveness of natural zeolite in treating AMD from Wheal Jane mine under continuous flow conditions.

9.3.1 Adsorption and desorption studies

A 50 cm column as described earlier (Figure 8.1) was used to treat AMD. The bed height was 50 cm and the AMD flow rate was 20 ml/min up flow. Breakthrough curves for the removal of iron, copper, zinc and manganese are shown in Figure 9.5.

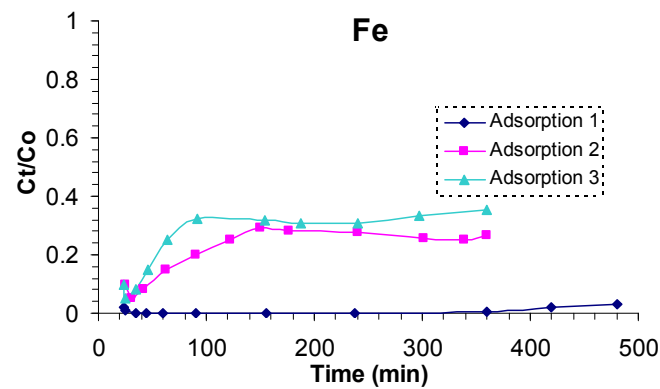
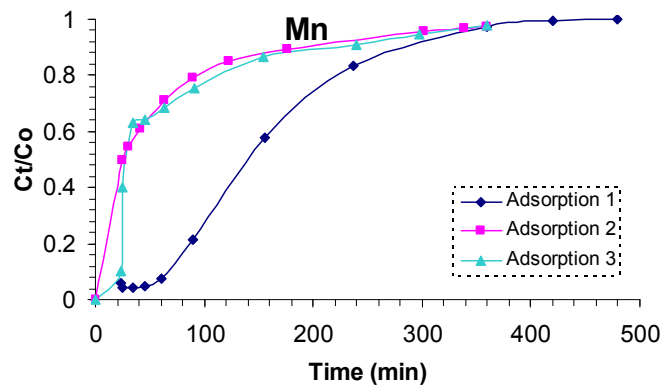
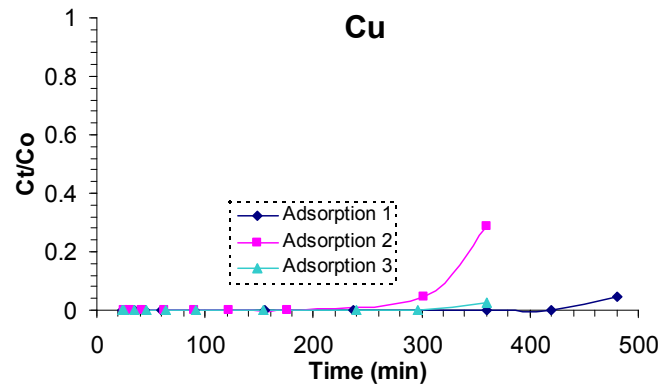
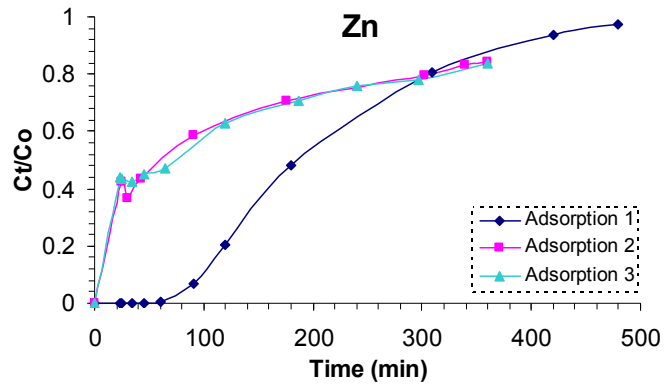


Figure 9.5: Breakthrough curves for the treatment of Wheal Jane AMD; bed height 50 cm and flow rate 20 ml/min.

Natural zeolite was regenerated and re-used to treat fresh AMD for three cycles. From Figure 9.5 it can be seen that the effectiveness of natural zeolite in treating AMD from cycle 1 to cycle 2 (that is, adsorption 1 and adsorption 2) was reduced significantly, but remained almost the same for cycle 2 and 3. The reduction in effectiveness may be caused by the electrostatic repulsion of heavy metal ions by the protonated natural zeolite surface (Cabrera et al., 2005).

The efficiency of the column in removing/adsorbing heavy metals from AMD can also be calculated from the ratio of the total amount of heavy metals adsorbed (m_{ads}) to the total amount of heavy metals fed to the column (m_f).

$$m_f = \frac{C_o Q_v t_t}{1000} \quad (1)$$

$$Adsorption(\%) = \frac{m_{ads}}{m_f} \times 100 \quad (2)$$

Where C_o is the initial solution concentration, mg/l; Q_v is the volumetric flow rate, ml/min; and t_t is the total flow time, min.

The efficiencies of the column in removing iron, copper, zinc and manganese from Wheal Jane AMD are presented in Table 9.5.

Table 9.5: Calculated column efficiencies for the 3 cycles (Contact time for each cycle was about 500 minutes).

Heavy Metals	Total amount adsorbed from solution, m_{ads} (mg)	Total amount fed into column, m_f (mg)	Column efficiency (%)
Iron			
<i>Cycle 1</i>	139.2	140.2	99
<i>Cycle 2</i>	89.8	116.1	77
<i>Cycle 3</i>	86.5	121.1	71
Manganese			
<i>Cycle 1</i>	12.4	38.1	33
<i>Cycle 2</i>	4.6	27.1	17
<i>Cycle 3</i>	4.7	27.1	17
Copper			
<i>Cycle 1</i>	0.624	0.628	99
<i>Cycle 2</i>	0.457	0.471	97
<i>Cycle 3</i>	0.468	0.471	99
Zinc			
<i>Cycle 1</i>	122	277.5	44
<i>Cycle 2</i>	71.5	210.7	34
<i>Cycle 3</i>	72.5	207.7	35

Table 9.5 shows a decrease in the column efficiency with regeneration for the removal of heavy metals from AMD. This reduction in efficiency may be attributed to the electrostatic repulsion of heavy metals by the protonated zeolite surface, as previously discussed (Cabrera et al., 2005).

Table 9.6 shows a comparison between the final solution concentrations obtained from column studies (in this research) and those from the active treatment plant at Wheal Jane mine.

Table 9.6: Comparison between results from Wheal Jane (W.J.) active treatment plant and those found in this study (fixed bed column studies).

Heavy metal	Final solution concentration after treatment (mg/l)		Wheal Jane Consent (mg/l) ^b
	W.J. Active treatment plant ^a	Fixed bed column (this study)	
Iron	0.47	0	5.0
Zinc	0.12	4.02	2.5
Manganese	0.18	1.19	1.0
Copper	< 0.01	0	0.08

^a United Utilities, 2007; ^b Bone, 2003; Coulton et al., 2003.

The final solution concentrations obtained from fixed bed column studies (this study) were calculated using 30 % breakthrough for manganese. The residence time required for 30 % breakthrough to be achieved was calculated and obtained as about 106 minutes. Natural zeolite has a low affinity for manganese (as shown in equilibrium studies) and hence its use as the basis for the determination of residence time.

Table 9.6 shows that the treatment of Wheal Jane AMD by natural zeolite is not as effective as that from the active treatment plant employed at Wheal Jane mine, mainly for zinc and manganese removal. Nevertheless, the final metal concentrations in the effluent from the fixed bed column (this study, at 30 % breakthrough) were close to the consent limit for Wheal Jane mine-water discharges. Actually, no iron or copper were present in the effluent from the column, indicating that if the column is optimised, it might actually become an economical method of treating Wheal Jane AMD. Optimising the column might involve increasing the column residence time. Residence time can be increased by slowing the volumetric flow rate or by increasing the column bed height. The results presented in Table 9.6 show that natural zeolite has great potential as a low cost adsorbent for the treatment of Wheal Jane AMD. Natural zeolite should nevertheless be

used to treat relatively dilute AMD, rather than concentrated AMD coming directly from the mine. The reason for this being that natural zeolite becomes exhausted quite fast, as shown earlier; it only took 106 minutes of treatment before the column reached 30 % breakthrough. Breakthrough times can be increased if more dilute solutions are passed through natural zeolite.

There has been other research work carried out at the University of Birmingham for the treatment of Wheal Jane mine AMD using different methods and materials, these include, the use of blast furnace slag, calcium alginate beads and column flotation. Table 9.7 presents the results obtained in these studies.

Table 9.7: Research carried out at the University of Birmingham for the treatment of Wheal Jane mine AMD and the results obtained.

Heavy Metals	Natural Zeolite ^a (This Study)	Calcium Alginate Beads ^b	Blast Furnace Slag ^c	Column Flotation ^d
Iron (%)	99	90	97	76
Copper (%)	99	42	---	99
Zinc (%)	44	32	67	89
Manganese (%)	33	32	22	---

- a. Column studies, bed height 50 cm, flow rate 20 ml/min, 1 cycle, contact time 480 minutes
- b. Nantumbwe, B.B., 2007. Experimental conditions: Column height 100 cm; flow rate 50 ml/min; contact time ≈ 500 minutes.
- c. Darkwah, L., 2005. Experimental conditions: 0.5 g blast furnace slag in 50 ml solution in a batch reactor. Agitation rate 200 rpm.
- d. Lynch, B., 2003. Experimental conditions: Protocol CA540 dosage 15ml/l, pH 9.0, froth depth 16 cm, air flow 600 cm³/min.

Table 9.7 shows the performance of natural zeolite in treating Wheal Jane mine AMD compared to previous work carried out in this area at the University of Birmingham. These results further show the potential that natural zeolite has as a low cost material/adsorbent for the treatment of AMD.

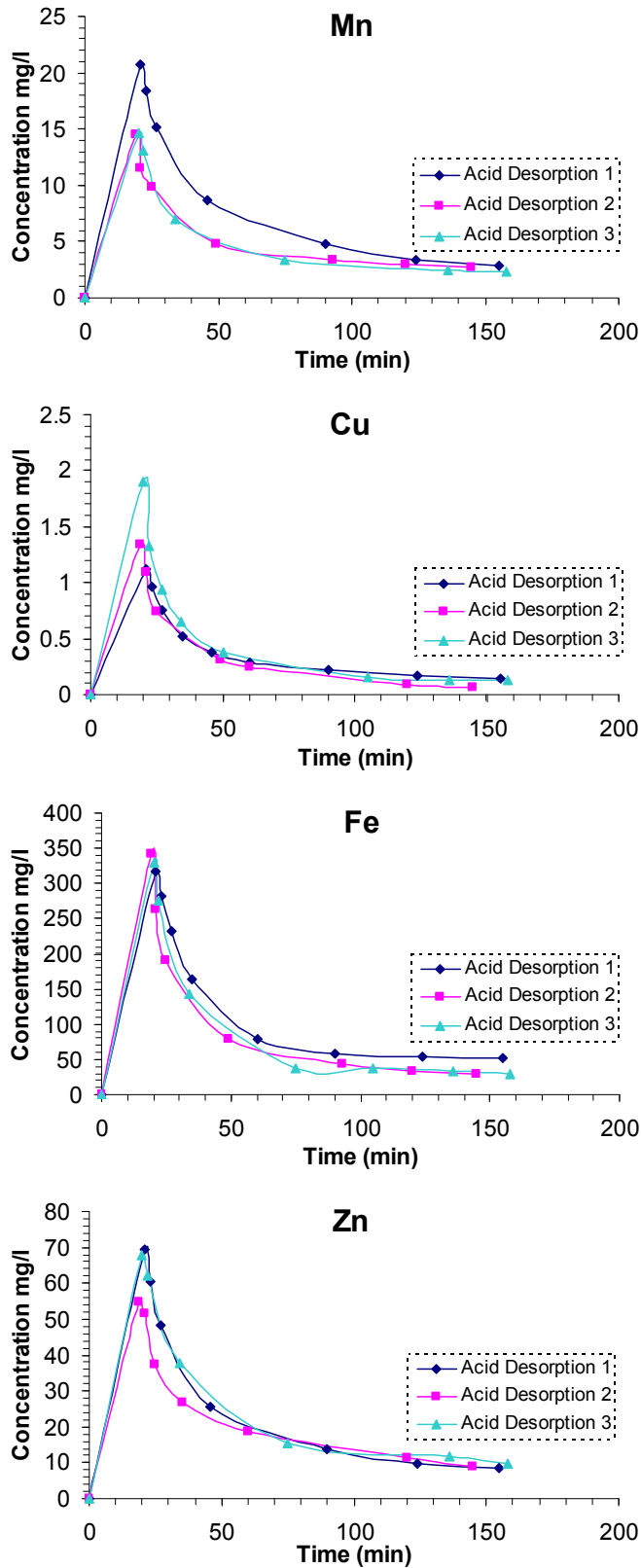


Figure 9.6: Desorption of heavy metals from natural zeolite using 2 % (w/w) sulphuric acid at 40 °C; flow rate 20 ml/min; column bed height 50 cm.

Figure 9.6 shows desorption curves for the removal of heavy metals from natural zeolite during regeneration. Most of the heavy metals are desorbed within the first 50 minutes. The rate of desorption begins to decrease from about 20 minutes, this is mainly due to a reduction in the concentration of heavy metals within the zeolite structure. A reduction in the concentration of heavy metals in the solid, results in a decrease in the concentration driving force of desorption, which eventually leads to a reduction in desorption rate (Cooney, 1999).

9.4 Conclusions

The results obtained from batch experiments for the treatment of Wheal Jane mine AMD, showed that thermally treating natural zeolite enhanced the capacity and efficiency of natural zeolite in treating AMD. Natural zeolite and synthetic zeolite were also used to treat AMD in batch mode, the adsorption capacity of synthetic zeolite was found to be ten times that of natural zeolite. The major disadvantage of using synthetic zeolite in treating AMD is its price, which is quite high, that is USD 50 – 60 per kg synthetic zeolite compared to USD 50 – 70 per ton natural zeolite.

Standing tests were also performed and the results were found to be comparable with removal capacities from other treatment processes that were used at the Wheal Jane passive treatment plant. From these results a reactor vessel was designed which is expected to give comparable removal rates with the Anoxic limestone drain system (ALD), Lime dosed system (LD) or the Lime free system (LF) systems used at Wheal Jane mine.

Fixed bed column tests revealed that natural zeolite has the potential to treatment AMD in a continuous process. Heavy metals were efficiently removed from AMD within the first cycle, but this efficiency reduced with regeneration. Regeneration may have caused the protonation of natural zeolite surface, which meant that the heavy metals in solution were being repelled from the zeolite surface resulting in a decrease in the adsorption rate. This problem could be solved by reducing the concentration of acid used in regeneration or using other reagents such as NaCl, NaNO₃ or EDTA. The fixed bed column had high removal efficiencies for iron and copper. The removal efficiency of the fixed bed column in treating AMD was compared with the efficiency of the Active treatment plant at Wheal Jane mine; this revealed that natural zeolite has the potential to effectively treat AMD. It was also observed that natural zeolite was easily saturated, and thus not economical in treating highly concentrated AMD. Therefore, any technology that incorporates natural zeolite as an adsorbent in treating AMD should be downstream of other treatment technologies which reduce the heavy metal concentration in AMD, thus insuring that the natural zeolite based technology handles only relatively dilute solutions.

The results from this study were generally better than those from other research work carried out at the University of Birmingham for the treatment of Wheal Jane mine AMD, that is, the use of blast furnace slag, calcium alginate beads and column flotation.

CHAPTER 10

CONCLUSIONS AND RECOMMENDATIONS

10.1 Conclusions

The potential of natural zeolite as a low cost material for the removal of iron, copper, zinc and manganese from synthetic metal solutions and real AMD from Wheal Jane mine was assessed in this study. A number of experiments were performed in order to determine this potential; these included characterisation of natural zeolite, equilibrium experiments, kinetic experiments and column studies. A summary of the conclusions of the experimental results will be presented in this chapter.

10.1.1 Characterisation of natural zeolite

SEM micrographs revealed that the natural zeolite samples used in this study have a heterogeneous and porous structure, with well defined clinoptilolite crystals. Micrographs of thermally pre-treated natural zeolite revealed that natural zeolite lost its porosity with an increase in thermal temperature, from 200 to 800 °C, and an increase in exposure time to microwave radiation from 15 to 45 minutes. Natural zeolite that was exposed to extreme temperatures lost all its porosity and its surface became a solid – glass like material.

The EDS technique was also performed to determine the elemental composition of natural zeolite. It was proved by use of this method that the main exchangeable cations in the structure of natural zeolite were Na^+ , Mg^{2+} , K^+ and Ca^{2+} .

The particle density of natural zeolite (particle size ranging from 1 – 3 mm) was determined to be approximately 2.28 g/cm^3 , using a helium gas pycnometer. The other particle characteristics determined were porosity, surface area and moisture content and these were 47.6 %, $15.9 \text{ m}^2/\text{g}$ and 9.4 % respectively.

10.1.2 Equilibrium studies

Results from equilibrium studies showed that natural zeolite was capable of removing heavy metals from solution. The maximum experimental removal capacities, $q_{e \text{ exp}}$, were 5.77, 6.51, 6.56 and 2.84 mg metal/ g natural zeolite for copper, zinc, iron and manganese respectively. The adsorption capacity increased with an increase in initial solution pH, from 2.5 to 5.7. The maximum adsorption capacities were all obtained at pH 5.7.

The Langmuir and Freundlich adsorption isotherms were used to evaluate the adsorption behaviour of natural zeolite for copper, zinc, manganese and iron. These models were able to give good fits to experimental data, with correlation coefficients, R^2 , ranging from about 0.9 – 0.99. However, at low initial solution pH, that is, pH = 2.5, the models were not effective in describing the equilibrium data.

Analysis of the exchangeable cations (Ca^{2+}) in aqueous solution at equilibrium showed an increase in these ions as the initial metal concentration increased. This was an indication that ion exchange between the heavy metals in solution and the exchangeable cations in the zeolite structure was taking place. Therefore, ion exchange was one of the processes responsible for the removal of heavy metals from solution by natural zeolite.

The removal of heavy metals from solution was not only due to adsorption and ion exchange but also due to metal precipitation. This was visually evident for iron removal; since its equilibrium pH was greater than the minimum pH (4.3) necessary for precipitation to occur.

Equilibrium studies were also used to determine the selectivity series of natural zeolite for the adsorption of iron, copper, zinc and manganese from solution, according to the Langmuir isotherm. The series was found to be: $\text{Fe}^{3+} > \text{Zn}^{2+} > \text{Cu}^{2+} > \text{Mn}^{2+}$.

10.1.3 Kinetic studies

Kinetic studies indicated that the rate of adsorption of the heavy metals by natural zeolite was rapid for the first 40 minutes and then gradually decreased as equilibrium was approached. About 80%, 95%, 90% and 99% of iron, manganese, zinc and copper respectively were adsorbed from their single component solutions in this first stage. This rapid removal of the heavy metals from solution is an advantage in waste water treatment processes.

There were a number of operational conditions which were found to influence the rate of metal uptake by natural zeolite; these include speed or rate of agitation, initial solution pH, initial solution concentration, particle size, presence of competing cations and thermal pre-treatment.

The speed of agitation mainly enhanced the rate of removal at the beginning of the process, thus it was observed that an increase in agitation speed resulted in an increase in the initial rate of adsorption, but the total amount adsorbed after equilibrium was

approximately the same for the different agitation speeds. An increase in the initial solution pH from 2.5 to 4.5 resulted in an increase in the equilibrium adsorption capacity, q_e , of natural zeolite for Mn^{2+} , Zn^{2+} and Cu^{2+} by 43%, 34% and 23% respectively. Therefore, the efficiency of natural zeolite for metal adsorption is dependent on the initial solution pH.

An increase in initial solution concentration resulted in an increase in the amount of heavy metals adsorbed, q , and a decrease in the efficiency of natural zeolite for the removal of heavy metals from solution. This decrease in efficiency was seen by a general reduction in the percentage adsorption (which represents the efficiency of the process) from about 100 % to 25 % for an increase in initial concentration from about 10 – 600 mg/l for the four heavy metals.

The results also showed that decreasing the particle size distribution of natural zeolite resulted in higher heavy metal removal rates and efficiencies, but as contact time increased, (that is, tending toward equilibrium) there was a decrease in the degree of the effect of particle size on adsorption. Thus at equilibrium the amount of heavy metals removed from solution by the different particle sizes should be approximately equal.

The effect of competing cations was also investigated and it was observed that the adsorption of Fe^{3+} was not significantly affected by the presence of competing ions. This may be because one of the mechanisms responsible for Fe^{3+} removal from solution is thought to be precipitation. The other 3 heavy metals were significantly affected by the presence of competing cations: the amount adsorbed from multi-component solutions,

decreased by 33%, 41% and 39% for Cu^{2+} , Zn^{2+} and Mn^{2+} respectively compared to that from single component solutions.

Thermal pre-treatment resulted in an increase in the rate and capacity of natural zeolite for heavy metals. The natural zeolite exposed to extreme thermal conditions lost its ability to remove significant amounts of heavy metals from solution due to the collapse of the porous zeolite structure. It was observed that natural zeolite exposed to microwave radiation for 15 minutes and natural zeolite heated in a muffle furnace at 200 °C for 30 minutes gave the best removal rates and efficiencies.

It was possible to regenerate natural zeolite using 2 % (wt.) sulphuric acid and NaCl (20 g/l). Sulphuric acid at 40 °C gave the best desorption efficiencies. Regeneration resulted in a decrease in the adsorption capacity of natural zeolite. For example, over 3 cycles of adsorption-desorption, the adsorption capacity of natural zeolite for iron, copper, zinc and manganese decreased by approximately 20.2, 9.8, 20.4 and 21.4 % respectively. This may be due to the destructive nature of sulphuric acid.

The rate limiting step for the removal of heavy metals from solution by natural zeolite was found to be intraparticle diffusion. The Nernst-Planck model gave a good fit of the experimental results; the correlation coefficient, R^2 , for the heavy metals ranged from 0.94 – 0.99.

10.1.4 Column studies

According to results obtained from fixed bed column studies, the adsorption of heavy metals from solution was affected by operational conditions such as flow rate and bed

height. Slower flow rates gave better removal efficiencies and capacities compared to faster ones, and longer bed heights also resulted in greater adsorption efficiencies due to an increase in residence time and available adsorption sites. Moreover, the breakthrough time increased with increasing bed height and decreasing flow rate.

The bed depth service time model (BDST) was successfully used to simulate experimental results at 30 % breakthrough. The breakthrough curves for copper, zinc, manganese and iron obtained from the BDST model deviated from experimental results by between 12 – 14 %.

Column studies were performed using synthetic AMD, which simulates Wheal Jane mine AMD. Natural zeolite was contacted with the solution for three adsorption – desorption cycles. There was a large decrease in the efficiency of the column in adsorbing heavy metals from cycle 1 to cycle 2, that is, at 40 % breakthrough. This reduction in efficiency, which occurred after regeneration, proves that acid regeneration negatively affected natural zeolite. It is recommended that another regenerating reagent be used, for example NaCl, NaNO₃ or EDTA. The reduction in efficiency may have been caused by the protonation of the zeolite surface by sulphuric acid. The protonated surface repels any heavy metals that may be approaching the zeolite surface, resulting in the evident reduction in efficiency of the acid regenerated zeolite.

The total amount of heavy metals adsorbed from solution after about 540 minutes, for the 3 cycles, was almost the same. This is an indication that the capacity of natural zeolite was not drastically altered by regeneration; rather its efficiency is the one that was affected. Therefore, the rate of adsorption was mainly affected by acid regeneration.

10.1.5 Treatment of Wheal Jane AMD

Batch experiments were performed for the treatment of Wheal Jane mine AMD, and these showed that thermally treating natural zeolite enhanced the capacity and efficiency of natural zeolite in treating AMD. The treatment of Wheal Jane AMD by thermally pre-treated natural zeolite gave final concentrations of iron below the maximum consent limit; the concentrations of copper, manganese and zinc were still higher than the acceptable legal concentrations. This indicates that natural zeolite is not capable of treating highly concentrated metal solutions in one pass.

Natural zeolite and synthetic zeolite were also used to treat AMD in batch mode, the adsorption capacity of synthetic zeolite was found to be ten times that of natural zeolite. The major disadvantage of using synthetic zeolite in treating AMD is its price, which is much higher than that of natural zeolite, that is, USD 50 – 60 per kg synthetic zeolite compared to USD 50 – 70 per ton natural zeolite. Therefore, only natural zeolite was used in this study, since one of the objectives was to develop a low cost process for the treatment of AMD.

Standing tests for the treatment of AMD were also performed and the results were found to be comparable with removal capacities from other treatment processes that were used at Wheal Jane passive treatment plant. From these results a reactor vessel was designed which is expected to give comparable removal rates and capacities to those obtained from the Anoxic limestone drain system (ALD), Lime dosed system (LD) or the Lime free system (LF) systems used at Wheal Jane passive treatment plant, see Appendix C.

Column studies revealed that natural zeolite has the potential to treatment AMD in a continuous process. Iron and copper were efficiently removed from Wheal Jane mine AMD, that is, between 71 – 99 % iron removal and 97 – 99 % copper removal for 3 adsorption-desorption cycles. The removal of manganese and zinc was not efficient, these ranged from 17 – 33 % and 34 – 44 % respectively. The removal efficiency of the column decreased with regeneration. The removal efficiency of the fixed bed column (cycle 1) in treating AMD was compared with the efficiency of the Active treatment plant at Wheal Jane mine; this revealed that natural zeolite has the potential to effectively treat AMD. It was also observed that natural zeolite was easily saturated, and thus not economical in treating concentrated AMD. Therefore, any technology that incorporates natural zeolite as an adsorbent in treating AMD should be downstream of other treatment technologies which reduce the heavy metal concentration in AMD, thus insuring that the natural zeolite based technology handles only relatively dilute solutions.

The results from this study were comparable with those from other research work carried out at the University of Birmingham for the treatment of Wheal Jane mine AMD, see Table 9.7.

10.2 Recommendations

The research carried out and presented in this thesis has shown that natural zeolite has potential for use in treating AMD. However, further research and studies are needed in this area if this technology is to be fully utilised on an industrial scale economically. There are several areas of research that could be pursued in the future, these are presented below.

Natural zeolite was thermally pre-treated in this study; other pre-treatment methods were not investigated. This could be a potential area of further study, which could result in an increase in the capacity and efficiency of natural zeolite in treating AMD. There are a number of pre-treatment methods that can be used for activating natural zeolite these include, chemical treatment using NaCl or NaNO₃ solutions, dilute concentrations of acid (HCl), NH₄Cl solution and cationic surfactants such as HDMTA-Br (hexadecyltrimethylammonium bromide).

In this study equilibrium studies were carried out using single component solutions, and these were modelled using the Langmuir and Freundlich isotherms. In practice, AMD contains a mixture of different cations, hence to get a clear picture of the maximum adsorption capacity of natural zeolite when treating AMD; equilibrium studies have to be performed using solutions containing a mixture of cations. The competitive Langmuir model could be used to model such a system.

Acid mine drainage not only contains metal cations but also anions such as SO₄²⁻, HPO₄²⁻, Cl⁻ and NO₃²⁻. Ion exchange of certain cations is strongly influenced and affected by the presence of complexing reagents such as the above mentioned anions (Helfferich, 1962; Inglezakis et al., 2003). This research only focused on the removal of heavy metals and did not take into account the effect of these anions on the capacity and effectiveness of natural zeolite. Further, research could be carried out to determine whether natural zeolite was able to reduce the concentration of these anions from solution and how the anions affect the heavy metal uptake capacity of natural zeolite.

Another potential area of research is the determination of the best regenerating solution. It is important to optimise this process, since the effectiveness of natural zeolite for subsequent adsorption stages is influenced by the effectiveness of the regeneration process. The optimisation of sulphuric acid can be carried out, by using a wide range of concentrations and determining the optimal acid concentration. The effectiveness of other regenerating solutions such as HCl, EDTA, NaCl and CaCl₂ at various concentrations and temperatures could be investigated as well.

The disposal of solutions from regeneration of natural zeolite and the disposal of exhausted natural zeolite are potential areas of further study. In this study, acid was used and recycled in regenerating natural zeolite so as to increase the metal concentration in a small volume of acid. This achieved the desired objective of reducing the volume of waste, but the problem of how to dispose this metal concentrated acidic solution was not dealt with. There are a number of potential solutions, these include the reclamation of metals from the acidic solutions by processes such as electrolysis and electro-dialysis; investigations could be carried out to determine the economic feasibility of each potential solution.

One of the conclusions drawn from this study was that natural zeolite was not capable of treating very concentrated solutions of heavy metals. It is recommended that instead of a single column set up, as used in this study, a multi – column set up be used and optimised for further study on the potential of natural zeolite in treating AMD. The advantage of this system would be that each column could have different operating parameters to maximise the efficiency of the total system.

Before this technology is implemented on an industrial scale, the construction of a pilot plant using natural zeolite to treat AMD would be a good way forward. Investigations could be carried out to determine different operating conditions that simulate real plant operation. From the pilot plant the required data for industrial application can be obtained and also a cost estimate of the implementation of the technology can be determined more accurately.

REFERENCES

1. Abadzic, S. D., and Ryan, J.N., 2001. Particle release and permeability reduction in a natural zeolite (clinoptilolite) and sand porous medium. *Environmental Science and Technology*, 35, 4501-4508.
2. Akdeniz, Y., and Ulku, S., 2007. Microwave effect on ion-exchange and structure of clinoptilolite. *Journal of Porous Materials*, 14, 55-60.
3. Altin, O., Ozbelge, H.O., Dogu, T., 1998. Use of general purpose adsorption isotherms for heavy metal-clay mineral interactions. *Journal of Colloid and Interface Science*, 198, 130 – 40.
4. Alvarez-Ayuso, E., Garcia-Sanchez, A., Querol, X., 2003. Purification of metal electroplating waste waters using zeolites. *Water Research*, 37, 4855-4862.
5. Amarasinghe, B.M.W. and Williams, R.A., 2007. Tea waste as a low cost adsorbent for the removal of Cu and Pb from wastewater. *Chemical Engineering Journal*, Volume 132, 299 – 309.
6. Ames, L. L., Jr., 1965. Self diffusion of some cations in open zeolites. *The American Mineralogist*, Volume 50, 465 – 475.
7. Atmosphere, Climate and Environment Information Programme, 2004. Industrial emission controls: Sulphur dioxide. Air Pollution and Acid Rain Fact Sheets Series: KS4 and A. [Available at: http://www.ace.mmu.ac.uk/Resources/Fact_Sheets/Key_Stage_4/Air_Pollution/pdf/27.pdf : last accessed 14/09/09].
8. Baerlocher, C., McCusker, L.B., Olson, D.H., 2007. Atlas of zeolite framework types. Elsevier on behalf of Structure Commission of the International Zeolite Association, 6th Edition.
9. Bailey, S. E., Trudy, J., Olin, T. J., Bricka, M. R., Adrian, D. D., 1999. A review of potentially low-cost sorbents for heavy metals. *Water Research*, 33 [11], 2469-2479.
10. Barrer, R.M., Papadopoulos, R., Rees, L.V.C., 1967. Exchange of sodium in clinoptilolite by organic cations. *Journal of Inorganic and Nuclear Chemistry*, 29, 2047 – 2063.
11. Barrer, R.M., 1978. Zeolites and clay minerals as sorbents and molecular sieves. Academic Press Inc., London.
12. Bektas, N. and Kara, S., 2004. Removal of lead from aqueous solutions by natural clinoptilolite: equilibrium and kinetic studies. *Separation and Purification Technology*, 39, 189 – 200.

13. Bell R.G., 2001. Zeolites. British Zeolite Association (<http://www.bza.org/>).
14. Bhattacharyya, K.G. and Gupta, S.S., 2006. Kaolinite, montmorillonite, and their modified derivatives as adsorbents for removal of Cu (II) from aqueous solution. *Separation and Purification Technology*, 50, 388-397.
15. Biesinger, K.E., Christensen, G.M. and Fiandt, J. T., 1986. Effects of metal salt mixtures on *Daphnia magna* reproduction. *Ecotoxicology and Environmental Safety*, 11, 9 – 14.
16. Blanchard, G., Maunaye, M., Martin, G., 1984. Removal of heavy metals from waters by means of natural zeolite. *Water Research*, 18, 1501 – 1507.
17. Bohart, G.S. and Adams, E.Q., 1920. Some aspects of the behaviour of charcoal with respect to chlorine. *Journal of the American Chemical Society*, 42, 523 – 544.
18. Bone, B., 2003. Remediation scheme to mitigate the impacts of abandoned mines. Environmental Agency for England and Wales [Available at: http://www.cluin.org/romania/presentations/natoccms_uk_cases.pdf: accessed 14/09/09].
19. Brigatti, M.F., Lugli, C., Poppi, L., 2000. Kinetics of heavy metal removal and recovery in sepiolite. *Applied Clay Science*, 16, 45 – 57.
20. Brown, D.J.A. and K. Sadler, 1989. Fish survival in acid waters. In: *Acid Toxicity and Aquatic Animals*. Society for Experimental Biology Seminar Series: 34, (Morris, R. et al., eds.), Cambridge University Press, 31 – 44.
21. Brown, M., Barley, B., Wood, H., 2002. *Mine water treatment: Technology, application and policy*. London: IWA Publishing, p. 448.
22. Brunauer, S., Emmett, P.H., Teller, E., 1938. Adsorption of gases in multimolecular layers. *Journal of the American Chemical Society*, 60, 309-319.
23. Brunauer, S., 1943. *The adsorption of gases and vapours*. Oxford University Press.
24. Cabrera, C., Gabaldon, C., Marzal, P., 2005. Sorption characteristics of heavy metal ions by a natural zeolite. *Journal of Chemical Technology and Biotechnology*, 80, 477-481
25. Celik, M.S., Ozdemir, B., Turan, M., Koyuncu, I., Atesok, G., Sarikaya, H.Z., 2001. Removal of ammonia by natural clay minerals using fixed and fluidised bed column reactors. *Water Science and Technology: Water Supply*, 1, 81 – 88.
26. Chiron, N., Guilet, R., Deydier, E., 2003. Adsorption of Cu (II) and Pb(II) onto a grafted silica: isotherm and kinetic models. *Water Research*, 37, 3079 – 3086.

27. Cincotti, A., Mameli, A., Locci, M. A., Orru, R., Cao, G., 2006. Heavy metal uptake by Sardinian natural zeolites: Experiment and modelling. *Industrial and Engineering Chemistry Research*, 45, 1074-1084.
28. Connors, K., 1990. Chemical Kinetics: The study of reaction rates in solution. VCH Publishers, USA.
29. Cooney, D.O., 1998. Adsorption design for wastewater treatment. CRC Press.
30. Cooney, E.L., Booker, N.A., Shallcross, D.C., Stevens, G.W., 1999. Ammonia removal from wastewaters using natural Australian zeolite. II. Pilot-scale study using continuous packed column process. *Separation Science and Technology*, 34, 2741-2760.
31. Cortes-Martinez, R., Solache-Rios, M., Martinez-Miranda, V., Alfaro-Cuevas, R., 2008. Removal of cadmium by natural and surfactant modified Mexican zeolitic rocks in fixed bed columns. *Water, Air and Soil Pollution*, Volume 196, 199 – 210.
32. Costello, C., 2003. Acid Mine Drainage: Innovative treatment technologies. U.S. Environmental Protection Agency.
33. Coulton, R., Bullen, C., Dolan, J., Hallett, C., Wright, J., Marsden, C., 2003. Wheal Jane mine water active treatment plant – design, construction and operation. *Land Contamination and Reclamation*, 11 (2), 245 – 252.
34. Coulton, R., Bullen, C., Hallet, C., 2003. The design and optimization of active mine water treatment plants. *Land Contamination and Reclamation*, 11, 273–279.
35. Cresser, M.S and Marr, I.L., 1991. Optical spectrometry in the analysis of pollutants *in Instrumental Analysis of Pollutants*. Hewitt, C.N. (editor). Elsevier Applied Science, London, 99 – 145.
36. Csicsery, S.M., 1985. Chemistry in Britain. Royal Society of Chemistry, p. 473.
37. Culfaz, M. and Yagiz, M., 2004. Ion exchange properties of natural clinoptilolite: lead-sodium and cadmium-sodium equilibria. *Separation and Purification Technology*, 37, Volume 2, 93-105.
38. Curkovic, L., Cerjan-Stefanovic, S., Philippan, T., 1997. Metal ion exchange by natural and modified zeolites. *Water Research*, 31, 1379 – 1382.
39. Darkwah, L., 2005. Remediation of acid mine drainage. The University of Birmingham, Thesis.
40. Doula, M., Ioanou, A., Dimirkou, A., 2002. Copper adsorption and Si, Al, Ca, Mg and Si release from clinoptilolite. *Journal of Colloid and Interface Science*, 245, 237-250.

41. Doula, M., 2006. Removal of Mn^{2+} ions from drinking water by using clinoptilolite and a clinoptilolite-Fe oxide system. *Water Research*, 40, 3167 – 3176.
42. Du, Q., Liu, S., Cao, Z., Wang, Y., 2005. Ammonia removal from aqueous solution using natural Chinese clinoptilolite. *Separation and Purification Technology*, 44 [3], 229-234.
43. Dyer, A., 1988. An introduction to zeolite molecular sieves. John Wiley & Sons, Toronto.
44. Earle, J. and Callaghan, T., 1998. Coal mine drainage prediction and pollution prevention in Pennsylvania. Department of Environmental Protection, Chapter 4, 4.1 – 4.10.
45. Englert, A.H. and Rubio, J., 2005. Characterisation and environmental application of a Chilean natural zeolite. *International Journal of Mineral Processing*, 75, 21 – 29.
46. Environmental Agency, 2007. Wheal Jane mine-water treatment plant Baldhu, Cornwall.
47. Erdem, E., Karapinar, N., Donat, R., 2004. The removal of heavy metal cations by natural zeolite. *Journal of Colloid and Interface Science*, 280, 309-314.
48. Ersoy, B. and Celik, M.S., 2002. Electro-kinetic properties of clinoptilolite with mono and multivalent electrolytes. *Microporous and Mesoporous Materials*, 55, 305-312.
49. Evangelou, V.P., 1998. Pyrite chemistry: the key for abatement of acid mine drainage. In: Geller, A., Klapper, H., Salomons, W., editors. *Acidic Mining Lakes: Acid Mine Drainage, Limnology and Reclamation*. Berlin: Springer; 197– 222.
50. Faulkner, B.B. and Skousen J.G., 1995. Effects of land reclamation and passive treatment systems on improving water quality. *Green Lands* 25 (4), 34 – 40.
51. Fripp, J., Ziemkiewicz, P.F., Charkavork, H., 2000. Acid mine drainage treatment - Technical Notes Collection. Vicksburg: Army Engineer Research and Development Center; Report No.: ERDC TN-EMRRPSR-14.
52. Furusawa, T. and Smith, J.M., 1973. Fluid-particle and intraparticle mass transport rates in slurries. *Industrial and Engineering Chemistry Fundamentals*, Volume 12, [2], 197-203.
53. Garcia-Mendiata, A., Solache-Rios, M., Olguin, M.T., 2009. Evaluation of the sorption properties of a Mexican clinoptilolite-rich tuff for iron, manganese and iron-manganese systems. *Microporous and Mesoporous Materials*, 118, 489 – 495.
54. Gazea, B., Adam, K., Kontopoulos, A., 1996. A review of passive systems for the treatment of acid mine drainage. *Minerals Engineering*, Volume 9 [1], 23 – 42.

55. Goldstein, J., Newbury, D., Joy, D., Lyman, C., Echlin, P., Lifshin, E., Sawyer, L., Michael, J., 2003. Scanning electron microscopy and X-Ray microanalysis. Kluwer Academic/Plenum Publishers, New York.
56. Griffiths, D., 2005. Abandoned mine drainage. Environmental Agency.
57. Gunay, A., Arslankaya, E., Tosun, I., 2007. Lead removal from aqueous solution by natural and pretreated clinoptilolite: Adsorption equilibrium and kinetics. *Journal of Hazardous Materials*, 146, 362 – 371.
58. Hallberg, K.B. and Johnson, B.D., 2003. Passive mine water treatment at the former Wheal Jane tin mine, Cornwall: important biogeochemical and microbiological lessons. *Land Contamination and Reclamation*, Volume 11 [2], 213 – 220.
59. Hamilton, R.M., Bowen, G.G., Postlethwaite, N.A., Dussek, D.J., 1994. The abandonment of Wheal Jane, a tin mine in S.W. England. In: Proceedings of the 5th International Mine water Congress, Nottingham, UK, 543 – 551.
60. Harland, C.E., 1994. Ion Exchange: Theory and Practice, second edition, The Royal Society of Chemistry.
61. Hedin, R.S. and Watzlaf, G.R., 1994. The effects of anoxic limestone drains on mine water chemistry. p. 185-194. In Proceedings of the International Land Reclamation and Mine Drainage Conference, Pittsburgh, PA.
62. Hedin, R.S., Nairn R.W., Kleinmann, R.L.P., 1994. Passive treatment of coal mine drainage. USDI, Bureau of Mines Information Circular IC 9389. Pittsburgh, PA.
63. Helfferich, F. and Plesset, M.S., 1958. Ion exchange kinetics. A nonlinear diffusion problem. *Journal of Chemical Physics*, Volume 28 [3], 418-424.
64. Helfferich, F., 1962. Ion exchange, Chapter 6, Dover, New York.
65. Hem, J.D., 1970. Study and interpretation of the chemical characteristics of natural waters, Second edition. United States Geological Survey Water Supply Paper No. 2254, pg 363.
66. Heping, C., Li, L.Y., Grace, J.R., 2006. Exploration of remediation of acid rock drainage with clinoptilolite as sorbent in a slurry bubble column for both heavy metal capture and regeneration. *Water Research*, 40, 3359-3366.
67. Hodge, W.W., 1937. Pollution of streams by coal mine drainage. *Industrial and Engineering Chemistry*, Volume 29, 1048 – 1055.
68. Hoehn, R.C. and Sizemore, D.R., 1977. Acid mine drainage (AMD) and its impact on a small Virginia stream. *Water Resources Bulletin*, Volume 13, 153-160.

69. Hughes, P., 1994. Water pollution from abandoned coal mines. Library Research Paper 94/43.
70. Hull, A.W., 1919. A new method of chemical analysis. *Journal of the American Chemical Society*, 41 (8), 1168 – 1175.
71. Hutchins, R.A., 1974. New method simplifies design of activated carbon systems. *Chemical Engineering*, 80, 133 – 138.
72. Inglezakis, V.J., Diamandis, N.A.D., Loizidou, M.D., Grigoropoulou, H.P., 1999. Effect of pore clogging on kinetics of lead uptake by clinoptilolite. *Journal of Colloid and Interface Science*, 215, 54 – 57.
73. Inglezakis, V.J., Loizidou, M.D., Grigoropoulou, H.P., 2001. Applicability of simplified models for the estimation of ion exchange diffusion coefficients in zeolites. *Journal of Colloid and Interface Science*, 234, 434-441.
74. Inglezakis, V.J., Hadjiandreou, K.J., Loizidou, M.D., Grigoropoulou, H.P., 2001. Pretreatment of natural clinoptilolite in a laboratory-scale ion exchange packed bed. *Water Research*, 35 [9], 2161-2166.
75. Inglezakis, V.J., Loizidou, M.D., Grigoropoulou, H.P., 2002. Equilibrium and kinetic ion exchange studies of Pb^{2+} , Cr^{3+} , Fe^{3+} and Cu^{2+} on natural clinoptilolite. *Water Research*, 36, 2784-2792.
76. Inglezakis, V.J., Loizidou, M.D., Grigoropoulou, H.P., 2003. Ion exchange of Pb^{2+} , Cu^{2+} , Fe^{3+} and Cr^{3+} on natural clinoptilolite: selectivity determination and influence of acidity on metal uptake. *Journal of Colloid and Interface Science*, 261, 49-54.
77. Inglezakis, V.J., Zorpas, A.A., Loizidou, M.D., Grigoropoulou, H.P., 2003. Simultaneous removal of metals Cu^{2+} , Fe^{3+} and Cr^{3+} with anions SO_4^{2-} and HPO_4^{2-} using clinoptilolite. *Microporous and Mesoporous Materials*, 61, 167-171.
78. Inglezakis, V.J., Grigoropoulou, H., 2004. Effects of operating conditions on the removal of heavy metals by zeolite in fixed bed reactors. *Journal of Hazardous Materials*, 12, 37-43.
79. Inglezakis, V.J., 2005. The concept of “capacity” in zeolite ion-exchange systems. *Journal of Colloid and Interface Science*, 281, 68 - 79.
80. Jenkins, D.A., Johnson, D.B., Freeman, C., 2000. Mynydd Parys Cu-Pb-Zn mines: mineralogy, microbiology and acid mine drainage. In: Cotter-Howells, J.D., Campbell, L.S., Valsami-Jones, E., Batchelder, M. (editors.) *Environmental mineralogy: microbial interactions, anthropogenic influences, contaminated land and waste management*. The Mineralogy Society Series no.9. Mineralogical Society, London, UK, 161-180.

81. Johnson, B.D. and Hallberg, K.B., 2005. Acid mine drainage remediation options: a review. *Science of the Total Environment*, 338, 3 – 14.
82. Jusoh, A., Shiung, L.S, Ali, N., Noor, M.J, 2007. A simulation study of the removal efficiency of granular activated carbon on cadmium and lead. *Desalination*, 206, 9 – 16.
83. Kadirvelu, K. and Namasivayam, C., 2003. Activated carbon from coconut coirpith as metal adsorbent: adsorption of Cd (II) from aqueous solution. *Advances in Environmental Research*, 7, 471 – 478.
84. Kepler, D.A. and McCleary, E.C., 1994. Successive alkalinity-producing systems (SAPS) for the treatment of acidic mine drainage. In Proceedings of the International Land Reclamation and Mine Drainage Conference, Pittsburgh, PA., p. 195-204.
85. Kepler, D.A. and McCleary, E.C., 1997. Passive aluminium treatment successes. In Proceedings of the National Association of Abandoned Mine Lands Programs. Davis, WV.
86. Kesraoui-Ouki, S., Cheeseman, C.R., Perry, R., 1994. Natural zeolite utilisation in pollution control: A review of applications to metals' effluents. *Journal of Chemical Technology and Biotechnology*, 59, 121 – 126.
87. Kimmel, W.G., 1983. The impact of acid mine drainage on the stream ecosystem. In: Pennsylvania Coal: Resources, Technology and Utilization, (S. K. Majumdar and W. W. Miller, editors). *The Pennsylvania Academy of Sciences Publishing*, 424-437.
88. Ko, D.C, Lee, V.K, Porter, J.K., McKay, G., 1999. Correlation based approach to the optimisation of fixed bed sorption units. *Industrial and Engineering Chemistry Research*, 38, 4868 – 4877.
89. Kocaoba, S., Orhan, Y., Akyuz, T., 2007. Kinetics and equilibrium studies of heavy metal ions removal by use of natural zeolite. *Desalination*, 214, 1 – 10.
90. Kocaoba, S. and Akcin, G, 2008. A kinetic investigation of the removal of chromium from aqueous solutions with a strong cation exchange resin. *Monatshefte fur Chemie*, 139, 873 – 879.
91. Korkuna, O., Lebeda, R., Skubiszewska-Zieba, J., Vrublevs'ka, T., Gun'ko, V.M., Ryczkowski, J., 2006. Structural and physicochemical properties of natural zeolites: clinoptilolite and mordenite. *Microporous and Mesoporous Materials*, 87, 243 – 254.
92. Koryak, M., Shapiro M.A., Sykora, J.L., 1972. Riffle zoobenthos in streams receiving acid mine drainage. *Water Research*, Volume 6, 1239-1247.
93. Langmuir, I., 1918. The adsorption of gases on plane surfaces of glass, mica and platinum. *Journal of American Chemical Society*, 40, 1361 – 1403.

94. Leinonen, H., Letho, J., 2001. Purification of metal finishing waste waters with zeolites and activated carbons. *Waste Management and Research*, 19, 45-57.
95. Li, M.G., Aube, B.C., St-Arnaud, L.C., 1997. Considerations in the use of shallow water covers for decommissioning reactive tailings. Proceedings of the Fourth International Conference on Acid Rock Drainage, Vancouver, Volume I, 115–130.
96. Lide, D.R., 1997. Handbook of chemistry and physics, 78th edition.
97. Loos, M.A., Bosch, C., Mare, J., Immelman, E., Sanderson, R.D., 1989. Evaluation of sodium lauryl sulphate, sodium benzoate and sorbic acid as inhibitors of acidification of South African coal waste. Groundwater and Mining: Proceedings of the 5th Biennial Symposium of the Groundwater Division of the Geological.
98. Low, K.S., Lee, C.K., Ng, A.Y., 1999. Column study on the sorption of Cr (VI) using quaternized rice hulls. *Bioresource Technology*, 68, 205 – 208.
99. Lynch, B, 2003. The remediation of acid mine drainage using column flotation. The University of Birmingham, Thesis.
100. McGinness, S., 1999. Treatment of Acid Mine Drainage. Research Paper 99/10. House of Commons, London.
101. Malliou, E., Loizidou, M., Spyrellis, N., 1994. Uptake of lead and cadmium by clinoptilolite. *Science of the Total Environment*, 149, 139 – 144.
102. Marcus, Y., 1991. Thermodynamics of Solvation of Ions. *Journal of Chemical Society, Faraday Transactions*, 87, 2995-2999.
103. Markovska, L.T., Meshko, V.D., Marinkovski, M.S., 2006. Modelling of the adsorption kinetics of zinc onto granular activated carbon and natural zeolite. *Journal of Serbian Chemical Society*, 71 (8-9), 957 – 967.
104. Mehling, P.E., Day, S.J., Sexsmith, K.S., 1997. Blending and layering waste rock to delay, mitigate or prevent acid generation: a case review study. Proceedings of the Fourth International Conference on Acid Rock Drainage, Vancouver, BC, vol. II, p. 953–70.
105. Mier, M.V., Callejas, R.L., Gehr, R., Cisneros, B.E.J., Alvarez P.J.J., 2001. Heavy metal removal with Mexican clinoptilolite: multi – component ionic exchange. *Water Research*, 35 [2], 373 – 378.
106. Mohan, S. and Sreelakshmi, G., 2008. Fixed bed column study for heavy metal removal using phosphate treated rice husk. *Journal of Hazardous Materials*, 153, 75-82.

107. Moreno, N., Querol, X., Ayora, C., 2001. Utilization of zeolites synthesised from coal fly ash for the purification of acid mine waters. *Environmental Science and Technology*, 35, 3526-3534.
108. Moreno-Pirajan, J.C., Rangel, D., Amaya B., Vargas, E.M., Giraldo, L., 2006. Scale up of pilot plant for the adsorption of heavy metals. *Journal the Argentine Chemical Society*, Volume 94, 365 – 375.
109. Morris, R., Taylor, E.W., Brown, D.J.A., Brown, J.A., 1989. Acid toxicity and aquatic animals. Society for Experimental Biology Seminar Series, Volume 34, Cambridge University Press, p. 282.
110. Mortier, W.J. and Structure Commission of the International Zeolite Association, 1982. Compilation of extra framework sites in zeolites. Butterworth Scientific Ltd.
111. Mumpton, F.A. and Fishman, P.H., 1977. The application of natural zeolite in animal science and aquaculture. *Journal of Animal Science*, 45, 1188 – 1203.
112. Nantumbwe, B.B., 2007. Removal of metals from minewater and synthetic metal solutions using calcium alginate beads. The University of Birmingham, Thesis.
113. Neal, C., Whitehead, P.G., Jeffery, H., Neal, M., 2004. The water quality of the River Carnon, West Cornwall, November 1992 to March 1994: the impacts of Wheal Jane discharges. *Science of the Total Environment*, 338, 23–39.
114. Nieto, J.M., Sarmiento, A.M., Olias, M., Canovas, C.R., Riba, I., Kalman, J., Delvalls, T.A., 2007. Acid mine drainage pollution in the Tinto and Odiel rivers (Iberian Pyrite Belt, S.W. Spain) and bioavailability of the transported metals to the Huelva Estuary. *Environmental International*, 33, 445 – 455.
115. Nightingale, E.R.J., 1959. Phenomenological theory of ion solvation. Effective radii of hydrated ions. Department of Chemistry, University of Nebraska.
116. Omer, Y., Altunkaynak, Y., Guzel, F., 2003. Removal of copper, nickel, cobalt and manganese from aqueous solution by kaolinite. *Water Research*, 37, 948-952.
117. Panayotova, M. and Velikov, B., 2002. Kinetics of heavy metal ions removal by use of natural zeolite. *Journal of Environmental Science and Health*, A37 [2], 139–147.
118. Papageorgiou, K.S., Katsaros, K.F., Kouvelos, P.E., Nolan, W.J., LeDeit, H., Kanellopoulos, K.N., 2006. Heavy metal sorption by calcium alginate beads from *Laminaria digitata*. *Journal of Hazardous Materials*, B137, 1765 – 1772.
119. Penreath, R.J., 1994. The discharge of waters from active and abandoned mines. In: Hester, R.E. and Harrison, R.M. (editors.) Mining and its environmental impact. Issues in Environmental Science and Technology no. 1. Royal Society of Chemistry, Herts, UK, 121-132.

120. Peric, J., Trgo, M., Medvidovic, N.V., 2004. Removal of zinc, copper and lead by natural zeolite-a comparison of adsorption isotherms. *Water Research*, 38, 1893-1899.
121. Richardson, J.F., Harker, J.H., Backhurst, J.R., 2002. Coulson & Richardson's Chemical Engineering Volume 2, Fifth edition, Butterworth Heinemann.
122. Rozic, M., Stefanovic, S.J., Kurajica, S., Maeefat, M.R., Margeta, K., Farkas, A., 2005. Decationization and dealumination of clinoptilolite tuff and ammonium exchange on acid modified tuff. *Journal of Colloid and Interface Science*, 284, 48-56.
123. Ruthven, D.M., 1984. Principles of adsorption and adsorption processes. A Wiley – Interscience Publication, John Wiley and Sons Inc.
124. Sanchez, E., Lopez-Pamo, E., Santofimia, E., Aduvire, O., Reyes, J., Baretino, D., 2005. Acid mine drainage in the Iberian Pyrite Belt (Spain): Geochemistry, mineralogy and environmental implications. *Applied Geochemistry*, 20 [7], 1320 – 1356.
125. Sand, L.B. and Mumpton, F.A., 1978. Natural Zeolites (Occurrence, properties, Use). Pergamon Press Ltd.
126. Semmens, M. and Martin, W., 1988. The influence of pretreatment on capacity and selectivity of clinoptilolite for metal ions. *Water Research*, 22, 537 – 542.
127. Sheta, A.S., Falatah, A.M., Al-Sewailem, M.S., Khaled, E.M., Salam, A.S.H., 2003. Sorption characteristics of zinc and iron by natural zeolite and bentonite. *Microporous Mesoporous Material*, 61, 127–136.
128. Sidheswaran, P. and Bhat, A.N., 1998. Impact of zeolitic water content on exchange of calcium ions. *Thermochimica Acta*, 298 [1-2], 55 – 58.
129. Singer, P.C. and Strumm, W., 1970. Acid mine drainage: the rate determining step. *Science*, 167, 1121 – 1123.
130. Skousen, J., Rose, A., Geidel, G., Foreman, J., Evans, R., Hellier, W., Members of the Avoidance and Remediation Working Group of ADTI, 1998. Handbook of technologies for avoidance and remediation of acid mine drainage. The national Mine Land Reclamation Centre, West Virginia.
131. Sprynskyy, M., Boguslaw B., Terzyk, A.P., Namiesnik, J., 2006. Study of the selection mechanism of heavy metal (Pb^{2+} , Cu^{2+} , Ni^{2+} and Cd^{2+}) adsorption on clinoptilolite. *Journal of Colloid and Interface Science*, 304, 21-28.
132. Srivastava, S. K., Tyagi, R., Pant, N., Pal, N., 1989. Studies on the removal of some toxic metal ions. Part II (removal of lead and cadmium by montmorillonite and kaolinite). *Environmental Technology*, Volume 10, 275 - 282.

133. Steffen, Robertson and Kirsten, Inc., 1989. Acid Drainage Draft Technical Guide, Volume 2 – Summary Guide.
134. Stylianou, M.A., Inglezakis, V.J., Moustakas, K.G., Malamis, S., Loizidou, M.D., 2007. Removal of Cu (II) in fixed bed and batch reactors using natural zeolite and exfoliated vermiculite as adsorbents. *Desalination*, 215, 133 – 142.
135. Survey of South Africa Randberg, Transvaal. Pretoria: Geological Society of South Africa, pp. 193– 200.
136. Swanson, D.A., Barbour, S.L., Wilson, G.W., 1997. Dry-site versus wet-site cover design. Proceedings of the Fourth International Conference on Acid Rock Drainage, Vancouver, BC, vol. IV, p. 1595–610.
137. Swash, P.M. and Monhemius, A.J., 2005. Characteristics and stabilities of residues from the Wheal Jane constructed wetlands. *Science of the Total Environment*, 338, 95 – 105.
138. Tatsuo, O. and Nagae M., 2003. Quick activation of optimized zeolites with microwave heating and utilization of zeolite for re-useable desiccant. *Journal of Porous Materials*, 10, 139-143.
139. Tatsuo, O. and Nagae M., 2005. Durability of zeolite against repeated activation treatments with microwave heating. *Journal of Porous Materials*, 12, 256-271.
140. The Water Supply (Water Quality) Regulations 2000, Statutory Instrument 2000 No. 3184.
141. Tien, Chi, 1994. Adsorption calculations and modelling. Butterworth – Heinemann, New York.
142. Tissue, B.M., 1996. Atomic transitions: Theory. Available at <http://elchem.kaist.ac.kr/vt/chem-ed/spec/atomic/aa.htm> [last accessed 11/09/09].
143. Treybal, R.E., 1980. Mass transfer operations, 3rd Edition. McGraw – Hill Book Company.
144. Trgo, M. and Peric, J., 2003. Interaction of the zeolitic tuff with Zn containing simulated pollutant solutions. *Journal of Colloid and Interface Science*, 260, 1017-1021.
145. Tsitsishvili, G.V., Andronikashvili, T.G., Kirov, G.M., Filizova, L.D., 1992. Natural Zeolites. Ellis Horwood Limited, Chichester, UK.
146. Turner, M.D., Laurence, R.L., Conner, W.C., 2000. Microwave radiation's influence on sorption and competitive sorption of zeolites. *AIChE Journal*, Volume 46 [4], 758 – 768.

147. United Utilities, 2007. Wheal Jane minewater treatment plant (Brochure).
148. Valenzuela, F., Cabrera, J., Basualto, C., Sapag-Hagar, J., 2005. Kinetics of copper removal from acidic mine drainage by a liquid emulsion membrane. *Minerals Engineering*, 18, 1224 – 1232.
149. Walker, G.M. and Weatherley, L.R., 2001. COD removal from textile industry effluent: pilot plant studies. *Chemical Engineering Journal*, 84, 125 – 131.
150. Whitehead, P.G., Cosby, B.J., Prior, H., 2005. The Wheal Jane wetlands model for bioremediation of acid mine drainage. *Science of the Total Environment*, 338, 125 – 135.
151. Whitehead, P.G., Hall, G., Neal, C., Prior, H., 2005. Chemical behaviour of the Wheal Jane bioremediation system. *Science of the Total Environment*, 338, 41 – 51.
152. Wingenfelder, U., Hansen, C., Furrer, G., Schulin R., 2005. Removal of heavy metals from mine waters by natural zeolites. *Environmental Science and Technology*, 35, 4606-4613.
153. Wong, M.H., Luk, K.C., Choi, K.Y., 1977. The effects of zinc and copper salts on *Cyprinus carpio* and *Ctenopharyngodon idellus*. *Acta Anatomica*, 99, 450 – 454.
154. Younger, P.L., Banwart, S. A., Hedin, R. S., 2002. Mine Water: Hydrology, Pollution, Remediation. The Netherlands: Kluwer Academic Press.
155. Younger, P.L., Coulton, R.H., Froggatt, E.C., 2004. The contribution of science to risk-based decision-making: lessons from the development of full-scale treatment measures for acidic mine waters at Wheal Jane, UK. *Science of the Total Environment*, 338, 137–54.
156. Yuan, G., Seyama, H., Soma, M., Theng, B.K.G., Tanaka, A., 1999. Adsorption of some heavy metals by natural zeolites: XPS and batch studies. *Journal of Environmental Science and Health*, 34, 625 – 648.
157. Zamzow, M.J., Eichbaum, B.R., Sandgren, K.R., Shanks, D.E., 1990. Removal of heavy metals and other cations from waste water using zeolites. *Separation Science and Technology*, 25 [13-15], 1555 – 1569.
158. Ziemkiewicz, P., Skousen, J., Brant, D., Sterner, P., Lovett, R.J., 1997. Acid mine drainage treatment with armoured limestone in open channels. *Journal of Environmental Quality*, 26, 1017-1024.
159. Zipper, C. and Jage, C., 2001. Passive treatment of acid mine drainage with vertical – flow systems. Virginia co-operative extension publication No. 460 – 133.

APPENDICES

APPENDIX A

Atomic absorption spectroscopy (AAS)

Atomic absorption spectroscopy (AAS) uses the absorption of light to measure the concentration of gas-phase atoms. Since samples are usually liquid, the metal atoms or ions must be vaporized in a flame. The vaporised atoms absorb ultraviolet or visible light and make transitions to higher electronic energy levels. The metal concentration is determined from the amount of light absorbed by the vaporised atoms (Tissue, 1996). The amount of light absorbed by the atoms is simply the total amount of light produced at the light source (lamp) minus the total amount received by the detector, see Figure A1. The measurable decrease in intensity of the light beam due to absorption at a specific wavelength is characteristic to a specific element according to the Beer-Lambert Law:

$$\log \frac{I_o}{I_t} = \varepsilon.C.I \quad (1)$$

Where I_o – Incident light intensity,

I_t – Transmitted light intensity,

ε – Species constant as specified wavelength,

C – Concentration of absorbing species,

I – Optical path length.

The percentage transmission ($100 \times I_o/I_t$) which varies linearly with concentration of the element is referred to as absorbance value (Cresser and Marr, 1991).

Concentration measurements are usually determined from a working curve after calibrating the instrument with standards of known concentration.

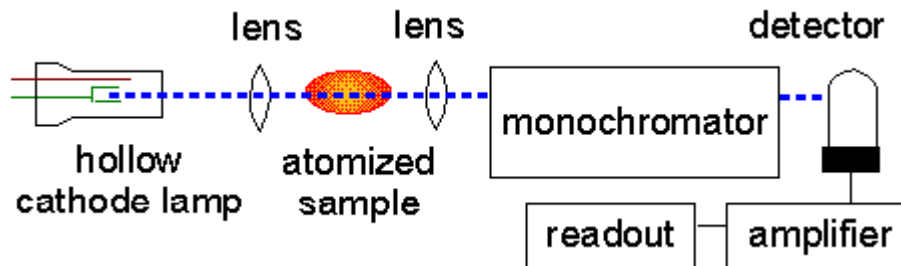


Figure A1: Schematic of atomic absorption spectrometer (Tissue, 1996). [Reprinted from: <http://elchem.kaist.ac.kr/vt/chem-ed/spec/atomic/aa.htm>].

Light source

The light source is usually a hollow-cathode lamp of the element that is being measured. Lasers are also used in research instruments. Since lasers are intense enough to excite atoms to higher energy levels, they allow AAS and atomic fluorescence measurements in a single instrument. The disadvantage of these narrow-band light sources is that only one element is measurable at a time.

Atomizer

AAS requires that the metal atoms be in a gaseous phase. Ions or atoms in a sample must be vaporised in a high-temperature source such as a flame (2100 – 2400 K) or graphite furnace. Flame AAS can only analyse solutions, while graphite furnace AAS can accept solutions, slurries, or solid samples.

Flame

AAS uses a slot type burner to increase the path length, and therefore to increase the total absorbance (Beer-Lambert law). Sample solutions are usually aspirated with the gas flow

into a nebulising/mixing chamber to form small droplets before entering the flame. Table A1 presents examples of different fuels used to produce a flame for the AAS.

Light separation and detection

AAS use monochromators and detectors for UV and visible light. The main purpose of the monochromator is to isolate the absorption line from background light due to interferences. Simple dedicated AAS instruments often replace the monochromator with a band-pass interference filter. Photomultiplier tubes are the most common detectors for AAS.

Excitation

A flame provides a high-temperature source for desolvating and vaporising a sample to obtain free atoms for spectroscopic analysis. In atomic absorption spectroscopy ground state atoms are desired. For atomic emission spectroscopy the flame must also excite the atoms to higher energy levels. The following table lists temperatures that can be achieved in some commonly used flames.

Table A1: Examples of common fuels used in AAS and the temperature of the flames they produce.

Fuel	Oxidant	Temperature, K
Hydrogen	Air	2000-2100
Acetylene	Air	2100-2400
Hydrogen	Oxygen	2600-2700
Acetylene	Nitrous Oxide	2600-2800

The atomic absorption spectrometer (AAS) used in this study uses an air – acetylene flame to vaporise solution samples and single element hollow cathode lamps a light sources.

Sample analysis

The atomic absorption spectrometer (AAS) had to be calibrated for each metal before analysing any sample. This was achieved by passing samples of known concentration through the AAS. These samples were made from standard metal solutions which were diluted to the required metal concentration. The results of analysing these diluted standard solutions gave a calibration curve for each metal. Figure A2 presents the typical calibration curves for iron, copper, zinc and manganese used in this study. The error in analysing copper, zinc, manganese and iron was $\pm 6.5 \%$, 6.6% , 5.7% and 6.6% .

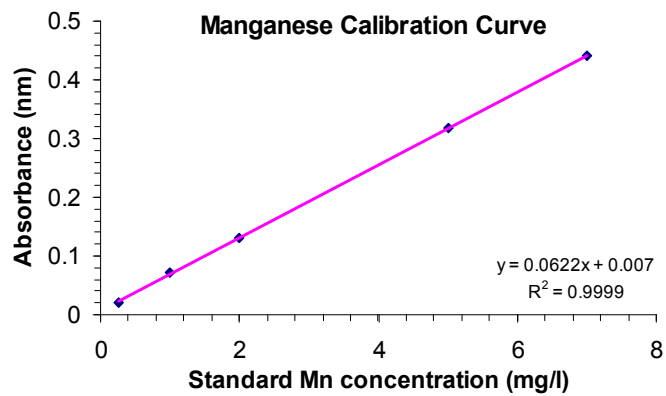
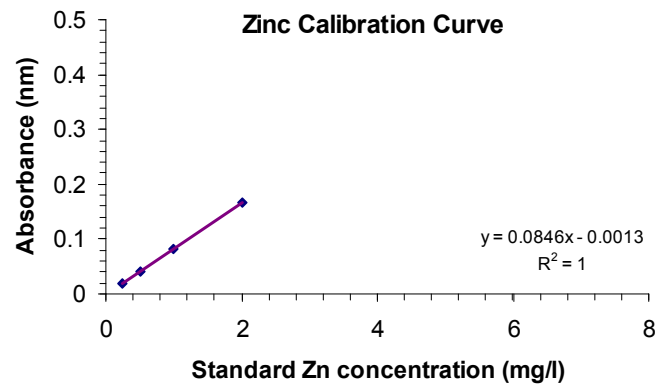
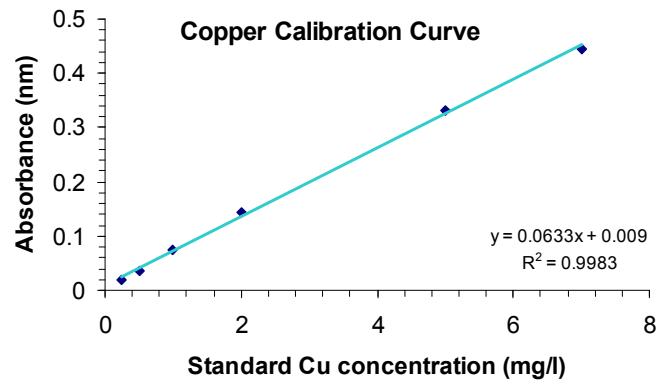
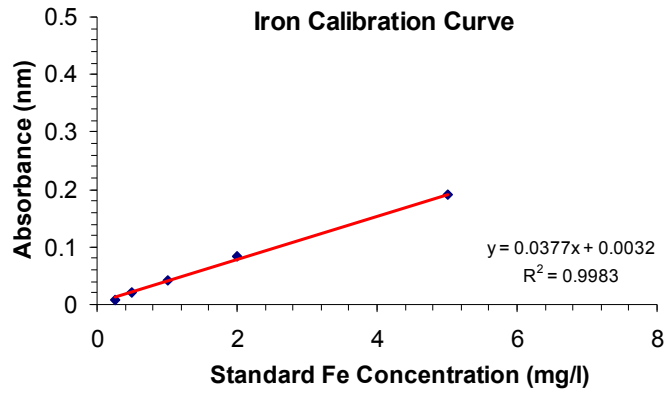


Figure A2: Typical calibration curves for iron, copper, zinc and manganese obtained using the AAS.

The calibration curve for the analysis of Ca²⁺ ions in solution is shown in Figure A3.

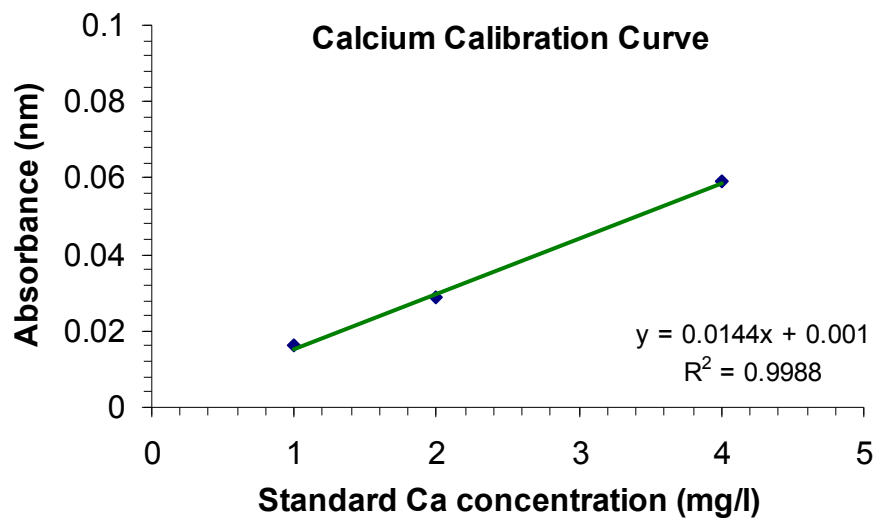


Figure A3: Typical calibration curve for calcium obtained using the AAS.

APPENDIX B

Characterisation of natural zeolite by supplier

Exploration Samples (No. ES7661)

Date 01/06/2004

Originator: J.Hooper/PMGI

Country: Turkey

Region: Asia

Location: Gordes

Source: Euremica Enviromental

Samples processed 2

Mineral: Zeolite Clinoptilolite

Testing Required: XRF XRD (PMC and CSM)

Results required

Notes:

Samples sourced by JJH through Rob Sampson of Euremica Environmental Ltd.

Potential feed material for micro-sphere project.

1/5K 1-3mm Buff coloured

2/5k <45mic powder Buff coloured



Chemical Analysis XRF (wt. %)

Sample details	Al ₂ O ₃	SiO ₂	Fe ₂ O ₃	TiO ₂	K ₂ O	CaO	MgO	Na ₂ O	LOI
1 – 3 mm	11.92	72.43	1.18	0.08	3.38	2.12	1.38	1.10	6.40
< 45 μm	11.45	71.79	1.27	0.04	3.22	2.20	1.42	0.67	7.92

Mineralogical Analysis XRD (wt. %)

Sample Details	Clinoptilolite	Mica	Quartz	Unidentified
1 – 3 mm	Majority	Trace	4	---
< 45 μm	Majority	---	---	---

APPENDIX C

Proposed design of a passive AMD treatment reactor vessel

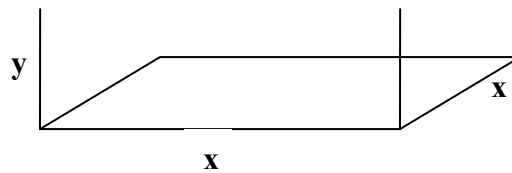
Flow rate into Passive treatment plant = 6 L/s

Residence time = 48 hours

Calculations:

Total volume passed in 48 hours = 1036.8 m³

Assuming the tank has a square base and a height that is half of the length of one side of the square base:



Where $y = x / 2$,

Therefore, volume of tank = x^2y

Volume, m³ = 1036.8 = $x^2y = x^3/2$

The value of x = 12.75 m

And, y = 6.38 m

This is a very massive reactor, which poses a number of challenges, the main being maintenance. Instead, two smaller vessels were designed with a total residence time of 48 hours.

The dimensions of the reactors are:

$$x = 10 \text{ m}$$

$$y = 5.5 \text{ m.}$$

The outlet nozzle diameter:

$$\text{Volumetric flow rate, } V = Au,$$

Where u is the linear velocity = 2 m/s.

$$V = Au = A \times 2 = 0.006 \text{ m}^3/\text{s}$$

$$A = 0.003 \text{ m}^2$$

From, Area, $A = \pi d^2/4$, the value of d , the diameter of the nozzle can be calculated.

$$\text{Therefore, the nozzle diameter for the outlet pipe} = 0.0618 \text{ m.}$$

$$\approx 6.2 \text{ cm.}$$

Material of Construction:

The vessel will be constructed using concrete; this is resistant to the acidic nature of AMD and results in a longer life of the reactor vessel.

APPENDIX D

Publications:

- ✚ Motsi, T, Rowson, N.A., Simmons, M.J., 2009. Adsorption of heavy metals from acid mine drainage by natural zeolite. *International Journal of Minerals Processing*, 92, 42 – 48.
- ✚ Motsi, T, Rowson, N.A., Simmons, M.J., 2009. Kinetic Studies of the Removal of Heavy Metals from Solution by Natural Zeolite. Manuscript submitted to the *International Journal of Minerals Processing* (2009).

Poster Presentations:

- ✚ Motsi, T, Rowson, N.A., Simmons, M.J., 2008. Adsorption of heavy metals from acid mine drainage (AMD), by natural zeolite (clinoptilolite). *31st British Zeolite Association Conference*, University of Keele, 1st April.
- ✚ Motsi, T, Rowson, N.A., Simmons, M.J., 2008. Adsorption of heavy metals from solution by clinoptilolite. *18th International Congress of Chemical and Process Engineering*, Prague, Czech Republic, 25th August.